

UNIVERSITA' DEGLI STUDI
DI PADOVA



UNIVERSITE DES SCIENCES ET
TECHNOLOGIES DE LILLE



N° d'ordre: 4176

THÈSE EN COTUTELLE

présentée par

Roberto MILANI

pour obtenir le grade de

Docteur de l'Université de Padova

Spécialité : Science des Matériaux

Docteur de l'Université de Lille 1

Spécialité : Structure et dynamique des systèmes réactifs

Thème

**Matériaux à base de phosphazènes chlorés pour la fonctionnalisation
de surface, la synthèse de précurseurs monomères
et la chimie supramoléculaire**

Soutenue le 7 Avril 2008 devant le jury composé de :

Président : R. Bertani Professeur, Faculté d'Ingénierie de Padova

Examineurs :

G. Mistura Professeur, Faculté de Sciences MM.FF.NN. de Padova

C. Jama Maître de Conférence, HDR, ENSC de Lille

A. Sassi Docteur, Chercheur au CNR de Padova

Directeurs de thèse : M. Gleria Docteur, Chercheur au CNR de Padova

A. Mazzah Professeur, Université de Lille 1

*For long you'll live and high you'll fly
And smiles you'll give and tears you'll cry
And all you touch and all you see
Is all your life will ever be*

(R. Waters)

INDEX

| | |
|---|----|
| List of Abbreviations..... | 1 |
| Abstract in lingua italiana | 3 |
| Resumé en langue française | 5 |
| 1. General Aim | 7 |
| 2. Introduction | 11 |
| 2.1. Phosphazene synthesis..... | 11 |
| 2.2. Phosphazene copolymers and multifunctionality | 12 |
| 2.3. Functionalization of phosphazenes..... | 14 |
| 2.4. Previous surface studies on phosphazenes | 18 |
| 3. Experimental Section | 25 |
| 3.1 Materials and Instrumentation | 25 |
| 3.1.1. Solvents..... | 25 |
| 3.1.2. Reagents | 25 |
| 3.1.3. Other materials | 26 |
| 3.1.4. Equipment for characterization..... | 27 |
| 3.2. Experimental procedures for surface functionalization of sodalime glasses and crystalline Silicon (100) wafers with chlorophosphazenes: a theoretical and experimental approach (Chapter 4.1)..... | 30 |
| 3.2.1. Theoretical Calculations | 30 |
| 3.2.2. Experimental Approach | 31 |
| 3.2.2.1. Surface activation of fused quartz slides..... | 31 |
| 3.2.2.2. Grafting of HCCP by “immersion” procedure | 32 |
| 3.2.2.3. Grafting of HCCP by “droplet deposition” procedure | 32 |
| 3.3. Experimental procedures for silicon-based surfaces functionalization using thin chlorophosphazene films deposited by glow-discharge induced sublimation as coupling agents (Chapter 4.2) | 32 |
| 3.3.1. Experimental apparatus..... | 32 |
| 3.3.2. Activation of crystalline silicon substrates | 33 |
| 3.3.3. Deposition procedure | 33 |
| 3.3.4. Reaction in solution | 34 |

| | |
|---|----|
| 3.4. Experimental procedures for surface functionalization of polymeric substrates using chlorophosphazenes as coupling agents (Chapter 4.3) | 34 |
| 3.4.1. Plasma activation of polymeric substrates..... | 35 |
| 3.4.2. Grafting of chlorophosphazenes..... | 35 |
| 3.4.3. Substitution of residual chlorines with nucleophiles..... | 35 |
| 3.5. Experimental procedures for the surface functionalization of silicon-based substrates and the preparation of new bulk materials and thin films using cyclophosphazenes partially substituted with trialkoxysilane derivatives (chapter 4.4)..... | 37 |
| 3.5.1 Starting and reference compounds | 37 |
| 3.5.1.1. Synthesis of hexakis(4CNP)cyclophosphazene | 37 |
| 3.5.1.2. Synthesis of tris(4CNP)tris(chloro)cyclophosphazene | 38 |
| 3.5.1.3. Synthesis of 2,2-dichloro-4,4,6,6-bis[spiro(2',2'')-dioxo-1',1''-biphenyl)]-cyclophosphazene | 39 |
| 3.5.1.4. Synthesis of 2,2-bis(2,2,3,3-tetrafluoropropoxy)-4,4,6,6-bis[spiro(2',2'')-dioxo-1',1''-biphenyl)]cyclophosphazene (C-2-TFP) | 40 |
| 3.5.2. Synthesis of sol-gel precursors | 41 |
| 3.5.2.1. Synthesis of tris(4CNP)tris(APTES)cyclophosphazene | 41 |
| 3.5.2.2. Synthesis of tris(TFP)tris(APTES)cyclophosphazene | 42 |
| 3.5.2.3. Synthesis of tris(PEG-750-ME)tris(APTES)-cyclophosphazene | 43 |
| 3.5.2.4. Synthesis of tris(AzB)tris(APTES)cyclophosphazene..... | 44 |
| 3.5.3. Surface functionalization of silica gel | 45 |
| 3.5.3.1. Silica gel activation..... | 45 |
| 3.5.3.2. Surface functionalization of silica gel beads with cyclophosphazenes cosubstituted with APTES and with TFP, PEG-750-ME or AzB..... | 45 |
| 3.5.4. Preparation of monoliths and thin films | 47 |
| 3.5.4.1. Preparation of monoliths and thin films starting from tris(4CNP)tris(APTES)cyclophosphazene via sol-gel technique | 47 |
| 3.5.4.2. Preparation of monoliths and thin film coatings on Si(100) by sol-gel technique from cyclophosphazenes co-substituted with APTES and TFP, PEG-750-ME or AzB..... | 49 |

| | |
|--|----|
| 3.6. Experimental procedures for the synthesis of cyclophosphazenes substituted with oxazoline groups as starting products for the preparation of new materials (Chapter 4.5)..... | 51 |
| 3.6.1. Synthesis of hydroxyphenyloxazoline derivatives..... | 51 |
| 3.6.1.1. Synthesis of N-2-hydroxyethyl-4-hydroxybenzamide (I) and of chiral R-(-) (II), S-(+) (III) and racemic (±) (IV) N-2-hydroxypropyl-4-hydroxybenzamides..... | 51 |
| 3.6.1.2. Synthesis of 2-(4-hydroxyphenyl)-2-oxazoline (a) and of S-(+) (b), R-(-) (c) and (±) (d) -2-(4-hydroxyphenyl)-5-methyl-2-oxazolines.... | 52 |
| 3.6.2. Synthesis of chlorophosphazenes..... | 54 |
| 3.6.2.1. Synthesis of pentakis(phenoxy)monochlorocyclophosphazene, C-1-Cl (1)..... | 54 |
| 3.6.2.2. Synthesis of 2,2-dichloro-4,4,6,6-bis[spiro(2',2''-dioxo-1',1''-biphenyl)]-cyclophosphazene, C-2-Cl (2)..... | 54 |
| 3.6.3. Synthesis of cyclophosphazene derivatives substituted with 2-oxazoline groups..... | 54 |
| 3.6.3.1. Synthesis α: Reaction carried out in anhydrous THF in the presence of NaH 60% oil dispersion | 55 |
| 3.6.3.2. Synthesis β: Synthesis carried out in anhydrous acetone in the presence of Cs ₂ CO ₃ | 55 |
| 3.6.3.3. Synthesis of pentakisphenoxy-mono-4-(oxazolinophenoxy) cyclophosphazene (1a) (C-1-OXA)..... | 55 |
| 3.6.3.4. Synthesis of chiral S-(+) pentakisphenoxy-mono[4-(5-methyl)-oxazolinophenoxy] cyclophosphazene (C-1-OXA S+) (1b) | 56 |
| 3.6.3.5. Synthesis of chiral R-(-) pentakisphenoxy-mono[4-(5-methyl)-oxazolinophenoxy] cyclophosphazene (C-1-OXA R-) (1c)..... | 56 |
| 3.6.3.6. Synthesis of racemic pentakisphenoxy-mono[4-(5-methyl)-oxazolinophenoxy] cyclophosphazene (C-1-OXA±) (1d) | 57 |
| 3.6.3.7. Synthesis of 2,2-bis(4-oxazolinophenoxy)-4,4,6,6-bis-[spiro(2',2''-dioxo-1',1''-biphenyl)] cyclophosphazene (C-2-OXA) (2a) .. | 57 |
| 3.6.3.8. Synthesis of chiral [S-(+)] 2,2-bis[4-(5-methyl)-oxazolinophenoxy]-4,4,6,6-bis[spiro(2',2''-dioxo-1',1''-biphenyl)]cyclophosphazene (C-2-OXA S+) (2b) | 58 |

| | |
|--|----|
| 3.6.3.9. Synthesis of chiral [R(-)] 2,2-bis[4-(5-methyl)-oxazolinophenoxy]-4,4,6,6-bis[spiro(2',2''-dioxo-1',1''-biphenyl)]cyclophosphazene (C-2-OXA R-) (2c)..... | 58 |
| 3.6.3.10. Synthesis of racemic 2,2-bis[4-(5-methyl)-oxazolinophenoxy]-4,4,6,6-bis[spiro(2',2''-dioxo-1',1''-biphenyl)]cyclophosphazene (C-2-OXA \pm) (2d) | 59 |
| 3.6.3.11. Synthesis of hexakis(oxazolinophenoxy)cyclophosphazene (C-6-OXA) (3a) | 59 |
| 3.6.3.12. Synthesis of chiral [S(+)]hexakis(4-(5-methyl)-oxazolinophenoxy)-cyclophosphazene (C-6-OXA S+) (3b) | 60 |
| 3.6.3.13. Synthesis of chiral [R(-)]hexakis(4-(5-methyl)-oxazolinophenoxy)-cyclophosphazene (C-6-OXA R-) (3c) | 60 |
| 3.6.3.14. Synthesis of racemic hexakis[4-(5-methyl)-oxazolinophenoxy]-cyclophosphazene (C-6-OXA \pm) (3d)..... | 60 |
| 3.7. Experimental section for the synthesis of supramolecular rods via halogen bonding-based self-assembly of fluorinated phosphazene nanopillars (Chapter 4.6)..... | 61 |
| 3.7.1. Synthesis of 2,2-bis(4-formylphenoxy)-4,4,6,6-bis[spiro(2',2''-dioxo-1',1''-biphenyl)]cyclophosphazene (C-2-pCHO) | 61 |
| 3.7.2. Synthesis of hexakis(4-formylphenoxy)cyclophosphazene (C-6-pCHO) | 62 |
| 3.7.3. Synthesis of 2,2-bis(4-hydroxymethylenphenoxy)-4,4,6,6-bis[spiro(2',2''-dioxo-1',1''-biphenyl)]cyclotriphosphazene (C-2-pOH) | 63 |
| 3.7.4. Synthesis of hexakis(4-hydroxymethylenphenoxy)cyclophosphazene (C-6-pOH)..... | 64 |
| 3.7.5. Synthesis of 2,2-bis[4-(2,3,5,6-tetrafluoro-4-iodophenoxy)methylenphenoxy]-4,4,6,6-bis[spiro(2',2''-dioxo-1',1''-biphenyl)]cyclophosphazene (C-2-ITFB) | 65 |
| 3.7.6. Synthesis of hexakis[4-(2,3,5,6-tetrafluoro-4-iodophenoxy)methylenphenoxy]-cyclophosphazene (C-6-ITFB) | 66 |
| 3.7.7. Self-assembly..... | 67 |

| | |
|---|-----|
| 4. Results and Discussion..... | 68 |
| 4.1. Surface functionalization of sodalime glasses and crystalline silicon (100) wafers with chlorophosphazenes: a theoretical and experimental approach | 68 |
| 4.1.1. Preliminary considerations..... | 68 |
| 4.1.2. <i>Ab initio</i> calculations..... | 71 |
| 4.1.2.1. Structure of the HCCP molecule | 71 |
| 4.1.2.2. Reaction between HCCP and hydroxylated silicon surface: thermodynamic data | 72 |
| 4.1.2.3. Reaction between HCCP and hydroxylated silicon surface: kinetic data | 78 |
| 4.1.3. Experimental approach | 81 |
| 4.1.3.1. Influence of the solvent | 83 |
| 4.1.3.2. Influence of surface-adsorbed water | 84 |
| 4.1.3.3. Influence of temperature and treatment duration | 87 |
| 4.1.4. Conclusions..... | 91 |
| 4.1.5. Acknowledgements..... | 92 |
| 4.2. Thin phosphazene films deposition by glow discharge-induced sublimation (GDS)..... | 92 |
| 4.2.1. Preliminary considerations..... | 92 |
| 4.2.2. Deposition rate of HCCP derived thin films..... | 93 |
| 4.2.3. Plasma composition by mass spectrometry | 94 |
| 4.2.4. Characterization of HCCP-derived thin films..... | 97 |
| 4.2.5. Behaviour of chlorophosphazene coatings towards washing | 99 |
| 4.2.6. Substitution reactions in solution..... | 100 |
| 4.2.7. Conclusions..... | 102 |
| 4.2.8. Acknowledgements..... | 102 |
| 4.3. Surface functionalization of polymeric substrates using chlorinated phosphazenes as coupling agents..... | 103 |
| 4.3.1. Step 1: Plasma treatment of HDPE and PA6 | 104 |
| 4.3.1.1. Contact angle study | 105 |
| 4.3.1.2. Infrared study | 106 |
| 4.3.1.3. XPS study | 107 |
| 4.3.2. Step 2: Grafting of chlorophosphazenes | 110 |

| | |
|---|-----|
| 4.3.3. Step 3: Nucleophilic replacement of phosphazene residual chlorines .. | 110 |
| 4.3.3.1 Infrared characterization | 111 |
| 4.3.3.2. Contact angle characterization | 112 |
| 4.3.3.3. XPS characterization..... | 114 |
| 4.3.3.4. UV-Vis characterization | 119 |
| 4.3.4. Conclusions | 120 |
| 4.3.5. Acknowledgements | 121 |
| 4.4. Cyclophosphazenes partially substituted with trialkoxysilane derivatives for the surface functionalization of silicon-based substrates and for the preparation of new bulk materials and thin films..... | 122 |
| 4.4.1. Preliminary considerations | 122 |
| 4.4.2. Synthesis of cyclophosphazenes..... | 124 |
| 4.4.2.1 Preliminary synthesis of hexakis(4CNP)cyclophosphazene..... | 124 |
| 4.4.2.2. First reaction step: partial substitution of HCCP with nucleophiles... | 124 |
| 4.4.2.3. Second step: residual chlorines substitution with APTES | 126 |
| 4.4.3. Surface functionalization of silica gel | 127 |
| 4.4.4. Monoliths and thin films preparation | 132 |
| 4.4.4.1. Self-condensation processes | 132 |
| 4.4.4.2. Monolith preparation from self-condensation processes | 132 |
| 4.4.4.3. Thin film coating deposition from self-condensation processes ... | 135 |
| 4.4.4.4. Condensation processes in the presence of TEOS | 135 |
| 4.4.4.5. Monolith Preparation from condensation processes in the presence of TEOS | 136 |
| 4.4.4.6. Thin films deposition from condensation processes in the presence of TEOS | 139 |
| 4.4.5. Conclusions | 140 |
| 4.4.6. Acknowledgements | 141 |
| 4.5. Cyclophosphazenes substituted with 2-oxazoline groups as starting products for the preparation of new materials..... | 141 |
| 4.5.1. Preliminary considerations | 141 |
| 4.5.2. Synthesis and characterization of the oxazoline-containing phosphazenes.. | 143 |
| 4.5.3. Conclusions | 146 |
| 4.5.4. Acknowledgements | 146 |

| | |
|---|-----|
| 4.6. Supramolecular rods via halogen bonding-based self-assembly of fluorinated phosphazene nanopillars | 149 |
| 4.6.1. Preliminary considerations..... | 149 |
| 4.6.2. Synthesis and characterization of the phosphazene precursor | 150 |
| 4.6.3. Formation of supramolecular assemblies..... | 152 |
| 4.6.4. Conclusions..... | 157 |
| 4.6.5. Acknowledgements | 158 |
| 5. Conclusions | 159 |
| References | 161 |
| Appendices | 186 |
| A1. Characterization techniques..... | 186 |
| A1.1. X-ray Photoelectron spectroscopy (XPS) | 186 |
| A1.2. Contact angle and surface energy measurement | 188 |
| A1.3. Fourier Transform Infrared Spectroscopy in Attenuated Total Reflection mode (FTIR-ATR) | 190 |
| A2. Experimental techniques..... | 192 |
| A2.1. Glow Discharge-induced Sublimation (GDS) | 192 |
| A2.2. Sol-gel technique..... | 195 |
| List of Publications..... | 198 |
| Acknowledgements | 200 |

LIST OF ABBREVIATIONS

| | |
|-----------|---|
| 4CNP | 4-Hydroxybenzonitrile (also referred to as 4-Cyanophenol) |
| APTES | 3-aminopropyltriethoxysilane |
| AzB | 4-Phenylazophenol (also referred to as 4-Hydroxyazobenzene) |
| BE | Binding Energy |
| C-1-Cl | Pentakis(phenoxy)monochlorocyclotriphosphazene |
| C-1-OXA | Pentakis(phenoxy)mono-4-oxazolinophenoxy)cyclotriphosphazene |
| C-2-Cl | 2,2-Dichloro-4,4,6,6-bis[spyro(2',2''-dioxo-1',1''-biphenyl)]-cyclotriphosphazene |
| C-2-OXA | 2,2-Bis(4-oxazolinophenoxy)-4,4,6,6-bis[spyro(2,2'-dioxo-1,1'-biphenyl)] cyclotriphosphazene |
| C-2-pCHO | 2,2-Bis(4-formylphenoxy)-4,4,6,6-bis[spyro(2',2''-dioxo-1',1''-biphenyl)]cyclotriphosphazene |
| C-2-pITFB | 2,2-Bis[4-(2,3,5,6-tetrafluoro-4-iodophenoxymethylen)phenoxy]-4,4,6,6-bis[spyro(2',2''-dioxo-1',1''-biphenyl)]cyclotriphosphazene |
| C-2-pOH | 2,2-Bis(4-hydroxymethylenphenoxy)-4,4,6,6-bis[spyro(2,2'-dioxo-1,1'-biphenyl)]cyclotriphosphazene |
| C-2-TFP | 2,2-bis(2,2,3,3-tetrafluoropropoxy)-4,4,6,6-bis[spyro(2,2'-dioxo-1,1'-biphenyl)]cyclotriphosphazene |
| C-6-OXA | Hexakis(4-oxazolinophenoxy)cyclotriphosphazene |
| C-6-pCHO | Hexakis(4-formylphenoxy)cyclotriphosphazene |
| C-6-pITFB | Hexakis[4-(2,3,5,6-tetrafluoro-4-iodophenoxymethylen)phenoxy]cyclo-triphosphazene |
| C-6-pOH | Hexakis(4-hydroxymethylenphenoxy)cyclotriphosphazene |
| DPE | 1,2-di(4-pyridyl)ethylene |
| DPy | 4,4'-dipyridyl |
| EVOH | Poly(ethylene-co-vinylalcohol) |
| GDS | Glow Discharge-induced Sublimation |
| HCCP | Hexachlorocyclotriphosphazene |
| HDFN | 2,2,3,3,4,4,5,5,6,6,7,7,8,8,9,9-Heptafluoro-1-nonanol (also referred to as <i>1H,1H</i> -heptafluorononanol) |

| | |
|------------|--|
| HDPE | High Density Polyethylene |
| NLO | Non-Linear Optics |
| OCCP | Octachlorocyclotetraphosphazene |
| OXA | 2-Oxazoline |
| PA6 | Polyamide-6 |
| PDCP | Poly(dichlorophosphazene) |
| PEG-750-ME | Poly(ethyleneglycol)monomethylether (average molec. weight 750 Dalton) |
| POPs | Poly(organophosphazenes) |
| PTFEP | Poly[bis(2,2,2-trifluoroethoxy)phosphazene] |
| TBAB | Tetrabutylammonium bromide |
| TEA | Triethylamine |
| TEAB | Tetraethylammonium bromide |
| TEOS | Tetraethylorthosilicate (also referred to as Tetraethylorthosilicate) |
| TFE | 2,2,2-Trifluoroethanol |
| TFP | 2,2,3,3-Tetrafluoropropanol |
| THF | Tetrahydrofuran |

ABSTRACT IN LINGUA ITALIANA

Il progetto di ricerca descritto in questa tesi è basato essenzialmente su due aree principali di studio: l'utilizzo di esaclorociclofosfazene (HCCP) e poli(diclorofosfazene) (PDCP) come agenti di accoppiamento per la funzionalizzazione superficiale di substrati solidi (materiali silicei inorganici e materiali polimerici organici) e la sintesi di composti fosfazenici di partenza per la produzione di nuovi materiali e di strutture supramolecolari.

La prima tematica di questa tesi è stata affrontata per stadi, investigando in primo luogo la fattibilità della reazione di funzionalizzazione superficiale di substrati silicei inorganici (wafer di silicio, vetrini sodalime, quarzo fuso elettricamente e gel di silice) mediante calcoli teorici *ab initio*. Questi calcoli hanno dimostrato la fattibilità termodinamica dell'aggraffaggio di HCCP sulla superficie di tali substrati, ma anche la presenza di sostanziali barriere energetiche dal punto di vista cinetico, che però possono verosimilmente essere abbassate mediante scelta di un opportuno solvente per la reazione. Le prove di laboratorio, effettuate per immersione di vetrini sodalime e di quarzo fuso elettricamente in soluzioni di HCCP, hanno mostrato all'analisi XPS che il fosfazene forma dei legami forti con la superficie dei substrati, ma è d'altro canto soggetto a successivi fenomeni di degradazione idrolitica. Inoltre, film derivati da HCCP aventi una maggiore stabilità sono stati ottenuti su wafer di Si(100) con la tecnica GDS (Glow Discharge-induced Sublimation, ovvero sublimazione assistita da plasma), anche se la loro caratterizzazione FTIR ha indicato che l'originale struttura ciclica del precursore viene sostanzialmente perduta durante la deposizione. Successive reazioni di sostituzione nucleofila hanno permesso l'introduzione di 4-cianofenolo (4CNP) e 2,2,2-trifluoroetanolo (TFE) sulla superficie dei campioni, analizzati mediante tecniche FTIR e XPS. Come secondo stadio della nostra indagine, HCCP e PDCP sono stati utilizzati con successo come agenti di accoppiamento per la funzionalizzazione superficiale di substrati polimerici, permettendo l'aggraffaggio di alcool fluorurati di diversa lunghezza e di funzioni azobenzeniche sulle superfici di poli(etilene-co-vinil alcool) (EVOH), e di polietilene ad alta densità (HDPE) e poliammide-6 (PA6) preventivamente trattati con un plasma ad argon. Le analisi effettuate mediante spettroscopie FTIR-ATR, UV-Vis e XPS, e mediante misura dell'angolo di contatto, hanno confermato la modifica dell'energia superficiale e della bagnabilità di questi

materiali, nonché l'introduzione di proprietà fotocromiche di superficie nel caso dell'azo-composto. Ci siamo occupati infine della sintesi di derivati di HCCP contenenti nella stessa molecola gruppi 3-amminopropiltriethossisilano (APTES) e sostituenti organici differenti (4-cianofenossi, poli(etilen glicole) monometiltere, 2,2,3,3-tetrafluoropropossi o fenilazofenossi). Questi composti sono stati utilizzati sia per funzionalizzare la superficie di particelle di gel di silice, che nel processo sol-gel per depositare film sottili su vetro sodalime e silicio, e per ottenere materiali massivi ibridi organico-inorganici. La caratterizzazione effettuata mediante FTIR, NMR in stato solido, spettroscopia UV-Vis e le analisi termiche DSC e DMTA, ha confermato che i diversi prodotti così ottenuti hanno caratteristiche chimico-fisiche differenti, e che queste sono determinate dalla natura dei composti organici scelti come gruppi sostituenti sul precursore fosfazenico. E' opportuno sottolineare che le procedure di funzionalizzazione proposte hanno carattere generale, e possono essere estese in linea di principio alla modifica delle superfici di substrati solidi differenti con un'ampia gamma di composti organici, grazie alla versatilità sintetica della chimica dei fosfazeni.

Per quanto riguarda la seconda tematica di questa tesi, sono stati preparati dodici composti ciclotrifenilfosfazenici contenenti gruppi 2-ossazolina di natura chirale, achirale oppure racema come composti di partenza adatti per la produzione di nuovi materiali. Tali composti sono stati caratterizzati mediante FTIR, NMR, analisi elementare, misura del punto di fusione e del potere rotatorio ottico, confermandone la struttura prevista. Possibili applicazioni per questi derivati includono la sintesi di polimeri ciclomatrice reticolati per la separazione cromatografica di specie enantiomeriche, e l'utilizzo come estensori di catena per il riciclo di materiali polimerici. Infine, sono stati preparati ciclofosfazeni contenenti due o sei gruppi 4-iodotetrafluorofenossi. Il composto esasostituito è stato utilizzato in presenza di derivati dipiridilici per la produzione di nanostrutture tridimensionali autoassemblate, generate da interazioni supramolecolari basate su legame alogeno. Tali strutture sono state caratterizzate mediante tecniche FTIR, NMR, DSC e diffrazione X. Va sottolineato che il menzionato ciclofosfazene contenente sei gruppi 4-iodotetrafluorofenossi costituisce il primo esempio di donatore esadentato di legame alogeno.

RESUMÉ EN LANGUE FRANÇAISE

Aux recherches décrites dans cette thèse correspondent deux thèmes d'étude principaux :

- L'utilisation de l'hexachlorocyclotriphosphazène (HCCP) et du poly(dichlorophosphazène) (PDCP) en tant qu'agents de couplage pour la fonctionnalisation de surface de substrats solides (matériaux inorganiques à base de silicium et matériaux polymères organiques),
- La synthèse de composés phosphazéniques pour la production de nouveaux matériaux et de structures supramoléculaires.

La première thématique a été abordée par étapes. Dans un premier temps en étudiant à l'aide de calculs théoriques *ab initio*, la faisabilité de la réaction de fonctionnalisation de surface de substrats siliceux inorganiques (wafers de silicium, lamelles de verre sodalime et de quartz fondu électriquement, gel de silice). Ces calculs ont démontré, d'un point de vue thermodynamique, la faisabilité du greffage de HCCP à la surface de tels substrats mais aussi l'existence de barrières énergétiques importantes, lesquelles pourraient raisonnablement être diminuées par un choix adéquat du solvant de réaction. L'analyse XPS effectuée sur des échantillons de verre sodalime et de quartz fondu électriquement fonctionnalisés par immersion dans une solution de HCCP, a montré la formation de liaisons fortes entre le phosphazène et la surface des substrats, ainsi que l'intervention de phénomènes de dégradation hydrolytique. Des couches minces dérivées de HCCP possédant une meilleure stabilité ont été obtenues sur wafers de Si(100) par la technique GDS (*Glow Discharge-induced Sublimation*, c'est-à-dire sublimation induite par plasma), même si la caractérisation FTIR suggère que la structure cyclique originale du précurseur est en majorité perdue pendant la déposition. Des réactions successives de substitution nucléophile ont permis l'introduction de 4-cyanophénol (4CNP) et de 2,2,2-trifluoroéthanol (TFE) à la surface des échantillons, lesquels ont été analysés par spectroscopies FTIR et XPS. Dans un deuxième temps, HCCP et PDCP ont été utilisés avec succès en tant qu'agents de couplage pour la fonctionnalisation de surface de substrats polymères organiques. Ils ont permis de greffer des alcools fluorés de longueurs différentes ainsi que des fonctions azobenzènes à la surface de poly(éthylène-co-vinyl alcool) (EVOH), de polyéthylène haute densité (HDPE) et de polyamide-6 (PA6) traités préalablement par un plasma froid d'argon à basse pression. Les analyses effectuées par

spectroscopies FTIR, UV-Vis et XPS, ainsi que les mesures d'angles de contact, ont confirmé les modifications de l'énergie de surface et de la mouillabilité des substrats, et l'introduction de propriétés photochromiques de surface dans le cas de l'*azo*-composé. La synthèse de dérivés de HCCP contenant tous dans la même molécule des substituants 3-aminopropyltriethoxysilane (APTES), associés à des substituants organiques différents (4CNP, poly(éthylène glycol)monométhyléther, 2,2,3,3-tetrafluoropropanol ou 4-phénylazophénoxy) a enfin été réalisée. Les composés obtenus ont été utilisés soit pour fonctionnaliser la surface de particules de gel de silice, soit en utilisant la technique sol-gel, pour le dépôt de couches minces sur silicium et verre sodalime et pour la synthèse de nouveaux matériaux hybrides organiques-inorganiques. Les caractérisations par spectroscopies FTIR, RMN à l'état solide, UV-Vis et analyses thermiques DSC et DMTA, ont montré que les propriétés chimiques et physiques des matériaux obtenus étaient déterminées par la nature des fonctions organiques introduites sur le phosphazène précurseur. Il est bon de signaler le caractère général des procédures de fonctionnalisation proposées. L'étendue des réactions possibles de substitution des phosphazènes (cycliques ou polymères) devrait en effet permettre d'introduire de nombreux composés organiques à la surface de substrats solides différents.

En ce qui concerne la seconde thématique, douze cyclotriphosphazènes contenant des groupements 2-oxazoline de natures chirale, non chirale ou racémique ont été synthétisés en tant que composés de base pour la préparation de nouveaux matériaux. Les structures prévues pour ces composés ont été confirmées par spectroscopies FTIR et RMN, analyse élémentaire, mesure d'angles de contact et mesure du pouvoir rotatoire optique. Les applications potentielles de tels composés incluent la synthèse de matériaux réticulés (cyclomatrix polymères) pour la séparation d'espèces énantiomères, et leur utilisation en tant qu'espaceurs de chaînes pour le recyclage de matériaux polymères. Des cyclophosphazènes contenant deux et six fonctions 4-iodotetrafluorophénoxy ont enfin été préparés et caractérisés par spectroscopies FTIR et RMN. Le composé hexasubstitué a été utilisé en présence de dérivés dipyridyliques pour produire des nanostructures tridimensionnelles auto-assemblées, générées par interactions supramoléculaires basées sur des liaisons halogène. Ces structures ont été caractérisées par spectroscopies FTIR et RMN, DSC et diffraction X. Il est intéressant de souligner que le composé contenant six groupements 4-iodotetrafluorophénoxy constitue le premier exemple de donneur hexadenté de liaisons halogène.

CHAPTER 1

GENERAL AIM

In this thesis we disclose a few, very simple synthetic strategies to achieve the surface functionalization of silicon-based materials and of organic polymer plates with cyclic and polymeric phosphazene substrates acting as coupling agents.

To achieve this goal we took advantage of the well known and established reactivity of the P-Cl groups present in chlorophosphazene substrates with different nucleophiles to prepare poly(organophosphazenes) and cyclo(organophosphazenes), respectively¹⁻⁴.

The general process we used can be summarized in two steps, *i.e.* we reacted first hexachlorocyclophosphazene (HCCP) and poly(dichlorophosphazene) (PDCP) with the surface of materials already containing free hydroxylic groups, using in this process only a part of the chlorines available in these compounds. The residual P-Cl moieties were then substituted with a variety of nucleophiles to eventually functionalize the surface with these molecules.

As possible materials for surface functionalization we selected silicon-based materials such as crystalline (100) silicon wafers, silica beads, and sodalime glasses; we functionalized also the surface plates of an organic copolymer, *e.g.* poly(ethylene-co-vinyl alcohol) (EVOH), already containing free hydroxylic groups in its chemical structure.

These processes are reported in Figure 1.

The feasibility of surface functionalization reactions was first evaluated by semiempirical and *ab initio* theoretical calculations⁵ and subsequently achieved experimentally by solution⁶⁻⁸ (*Chapter 4.1*) and by Glow Discharge-induced Sublimation⁹ (*Chapter 4.2*) techniques. In the second case the residual chlorines of the surface-grafted phosphazene were eventually substituted with 2,2,2-trifluoroethanol (TFE) and with 4-cyanophenol (4CNP) groups. These results are indicated as Process A in the scheme of Figure 1.

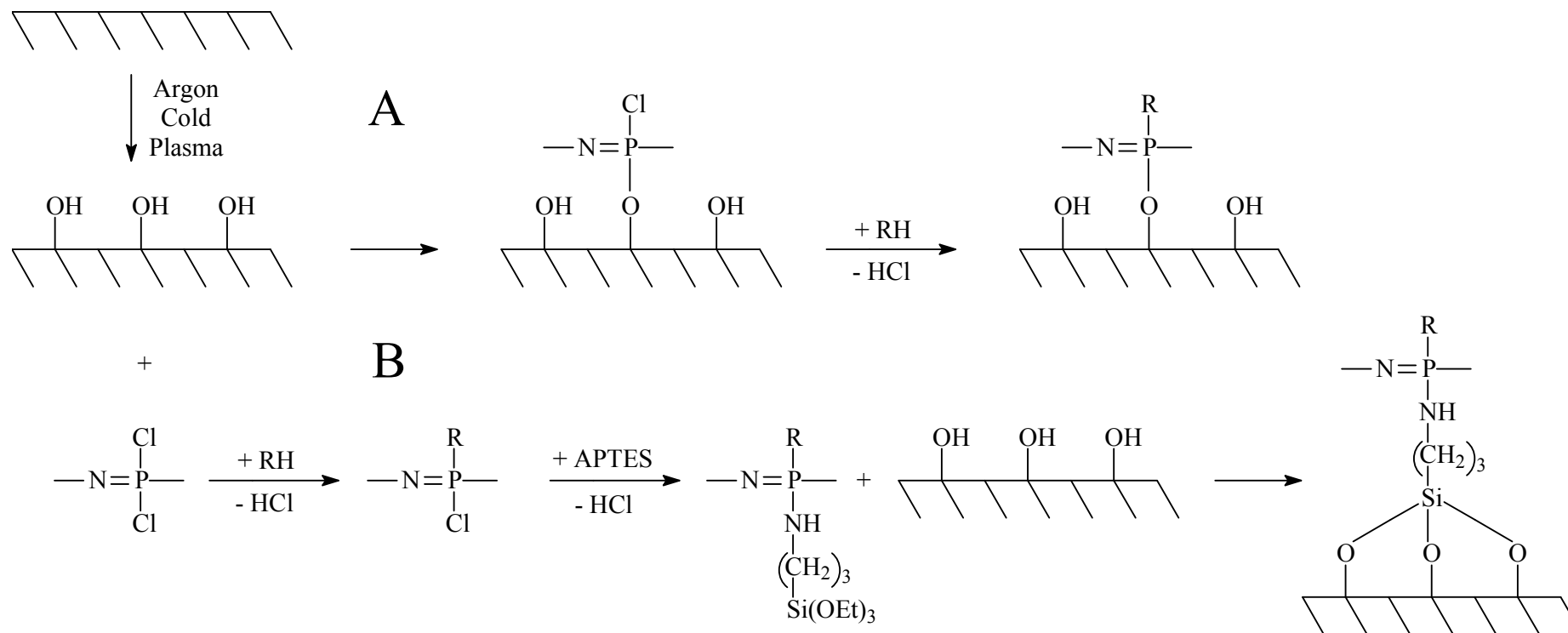


Figure 1. General scheme of the employed strategies to achieve surface functionalization of solid substrates with phosphazenes.
 APTES = γ -aminopropyltriethoxysilane; RH is an alcohol, a phenol or a primary or secondary amine.

The same pathway holds true also in the case of the surface functionalization of polymeric plates of EVOH¹⁰, High Density Polyethylene (HDPE)¹¹ and polyamide-6 (PA6)¹². Previous treatment with cold low pressure argon plasma was exploited to introduce onto the surface of HDPE and PA6 the hydroxylic groups necessary for the reaction with HCCP or PDCP. In all these cases TFE, *1H,1H*-heptadecafluoro-1-nonanol (HDFN), and 4-hydroxyazobenzene (AzB) were used to modify the polymeric surface (*Chapter 4.3*).

Finally, the surface functionalization process was reversed in the case of the functionalization of silica beads^{13,14} (*Chapter 4.4*), as we preliminarily synthesized cyclophosphazenes statistically substituted with about 50% of 4CNP, polyethylene glycol monomethyl ether (750 dalton of average molecular weight) (PEG-750-ME), 2,2,3,3-tetrafluoropropanol (TFP), or 4-hydroxyazobenzene (AzB), the residual 50% being saturated with γ -aminopropyltriethoxysilane (APTES). These latest groups were used to graft the synthesized cyclophosphazenes onto the surface of silica beads, and to produce new materials by monolith and thin coating preparation by sol-gel technique. This reaction sequence is indicated in Figure 1 as Pathway B.

As a second part of this thesis we also used HCCP for the preparation of 2-oxazoline (OXA)-containing cyclophosphazenes as potential monomers for the synthesis of cycloliner and/or cyclomatrix phosphazene polymers, or as chain extenders or crosslinkers for conventional organic macromolecules. This was done by using cyclophosphazenes containing 1, 2 or 6 reactive chlorines in their chemical structures and OXA derivatives, which were of both chiral and non-chiral nature^{15,16} (*Chapter 4.5*). We also explored the possibility of achieving solid crystalline assemblies by self-recognition processes based on the formation of halogen-bonding interactions between cyclophosphazenes containing 2,3,5,6-tetrafluoro-4-iodophenyl residues and tertiary amines¹⁷ (*Chapter 4.6*). These processes are indicated with the symbol “C” and “D” respectively in the scheme of Figure 2.

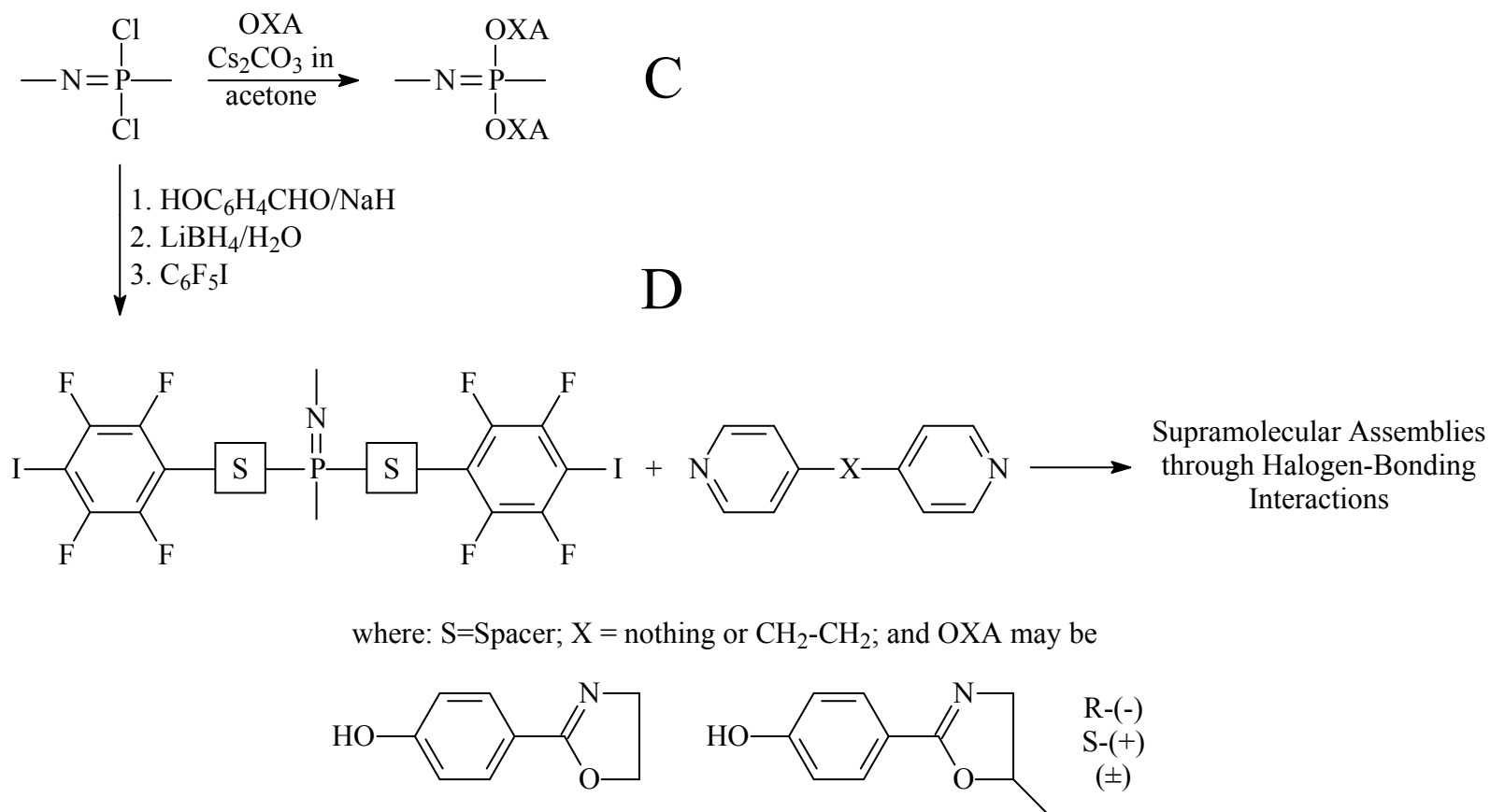


Figure 2. General scheme for the preparation of cyclophosphazenes containing 2-oxazoline and iodio-tetrafluoro benzene groups.

CHAPTER 2

INTRODUCTION

Phosphazenes are inorgano-organic materials, of both oligomeric (linear or cyclic) and polymeric nature⁴, characterized by the following structural units:

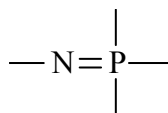


Figure 3. General structure of phosphazene derivatives.

Among the several thousands of existing phosphazenes, in this thesis we will deal mostly with compounds having the following structure:

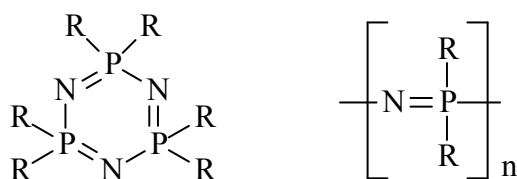


Figure 4. General structure of cyclotri- and polyphosphazenes.

in which the general formulas of cyclotriphosphazenes and of linear poly(organophosphazenes), POPs, respectively, are represented³.

Phosphazenes have at least three extremely important features that make them very attractive:

- 1) very peculiar synthetic versatility¹⁸;
- 2) multifunctionality and possibility of synthesizing phosphazene copolymers¹⁹;
- 3) very good functionalization possibility²⁰.

These characteristics will be examined in details hereafter.

2.1. Phosphazene Synthesis

The high versatility of the synthetic approach to the synthesis of phosphazene materials is based on the remarkable reactivity of the P-Cl groups existing in a series of phosphazene precursors, *i.e.* HCCP, octachlorocyclotetraphosphazene (OCCP) and PDCP, having the following structures respectively (Figure 5):

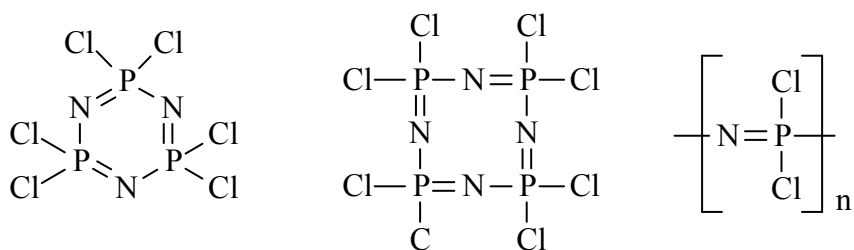


Figure 5. General Structure of Chlorinated Cyclo- and Poly-phosphazenes.

that can be easily reacted with a large variety of different nucleophiles to give rise to several different classes of cyclo- and polyphosphazenes^{1,21,22}, as reported in Figure 6.

In this Figure the general structures of nine different classes of cyclophosphazenes and poly(organophosphazenes) are reported. It can be realized immediately that in the Figure only homogeneously substituted cyclo- and polyphosphazenes (*i.e.* phosphazene homopolymers) are represented. Among these latter materials, poly(alkoxy)-²³, poly(aryloxy)-²⁴, poly(alkyl/aryl-amino)-²⁵ and polyspyrophosphazenes²⁶ represent the most important classes of phosphazene macromolecules both from an academic and from an applicative/technological point of view. It can be also observed that the substituent groups used to prepare hydrolytically stable polyphosphazenes are mostly aliphatic and aromatic alcohols or amines, which are commercial products easily available in high quantities and low prices. From this observation it can be expected that the class of phosphazene homopolymers could be formed by a considerably high number of polymeric compounds.

2.2. Phosphazene copolymers and multifunctionality

During the history of phosphazene compounds, attempts have been successfully carried out to simultaneously substitute two (or more than two) different nucleophiles on the same chlorophosphazene substrate¹⁹. This approach resulted in the synthesis of *substituent* phosphazene copolymers.

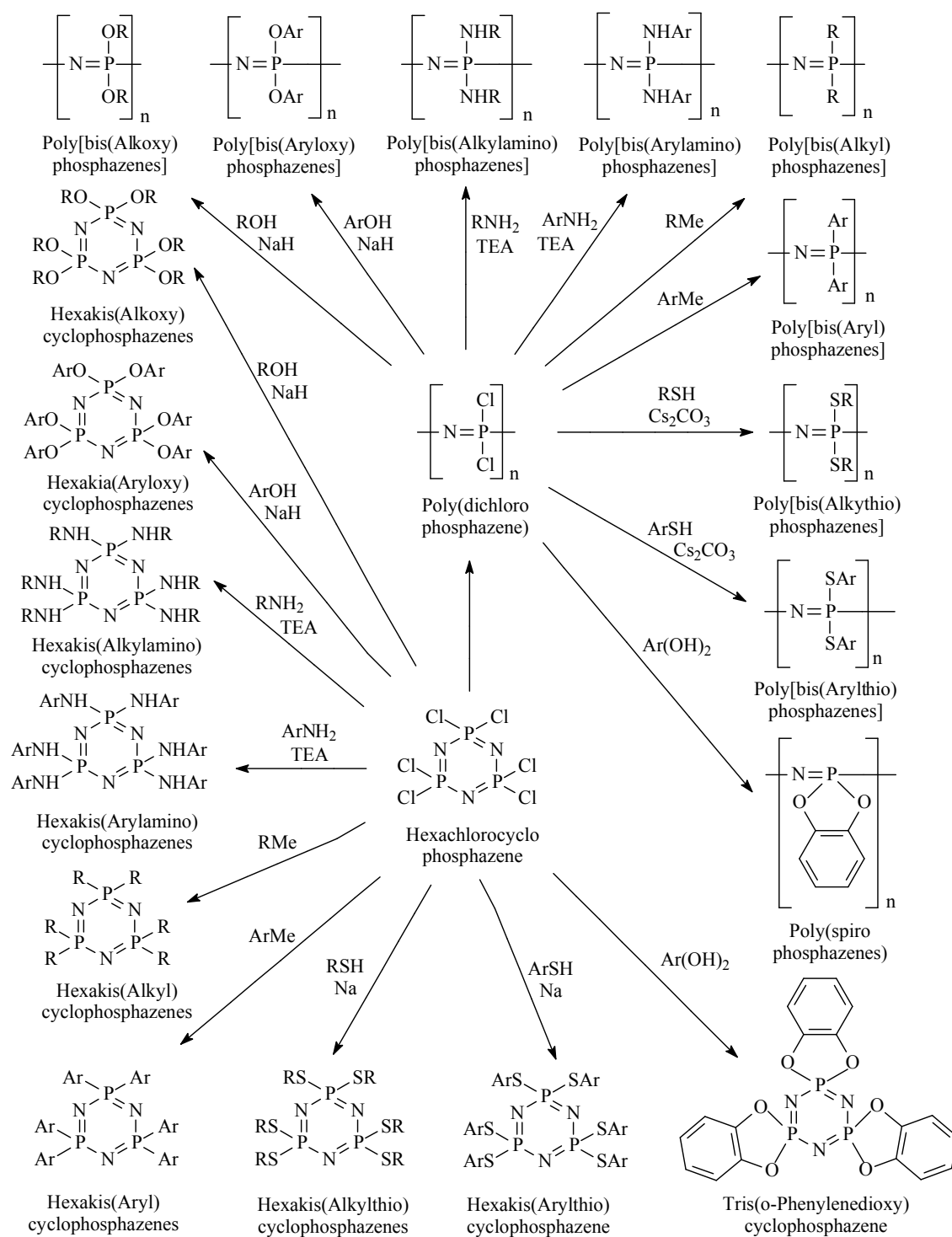


Figure 6. General synthesis of cyclo(organo)- and poly(organo)-phosphazenes.

The general structure of this last class of materials is reported in Figure 7 below:

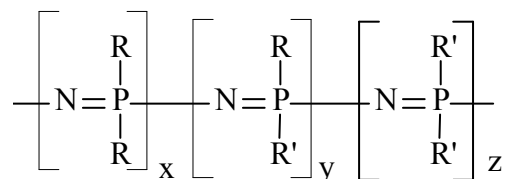


Figure 7. General Structure of *substituent* phosphazene copolymers

in which both homo-substituted (*i.e.* with R or R') and hetero-substituted (*i.e.* R and R') phosphazene repeat units are present on the same polyphosphazene skeleton.

These phosphazene copolymers are extremely attractive materials because their properties can be varied very easily and in a predictable way by changing the type and the relative percentage of the substituent groups to be reacted with polydichlorophosphazene, thus opening for these materials very valuable applicative domains, *e.g.* water solubility²⁷, low temperature elastomericity^{19,28}, photochemical activity²⁹, catalytic activity^{30,31}, etc.

This very attractive feature of phosphazene materials, *i.e.* multifunctionality⁴, could be equally extended to cyclophosphazenes. In fact, as reported in Figure 4, these phosphazene oligomers bear six or eight substituent groups in their chemical structure that can be heterogeneously substituted with different nucleophiles, giving rise to products showing a very interesting series of applicative features, for instance as water-soluble photoinitiators³², hydraulic fluids and lubricants³³⁻³⁵, cyclophosphazenes bearing biologically-important substituent groups^{36,37}, anticancers^{38,39}, etc.

2.3. Functionalization of phosphazenes

Functionalization of both cyclo- and polyphosphazenes can lead to the preparation of a variety of derivatives not readily accessible from direct substitutional processes on chlorophosphazenes.

A general representation of the reaction sequences usually exploited for functionalizing phosphazenes is reported in Figure 8.

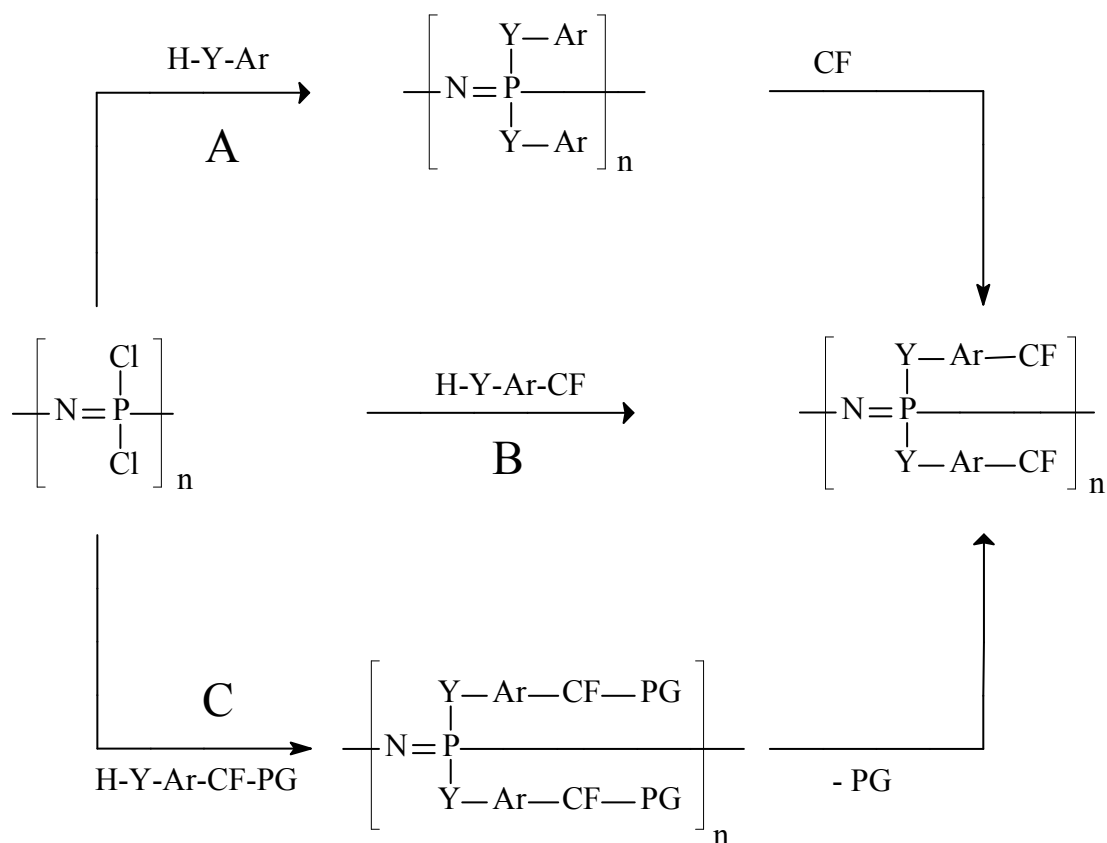


Figure 8. General scheme for the functionalization reactions of poly(organophosphazenes). Note that Y= -O- or -NH-; Ar = Aromatic ring; CF = Chemical Function; PG = Protective Group

Process “A” in Figure 8 represents the usual way of preparing phosphazene polymers by reaction of PDClP with suitable nucleophiles (H-Y-Ar) to obtain a substituted material, which undergoes successively a functionalization reaction according to classical organic chemistry^{40,41} to produce the functionalized polyphosphazene that contains a selected chemical functionality (“CF”). Several different polymers have been prepared according to this method, such as polyphosphazenes functionalized with sulfonic groups⁴²⁻⁴⁹, and nitro groups⁵⁰. In this context, this functionalization process is similar to that usually exploited in the functionalization processes of organic polymers⁵¹.

In the Process “B” is described an alternative method for preparing directly functionalized poly(organophosphazenes) which is peculiar of this class of materials. This process consists in the reaction between polydichlorophosphazene with bi-functional nucleophiles that possess only one chemical function having nucleophilic character, the second one being totally inert against the substitutional process. In this

way it could be possible to prepare a variety of functionalized phosphazene macromolecules by direct insertion of the desired chemical groups into the polyphosphazene substrate.

Examples of phosphazene macromolecules prepared according to this synthetic procedure could be poly[bis(4-formylphenoxy)phosphazene]⁵², poly[bis(4-nitrophenoxy)phosphazene]⁵², poly[bis(methoxy-ethoxy-ethoxy)phosphazene] (MEEP)^{53,54}, poly[bis(methyl-⁵⁵⁻⁶¹, ethyl-^{56,57,59,61-63}, *iso*-propyl-^{57,61,64-71}, *tert*-butyl-⁵⁷, and *sec*-butyl-^{56,57,59,61,72} phenoxy)phosphazenes], and phosphazene copolymers containing a variable percentage of 4-cyanophenoxy-⁷³⁻⁷⁷ or 4-(-2-oxazoline)phenoxy-⁷⁸⁻⁸¹ substituents, etc.

When in the reaction with PDCP are used bifunctional nucleophiles with both functions having nucleophilic character (Path “C” in Figure 8), the usual strategy selected to obtain phosphazene macromolecules is to block one of them with a suitable protective group. This monofunctional substituent is then reacted with PDCP and the second reactive functionality is subsequently deprotected to prepare the functionalized polyphosphazene. This is the case of polyphosphazenes substituted with 4-methoxyphenol (an -OH group protected by the CH₃ residue)⁸², and *n*-propyl-4-hydroxybenzoate (in which a -COOH group is protected by the *n*-propyl ester group)⁸³.

What is really important to stress in the above described functionalization processes is that the functional groups introduced into the polyphosphazenes can be easily modified according to classical organic chemistry reactions, and that during these additional modifications the phosphazene skeleton usually undergoes only minor modification, *i.e.* degradation or crosslinking phenomena²⁰.

In Figure 9 below, a general scheme is reported of several functionalization processes that have been carried out over time on functional groups present on the aromatic rings of the phenoxy substituents of suitable functionalized phosphazene macromolecules.

The conclusive remarks that can be drawn from the above reported statements on the synthesis, copolymerization and functionalization processes carried out on poly(organophosphazene) substrates are that a very high number of different phosphazene macromolecules can be prepared by carefully changing, mixing (even at different relative percentages) and chemically modifying the substituent groups attached to the skeletal phosphorus of the -P=N- chain.

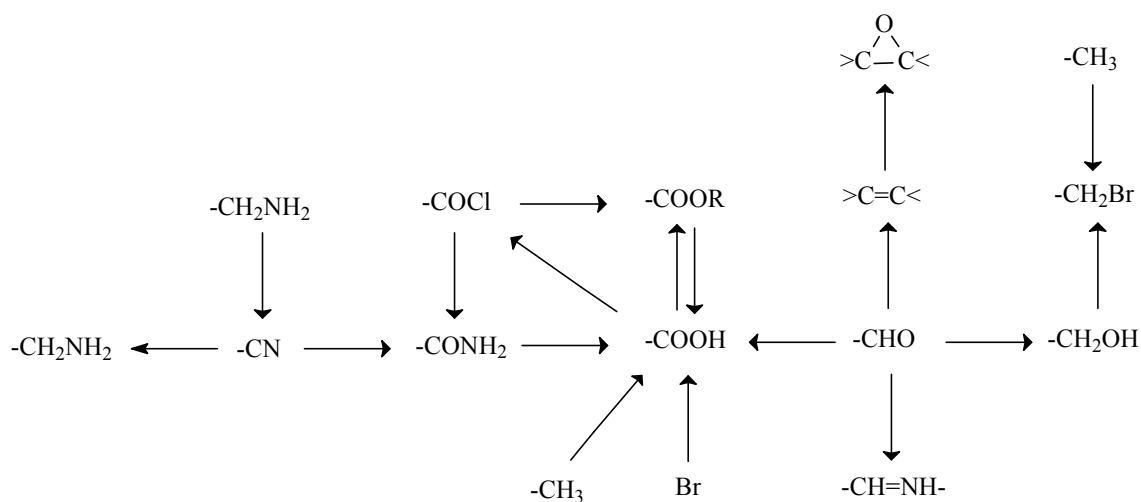


Figure 9. General scheme of the functionalization reactions carried out on poly(phenoxy)phosphazenes.

Up to now, more than 700 different polyphosphazenes have been synthesized and characterized⁸⁴, covering the following potential practical applications: polymers with an unusual low temperature flexibility⁸⁵⁻⁸⁷, high thermal stability^{88,89}, flame resistance⁹⁰⁻⁹⁹, high oxygen-index values^{4,91,96-98}, low smoke evolution properties¹⁰⁰, chemical stability against strong acids, bases and chemical aggressives¹⁰¹, potential applications in biomedicine¹⁰²⁻¹⁰⁵, photochemistry¹⁰⁶⁻¹¹⁰, resist technology¹¹¹⁻¹¹⁸, organometallic and coordination chemistry^{30,31,119-122}, membranes^{123,124}, liquid crystals¹²⁵⁻¹³¹, nonlinear optics^{129,132-134}, photochromism^{135,136}, catalysis^{30,31,137-139}, electric conductivity^{53,54,140-161}, hybrid materials¹⁶²⁻¹⁷², silicon-containing substrates¹⁷³⁻¹⁸², ceramics^{183,184}, piezoelectricity^{185,186}, electrochromism¹⁸⁷, etc.

Similarly in the case of cyclophosphazenes, the number of compounds presently prepared and characterized is above 5000 (in this number a series of linear phosphazene oligomers is included)¹⁸⁸, that have been exploited as follows: as biologically active materials due to their antitumor^{38,39,189-201}, insect chemosterilant^{195,202,203}, pesticide²⁰⁴, and fertilizer^{195,203,205-209} activity, potential applicability as flame retardant additives^{98,99,195} (for cellulose materials, synthetic fibers, textiles, polyurethanes and several different commercial organic macromolecules) with a considerably high Limiting Oxygen Index (LOI)^{4,98,99}, clathrates²¹⁰⁻²¹⁶ and high temperature resistant fluids³³⁻³⁵. Recently, they have also been found to be excellent phase transfer catalysts as polypodants^{139,217-221}, or cryptands²²²⁻²²⁵, and showed activity as good photoinitiators

for radical polymerizations^{4,109,226-228}, photostabilizers^{4,109,229-235}, antioxidants^{236,237} for organic commercial polymers (e.g. polystyrene or polyolefins), and as substrates able to form dendrimers²³⁸⁻²⁴².

2.4. Previous surface studies on phosphazenes

In spite of such a great number of practical applications already explored, the utilization of POPs for surface modification can be considered an underserved area. Looking through literature, in fact, it can be realized that surface issues in phosphazene chemistry have been faced over time according to two main strategies:

- 1) modification of the surface of solid poly(organophosphazene) films through a variety of experimental techniques, and
- 2) modification of the surface of conventional, carbon-backed macromolecules by exploiting polyphosphazene derivatives.

As far as the first point is concerned, the surface modification of polyphosphazene films has been obtained in the past by UV⁶⁷ irradiation of films of poly[bis(4-isopropylphenoxy)phosphazene]

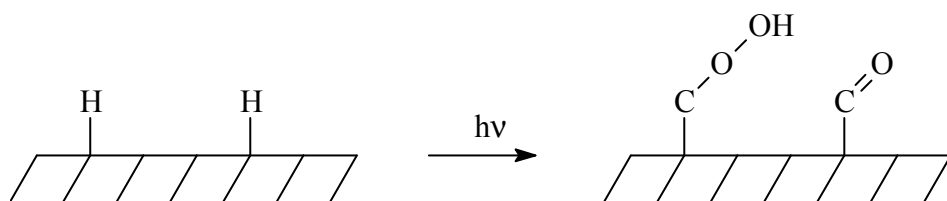


Figure 10. Photochemically-induced surface modification of poly[bis(4-isopropylphenoxy)phosphazene] films.

to form surface hydroperoxides and carbonyl groups; by laser surface treatment²⁴³, that induced extensive damage in films of poly[phenylamino]phosphazene, poly[bis(piperidino)phosphazene], and PDGP deposited on silica; and plasma treatment²⁴⁴ that brought about branching/crosslinking and oxidation phenomena with skeletal rearrangements of a series of phosphazene macromolecules and formation of structures reported below:

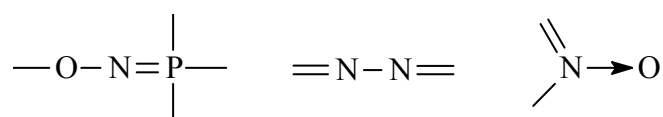


Figure 11. General modifications introduced in POPs by plasma treatments.

Nitration reactions⁵⁰ of poly[bis(phenoxy)phosphazene] to graft onto the surface of this polymer variable types of enzymes have been also explored, as reported in Figure 12,

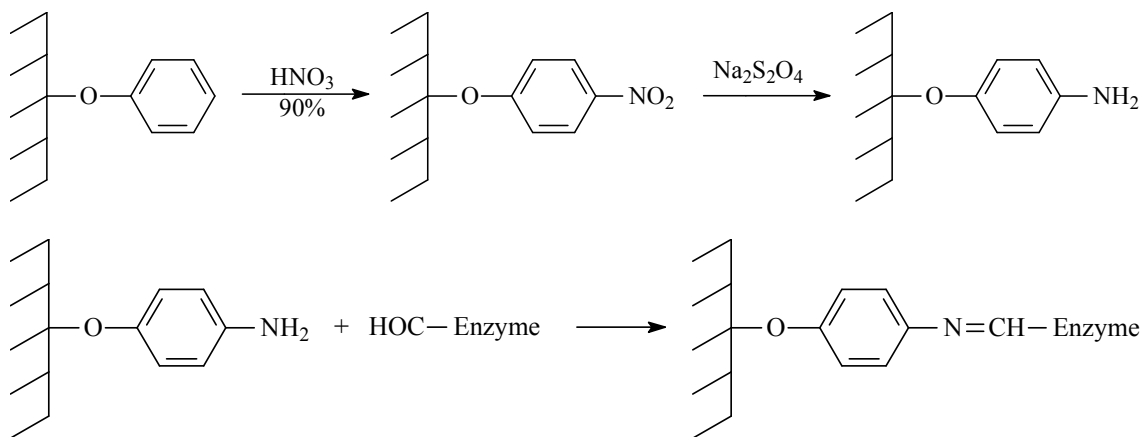


Figure 12. Nitration of poly[bis(phenoxy)phosphazene] and subsequent grafting of enzymes.

as well as sulfonation⁴⁵ processes of aryloxy-substituted poly(organophosphazenes) with different sulfonating agents, such as SO_3 , H_2SO_4 , SOCl_2 , etc. according to Figure 13.

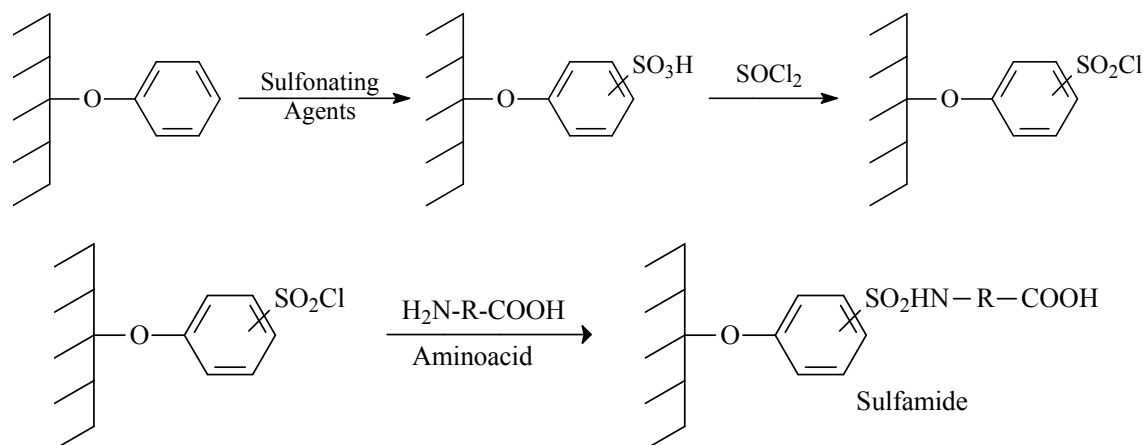


Figure 13. Sulfonation of poly[bis(phenoxy)phosphazene] and subsequent grafting of aminoacids.

Bromomethylation of poly[bis(4-methylphenoxy)phosphazene] to graft heparin residues for biomedical applications²⁴⁵ is also an useful approach to modify surface properties of phosphazene materials, as it can be seen in Figure 14.

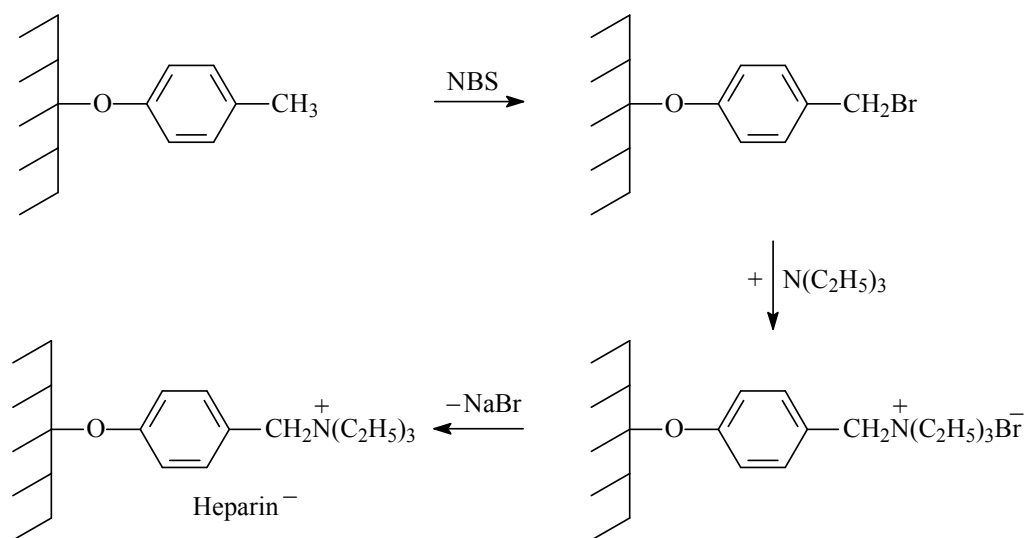


Figure 14. Surface modification of poly[bis(4-methylphenoxy)phosphazene] with heparin.

Oxidation^{246,247} reactions of 4-methylphenoxy substituents in the same polymer as above or hydrolysis reactions of propyl-4-carboxylatephenoxy moieties²⁴⁷ in poly[bis(4-carboxylatephenoxy propylester)phosphazene] to form surfaces functionalized with free carboxylic groups are also useful reactions to obtain surface modification in films of aryloxy-substituted POPs, as described in Figure 15.

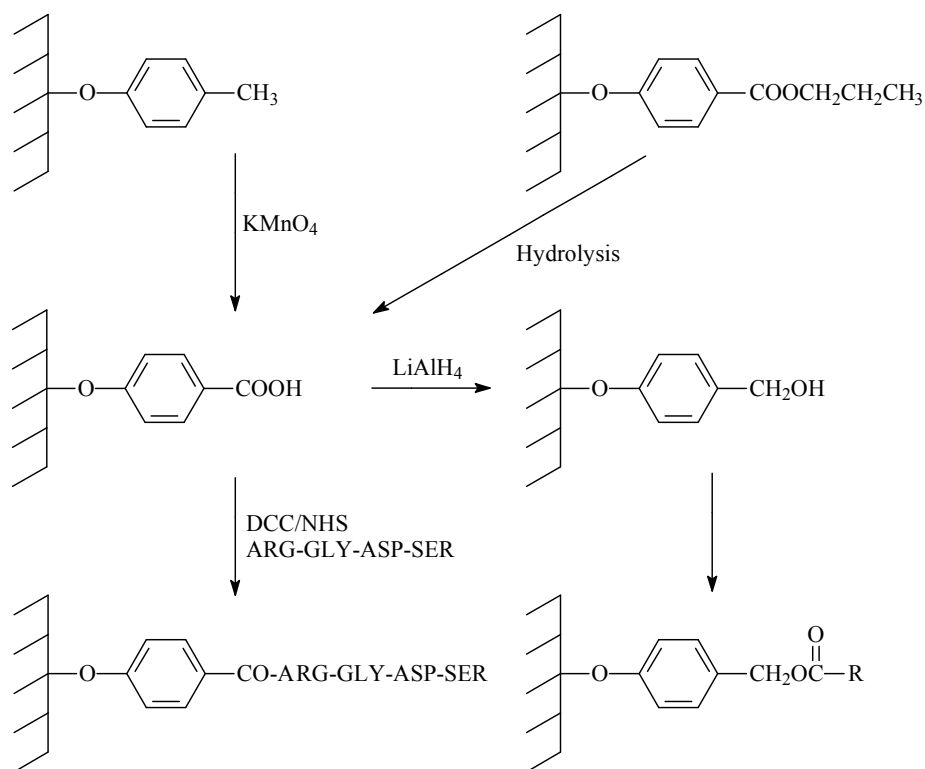


Figure 15. Surface preparation and modification of POPs functionalized with carboxylic groups.

Surface hydrosilylation processes²⁴⁸ of allyl group-containing polyphosphazenes have been also attempted to graft silyl derivatives in unsaturated polyphosphazenes (see Figure 16).

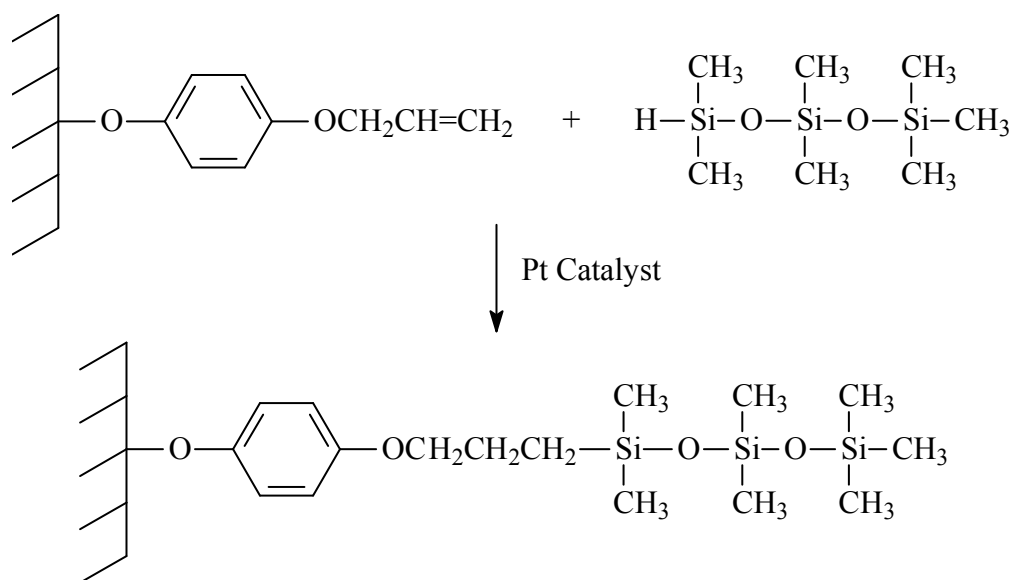


Figure 16. Surface hydrosilylation reaction of allyl group-containing POPs.

Another very useful synthetic strategy to modify the surface features of poly(organophosphazenes) is based on the utilization of metathetical exchange of trifluoroalkoxy substituents in poly[bis(trifluoroethoxy)phosphazene] with diethylenglycol monomethylether^{249,250}, different fluorine-containing alkoxides, or with other alkoxides containing OH²⁵², NH₂²⁵²⁻²⁵⁵, CN²⁵² functions or hydroxylic groups²⁵⁶ according to the general scheme reported in Figure 17.

Metal complexes or clusters have been supported on the surface of polyphosphazenes through metallation reactions^{30,257-259} carried out on polyphosphazene films, mostly for catalytic purposes, giving rise to polymers having the structures described in Figure 18.

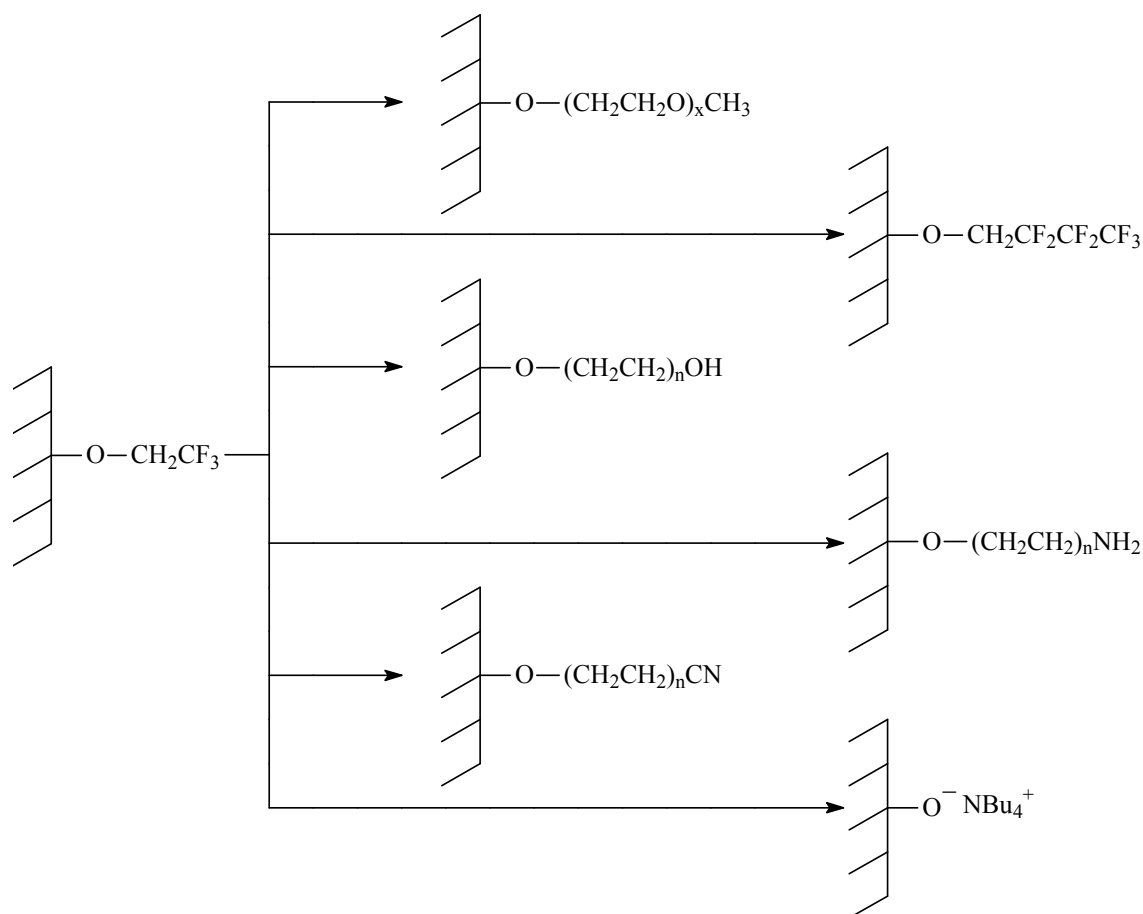


Figure 17. Surface modification of POPs containing trifluoroethoxy moieties.

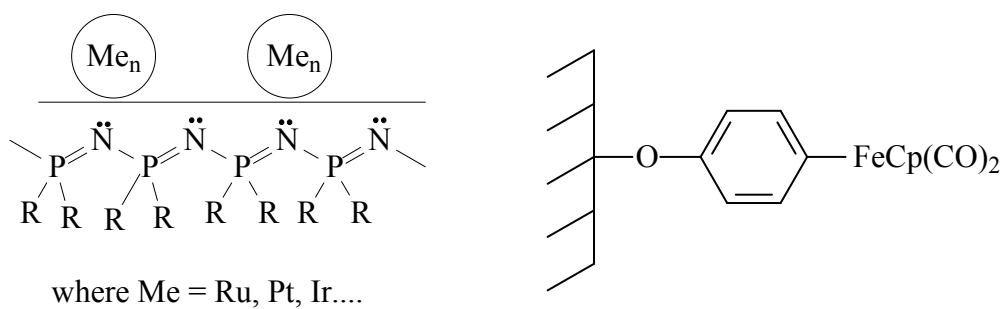


Figure 18. Metallation reactions on POPs.

Eventually, thermally-, photochemically- and/or γ -radiolytically-induced grafting reactions of organic conventional macromolecules onto the surface of polyphosphazene films^{56,71} have been deeply investigated according to the processes reported in Figure 19, to change surface polarity and wettability of phosphazene materials.

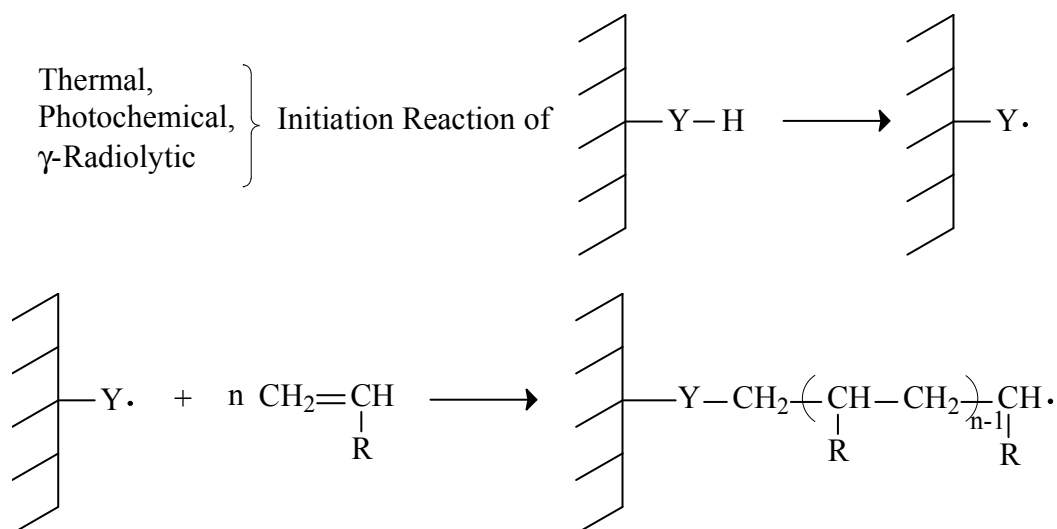


Figure 19. Grafting reactions on POPs.

On the other side, surface modification of conventional organic polymeric materials using poly(organophosphazenes) has been achieved basically by two different synthetic approaches, *i.e.* surface coating^{260,261} and surface grafting reactions of different phosphazene macromolecules on poly(ethylene)²⁶², poly(propylene)²⁶³, poly(vinyl chloride)²⁶³, poly(ethylene terephthalate)²⁶³, poly(bisphenol A carbonate)²⁶³, poly(methylmethacrylates)²⁶³, poly(vinyl alcohol)²⁶⁴⁻²⁶⁶, poly(ethylene-*co*-vinyl alcohol)²⁶⁶, using a variety of chemical reactions. The general method has been summarized in Figure 20, and consists first of coating the surface of organic macromolecules with polyphosphazenes using a variety of chemical reactions, followed by crosslinking of the inorganic coating, which eventually yields the surface modification of the organic film.

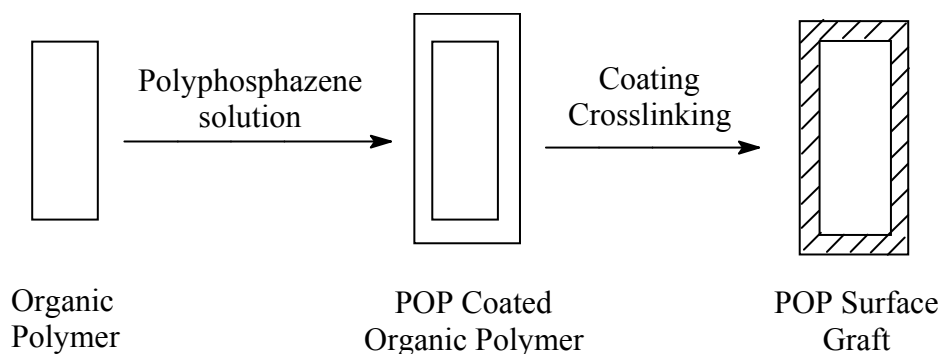


Figure 20. Organic polymer surface coatings with POPs.

An alternative method to modify the surface of organic substrates is based on the grafting of polydichlorophosphazene onto carbon black, followed by substitution of the residual chlorines present in this polymer with alkoxy, aryloxy, or amino groups²⁶⁷. The overall reaction sequence is reported in Figure 21.

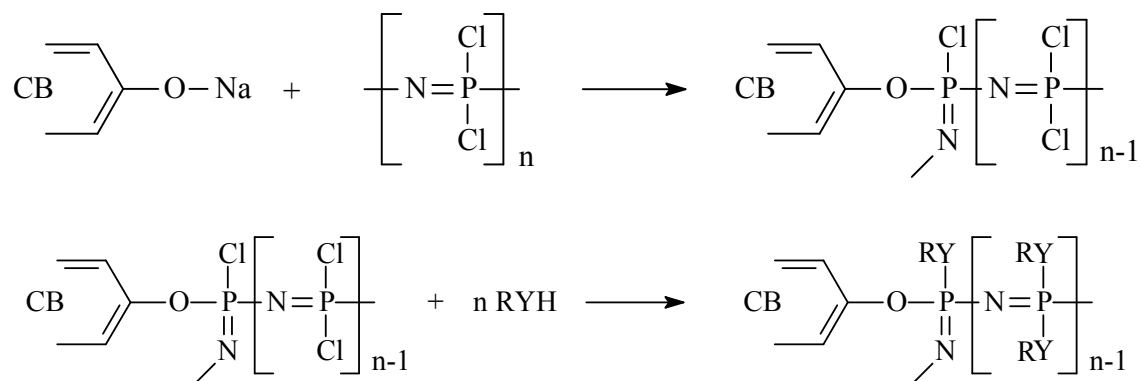


Figure 21. Phosphazene grafting on the surface of carbon black. Y may be --O-- or --NH-- , and R may be an aromatic or aliphatic residue.

All these functionalization reactions brought about the modification of the surface properties of different polymeric materials, both organic and inorganic in nature, thus widening the opportunities for their practical utilization in a significant way.

As a consequence of these previous studies, a few years ago we started a long-range research project in this area aimed to design general strategies to reach the surface functionalization of solid materials using cyclic and polymeric phosphazene derivatives as coupling agents^{6,7}. Preliminary work in this area has been carried out a few years ago by Grunze²⁶⁸⁻²⁷⁴ who succeeded in grafting PDCP onto oxidized human tissues, successively reacting the residual chlorines with trifluoroethoxy groups.

CHAPTER 3

EXPERIMENTAL SECTION

3.1. MATERIALS AND INSTRUMENTATION

3.1.1. Solvents

Tetrahydrofuran (THF), diethyl ether, chloroform, dichloromethane, methanol, ethanol, toluene, chlorobenzene, *n*-hexane and acetone were analytical grade Carlo Erba solvents. Benzene, chlorobenzene and trichlorobenzene were Aldrich products. Anhydrous acetone was purchased from Acros, while acetonitrile and orthodichlorobenzene were LAB-SCAN and Riedel de Haen solvents, respectively. When specified, solvents were dried according to classical methods^{40,275}, otherwise they were used as received.

3.1.2. Reagents

Hexachlorocyclophosphazene, $N_3P_3Cl_6$, HCCP, (95-98%) was purchased from Shin Nissho Kako, and purified by vacuum sublimation at 45-50°C, followed by repeated crystallizations from *n*-hexane¹.

Polydichlorophosphazene (PDCP) was prepared by thermally-induced polycondensation reaction of dichlorophosphinoyliminotrichlorophosphorane, $Cl_3PNP(O)Cl_2$, at 290°C, according to literature²⁷⁶⁻²⁷⁸. This polymer with an intrinsic viscosity of 44 ml/g was stored as a 37% w/w solution in 1,2,4-trichlorobenzene. It was also stabilized with 1% w/w $SOCl_2$ ²⁷⁹.

Sodium hydride 60% dispersion in mineral oil, tetraethylammonium bromide (TEAB), tetrabutylammonium bromide (TBAB), 2,2'-dihydroxybiphenyl, 4-hydroxybenzaldehyde, lithium borohydride, phosphorus tribromide, iodopentafluorobenzene, 4-nitrophenol, cesium carbonate, thionyl chloride, 4-cyanophenol (4CNP), polyethylenglycole monomethyl ether with average weight 750 dalton (PEG-750-ME), 2,2,3,3-tetrafluoropropanol (TFP), 4-phenylazophenol (AzB), 3-aminopropyltriethoxysilane (APTES), tetraethylorthosilicate (TEOS), 2,2,2-trifluoroethanol (TFE), 2,2,3,3,4,4,5,5,6,6,7,7,8,8,9,9,9-heptafluorononanol (HDFN), potassium carbonate, calcium hydride, benzophenone, sodium in mineral oil, 4,4'-dipyridyl (DPy) and 1,2-di(4-pyridyl)ethylene (DPE) were purchased from Aldrich.

PEG-750-ME was first dried by dissolution in toluene and reflux on a Marcusson apparatus, followed by evaporation of the solvent under reduced pressure. The compound was further dried under vacuum at 60°C for 16 hours and stored under nitrogen.

Methyl-4-hydroxybenzoate, R-(-)-1-amino-2-propanol, S-(+)-1-amino-2-propanol and the corresponding racemic derivative (\pm)-1-amino-2-propanol were Fluka products; 2-aminoethanol was Janssen. All these products were used as received.

Triethylamine (TEA), Sodium sulfate, 37% hydrochloric acid and triethylamine (TEA) were purchased from Carlo Erba. TEA was dried by refluxing under CaO ²⁷⁵.

All reagents were utilized as received unless where otherwise specified.

3.1.3. Other Materials

Crystalline Silicon wafers (100) used for surface functionalization with APTES-substituted cyclophosphazenes (Chapter 4.4) were purchased from Jocam s.r.l. (Milan) with the following features: crystal orientation (100), *p*-type by doping with boron, 20 Ω cm resistivity, thickness 440 μm . These crystals have been cut in squares of 1x1 cm before using.

Silicon wafers used for phosphazene deposition by GDS technique (Chapter 4.2) were purchased from Atomergic Chemetals Inc. with the following features: crystal orientation (100), *p*-type by doping with boron, thickness 350 μm . These crystals have been cut in squares of 1x1 cm before using.

Silica gel 60 (diameter 0.063-0.2 mm) was purchased from Fluka, and was previously activated with HCl according to the procedure described in section 3.5.3.¹²⁸⁰

Electrically fused quartz HSQ-300 type II was purchased from Heraeus Tenevo as 1 mm thick slides. It was cut into 6x6 mm squares, and was previously cleaned in an ethanol ultrasonic bath for 15 min. Sample surfaces were activated as described in section 3.2.2.1 before use.

High density polyethylene (HDPE) and polyamide-6 (PA6) were purchased from Goodfellow as 0.5 mm thick films, with a density of 0.95 g/cm^3 for HDPE and 1.13 g/cm^3 for PA6.

Poly(ethylene-*co*-vinyl alcohol) random copolymer (Soarnol-A, EVOH) has been purchased from Nippon Gohsei, and has an ethylene molar concentration of 44%, a density of 1.14 g/cm^3 , and a weight fraction crystallinity of 0.60 as assessed from

melting enthalpy. The material was melt-cast into films about 200 μm thick from a T-die extruder at 210°C.

All HDPE, PA6 and EVOH samples were cut in squares or rectangles with dimensions ranging from 1x1 cm to 2.5x3.5 cm, depending on characterization needs, and cleaned by sonication in ethanol bath for 18 minutes. The samples were then dried overnight in an oven at 60°C (HDPE, PA6) or 110°C (EVOH) before use. EVOH samples were utilized for functionalization reactions immediately after extraction from the oven.

3.1.4. Equipment for characterization

Transmission FTIR. Analyses were performed on a Nicolet Avatar 320 FTIR spectrometer. Compounds were characterized by transmission FTIR on a KBr pellet, while deposited sol-gel films and phosphazenic films obtained by GDS technique on Si(100) were characterized by transmission FTIR directly on the samples, using clean untreated Si(100) to collect background spectrum.

Attenuated Total Reflection FTIR (FTIR-ATR). Infrared absorption spectra of surface functionalized polymeric substrates (Chapter 4.3) were collected on a Perkin Elmer Spectrum One spectrometer, equipped for measurements in Attenuated Total Reflection (ATR) conditions on a diamond crystal. Subtraction of the spectrum of virgin samples from the spectra of functionalized samples was always performed.

Solution NMR. Multinuclear NMR characterizations were performed with a Bruker Avance-400 spectrometer operating at 400.13 MHz for ^1H , 100.62 MHz for ^{13}C and 161.98 MHz for ^{31}P . All NMR measurements were performed at T 298 K in CDCl_3 , which was used as received. ^1H and ^{13}C chemical shifts were referenced to internal tetramethylsilane (TMS). ^{31}P chemical shifts were referenced to external 85% aqueous H_3PO_4 .

Solid State NMR. Solid state NMR characterization was performed on a Bruker AC200 spectrometer equipped for solid state analysis. Samples were spun at 3000 Hz in 7 mm diameter zirconia rotors with Kel-F caps. ^{13}C CP MAS NMR spectra were obtained at 50.26 MHz, using the standard Bruker cross polarization pulse sequence, with 3 ms contact time and 5 s Relaxing Delay, recording the free induction decay over a sweep width of 13 kHz, with an acquisition time of 0.09 s, and processed with a 10 Hz exponential line broadening. The 39.71 MHz ^{29}Si CP MAS NMR spectra were

performed using the standard Bruker cross polarization pulse sequence, with a 5 ms contact time, 10 s relaxing delay, sweep width 5.5 kHz, acquisition time 0.1 s, and processed with 10 Hz exponential line broadening. Solid state ^{31}P NMR spectra were obtained at 80.90 MHz using single pulse experiment (SPE) and high power proton decoupling, with a 10 s Relaxing Delay, sweep width 14 kHz, acquisition time 0.078 s. ^{13}C and ^{29}Si chemical shifts were externally referenced to solid sodium 3-(trimethylsilyl)-1-propane sulfonate at 0 ppm. ^{31}P chemical shifts were externally calibrated with respect to solid triphenylphosphine at -7.2 ppm²⁸¹, and were referenced to 85% H_3PO_4 . ^{13}C and ^{29}Si cross polarization experiments were optimized using adamantane and sodium 3-(trimethylsilyl)-1-propan sulfonate, respectively. Magic angle conditions were adjusted by observing ^{79}Br spinning side bands pattern in a rotor containing 5% of KBr ²⁸².

X-ray Photoelectron Spectroscopy (XPS). Analyses of surface functionalized fused quartz slides (Chapter 4.1) were performed on a PHI-5500 - Physical Electronics spectrometer, equipped with a monochromatized source with aluminum anode ($\text{K}\alpha = 1486.6 \text{ eV}$), operating at 200 W applied power, 5.85 eV pass-energy, 0.05 eV energy-step. During the experiments the vacuum level was around 10^{-9} Torr residual pressure. The spectrometer was calibrated assuming $\text{Ag}(3\text{d}_{5/2})$ binding energy (BE) at 368.3 eV with respect to the Fermi-level and the measured full width at half maximum (FWHM) is 0.46 eV. In order to neutralize the surface electrostatic charge of the non-conductive samples, an electron gun was used. Furthermore, the charging effect on the analysis was also corrected considering the $\text{Si}(2\text{p}_{3/2})$ peak at $\text{BE} = 103.6 \text{ eV}$, characteristic of SiO_2 , as internal reference²⁸³.

Analyses of phosphazenic films deposited by Glow Discharge-induced Sublimation on silicon wafers (Chapter 4.2) were performed on a Perkin-Elmer Φ 5600 ci spectrometer using monochromatized $\text{Al-K}\alpha$ radiation ($h\nu = 1486.6 \text{ eV}$), with a working pressure in the 10^{-8} Pa range. The binding energies are calibrated against the value of the C_{1s} hydrocarbon component centered at 285.0 eV.

XPS analyses of surface-modified polymeric substrates (Chapter 4.3) were performed using the ESCALAB 220XL spectrometer. The $\text{Mg}_{\text{K}\alpha}$ line (1253.6 eV) was used for excitation with a 300W applied power. The spectrometer was operated in a constant pass energy mode ($E_{\text{pass}} = 40 \text{ eV}$) for high-resolution spectra recording. Binding energies were referenced to the C_{1s} core level energy at the hydrocarbon

species. During the experiment the vacuum level was less than 10^{-7} Pa. The sample film was stucked on the sample holder using a double-face conducting adhesive tape. Experimental quantification and spectral simulation were obtained using the Eclipse software provided by VG Scientific.

XPS spectra were collected at a take-off angle of 45 deg, analyzing the surfaces in different points (analysis area is around 0.5 mm^2). Experimental quantification and spectral line decomposition were obtained using the softwares PC-ACCESS provided by Physical Electronics (Chapter 4.1) and XPS Peak 4.1 (Chapter 4.3). The quantitative analysis data were reported as atomic percentage of elements.

Contact angle and surface energy measurements. Measurements were carried out with a GBX Digidrop instrument at a controlled substrate temperature of 37°C and using solvent droplets of $5 \mu\text{l}$. The reported data are the average of 5 measurements taken in different locations of the surfaces. Surface energy calculations were performed by the Windrop++ software with the aid of the Owens-Wendt model using contact angle values with water, formamide and diiodomethane.

X-ray single crystal diffraction. Analyses were performed on a Bruker SMART 1000 CCD diffractometer, equipped with an OXFORD low temperature device, using Mo $K\alpha$ radiation ($\lambda = 0.71703 \text{ \AA}$) and collecting data at a temperature of 193 K. Data collection and reduction were performed using the SMART and SAINT programs²⁸⁴; an empirical absorption correction was applied using the SAD-ABS program²⁸⁵; the structures were solved by using SIR2002²⁸⁶ and refined by full-matrix least-squares on F^2 using SHELXL-97²⁸⁷.

Optical activity measurements. The measurements of the specific optical activity of both chiral cyclophosphazenes and intermediates were carried out at room temperature using a Perkin Elmer mod. M141 polarimeter, according to the following procedure: chiral products were dissolved in a suitable solvent (tetrahydrofuran or methanol) at a concentration of about $C = 0.60 \text{ g per 100 ml of solvent}$, transferred in a quartz cell having the standard length of 10 cm and about 1.5 ml capacity, and their rotatory power measured against the pure solvent at variable wavelengths (589, 578, 546, 436 and 365 nm). An angle of experimental deviation “ α ” was first measured, which was then transformed into specific rotatory power $[\alpha]$ for the selected wavelengths according to the following equation:

$$[\alpha] = \frac{\alpha_{\text{measured}} \bullet 100}{b \bullet c}$$

where:

“b” is the cell length in decimeter (in our case this value is 1);

“c” is the concentration of the product in g/100 ml;

“ α_{measured} ” is the rotation angle observed experimentally.

3.2. EXPERIMENTAL PROCEDURES FOR SURFACE FUNCTIONALIZATION OF SODALIME GLASSES AND CRYSTALLINE SILICON (100) WAFERS WITH CHLOROPHOSPHAZENES: A THEORETICAL AND EXPERIMENTAL APPROACH (CHAPTER 4.1)

3.2.1. Theoretical calculations

Ab initio calculations have been carried out within the Car-Parrinello approach²⁸⁸ in the framework of the Density Functional Theory, using gradient corrections in the BLYP implementation^{289,290}. Gradient-corrected functionals have been adopted in the most recent theoretical studies of adsorption of molecules on Si(100) because they are typically more accurate than the local density functional in describing chemical processes on the Si(100) surface²⁹¹⁻²⁹³. The calculations have been carried out by taking into account spin polarization, considering the Γ -point only of the Brillouin zone, and using norm-conserving pseudopotentials²⁹⁴. Wavefunctions were expanded in plane waves with an energy cutoff of 70 Ry. It was explicitly checked that, at this value of the energy cutoff, the structural and binding properties of the system are well converged.

The OH-terminated Si(100) surface is modeled by assuming a complete saturation of the surface Si dimers by hydroxyl groups (our *ab initio* calculations indicate that the reaction of a water molecule with the surface Si(100) dimers is facile, being characterized by a small energy barrier of 4 kcal/mol), and considering a periodically repeated slab made of 5 Si layers and a vacuum region of 13 Å: such a relatively large value is required in order to make the interactions between the system and its periodic images along the *z* axis negligible.

A monolayer of hydrogen atoms is used to saturate the dangling bonds on the lower surface of the slab. A supercell was used with $p(\sqrt{8} \times \sqrt{8})R 45^\circ$ surface periodicity, corresponding to 8 Si atoms/layer. On top of this substrate a single HCCP molecule is

located in different initial configurations and the structure of the whole system is then fully optimized. Structural relaxations of the ionic coordinates have been performed using the method of direct inversion in the iterative subspace²⁹⁵. During the ionic relaxations the lowest Si layer and the saturation hydrogens were kept fixed. The estimates of the energy barrier characterizing different reaction paths have been obtained using a recently proposed variant of the popular “Nudged Elastic Band” method, *i.e.* the “Climbing Image Nudged Elastic Band” (CI-NEB) method²⁹⁶⁻²⁹⁸, which has proven to be a very efficient technique to determine minimum energy paths in complex chemical reactions.

3.2.2. Experimental approach

All manipulations were performed by keeping the fused quartz samples standing on a teflon sample holder, with the exception of the “droplet deposition” procedure (see 3.2.2.3). Treatments were always carried out under nitrogen atmosphere, except for the surface activation (see 3.2.2.1) and the “droplet deposition” procedure.

The typical functionalization experiment consisted of the following steps:

1. Surface activation with hydrochloric acid
2. Pre-essiccation of the samples under vacuum, at a selected temperature for one hour (optional)
3. Reaction with HCCP solution in THF, by “immersion” or “droplet deposition” technique (see below)
4. Sample washing with THF
5. Final essiccation of the samples, performed in the air or under vacuum, at a selected temperature and for a selected time

Samples were stored under nitrogen, and analyses were always performed within few days from preparation. Table 4 (see 4.1.3) lists preparation conditions and procedures for all experiments.

3.2.2.1. Surface activation of fused quartz slides

The surface activation of fused quartz slides was performed according to an already reported procedure²⁸⁰. Samples were put standing on a teflon support inside a round bottomed flask equipped with a refrigerator connected to a KOH trap, and treated with

refluxing 37% HCl for 4 hours. They were subsequently extracted from solution, washed with abundant distilled water and finally dried in an oven at 50°C for 16 hours.

3.2.2.2. Grafting of HCCP by “immersion” procedure

Activated fused quartz samples were put standing on a teflon support inside a round bottomed flask, and they were in most cases kept under dynamic vacuum at a selected temperature for one hour. Then 20 ml of a 0.1M solution of HCCP in anhydrous THF were added *via* metal cannula, and the solution was kept at reflux temperature for the selected treatment duration before drawing out the samples from the mixture.

Subsequent washing of the samples was always performed with 20 ml of THF under vigorous stirring for 10 minutes, followed by the final essiccation under vacuum at a given temperature and for a given time.

3.2.2.3. Grafting of HCCP by “droplet deposition” procedure

This procedure consisted of simply letting one droplet of a 0.1M solution of HCCP in anhydrous THF onto the surface of an activated fused quartz sample. After ten minutes in the air at room temperature to allow solvent evaporation, a post-treatment essiccation in an oven at 50°C for 30 minutes was in some cases performed. Then the sample was washed with 20 ml of anhydrous THF under vigorous stirring for 10 minutes; the final drying was performed in the air at room temperature for 10 minutes, followed by further drying in an oven at 50°C for 30 minutes.

3.3. EXPERIMENTAL PROCEDURES FOR SILICON-BASED SURFACES FUNCTIONALIZATION USING THIN CHLOROPHOSHAZENE FILMS DEPOSITED BY GLOW-DISCHARGE INDUCED SUBLIMATION AS COUPLING AGENTS (CHAPTER 4.2)

3.3.1. Experimental apparatus

The experimental setup consisted of a vacuum chamber evacuated by a turbomolecular pump. The glow discharge was sustained by a 1-in. cylindrical magnetron sputtering source connected to a radio frequency power generator (600 W, 13.56 MHz) through a matching box. The glow discharge feed gas was Argon

(99.9999%), whose pressure inside the chamber was measured through a capacitance gauge.

In order to measure the deposition rate of the phosphazene-derived layer as a function of deposition time, the sample holder was replaced by a water-cooled quartz crystal microbalance (Maxtek Inc., model TM400, 0.375 ng/cm² mass resolution).

The plasma composition was monitored during deposition by means of a quadrupole mass analyzer (Hiden Analytical, model PSM001). The spectrometer was connected to the deposition chamber through an electrically grounded sampling orifice (100 μ m-diameter) and evacuated by a turbomolecular pump to a base pressure of 10⁻⁶ Pa. The sampled neutral and radical species (1 to 510 m/z range) from the plasma chamber were ionized by an electron beam emitted from a hot filament (70 eV energy) and detected by a secondary electron multiplier. With the hot filament off, only charged species were collected.

3.3.2. Activation of crystalline silicon substrates

Silicon substrates were in some cases subject to a preliminary surface activation treatment, consisting of a 2 minutes ion etching treatment performed immediately before phosphazene deposition. To this purpose, a mixture of 95%Ar - 5%O₂ was introduced into the deposition chamber and the glow discharge was ignited by RF biasing the substrate.

3.3.3. Deposition procedure

Crystalline HCCP powder (750 mg) was put on the surface of an aluminum target and then placed on the sputtering source. In order to avoid any sputtering of the aluminum target during the ion bombardment the deposition process was always stopped when the target was still completely covered by HCCP powder. Working pressure was 5.00 \pm 0.05 Pa. The RF power was set to 10 W and the target DC self-bias was in the range -100 to -300 V. The silicon substrates were mounted on a sample holder, whose distance from the target varied from 30 to 7 cm with the aim of obtaining uniform phosphazene deposits. Silicon substrates were used as received (AR samples) or after surface activation performed as described above (ACT samples).

Deposition time varied from 1 to 4 min, after which the samples were immediately stored under argon in a sealed vessel to avoid moisture contamination from the air.

3.3.4. Reaction in solution

Freshly deposited HCCP-derived films were reacted with an excess of two different nucleophiles, *i.e.* TFE or 4CNP, under nitrogen atmosphere. The typical experimental procedure is as follows: 10 mg of nucleophile were dissolved in a flask containing 25 ml of THF, the film was dipped into the solution and placed at the bottom of the flask. Sodium hydride (10 mg) was then added, and the mixture was left to react at room temperature for 1 hour: during this period the flask was manually shaken every 5 minutes. Before analysis, samples were rinsed with clean THF, in order to remove the excess of reactants from the film surface.

Two reference samples were prepared. Two clean silicon substrates were respectively treated with trifluoroethanol and cyanophenol solutions, employing the same above described reaction conditions (samples **blank-CF3** and **blank-CN**, respectively).

In order to verify the behaviour of deposited thin films towards THF washing, two samples, deposited with or without preliminary ion etching activation, were treated in anhydrous THF for 1 hour, (samples **ACT PN-washed** and **AR PN-washed**, respectively).

Exploited samples and their preparative history (substrate activation, phosphazene deposition, THF washing, reaction in solution) are summarized Table 1 (*section 4.2.1*).

3.4. EXPERIMENTAL PROCEDURES FOR SURFACE FUNCTIONALIZATION OF POLYMERIC SUBSTRATES USING CHLOROPHOSPHAZENES AS COUPLING AGENTS (CHAPTER 4.3)

Unless otherwise specified, all the treatments here reported were performed under nitrogen atmosphere using dry solvents.

The functionalization process consisted of three steps for HDPE and PA6, or two steps for EVOH: (1) plasma activation of the polymeric plate (HDPE and PA6 only), (2) Grafting of HCCP or PDCP, (3) Residual chlorine substitution with TFE, HDFN or AzB. All manipulations were performed under nitrogen atmosphere, with the only exception of plasma treatment and sample washing after substitution step 3.

3.4.1. Plasma activation of polymeric substrates

The typical plasma activation procedure was as follows. An HDPE or PA6 sample was put into the plasma reactor, and the pressure inside the chamber was brought down to 130 mTorr. Then the selected plasma gas was let inside with a controlled flux (0.30 dm³/min when Ar only was used; 0.26 dm³/min of Ar and 0.04 dm³/min of O₂ when the argon/oxygen mixture was employed) while keeping pumping going, and the system was allowed two minutes to reach a steady state. The microwave generator was turned on and its power was set at a specific value. The plasma treatment was carried on for the planned duration, and then the generator was turned off, the gas flux was interrupted and the chamber was finally brought back to atmospheric pressure by letting air inside. Treated samples were used for phosphazene grafting immediately after the plasma treatment.

Based upon the preliminary study reported in section 4.3.1, the standard conditions for functionalization experiments were set as follows: Ar only as a gas, generator power of 300 W, treatment duration of 3 minutes.

3.4.2. Grafting of chlorophosphazenes

Grafting of PDCP. Samples were immersed in 20 ml of a PDCP solution in anhydrous toluene (concentration = 0.110 g/ml), and kept at room temperature for 7.5 h. Then they were drawn out and washed with 20 ml of anhydrous THF under stirring for 10 minutes before utilization for the substitution step.

Grafting of HCCP. Samples were immersed in a solution of 0.35g (1.0 mmol) of HCCP and 0.9 ml (0.66 g, 6.5 mmol) of anhydrous TEA in 10 ml of anhydrous THF, and kept at 50°C for 24 h. Precipitation of a white solid was observed, and the solution turned brown. Then the samples were drawn out and washed with 20 ml of anhydrous THF under stirring for 10 minutes before being used in the substitution step.

3.4.3. Substitution of residual chlorines with nucleophiles

Substitution with TFE. Finely divided sodium (0.35 g, 15.2 mmol) was put into 10 ml of anhydrous THF, and 2 ml (2.75 g, 27.4 mmol) of TFE were cautiously added, causing hydrogen evolution. After consumption of all the sodium, PDCP- and HCCP-functionalized samples were dipped into the solution, which was stirred at room temperature for 16 h. PDCP-grafted samples were then washed with 10 ml of THF,

while 10 ml of chloroform were used in the case of HCCP-grafted plates. Final washings were the same for both kinds of samples, in sequence with 10 ml of THF, 10 ml of distilled water and finally with 10 ml of THF. The samples were dried in an oven at 50°C before characterization.

Substitution with HDFN. Finely divided sodium (0.09 g, 3.9 mmol) was put into 10 ml of anhydrous THF, and 2.25 g (5.0 mmol) of HDFN were cautiously added, causing hydrogen evolution. After 7h of stirring at room temperature, the remaining sodium was removed, 0.02 g (0.06 mmol) of tetrabutylammonium bromide were added. A phosphazene-functionalized sample was immersed in the solution, and the system was stirred at room temperature for 16 h. PDCP-grafted samples were then washed with 10 ml of THF, while 10 ml of chloroform were used in the case of HCCP-grafted plates. Final washings were the same for both kinds of samples, in sequence with 10 ml of THF, sonication for 30 minutes in a mixture of 15 ml of THF and 6 ml of distilled water, washing with 10 ml of distilled water and then with 10 ml of THF. Finally, all HDFN-functionalized samples were THF extracted for 8h in a Soxhlet and then dried in an oven at 50°C before characterization.

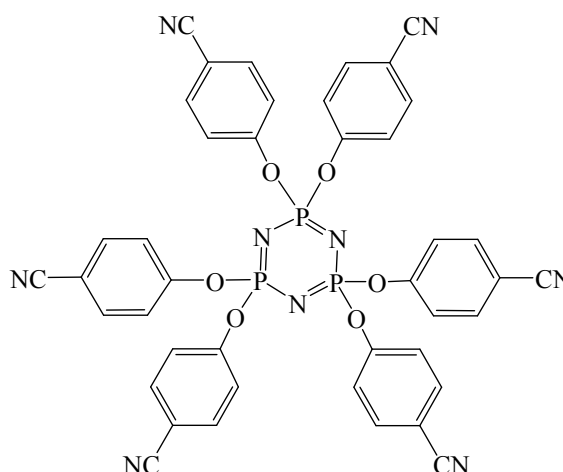
Substitution with AzB. Finely divided sodium (0.09 g, 3.9 mmol) was put into 10 ml of anhydrous THF, and 0.99 g (5.0 mmol) of AzB were cautiously added, causing hydrogen evolution. After consumption of all the sodium, 0.02 g (0.06 mmol) of tetrabutylammonium bromide were added. A phosphazene-functionalized sample was dipped into the solution, and the system was stirred at room temperature for 16 h. PDCP-grafted samples were washed with 10 ml of THF, while 10 ml of chloroform were used in the case of HCCP-grafted plates. Final washings were the same for both kinds of samples, in sequence with 10 ml of THF, 10 ml of distilled water and finally with 10 ml of THF. The samples were dried in an oven at 50°C before characterization.

3.5. EXPERIMENTAL PROCEDURES FOR THE SURFACE FUNCTIONALIZATION OF SILICON-BASED SUBSTRATES AND THE PREPARATION OF NEW BULK MATERIALS AND THIN FILMS USING CYCLOPHOSPHAZENES PARTIALLY SUBSTITUTED WITH TRIALKOXSILANE DERIVATIVES (CHAPTER 4.4)

Unless otherwise specified, all the syntheses hereby reported were performed under nitrogen atmosphere using dry solvents.

3.5.1 Starting and reference compounds

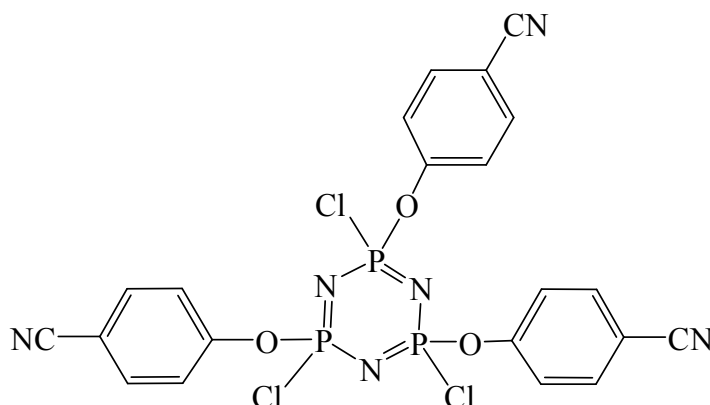
3.5.1.1. Synthesis of hexakis(4CNP)cyclophosphazene (C-6-pCN, MW = 843.62)



This synthesis was carried out according to the procedure previously set by G.A.Carriedo²⁹⁹. HCCP (0.30 g, 0.9 mmol), 4CNP (0.61 g, 5.2 mmol) and cesium carbonate (3.36 g, 10.3 mmol) were dissolved in 30 ml of anhydrous acetone, and the mixture was stirred at room temperature for 45 minutes. The solvent was evaporated under vacuum and the compound was extracted in a soxhlet for 3 hours with CH₂Cl₂, then the solvent was evaporated again.

Yield: 62% (0.45 g). Elemental analysis (expected values in brackets): C 59.6 (59.8); H 2.8 (2.9); N 14.6 (15.0). IR (KBr): 3100-3050 cm⁻¹ (ν aromatic CH); 2230 cm⁻¹ (ν C≡N); 1599, 1496 cm⁻¹ (breathing aromatic C=C); 1201, 1187 cm⁻¹ (ν_{as} P=N-); 944 cm⁻¹ (ν P-O-Ph). ¹H NMR (CDCl₃): δ 7.0 (m), 7.5 (m, aromatic protons). {¹H} ³¹P NMR (CDCl₃): δ 7.3 (s)

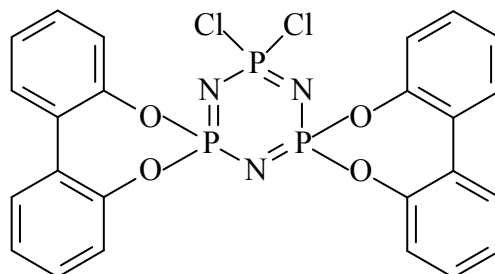
3.5.1.2. Synthesis of tris(4CNP)tris(chloro)cyclophosphazene



HCCP (1.78 g, 5.0 mmol) and 4CNP (1.79 g, 15.0 mmol) were dissolved in 100 ml of anhydrous toluene, and then anhydrous TEA (4.2 ml, 3.05 g, 30.1 mmol) was added. The solution was refluxed for 3 hours and filtered under nitrogen. The filtered triethylammonium chloride was washed three times with 10 ml of anhydrous toluene and dried under vacuum (2.00 g, 14.9 mmol, quantitative yield). The solvent was evaporated under vacuum at 60°C and subsequently at 110°C, to obtain a pale pink solid.

Elemental analysis (expected values in parentheses): C 41.67 (42.3); H 1.75 (2.0); N 13.73 (14.1). IR (KBr): 3100-3050 cm^{-1} (ν aromatic CH); 2230 cm^{-1} (ν -C \equiv N); 1599 and 1496 cm^{-1} (breathing aromatic C=C); 1201 and 1187 cm^{-1} (ν_{as} -P=N-); 944 cm^{-1} (ν P-O-Ph). ^1H NMR (CDCl_3): δ 7.7 \div 7.0 (m, aromatic protons). $\{^1\text{H}\}^{31}\text{P}$ NMR (CDCl_3): complex spectrum due to presence of compounds with different degrees of substitution of the chlorine atoms with 4CNP, and of different stereochemical structure. Multiplets are located in the δ 29 \div 25, 20 \div 14 and 7 \div -2 ranges.

3.5.1.3. Synthesis of 2,2-dichloro-4,4,6,6-bis[spiro(2',2''-dioxo-1',1''-biphenyl)]-cyclophosphazene (C-2-Cl, MW = 574.23)

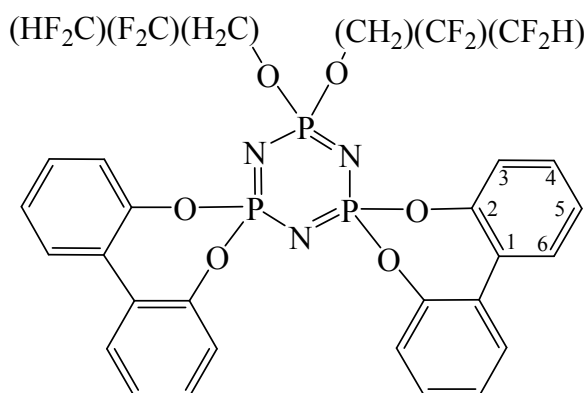


This product was prepared according to the procedure set by De Jaeger³⁰⁰.

HCCP (16.05 g, 86.1 mmol), 2,2'-dihydroxybiphenyl (16.05 g, 86.1 mmol), sodium hydroxide (6.87 g, 172.2 mmol) and TBAB (1.38 g, 4.29 mmol) were put into a flask with 150 ml of chlorobenzene and 150 ml of distilled water. The mixture was stirred at room temperature for three hours and subsequently at 70°C for three hours, then it was neutralized by addition of 37% hydrochloric acid. The chlorobenzene was evaporated under reduced pressure until precipitation of a brown solid, which was filtered on a gooch and washed with distilled water and then with small acetone portions until it became colorless.

Yield: 80% (23.80 g). Melting point: 309-312°C. Elemental analysis (theoretical values in brackets): C (50.2) 49.46; H (2.8) 2.59; N (7.3) 7.15. IR: 3066 cm⁻¹ (ν aromatic CH); 1605 e 1500 cm⁻¹ (ν aromatic C=C); 1229-1179 cm⁻¹ (ν_{as} P=N); 967 cm⁻¹ (ν, P-O-Ar). ¹H NMR (CDCl₃): δ 7.2-7.7 (m, aromatic system). ³¹P NMR (CDCl₃): δ 19.97 (d, ²J_{PP} = 78.70); 19.87 (d, ²J_{PP} = 81.32); 29.62 (dd 78.78, ²J_{PP} = 81.32).

3.5.1.4. Synthesis of 2,2-bis(2,2,3,3-tetrafluoropropoxy)-4,4,6,6-bis[spiro(2',2''-dioxo-1',1''-biphenyl)]cyclophosphazene (C-2-TFP, MW = 765.43)



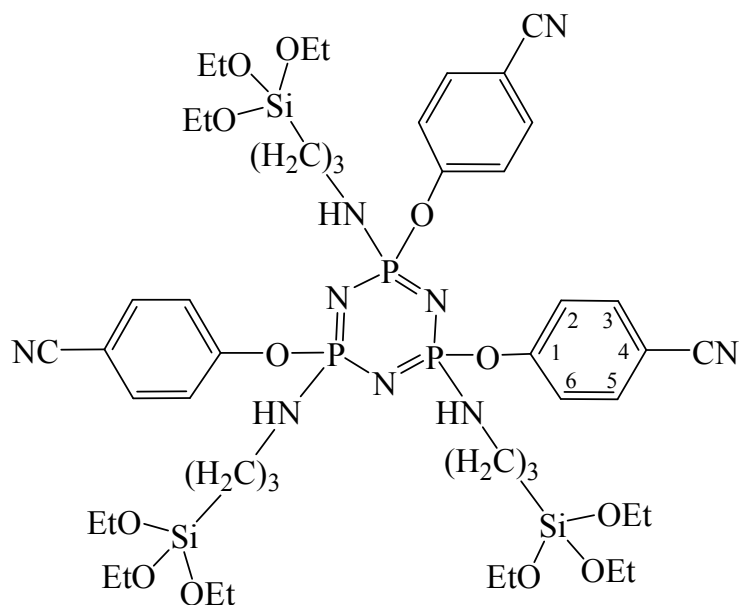
C-2-Cl (0.50 g, 0.9 mmol; see section 3.5.1.3), sodium hydride (60% dispersion in mineral oil, 0.10 g, 2.5 mmol) and TEAB (0.02 g, 0.1 mmol) were dissolved in 50 ml of anhydrous THF, and a solution of TFP (0.2 ml, 0.30 g, 2.2 mmol) in 50 ml of anhydrous THF was added dropwise causing hydrogen evolution. The mixture was stirred overnight at room temperature and filtered on a gooch, washing the filtered solid with THF. The mother and washing liquors were brought to dryness under reduced pressure, and the solid thus obtained was washed with distilled water, filtered on a gooch and finally dried under vacuum. The compound was then recrystallized from $\text{CH}_2\text{Cl}_2/n$ -hexane.

Yield: 87% (0.60 g). FTIR (KBr): 3027-3063 (ν aromatic CH), 1600-1500 cm^{-1} (breathing aromatic C=C), 1237-1175 cm^{-1} (ν_{as} P=N), 1093 cm^{-1} (ν CF), 968 cm^{-1} (ν P-O-Ph). ^1H NMR (CD_3COCD_3): δ 7.67 (d, $^3J_{\text{H,H}}=7.6$ Hz, biphenyl C6), 7.52 (t, $^3J_{\text{H,H}}=7.6$ Hz, biphenyl C4), 7.42 (t, $^3J_{\text{H,H}}=7.5$ Hz, biphenyl C5), 7.40 (d, $^3J_{\text{H,H}}=7.3$ Hz, biphenyl C3), 6.479 (CF_2H ; t, $J_{\text{H,F}}=52.3$ Hz, t $^2J_{\text{H,F}}=5.4$ Hz); 4.606 (CH_2 ; t $^3J_{\text{H,F}}=13.0$ Hz, d $^3J_{\text{H,P}}=7.8$ Hz, t $^4J_{\text{H,F}}=1.4$ Hz). $\{^1\text{H}\}^{31}\text{P}$ NMR (CD_3COCD_3): δ 26.31 (d, $^2J_{\text{P,P}}=93.9$ Hz); 26.29 (d, $^2J_{\text{P,P}}=92.3$ Hz); 19.15 (dd, $^2J_{\text{P,P}}=90.7$ Hz and 98.8 Hz). ^{31}P NMR (CD_3COCD_3): δ 26.59 (d, $^2J_{\text{P,P}}=4.2$ Hz); 26.01 (d, $^2J_{\text{P,P}}=3.2$ Hz); 19.15 (ddq $^2J_{\text{P,P}}=90.7$ Hz and 98.8 Hz, $^3J_{\text{P,H}}=7.8$ Hz; note: q=quintet). $\{^1\text{H}\}^{13}\text{C}$ NMR (CD_3COCD_3): δ 148.00 (s, biphenyl C2); 130.06 (s, biphenyl C4); 129.79 (s, biphenyl C6); 128.57 (s, biphenyl C1); 126.51 (s, biphenyl C5); 121.83 (s, biphenyl C3); 109.37 (tt, CF_2H ; $^1J_{\text{C,F}}=248.2$ Hz, $^3J_{\text{C,F}}=33.4$ Hz; note: in the same zone are the

undistinguishable signals from group $C-\underline{CF_2}-C$; 62.64 (td, OCH_2 ; $^2J_{C,F} = 29.4$ Hz, $^2J_{C,P} = 4.0$ Hz).

3.5.2. Synthesis of sol-gel precursors

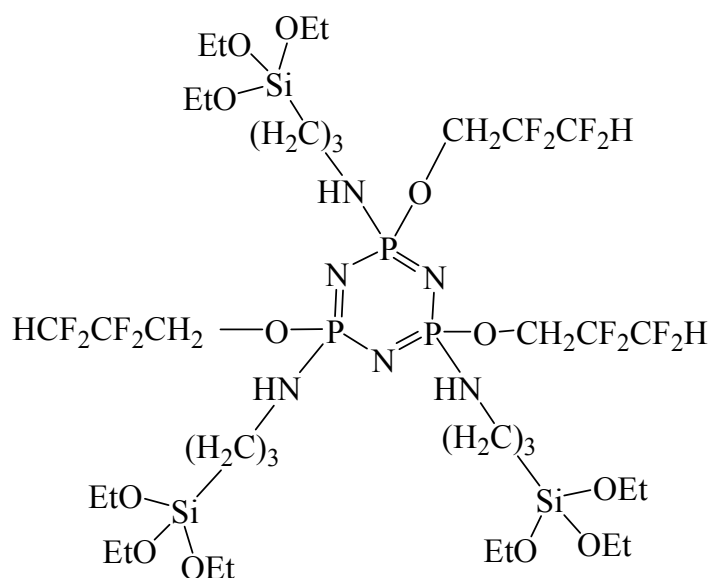
3.5.2.1. Synthesis of tris(4CNP)tris(APTES)cyclophosphazene



HCCP (2.50 g, 7.2 mmol) and 4CNP (2.57 g, 21.6 mmol) were dissolved in 100 ml of anhydrous THF, and anhydrous TEA (6 ml, 4.36 g, 43.0 mmol) was added. The solution was refluxed for 5 hours and filtered under nitrogen. The filtered triethylamine chloride was washed three times with 10 ml of anhydrous THF and dried under vacuum (2.97 g, 21.6 mmol, quantitative yield). APTES (5 ml, 4.73 g, 21.6 mmol) was then added, and the obtained mixture was stirred at room temperature for 72 hours and filtered under nitrogen. The separated triethylammonium chloride was washed three times with 10 ml of anhydrous THF and dried under vacuum (2.00 g, 14.5 mmol, 67% yield)³⁰¹. The solvent was evaporated under vacuum and the resulting colourless oil was washed twice with 30 ml of anhydrous *n*-hexane, introduced and removed *via* cannula. Then, the oil was dried under vacuum at 50°C and characterized by NMR.

$\{^1H\}^{31P}$ NMR ($CDCl_3$): complex spectrum due to presence of compounds with different substitution patterns and stereochemistry. 1H NMR ($CDCl_3$): δ 8.34 (NH); 3.85-3.72 (Si-O- $\underline{CH_2}$ -); 2.97-2.79 (- $\underline{CH_2-CH_2-NH-P}$); 1.57-1.44 (Si- $\underline{CH_2-CH_2}$ -); 1.24-1.13 (Si-O- $\underline{CH_2-CH_3}$); 0.56-0.45 (Si- $\underline{CH_2}$ -). $\{^1H\}^{13C}$ NMR ($CDCl_3$): δ 134.30-

3.5.2.2. Synthesis of tris(TFP)tris(APTES)cyclophosphazene

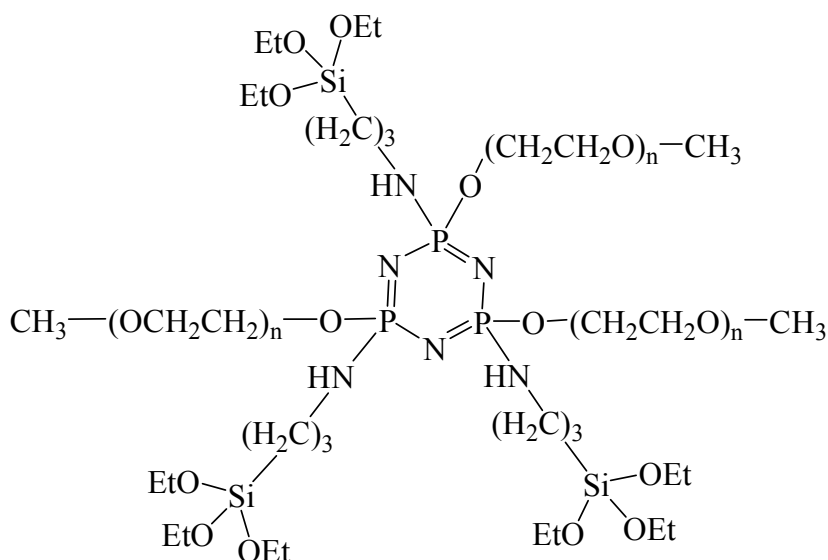


TEA (2.1 ml, 1.52 g, 15.1 mmol) and APTES (3.5 ml, 3.31 g, 15 mmol) were added, and the mixture was stirred at room temperature for 24 hours, refluxed at 65°C for 16 hours and subsequently filtered under nitrogen. The filtered triethylammonium chloride was washed twice with 10 ml of anhydrous THF, dried under vacuum and weighed (1.48 g, 10.8 mmol, 72% yield for the substitution reaction with APTES).

$\{^1\text{H}\}^{31}\text{P}$ NMR (CDCl_3) before substitution with APTES: complex spectrum due to presence of compounds with different degrees of substitution of the chlorine atoms of HCCP with APTES and TFP. A singlet at δ 17.78 comes from a molecule of phosphazene bearing one TFP substituent and one chlorine atom on each phosphorus.

Signals are located in the range δ 8÷30. ^1H NMR (CDCl_3) before substitution with APTES: δ 5.92 (m, $\text{C}(\text{F}_2)\text{H}$); 4.39 (m, CH_2); the OH signal of unreacted TFP is absent, so the yield of the first step is supposed to be quantitative.

3.5.2.3. Synthesis of tris(PEG-750-ME)tris(APTES)cyclophosphazene



In a 250 ml glass flask, HCCP (0.89 g, 2.5 mmol), PEG-750-ME (5.73 g, 7.5 mmol) and TEAB (0.02 g, 0.1 mmol) were dissolved in 50 ml of anhydrous THF. Sodium hydride (60% dispersion in mineral oil, 0.45 g, 11.3 mmol) was cautiously added, then the mixture was stirred at room temperature for 30 hours and filtered under nitrogen. The filtered solid residue was washed twice with 10 ml of anhydrous THF, which were added to the filtered solution.

The characterization of the first step is as follows:

$\{^1\text{H}\}^{31}\text{P}$ NMR (CDCl_3): complex spectrum due to presence of compounds with different degrees of substitution of the chlorine atoms of HCCP with PEG-750-ME. Signals are located at δ 26÷17, δ 12÷10 (weak), and 2÷-5. ^1H NMR (CDCl_3): δ 3.68÷3.48 (CH_2 of PEG in different positions); 3.31 (CH_3).

The filtered solution was treated with TEA (1.2 ml, 0.87 g, 8.6 mmol) and APTES (1.8 ml, 1.70 g, 7.5 mmol); the resulting mixture was stirred at room temperature for 48 hours and then filtered under nitrogen. The obtained triethylammonium chloride was washed twice with 10 ml of anhydrous THF, dried under vacuum and weighed (0.73 g, 5.3 mmol, 71% yield for the substitution reaction with APTES).

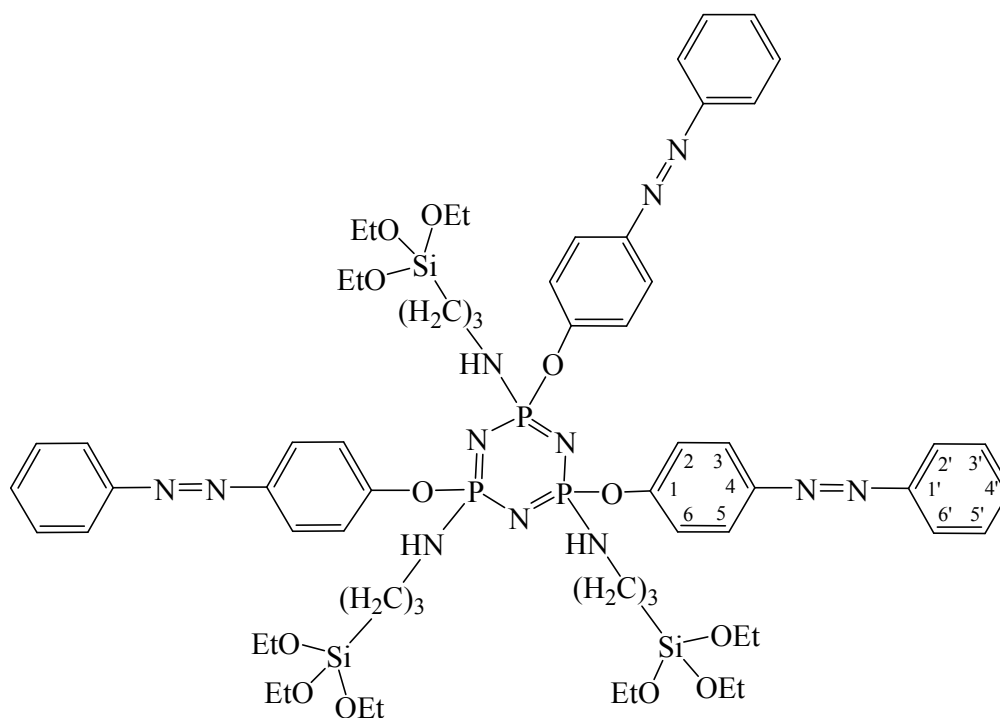
Evaporation of the solvent under reduced pressure at 50°C yielded a colorless oil.

NMR characterization of the final product gave:

$\{^1\text{H}\}^{31}\text{P}$ NMR (CDCl_3): complex spectrum due to presence of compounds with different degrees of substitution of the chlorine atoms of HCCP with APTES and PEG-750-ME. Signals are located at δ 25÷15 and 6÷-1. ^1H NMR (CDCl_3): δ 3.70 (q, Si-O-CH₂-CH₃); 3.47 (b, CH₂ of PEG in different positions, and Si-O-CH₂-); 3.27 (terminal CH₃ of PEG); 2.81 (b, -CH₂-CH₂-NH-P); 1.49 (b, Si-CH₂-CH₂-); 1.11 (t, Si-O-CH₂-CH₃); 0.53 (b, Si-CH₂-).

$\{^1\text{H}\}^{13}\text{C}$ NMR (CDCl_3): δ 73.00 (-CH₂-CH₂-O-P); 72.35 (-CH₂-O-CH₃); 70.99 (b, CH₂ of PEG in different positions); 61.97 (-CH₂-O-P); 59.42 (terminal CH₃ of PEG); 58.77 (Si-O-CH₂); 43.94 (-CH₂-CH₂-NH-P); 25.33 (Si-CH₂-CH₂-); 18.76 (Si-O-CH₂-CH₃); 8.06 (Si-CH₂-).

3.5.2.4. Synthesis of tris(AzB)tris(APTES)cyclophosphazene



HCCP (1.74 g, 5 mmol), sodium hydride (60% dispersion in mineral oil, 0.69 g, 17.3 mmol) and TEAB (0.02 g, 0.1 mmol) were dissolved in 100 ml of anhydrous THF. A solution of 4-phenylazophenol (2.97 g, 15 mmol) in 30 ml of anhydrous THF was added dropwise, then the mixture was stirred at room temperature for 72 hours and

filtered under nitrogen. The filtered solid residue was washed twice with 10 ml of anhydrous THF.

TEA (2.1 ml, 1.52 g, 15.1 mmol) and APTES (3.5 ml, 3.31 g, 15 mmol) were added, and the mixture was stirred at room temperature for 72 hours and subsequently filtered under nitrogen. The filtered triethylammonium chloride was washed twice with 10 ml of anhydrous THF, dried under vacuum and weighed (1.47 g, 10.8 mmol, 72% yield for the substitution reaction with APTES). Evaporation of the solvent under reduced pressure at 50°C yielded a dark red oil.

$\{^1\text{H}\}^{31}\text{P}$ NMR (CDCl_3): complex spectrum due to presence of compounds with different degrees of substitution of the chlorine atoms of HCCP with APTES and AzB. Signals are located at δ 30÷28, 23÷13 and 11÷5. ^1H NMR (CDCl_3): δ 8.02÷7.14 (m, aromatic protons); 3.77 (Si-O-CH₂-CH₃); 2.94 (b, -CH₂-CH₂-NH-P); 1.61 (b, Si-CH₂-CH₂-); 1.20 (Si-O-CH₂-CH₃); 0.62 (b, Si-CH₂-). $\{^1\text{H}\}^{13}\text{C}$ NMR (CDCl_3): δ 153.81 (aromatic C4); 153.01 (aromatic C1); 150.08 (aromatic C1'); 131.47 (aromatic C4'); 129.60 (aromatic C3',5'); 124.70 (aromatic C3,5); 123.39 (aromatic C2',6'); 122.40 (aromatic C2,6); 58.93 (Si-O-CH₂); 43.84 (-CH₂-CH₂-NH-P); 25.38 (Si-CH₂-CH₂-); 18.83 (Si-O-CH₂-CH₃); 8.01 (Si-CH₂-).

3.5.3. Surface functionalization of silica gel

3.5.3.1. Silica gel activation

The surface activation of SiO₂ beads was obtained according to an already reported procedure²⁸⁰ by suspending silica gel (11 g) in 120 ml of 37% HCl inside a round-bottomed flask equipped with a refrigerator connected to a KOH trap. The suspension was refluxed for 4 hours and then filtered. The recovered solid was washed with distilled water till neutrality of the washing liquors, and then dried at 110°C for 16 hours.

3.5.3.2. Surface functionalization of silica gel beads with cyclophosphazenes cosubstituted with APTES and with TFP, PEG-750-ME or AzB

A typical functionalization procedure is as follows: activated silica gel (0.60 g) was heated at 80°C under vacuum for 1 hour in a 250 ml flask, and treated with a solution of tris(4CNP, PEG-750-ME, TFP, or AzB)tris(APTES)cyclophosphazene (2.2 mmol) in 50 ml of anhydrous THF introduced *via* metal cannula. The mixture was stirred for

16 hours at reflux temperature (or at room temperature in the case of the azo compound) and then filtered under nitrogen. The gel obtained was washed twice with 10 ml of anhydrous THF and dried under vacuum at room temperature. The silica gels functionalized with TFP, PEG-750-ME and AzB-containing cyclophosphazenes were eventually washed with distilled water and diethyl ether, and dried at 50°C for 16 hours. The characterization of the resulting gels is reported below.

a) 4CNP

FTIR (KBr): 2970-2935 cm^{-1} (ν CH_2); 2233 cm^{-1} (ν CN); 1507 cm^{-1} (breathing aromatic $\text{C}=\text{C}$); shoulder 1170-1200 cm^{-1} (ν $\text{P}=\text{N}$); 1098 cm^{-1} (ν Si-O-Si). ^{13}C CP MAS NMR: δ 8.7 ($\text{Si}-\underline{\text{CH}_2}$ -), 15.9 ($\text{Si-O-CH}_2-\underline{\text{CH}_3}$), 21.1 ($\text{Si-CH}_2-\underline{\text{CH}_2}$ -), 42.5 ($-\text{CH}_2-\underline{\text{CH}_2}\text{-NH-P}$), 57.7 ($\text{Si-O}-\underline{\text{CH}_2}$ -), 107.7 (quaternary aromatic carbon C4), 121.8 (aromatic carbons C2, C6, and $-\underline{\text{C}}\equiv\text{N}$), 133.6 (aromatic carbons C3, C5), 154.5 (quaternary aromatic carbon C1). ^{31}P SPE MAS NMR: δ 19.9 ($W_{1/2}= 546$ Hz), 12.4 ($W_{1/2}= 942$ Hz). ^{29}Si CP MAS NMR: T^n units: δ -56.00 (T^1), -60.1 (T^2), -69.0 (T^3), $\text{AF}^{T^n}= 86\%$; Q^n units: -102.8 (Q^3), -112.0 (Q^4), $\text{AF}^{Q^n}= 88\%$, $T^n/Q^n= 0.23$.

b) TFP

FTIR (KBr): 2976-2894 cm^{-1} (ν CH_2 of APTES and TFP); shoulder 1170-1230 cm^{-1} (ν $\text{P}=\text{N}$); 1094 cm^{-1} (ν Si-O-Si , broad band covering ν C-F signal). ^{13}C CP MAS NMR: δ 10.0 ($\text{Si}-\underline{\text{CH}_2}$ -), 21.3 ($\text{Si-CH}_2-\underline{\text{CH}_2}$ -), 42.9 ($-\text{CH}_2-\underline{\text{CH}_2}\text{-NH-P}$), 61.7 ($\text{CF}_2-\underline{\text{CH}_2}\text{-O-P}$), 107-116 ($\text{H}-\underline{\text{CF}_2}-\underline{\text{CF}_2}$). ^{29}Si CP MAS NMR: T^n units: δ -59.2 (T^2), -68.9 (T^3), $\text{AF}^{T^n}= 91\%$; Q^n units: -102.4 (Q^3), -112.0 (Q^4), $\text{AF}^{Q^n}= 91\%$, $T^n/Q^n= 0.61$. ^{31}P SPE MAS NMR: δ 20.5 ($W_{1/2}= 817$ Hz), 6.7 ($W_{1/2}= 1067$ Hz).

c) PEG-750-ME

FTIR (KBr): 2971-2930 cm^{-1} (ν CH_2 of APTES and PEG); shoulder 1170-1230 cm^{-1} (ν $\text{P}=\text{N}$); 1097 cm^{-1} (ν Si-O-Si). ^{13}C CP MAS NMR: δ 9.8 ($\text{Si}-\underline{\text{CH}_2}$ -), 21.4 ($\text{Si-CH}_2-\underline{\text{CH}_2}$ -), 42.4 ($-\text{CH}_2-\underline{\text{CH}_2}\text{-NH-P}$), 57.7 ($\text{H}_3\underline{\text{C}}\text{OCH}_2$ -), 61.2 ($-\underline{\text{CH}_2}\text{-O-P}$), 70.3 ($\text{O}-\underline{\text{CH}_2}-\underline{\text{CH}_2}\text{-O}$). ^{29}Si CP MAS NMR: T^n units: δ -60.0 (T^2), -69.1 (T^3), $\text{AF}^{T^n}= 91\%$; Q^n units: δ -102.9 (Q^3), -112.0 (Q^4), $\text{AF}^{Q^n}= 89\%$. $T^n/Q^n= 0.33$. ^{31}P SPE MAS NMR: δ 18.8 ($W_{1/2}= 633$ Hz, 43%), 6.0 ($W_{1/2}= 858$ Hz, 57%).

d) AzB

FTIR (KBr): 2970-2883 cm^{-1} (ν CH_2 of APTES); 1500 cm^{-1} (breathing $\text{C}=\text{C}$ aromatic); shoulder 1173, 1234 cm^{-1} (ν $\text{P}=\text{N}$); 1094 cm^{-1} (ν Si-O-Si). ^{13}C CP MAS

NMR: δ 9.4 (Si-CH₂-), 21.4 (Si-CH₂-CH₂-), 42.1 (-CH₂-CH₂-NH-P), 121.6 (aromatic C2, C3, C5, C6, C2', C6'), 128.4 (aromatic C3', C4', C5'), 152.8 (aromatic C1, C4, C1'). ²⁹Si CP MAS NMR: Tⁿ units: δ -59.3 (T²), -68.9 (T³), AF^{Tⁿ} = 92 %; Qⁿ units: δ -102.8 (Q³), -112.4 (Q⁴), AF^{Qⁿ} = 89 %. Tⁿ/Qⁿ = 0.26. ³¹P SPE MAS NMR: δ 19.7 (W_{1/2} = 623 Hz), 6.2 (W_{1/2} = 1217 Hz).

3.5.4. Preparation of monoliths and thin films

The products described in the subsections of section 3.5.2 were used also for the preparation of monoliths and the deposition of thin films by sol-gel technique. The condensation of the cyclophosphazene precursor in the presence of an excess of TEOS was always performed, but for tris(APTES)tris(4CNP)cyclophosphazene self condensation without TEOS was also explored. Experiences involving this compound will therefore be treated separately.

3.5.4.1. Preparation of monoliths and thin films starting from tris(4CNP)tris(APTES)cyclophosphazene via sol-gel technique

A) Self condensation reactions

Tris(4CNP)tris(APTES)cyclophosphazene (0.87 mmol) was dissolved in 6 ml of THF, and treated with 0.1420 g of a 0.18 M aqueous HCl solution. The mixture was stirred at room temperature for 6 days; after this time, the solution was brought to pH 3 by addition of HCl, and stirred at room temperature for additional 24 hours.

Preparation of monoliths. The precursor solution, prepared as described above, was put in a 15 mm diameter polypropylene sample-tube, and the solvent evaporated at 50°C. Monoliths were characterized by FTIR and ¹³C, ²⁹Si and ³¹P NMR spectroscopy. The corresponding data are reported below.

FTIR (KBr): 2936-2873 cm⁻¹ (ν CH₂); 2233 cm⁻¹ (ν CN); 1602 and 1500 cm⁻¹ (breathing aromatic C=C); shoulder 1195, 1165 cm⁻¹ (ν P=N); 1102 cm⁻¹ (ν Si-O-Si); 922 cm⁻¹ (ν P-O-Ph).

¹³C CP MAS NMR: δ 11.5 (Si-CH₂-), 25.8 (Si-CH₂-CH₂-), 43.2 (-CH₂-CH₂-NH-P), 108.7 (quaternary aromatic carbon C4), 122.0 (aromatic carbon C2, C6, and -C≡N), 134.3 (aromatic carbon C3, C5), 154.5 (quaternary aromatic carbon C1). ²⁹Si CP MAS

NMR: δ -48.5 (T^1), -58.5 (T^2), -68.0 (T^3), AF=82%. ^{31}P SPE MAS NMR: δ 18.8 ($W_{1/2} = 637$ Hz), 12.2 ($W_{1/2} = 666$ Hz), 4.9 ($W_{1/2} = 756$ Hz).

Thin films deposition. A wafer (1×1 cm surface) of crystalline silicon (100) was dipped for one minute in the precursor solution prepared as described above. The sample was dried first at room temperature for 15 minutes and then at 110°C for 16 hours. The characterization was carried out by transmission FTIR spectroscopy.

FTIR: 2937-2870 cm^{-1} (ν CH_2); 2230 cm^{-1} (ν CN); 1603, 1501 cm^{-1} (breathing aromatic C=C); shoulder 1194, 1165 cm^{-1} (ν P=N); 1105 cm^{-1} (ν Si-O-Si); 925 cm^{-1} (ν P-O-Ph)

B) In the presence of TEOS

A solution of TEOS (19.12 g = 92 mmol), distilled water (6.56 g = 36.4 mmol) and 37% hydrochloric acid (0.09 g = 0.9 mmol) in THF (100 ml) was stirred for one hour at room temperature and then added to a solution of tris(4-cyanophenoxy)tris(3-triethoxysilyl-propylamino)cyclotriphosphazene (3.1 mmol) in 20 ml of anhydrous THF. The mixture was stirred at room temperature for 5 days.

Preparation of monoliths. Portions of 9.5 ml of the same precursor solution were put in 15 mm diameter polypropylene sample-tubes, and the solvent was evaporated at different temperatures and rates. The monoliths were characterized by FTIR and ^{13}C , ^{29}Si and ^{31}P NMR spectroscopy. The corresponding data are reported below:

FTIR (KBr): 2990-2940 cm^{-1} (ν CH_2); 2233 cm^{-1} (ν CN); 1598 and 1496 cm^{-1} (breathing aromatic C=C); shoulder 1163 cm^{-1} (ν P=N); 1078 cm^{-1} (ν Si-O-Si). ^{13}C CP MAS NMR: δ 9.6 (Si- $\underline{\text{C}}\text{H}_2$ -), 23.6 (Si- CH_2 - $\underline{\text{C}}\text{H}_2$ -), 43.2 ($-\text{CH}_2$ - $\underline{\text{C}}\text{H}_2$ -NH-P), 108.0 (quaternary aromatic carbon C4), 121.5 (aromatic carbon C2, C6, and $-\underline{\text{C}}\equiv\text{N}$), 134.3 (aromatic carbon C3, C5), 154.2 (quaternary aromatic carbon C1). ^{29}Si CP MAS NMR: T^n units: δ -58.2 (T^2), -66.7 (T^3), AF $^{T^n}$ = 93%; Q^n units: -92.8 (Q^2), -102.0 (Q^3), -110.9 (Q^4), AF $^{Q^n}$ = 79%. ^{31}P SPE MAS NMR: δ 19.5 ($W_{1/2} = 926$ Hz), 11.7 ($W_{1/2} = 633$ Hz).

Thin films deposition. Wafers (1×1 cm surface) of crystalline silicon (100) were dipped for one minute in the precursor solution prepared as described above, and dried first at room temperature for 15 minutes and then at 110°C for 16 hours. The silicon samples were characterized by transmission FTIR.

FTIR: 2992-2942 cm^{-1} (ν CH_2); 2228 cm^{-1} (ν CN); 1603, 1501 cm^{-1} (breathing aromatic $\text{C}=\text{C}$); shoulder 1170-1200 cm^{-1} (ν $\text{P}=\text{N}$); 1075 cm^{-1} (ν Si-O-Si).

3.5.4.2. Preparation of monoliths and thin film coatings on Si(100) by sol-gel technique from cyclophosphazenes co-substituted with APTES and TFP, PEG-750-ME or AzB

A solution of TEOS (9.57 g = 46 mmol) in THF (35 ml), and 0.14 M aqueous HCl (3.33 g; 0.45 mmol of HCl and 180 mmol of H_2O) were stirred together for one hour at room temperature and then added to a solution of tris(PEG-750-ME, TFP, or AzB)tris(APTES)cyclophosphazene (1.53 mmol) in 15 ml of THF. The mixture was stirred at room temperature for 5 days.

Preparation of monoliths. Portions of 9.5 ml of the precursor solution were put in 15 mm diameter polypropylene sample-tubes, and then the solvent was evaporated at different temperatures and rates. The obtained monoliths were characterized by FTIR and ^{13}C , ^{29}Si and ^{31}P solid state NMR spectroscopy. The corresponding data are reported below.

a) PEG-750-ME

FTIR (KBr): 2945-2878 cm^{-1} (ν CH_2 of APTES and PEG); shoulder 1194 cm^{-1} (ν $\text{P}=\text{N}$); 1082 cm^{-1} (ν Si-O-Si). ^{13}C CP MAS NMR: δ 9.5 ($\text{Si}-\underline{\text{CH}_2}$ -), 21.3 ($\text{Si}-\text{CH}_2-\underline{\text{CH}_2}$ -), 44.5 ($-\text{CH}_2-\underline{\text{CH}_2}-\text{NH-P}$), 70.7 ($\text{O}-\underline{\text{CH}_2}-\underline{\text{CH}_2}-\text{O}$ -). ^{29}Si CP MAS NMR: T^n units: δ -58.7 (T^2), -66.8 (T^3), $\text{AF}^{\text{T}^n} = 89.7\%$; Q^n units: δ -92.0 (Q^2)-102.0 (Q^3), -110.1 (Q^4), $\text{AF}^{\text{Q}^n} = 86.5\%$. $\text{T}^n/\text{Q}^n = 0.22$. ^{31}P SPE MAS NMR: δ 17.3 ($\text{W}_{1/2} = 601$ Hz), 8.6 ($\text{W}_{1/2} = 1088$ Hz), 1.8 ($\text{W}_{1/2} = 500$ Hz), -7.61 ($\text{W}_{1/2} = 802$ Hz).

b) TFP

FTIR (KBr): 2960-2847 cm^{-1} (ν CH_2 of APTES and TFP); shoulder 1203 cm^{-1} (ν $\text{P}=\text{N}$); 1081 cm^{-1} (ν Si-O-Si , broad band covering ν C-F signal). ^{13}C CP MAS NMR: δ 8.9 ($\text{Si}-\underline{\text{CH}_2}$ -), 22.7 ($\text{Si}-\text{CH}_2-\underline{\text{CH}_2}$ -), 43.7 ($-\text{CH}_2-\underline{\text{CH}_2}-\text{NH-P}$), 62.7 ($\text{CF}_2-\underline{\text{CH}_2}-\text{O-P}$), 107-116 ($\text{H}-\underline{\text{CF}_2}-\underline{\text{CF}_2}$)

^{29}Si CP MAS NMR: T^n units: δ -57.8 (T^2), -66.0 (T^3), $\text{AF}^{\text{T}^n} = 91\%$; Q^n units: δ -93.1 (Q^2)-101.7 (Q^3), -110.1 (Q^4), $\text{AF}^{\text{Q}^n} = 85\%$. $\text{T}^n/\text{Q}^n = 0.19$. ^{31}P SPE MAS NMR: δ 23.4 ($\text{W}_{1/2} = 435$ Hz), 19.0 ($\text{W}_{1/2} = 348$ Hz), 14.5 ($\text{W}_{1/2} = 471$ Hz), 4.7 ($\text{W}_{1/2} = 1105$ Hz), -8.7 ($\text{W}_{1/2} = 470$ Hz).

c) AzB

FTIR (KBr): 2976-2919 cm^{-1} (ν CH_2 of APTES); 1593, 1496 cm^{-1} (breathing $\text{C}=\text{C}$ aromatic); shoulder 1153 cm^{-1} (ν $\text{P}=\text{N}$); 1078 cm^{-1} (ν Si-O-Si)

^{13}C CP MAS NMR: δ 9.3 (Si-CH_2 -), 21.0 ($\text{Si-CH}_2\text{-CH}_2$ -), 43.0 ($-\text{CH}_2\text{-CH}_2\text{-NH-P}$), 122.7 (aromatic C2, C3, C5, C6, C2', C6'), 129.4 (aromatic C3', C4', C5'), 152.4 (aromatic C1, C4, C1').

^{29}Si CP MAS NMR: T^n units: δ -58.2 (T^2), -66.8 (T^3), $\text{AF}^{\text{T}^n} = 93\%$; Q^n units: δ -93.6 (Q^2)-102.0 (Q^3), -109.8 (Q^4), $\text{AF}^{\text{Q}^n} = 85\%$. $\text{T}^n/\text{Q}^n = 0.12$.

^{31}P SPE MAS NMR: δ 17.3 ($W_{1/2} = 942$ Hz), 4.8 ($W_{1/2} = 954$ Hz).

Thin films deposition. Crystalline silicon (100) wafers (1×1 cm surface), or in the case of azo compound-substituted cyclophosphazene also a sodalime glass slice, were dipped for one minute in one of the precursor solutions prepared as described above. They were subsequently dried, first at room temperature for 15 minutes, and then at 50°C for 16 hours. The samples were characterized by transmission FTIR spectroscopy. In the case of the thin film on sodalime glass slide bearing AzB groups, also UV-visible transmission spectroscopy was exploited.

a) PEG-750-ME

FTIR: 2945-2879 cm^{-1} (ν CH_2 of APTES and PEG); shoulder 1194 cm^{-1} (ν $\text{P}=\text{N}$); 1083 cm^{-1} (ν Si-O-Si).

b) TFP

FTIR (KBr): 2980-2894 cm^{-1} (ν CH_2 of APTES and TFP); shoulder 1200 cm^{-1} (ν $\text{P}=\text{N}$); 1078 cm^{-1} (ν Si-O-Si , broad band covering ν C-F signal).

c) AzB

FTIR: 2930-2870 cm^{-1} (ν CH_2 of APTES); 1598, 1496 cm^{-1} (breathing $\text{C}=\text{C}$ aromatic); shoulder 1168-1200 cm^{-1} (ν $\text{P}=\text{N}$); 1083 cm^{-1} (ν Si-O-Si). UV-Vis: two bands located at 330 and 430 nm attributed to the *trans* and to the *cis* isomer of the azobenzene substituents, respectively.

3.6. EXPERIMENTAL PROCEDURES FOR THE SYNTHESIS OF CYCLOPHOSPHAZENES SUBSTITUTED WITH OXAZOLINE GROUPS AS STARTING PRODUCTS FOR THE PREPARATION OF NEW MATERIALS (CHAPTER 4.5)

Unless otherwise specified, all the synthetic reactions hereby reported were performed under nitrogen atmosphere using dry solvents.

3.6.1. Synthesis of hydroxyphenyloxazoline derivatives

3.6.1.1. Synthesis of *N*-2-hydroxyethyl-4-hydroxybenzamide (I) and of chiral *R*-(-) (II), *S*-(+) (III) and racemic (\pm) (IV) -*N*-2-hydroxypropyl-4-hydroxybenzamides

These products were synthesized by reacting 1 mol of methyl-4-hydroxybenzoate with 2 mol of the corresponding amino alcohol at 140 °C for 4-6 h, according to literature³⁰². The methanol obtained and the excess of amino alcohol were distilled under rotative vacuum, and the solids obtained were recrystallized from ethanol or purified by column chromatography (silica gel; ethanol/water = 9:1) and dried in an oven under vacuum at room temperature for 8 h.

Characterization data were as follows (for NMR attributions see Figure 40, section 4.5.2):

Product (I):

Yield 80%. Melting point: 153°-155°C. Elemental analysis (calculated values in parentheses): C (59.67) 59.41; H (6.08) 6.18, N (7.73) 7.87. IR (KBr): 3500-2750 cm⁻¹ (v -OH); 3380 and 3240 cm⁻¹ (v NH); 2980-2930 cm⁻¹ (v CH aliphatic); 1615 cm⁻¹ (v C=O amide I); 1570 cm⁻¹ (v N-H amide II); 1600 and 1510 cm⁻¹ (v C=C of the aromatic ring). ¹H-NMR (DMSO-d₆): δ 9.7 (s, 1H, C₆H₄-OH); 8.2 (t, 1H, NHCO); 7.7-6.8 (m, 4H, H(2',3',5',6')); 4.8 (s, 1H, CH₂OH); 3.5 (m, 2H, H(5'')); 3.3 (m, 2H, H(4'')).

Product (II):

Yield 48%. Melting point: 148°-151°C. Elemental analysis (calculated values in parentheses): C (61.53) 60.94; H (6.71) 6.5, N (7.18) 7.1. IR (KBr): 3379 cm⁻¹ (v OH); 3243 cm⁻¹ (v NH secondary amide group); 3116 cm⁻¹ (v CH aromatic); 2976-2945 cm⁻¹ (v CH aliphatic); 1615 cm⁻¹ (v C=O amide I); 1584 and 1511 cm⁻¹ (breathing of the aromatic ring); 1537 cm⁻¹ (v NH amide II). ¹H-NMR (DMSO-d₆): δ 9.5 (s, 1H, C₆H₄-OH); 8.2 (t, 1H, NHCO); 7.8-6.9 (m, 4H, H(2',3',5',6')); 4.8 (s, 1H, CHOH); 3.9 (m, 1H, H(5'')); 3.3 (m, 2H, H(4'')), 1.2 (m, 3H, H(6'')). Specific Rotatory Power at

room temperature: $[\alpha]_{589} = -15.6^\circ$; $[\alpha]_{578} = -18.7^\circ$; $[\alpha]_{546} = -20.3^\circ$; $[\alpha]_{436} = -34.4^\circ$; $[\alpha]_{365} = -57.8^\circ$.

Product (III):

Yield 43%. Melting Point: 159° - 160°C . Elemental Analysis (calculated values in parentheses): C (61.53) 61.59; H (6.71) 6.73; N (7.17) 7.16. IR(KBr): 3378 cm^{-1} (ν OH); 3245 cm^{-1} (ν NH secondary amide group); 3122 cm^{-1} (ν CH aromatic); 2975 - 2944 cm^{-1} (ν CH aliphatic); 1615 cm^{-1} (ν C=O amide I); 1583 and 1509 cm^{-1} (breathing of the aromatic ring); 1537 cm^{-1} (ν NH amide II). $^1\text{H-NMR}$ (DMSO- d_6): δ 8.2 (t, 1H NHCO); 7.7-6.7 (m, 4H, $\text{H}(2',3',5',6')$); 4.7 (s, 1H, CHOH); 3.7 (m, 1H, $\text{H}(5'')$); 3.2 (m, 2H, $\text{H}(4'')$); 1.0 (m, 3H, $\text{H}(6'')$). Specific Rotatory Power at room temperature: $[\alpha]_{589} = 12.1^\circ$; $[\alpha]_{578} = 11.7^\circ$

Product (IV):

Yield 73%. Melting Point: 139° - 140°C . Elemental Analysis (calculated values in parentheses): C (61.53) 61.41; H (6.71) 6.91; N (7.17) 7.06. IR(KBr): 3364 cm^{-1} (ν OH); 3239 cm^{-1} (ν NH secondary amide group); 3127 cm^{-1} (ν CH aromatic); 2976 - 2940 cm^{-1} (ν CH aliphatic); 1617 cm^{-1} (ν C=O amide I); 1583 and 1509 cm^{-1} (breathing of the aromatic ring); 1538 cm^{-1} (ν NH amide II). $^1\text{H-NMR}$ (DMSO- d_6): δ 8.1 (t, 1H, NHCO); 7.7-6.7 (m, 4H, $\text{H}(2',3',5',6')$); 4.7 (s, 1H, CHOH); 3.7 (m, 1H, $\text{H}(5'')$); 3.1 (m, 2H, $\text{H}(4'')$); 1.0 (d, 3H, $\text{H}(6'')$).

3.6.1.2. Synthesis of 2-(4-hydroxyphenyl)-2-oxazoline (a) and of S-(+) (b), R-(-) (c) and (\pm) (d) -2-(4-hydroxyphenyl)-5-methyl-2-oxazolines

The synthesis of these products was performed according to literature³⁰² by reacting 1 mol of hydroxybenzamides (I-IV) dissolved in chilled (0°C) methylene chloride with 3 mol of freshly distilled thionyl chloride. Then the reaction mixture was kept at 0°C for 30 min and stirred at room temperature for additional 21 h. The product obtained was filtered on gooch, washed several times with CH_2Cl_2 and then added portionwise to a 0.4 M solution of NaHCO_3 in water (caution: effervescence was observed due to CO_2 evolution). The mixture was stirred for additional 30 min and filtered on gooch. The solid product was dried in an oven under vacuum at 60°C .

The products obtained showed the following characterization data (for NMR attributions see Figure 40, section 4.5.2):

Product (a):

Yield 63%. Melting Point: 215°-218°C. Elemental analysis (calculated values in parentheses): C (66.26) 66.07; H (5.52) 5.60; N (8.59) 8.49. IR (KBr): 3555-3342 cm^{-1} (v OH); 3044 cm^{-1} (v CH aromatic); 2995-2912 cm^{-1} (v CH aliphatic); 1635 cm^{-1} (v C=N oxazoline); 1607 cm^{-1} and 1510 cm^{-1} (v C=C); 1483 cm^{-1} , 1391 cm^{-1} , 1369 cm^{-1} and 1331 cm^{-1} (δ CH aliphatic). UV (THF): $\lambda_{\text{max}} = 257 \text{ nm}$. $^1\text{H-NMR}$ (DMSO- d_6): δ 10.0 (s, 1H, C₆H₄-OH); 7.7-6.8 (m, 4H, H(2',3',5'6')); 3.8-4.4 (m, 4H, H(4'',5'')).

Product (b):

Yield 76%. Melting Point: 200°-202°C. Elemental analysis (calculated values in parentheses): C (67.78) 66.51; H (6.26) 6.29; N (7.90) 7.63. IR (film on KBr): 3584-3333 cm^{-1} (v OH); 3059 cm^{-1} (v CH aromatic); 2976-2880 cm^{-1} ; (v CH aliphatic); 1635 cm^{-1} (v C=N oxazoline); 1604 cm^{-1} and 1516 cm^{-1} (v C=C of the aromatic ring); 1452 cm^{-1} and 1374 cm^{-1} and 1344 cm^{-1} (δ CH); 681 cm^{-1} (δ C=C). $^1\text{H-NMR}$ (DMSO- d_6): δ 10.1 (s, 1H, C₆H₄-OH); 7.8-6.9 (m, 4H, H(2',3',5',6')); 4.8 (m, 1H, H(5'')), 4.1 (m, 1H, H(4'')); 3.5 (m, 1H, H(4'')), 1.4 (m, 3H, H(6'')). Specific Rotatory Power at room temperature: $[\alpha]_{578} = +38.8^\circ$; $[\alpha]_{589} = +36.3^\circ$; $[\alpha]_{546} = +45.3^\circ$; $[\alpha]_{436} = +92.8^\circ$; $[\alpha]_{365} = +185.8^\circ$.

Product (c):

Yield 92%. Melting Point: 204°-206°C. Elemental analysis (calculated values in parentheses): C (67.78) 67.75; H (6.26) 6.25; N (7.90) 7.85. IR (KBr): 3433 cm^{-1} (v OH); 3072-3052 cm^{-1} (v CH aromatic); 2976-2879 cm^{-1} ; (v CH aliphatic); 1634 cm^{-1} (v C=N oxazoline); 1603 cm^{-1} and 1516 cm^{-1} (v C=C of the aromatic ring); 1452 cm^{-1} , 1374 cm^{-1} and 1344 cm^{-1} (δ CH); 680 cm^{-1} (δ C=C). $^1\text{H-NMR}$ (DMSO- d_6): δ 10.0 (s, 1H C₆H₄OH); 7.7-6.8 (4H, H(2',3',5'6')); 4.8 (m, 1H, H(5'')); 4.0 (m, 1H, H(4'')); 3.4 (1H, H(4'')); 1.3 (m, 3H, H(6'')). Specific Rotatory Power at room temperature: $[\alpha]_{589} = -28.1^\circ$; $[\alpha]_{578} = -30.5^\circ$

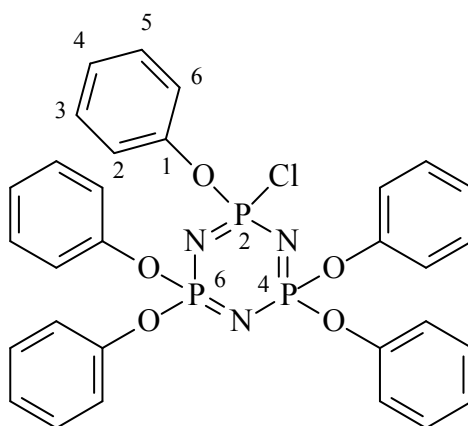
Product (d):

Yield 58%. Melting Point: 214°-217°C. Elemental analysis (calculated values in parentheses): C (67.78) 67.21; H (6.26) 6.15; N (7.90) 7.80. IR (KBr): 3441 cm^{-1} (v OH); 3072-3045 cm^{-1} (v CH aromatic); 2972-2891 cm^{-1} ; (v CH aliphatic); 1630 cm^{-1}

(ν C=N oxazoline); 1606 cm^{-1} and 1509 cm^{-1} (ν C=C of the aromatic ring); 1464 cm^{-1} , 1371 cm^{-1} and 1335 cm^{-1} (δ CH); 685 cm^{-1} (δ C=C). $^1\text{H-NMR}$ (DMSO- d_6): δ 10.1 (s, 1H, C₆H₄OH); 7.7-6.8 (m, 4H, H(2',3',5',6')); 4.8 (m, 1H, H(5'')); 4.0 (m, 1H, H(4'')); 3.4 (m, 1H, H(4'')); 1.3 (m, 3H, H(6'')).

3.6.2. Synthesis of chlorophosphazenes

3.6.2.1. Synthesis of pentakis(phenoxy)monochlorocyclophosphazene, C-1-Cl (1)



The synthesis of this cyclophosphazene has been carried out following literature¹. Yield = 72%. Elemental analysis (calculated values in parentheses): C: 57.09 (56.74); H 3.98 (3.96); N 6.54 (6.62). Melting point = 68°C . I.R. (Nujol): 3060 cm^{-1} (ν CH aromatic); 1605 and 1506 cm^{-1} (ν C=C); 1269 - 1179 cm^{-1} (ν P=N); 1050 cm^{-1} (δ CH aromatic); 947 cm^{-1} (ν P-O-Ph). $^1\text{H NMR}$ (CDCl₃): δ =7.29-6.90 (m, phenyl). $^{31}\text{P NMR}$ (CDCl₃): δ 22.53 (dd; $^2J_{\text{PP}} = 118\text{ Hz}$, $^2J_{\text{PP}} = 82\text{ Hz}$); 8.44 (d, $^2J_{\text{PP}} = 118\text{ Hz}$); 7.20 (d, $^2J_{\text{PP}} = 82\text{ Hz}$).

3.6.2.2. Synthesis of 2,2-dichloro-4,4,6,6-bis[spiro(2',2''-dioxo-1',1''-biphenyl)]-cyclophosphazene, C-2-Cl (2)

This compound was prepared as already described in section 3.5.1.3.

3.6.3. Synthesis of cyclophosphazene derivatives substituted with 2-oxazoline groups

The synthesis of OXA-containing cyclophosphazenes has been achieved basically with two different preparative strategies α and β , as described below:

3.6.3.1. Synthesis α : Reaction carried out in anhydrous THF in the presence of NaH 60% oil dispersion

In a three necked, round-bottomed flask, 1 eq of the selected chlorinated cyclophosphazene (1-3) was dissolved in anhydrous THF in the presence of 2 eq of NaH 60% oil-dispersion, and treated portionwise with 1.1-1.3 eq of solid hydroxyphenyl-2-oxazoline (a-d) (H_2 development was observed). Then the reaction mixture was refluxed for 24 h, allowed to cool to room temperature, filtered on gooch, and evaporated to dryness on a rotovap. The solid paste obtained was treated with methanol and filtered after 24 h standing. The solid residue was eventually washed with ethyl ether to give a white powder, that was analyzed and characterized.

3.6.3.2. Synthesis β : Synthesis carried out in anhydrous acetone in the presence of Cs_2CO_3

In a three-necked, round-bottomed flask of appropriate dimensions 1 eq of chlorinated cyclophosphazene and 1.1-1.2 eq of hydroxyphenyl-2-oxazoline (a-d) were suspended in anhydrous acetone under nitrogen. The reaction mixture was then refluxed until solubilization of the reagents was obtained. Eventually an excess (2.2-2.3 eq) of solid Cs_2CO_3 was added in one portion under a nitrogen blanket. The solution was stirred for 3 h and then cooled to room temperature. The solvent was finally evaporated on rotavapor. The solid paste obtained was dissolved in CH_2Cl_2 , filtered and evaporated to dryness. The solid residue was washed several times with small portions of a 10^{-2} M solution of NaOH, dissolved in methanol and evaporated to dryness.

3.6.3.3. Synthesis of pentakisphenoxy-mono-4-(oxazolinophenoxy)cyclophosphazene (1a) (C-1-OXA)

This product was prepared according to synthesis β . The characterization data are as follows: Yield 82% (deliquescent product). Elemental analysis (calculated values in parentheses): C (61.42) 61.60; H (4.36) 4.40; N (7.35) 7.31. IR (film on CsI): 3064 cm^{-1} (ν CH aromatic); $2976\text{-}2880\text{ cm}^{-1}$ (ν CH aliphatic); 1645 cm^{-1} (ν C=N of the oxazoline groups); 1589 cm^{-1} and 1485 cm^{-1} (ν C=C aromatic); 1461 cm^{-1} (ν CH aliphatic); $1261\text{-}1156\text{ cm}^{-1}$ (ν_{as} P=N); 1067 and 946 cm^{-1} (ν P-O-Ar). 1H -NMR (acetone- d_6): δ 7.78 (m, 2H, H(3',5')), 7.25 (m, 10H, H(3,5)), 7.17 (m, 5H, H(4)), 6.95 (m, 12H, H(2',6') and H(2,6)), 4.40 (t, 2H, H(5'')), 3.97 (t, 2H, H(4'')). ^{31}P -NMR (acetone- d_6):

δ 9.45 (m). ^{13}C -NMR (acetone- d_6): δ 162.73 (1C, C(2'')), 152.74 (1C, C(4')), 150.67, 150.64, 150.61, 150.56, 150.54 and 150.52 (6C (C1') and C(1)), 129.65, 129.62, 129.59, and 129.54 (12C, C(3',5') and C(3,5)), 125.77, 125.14, 125.13 and 125.11 (5C, C(4)), 120.87, 120.85, 120.84, 120.73, 120.71, 120.70 and 120.69 (12C, C(2,6) and C(2',6')), 67.53 (1C, C(5'')), 54.85 (1C, C(4'')).

3.6.3.4. Synthesis of chiral S-(+) pentakisphenoxy-mono[4-(5-methyl)-oxazolinophenoxy] cyclophosphazene (C-1-OXA S+) (1b)

This product was prepared according to synthesis β . The characterization data are as follows: Yield 61% (deliquescent product). Elemental Analysis (calculated values in parentheses): C (61.86) 61.58; H (4.54) 4.25; N (7.21) 7.00. IR (film on CsI): 3071 cm^{-1} (v CH aromatic); 2970-2867 cm^{-1} (v CH aliphatic); 1648 cm^{-1} (v C=N of the oxazoline group); 1590 cm^{-1} and 1484 cm^{-1} (v C=C aromatic groups); 1267-1157 cm^{-1} (v_{as} P=N); 1074 and 947 cm^{-1} (v P-O-Ar). ^1H - NMR (acetone- d_6): δ 7.77 (m, 2H, H(3',5')), 7.25 (m, 10H, H(3,5)), 7.17 (m, 5H, H(4)), 6.96 (m, 12H, H(2',6') and H(2,6)), 4.80 (m, 1H, H(5'')), 4.10 and 3.50 (2m, H(4''a) H(4''b)), 1.36 (d, 3H, CH₃). ^{31}P -NMR (acetone- d_6): δ 9.49 (m). ^{13}C -NMR (acetone- d_6): δ 161.86 (1C, C(2'')), 152.66 (1C, C(4')), 150.72, 150.67, 150.64, 150.60, 150.57 and 150.53 (6C (C1') and C(1)), 129.75, 129.64, 129.61, and 129.60, 129.46 (12C, C(3',5') and C(3,5)), 125.16, 125.10, 125.04 (5C, C(4)), 121.10, 120.84, 120.74, 120.70, 120.69 (12C, C(2,6) and C(2',6')), 76.17 (1C, C(5'')), 61.55 (1C, C(4'')), 20.49 (1C, CH₃). Specific Rotatory Power at room temperature: $[\alpha]_{578} = +3.72^\circ$; $[\alpha]_{589} = +4.57^\circ$

3.6.3.5. Synthesis of chiral R-(-) pentakisphenoxy-mono[4-(5-methyl)-oxazolinophenoxy] cyclophosphazene (C-1-OXA R-) (1c)

This product was prepared according to synthesis β . The characterization data are as follows: Yield 91%. (deliquescent product). Elemental analysis (calculated values in parentheses): C (61.86) 61.53; H (4.54) 4.29; N (7.21) 7.10. IR (film on CsI): 3068-3041 cm^{-1} (v CH aromatic); 2971-2870 cm^{-1} (v CH aliphatic); 1648 cm^{-1} (v C=N of the oxazoline group); 1591 cm^{-1} and 1489 cm^{-1} (v C=C aromatic groups); 1265-1157 cm^{-1} (v_{as} P=N); 1072 and 948 cm^{-1} (v P-O-Ar). ^1H -NMR (acetone- d_6): δ 7.73 (m, 2H, H(3',5')), 7.16 (m, 10H, H(3,5)), 7.11 (m, 5H, H(4)), 6.89 (m, 2H, H(2',6')), 6.93

(m, 10H, H(2,6)), 4.84 (m, 1H, H(5'')), 4.14 and 3.61 (2m, 2H, H(4''a and 4''b)), 1.42 (d, 3H, CH₃). ³¹P-NMR (acetone-d₆): δ 9.3 (m). ¹³C- NMR (acetone-d₆): δ 163.08 (1C, C(2'')), 152.86 (1C, C(4')), 150.50, 150.39, 150.24 (6C (C1') and C(1)), 129.52, 129.46, 129.39, 129.37, 129.34 (10C, C(3,5)), 129.45 (2C, C(3',5')), 125.49 (1C, C(4')), 125.22, 125.09, 125.02 (5C, C(4)), 121.27, 121.25, 121.23, 121.22, 121.19, 121.02, 120.99, 120.98, 120.96, 120.93 (10C, C(2,6)), 120.85 (2C, C(2'6')), 76.32 (1C, C(5'')), 61.67 (1C, C(4'')), 21.16 (1C, CH₃).

Specific Rotatory Power at room temperature: [α]₅₈₉ = -10.7°; [α]₅₇₈ = -11.8°.

3.6.3.6. Synthesis of racemic pentakisphenoxy-mono[4-(5-methyl)-oxazolinophenoxy]/cyclophosphazene (C-1-OXA±) (1d)

This product was prepared according to the synthesis β. The characterization data are as follows: Yield 70% (deliquescent product). Elemental Analysis (calculated values in parentheses): C (61.86) 61.54; H (4.54) 4.34; N (7.21) 7.26. IR (film on CsI): 3069 cm⁻¹ (ν CH aromatic); 2975-2864 cm⁻¹ (ν CH aliphatic); 1640 cm⁻¹ (ν C=N of the oxazoline group); 1587 cm⁻¹ and 1487 cm⁻¹ (ν C=C aromatic groups); 1272-1159 cm⁻¹ (ν_{as} -P=N-); 1067 and 945 cm⁻¹ (ν P-O-Ar). ¹H-NMR (acetone-d₆): δ 7.76 (m, 2H, H(3',5')), 7.25 (m, 10H, H(3,5)), 7.17 (m, 5H, H(4)), 6.96 (m, 2H, H(2',6')), 6.95 (m, 10H, H(2,6)), 4.85 (m, 1H, H(5'')), 4.08 and 3.53 (2m, 2H, H(4''a and 4''b)), 1.36 (d, 3H, CH₃). ³¹P-NMR (acetone-d₆): δ 9.43 (m). ¹³C-NMR (acetone-d₆): δ 161.86 (1C, C(2'')), 152.67 (1C, C(4')), 150.60 (6C (C1') and C(1)), 129.59 (10C, C(3,5)), 129.45 (2C, C(3',5')), 125.15, 125.09, 125.02 (5C, C(4)), 120.83 (10C, C(2,6)), 120.70 (2C, C(2'6')), 76.17 (1C, C(5'')), 61.53 (1C, C(4'')), 20.46 (1C, CH₃).

3.6.3.7. Synthesis of 2,2-bis(4-oxazolinophenoxy)-4,4,6,6-bis[spiro(2',2''-dioxo-1',1''-biphenyl)] cyclophosphazene (C-2-OXA) (2a)

The cyclophosphazene was prepared following method α, according to literature³⁰³. The characterization data are as follows: Yield 83%. Melting Point: 112°C. Elemental Analysis (calculated values in parentheses): C (60.95) 58.98; H (3.90) 3.78; N (8.46) 7.76. IR (KBr): 3059 cm⁻¹ (ν CH aromatic); 2969-2870 cm⁻¹ (ν CH aliphatic); 1645 cm⁻¹ (ν C=N of the oxazoline group); 1603 cm⁻¹ and 1500 cm⁻¹ (ν C=C aromatic); 1472 cm⁻¹ (ν CH aliphatic); 1272-1151 cm⁻¹ (ν_{as} P=N); 1088 and 943 cm⁻¹ (ν P-O-Ph).

$^1\text{H-NMR}$ (acetone- d_6): δ 8.00-7.10 (m, H_{ar} , 24H); 4.43 (t, O- CH_2 , 4H, $^3J_{\text{HH}} = 10.0$ Hz), 4.05 (t, N- CH_2 , 4H, $^3J_{\text{HH}} = 10$ Hz). $^{31}\text{P-NMR}$ (acetone- d_6): δ 11.14m, dd, $^2J_{\text{P,P}} = 90$ Hz, $^2J_{\text{P,P}} = 97$ Hz, P2; 26.79, d, $^2J_{\text{P,P}} = 94$ Hz and 26.75, d, $^2J_{\text{P,P}} = 93$ Hz, P4 and P6.

3.6.3.8. Synthesis of chiral [S-(+)] 2,2-bis[4-(5-methyl)-oxazolinophenoxy]-4,4,6,6-bis[spyro(2',2''-dioxo-1',1''-biphenyl)]cyclophosphazene (C-2-OXA S+) (2b)

The cyclophosphazene could be obtained with both the experimental procedures α and β described above. The characterization of the product gave the following results: Yield 78%. Melting Point: 219.7°C. Elemental Analysis (calculated values in parentheses): C (61.76) 59.26; H (4.24) 4.10; N (8.18) 7.52. IR (KBr): 3064 cm^{-1} (v CH aromatic); 2964-2864 cm^{-1} (v CH aliphatic); 1645 cm^{-1} (v C=N of the oxazoline group); 1598 cm^{-1} and 1498 cm^{-1} (v C=C of the aromatic groups); 1272-1167 cm^{-1} (ν_{as} P=N); 1094 and 930 cm^{-1} (v P-O-Ar). $^1\text{H-NMR}$ (acetone- d_6): δ 8.06 (4H, m, H(3',5')), 7.65 (d, 4H, H(5)), 7.49 (m, 4H, H(6)), 7.48 (d, 4H, H(2',6')), 7.41 (t, 4H, H(3)), 7.18 (t, 4H, H(4)), 4.87 (m, 2H, H(5'')), 4.09 and 3.55 (2m, 4H, H(4'')), 1.37 (d, 6H, CH_3). $^{31}\text{P-NMR}$ (acetone- d_6): δ 26.71 ($^2J_{\text{P,P}}$ 96 Hz), and 26.25, ($^2J_{\text{P,P}}$ 92 Hz): 2d, P4 and P6; 11.14 (dd, $^2J_{\text{P,P}}$ 97 and 90 Hz): P2. $^{13}\text{C-NMR}$ (acetone- d_6): δ 162.00 (2C, C(2'')), 152.74 (2C, C(4')), 147.94 (4C, C(6)), 129.98 (4C (2',6')), 122.25 (4C, C(5)), 129.69 (4C, C(3',5')), 128.52 (4C, C(1)), 126.41 (4C, C(3)), 126.05 (2C, C(1')), 121.83 (4C, C(4)), 121.08 (4C, C(3)), 76.27 (2C, C(5'')), 61.52 (4C, C(4'')), 20.42 (2C, CH_3). Specific Rotatory Power at room temperature: $[\alpha]_{578} = +7.81^\circ$; $[\alpha]_{589} = +7.18^\circ$.

3.6.3.9. Synthesis of chiral [R(-)] 2,2-bis[4-(5-methyl)-oxazolinophenoxy]-4,4,6,6-bis[spyro(2',2''-dioxo-1',1''-biphenyl)]cyclophosphazene (C-2-OXA R-) (2c)

The cyclophosphazene was prepared according to synthesis β described above. The characterization of the product gave the following results: Yield 74%. Melting Point: 214.4-216.0 °C. Elemental Analysis (calculated values in parentheses): C (61.76) 61.48; H (4.24) 4.25; N (8.18) 7.89). IR (KBr): 3060 cm^{-1} (v CH aromatic); 2971-2866 cm^{-1} (v CH aliphatic); 1650 cm^{-1} (v C=N of the oxazoline group); 1608 cm^{-1} and 1505 cm^{-1} (v C=C of the aromatic groups); 1230-1177 cm^{-1} (ν_{as} P=N); 1094 and 932 cm^{-1} (v P-O-Ar). $^1\text{H-NMR}$ (acetone- d_6): δ 8.06 (4H, m, H(3',5')), 7.68 (d, 4H, H(6)), 7.52 (m, 4H, H(3)), 7.51 (d, 4H, H(2',6')), 7.44 (t, 4H, H(4)), 7.21 (t, 4H, H(5)),

4.89 (m, 2H, H(5'')), 4.12 and 3.57 (2m, 4H, H(4'')), 1.40 (d, 6H, CH₃). ³¹P-NMR (acetone-d₆): δ 26.20 (²J_{P,P} 94 Hz) and 26.18 (²J_{P,P} 92 Hz), 2d, P4 and P6; 10.60 (dd, ²J_{P,P} 94 and 92 Hz), P2. ¹³C-NMR (acetone-d₆): δ 162.25 (2C, C(2'')), 153.13 (2C, C(1')), 148.35 (4C, C(2)), 121.51 (4C (2',6')), 122.25 (4C, C(5)), 130.12 (4C, C(3',5')), 128.93 (4C, C(1)), 121.49 (4C, C(3)), 126.45 (2C, C(4')), 126.83 (4C, C(4)), 121.49 (4C, C(3)), 76.68 (2C, C(5'')), 61.93 (4C, C(4'')), 20.83 (2C, CH₃). Specific Rotatory Power at room temperature: [α]₅₈₉ = -9.9°; [α]₅₇₈ = -11.7°.

3.6.3.10. Synthesis of racemic 2,2-bis[4-(5-methyl)-oxazolinophenoxy]-4,4,6,6-bis[spiro(2',2''-dioxy-1',1''-biphenyl)]cyclophosphazene (C-2-OXA ±) (2d)

This trimer was prepared according to both the above described α and β procedures. The characterization data are as follows: Yield 40 %. Melting Point: 214.3°C. Elemental analysis (calculated values in parentheses): C (61.76) 59.13; H (4.24) 4.20; N (8.18) 7.85. IR (KBr): 3069 cm⁻¹ (ν CH aromatic); 2965-2864 cm⁻¹ (ν CH aliphatic); 1645 cm⁻¹ (ν C=N of the oxazoline group); 1603 cm⁻¹ and 1503 cm⁻¹ (ν C=C aromatic ring); 1272-1172 cm⁻¹ (ν_{as} P=N); 1088 and 941 cm⁻¹ (ν P-O-Ar). ¹H NMR (acetone-d₆): δ 8.06 (m, 4H, H(3',5')), 7.66(d, 4H, H(5)), 7.749 (m, 8H, H(H2) and H(2',6')), 7.41 (t, 4H, H(H3)), 7.19 (m, 4H, H(4)), 4.78 (m, 2H, H(5'')), 4.10 and 3.55 (2m, 2H, H(4''a and 4''b)), 1.38 (d, CH₃). ³¹P NMR (acetone-d₆): δ 31,30 and 31,29 (2d, ²J_{P,P} 94 and 96 Hz, P4 and P6); 15,72 (dd, ²J_{P,P} 94 and 96 Hz, P2).

3.6.3.11. Synthesis of hexakis(oxazolinophenoxy)cyclophosphazene (C-6-OXA) (3a)

The synthesis of this product has been carried out following the procedure α, according to literature³⁰⁴. Melting Point: 221°C. Elemental Analysis (calculated values in parentheses): C (58.54) 57.92; H (4.34) 4.26; N (11.38) 11.58. IR (KBr): 3064 cm⁻¹ (ν CH aromatic); 2969-2878 cm⁻¹ (ν CH aliphatic); 1645 cm⁻¹ (ν C=N oxazoline groups); 1598 and 1505 cm⁻¹ (ν C=C); 1261-1156 cm⁻¹ (ν_{as} P=N); 943 cm⁻¹ (ν P-O-Ar). ¹H-NMR (acetone-d₆): δ 7.88 (d, 12H, H(3'5')), 7.10 (d, 12H, H(2',6')), 4.49 (t, 12H, H(5'')), 4.05 (t, 12H, H(4'')). ³¹P-NMR (acetone-d₆): δ 9.99.

3.6.3.12. Synthesis of chiral [*S*(+)]hexakis(4-(5-methyl)-oxazolinophenoxy)-cyclophosphazene (C-6-OXA *S*+) (3b)

This product was synthesized according to the procedure β . The characterization data are as follows: Yield 66%. Melting Point: 112°-116°C. Elemental Analysis (calculated values in parentheses): C (60.45) 59.61; H (5.07) 5.04; N (10.57) 10.6. IR (KBr): 3069 cm^{-1} (v CH aromatic); 2964-2843 cm^{-1} (v CH aliphatic); 1647 cm^{-1} (v C=N oxazoline); 1592 and 1505 cm^{-1} (v C=C); 1258-1156 cm^{-1} (ν_{as} P=N); 1067 and 943 cm^{-1} (v P-O-Ar). ^1H -NMR (acetone- d_6): δ 7.79 (m, 12H, H(3',5')), 6.99 (m, 12H, H(2'6')), 4.86 (m, 6H, H(5'')), 4.80 and 3.53 (2m, 12H, H(4''a and 4''b)), 1.38 (d, 18H, CH₃). ^{31}P -NMR (acetone- d_6): δ 9.33. ^{13}C -NMR (acetone- d_6): δ 161.74 (C(2'')), 152.29 (C (4')), 129.56 (C(3'5')), 125.90 (C (1')), 120.72 (C (2',6')), 76.26 (C(5'')), 61.55 (C(4'')), 20.45 (CH₃). Specific Rotatory Power at room temperature: $[\alpha]_{578} = +16.7^\circ$; $[\alpha]_{589} = +18.45^\circ$.

3.6.3.13. Synthesis of chiral [*R*(-)]hexakis(4-(5-methyl)-oxazolinophenoxy)-cyclophosphazene (C-6-OXA *R*-) (3c)

This product was synthesized according to the procedure β . The characterization data are as follows: Yield 80%. Melting Point: 109.6°-111.0°C. Elemental Analysis (calculated values in parentheses): C (60.45) 59.04; H (5.07) 5.05; N (10.57) 10.12. IR (KBr): 3072 cm^{-1} (v CH aromatic); 2971-2866 cm^{-1} (v CH aliphatic); 1648 cm^{-1} (v C=N oxazoline); 1605 and 1505 cm^{-1} (v C=C); 1262-1161 cm^{-1} (ν_{as} P=N); 1078 and 948 cm^{-1} (v P-O-Ar). ^1H -NMR (acetone- d_6): δ 7.90 (m, 12H, H(3',5')), 6.96 (m, 12H, H(2'6')), 4.85 (m, 6H, H(5'')), 4.14 and 3.59 (2m, 12H, H(4''a and 4''b)), 1.43 (d, 18H, CH₃). ^{31}P -NMR (acetone- d_6): δ 8.6. ^{13}C -NMR (acetone- d_6): δ 162.94 (C(2'')), 152.46 (C (4')), 129.67 (C(3'5')), 125.24 (C (1')), 120.67 (C (2',6')), 76.37 (C(5'')), 61.64 (C(4'')), 20.10 (CH₃). Specific Rotatory Power at room temperature: $[\alpha]_{589} = -24.6^\circ$; $[\alpha]_{578} = -26.4^\circ$.

3.6.3.14. Synthesis of racemic hexakis[4-(5-methyl)-oxazolinophenoxy]-cyclophosphazene (C-6-OXA \pm) (3d)

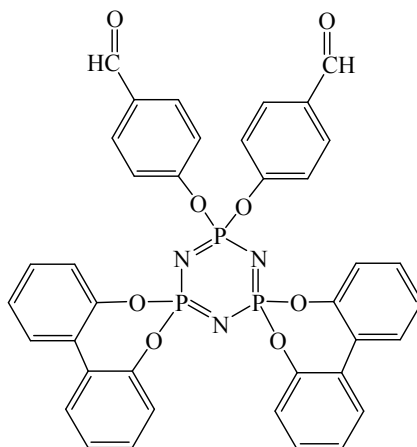
The product was obtained following procedure β . The characterization data are as follows. Yield 74 %. Melting Point: 78-81°C. Elemental Analysis (calculated values in

parentheses): C (60.45) 58.71; H (5.07) 4.92; N (10.57) 10.33. IR (KBr): 3064 cm^{-1} (ν CH aromatic); 2954-2870 cm^{-1} (ν CH aliphatic); 1645 cm^{-1} (ν C=N of the oxazoline groups); 1587 and 1503 cm^{-1} (ν C=C); 1256-1158 cm^{-1} (ν_{as} P=N); 1077 and 943 cm^{-1} (ν P-O-Ar). ^1H -NMR (acetone- d_6): δ 7.79 (m, 12H, H(3',5')), 6.99 (m, 12H, H(2'6')), 4.86 (m, 6H, H(5'')), 4.80 and 3.53 (2m, 12H, H(4''a and 4''b)), 1.38 (d, 18H, CH_3). ^{31}P -NMR (acetone- d_6): δ 9.32. ^{13}C -NMR (acetone- d_6): δ 161.7 (C(2'')), 152.25 (C(4')), 129.56 (C(3'5')), 125.90 (C(1')), 120.73 (C(2',6')), 76.26 (C(5'')), 61.55 (C(4'')), 20.45 (CH_3).

3.7. EXPERIMENTAL SECTION FOR THE SYNTHESIS OF SUPRAMOLECULAR RODS VIA HALOGEN BONDING-BASED SELF-ASSEMBLY OF FLUORINATED PHOSPHAZENE NANOPILLARS (CHAPTER 4.6)

Unless otherwise specified, all the synthetic reactions hereby reported were performed under nitrogen atmosphere using dry solvents.

3.7.1. Synthesis of 2,2-bis(4-formylphenoxy)-4,4,6,6-bis[spiro(2',2''-dioxo-1',1''-biphenyl)]cyclophosphazene (C-2-pCHO, MW = 745.55)

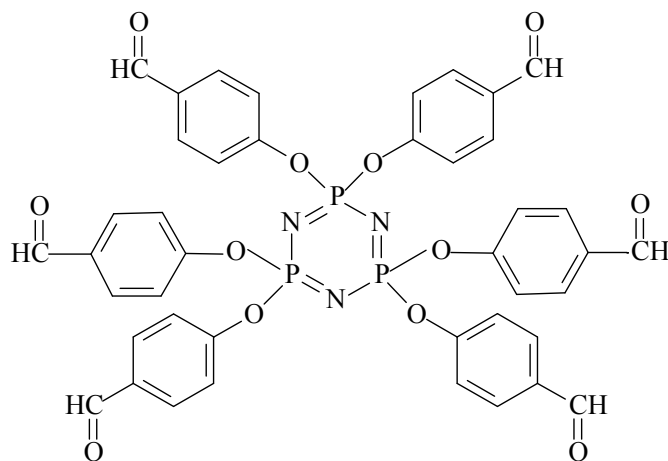


C-2-Cl (2 g, 3.5 mmol; see section 3.5.1.3 for preparation), sodium hydride (60% dispersion in mineral oil, 0.42 g, 10.5 mmol) and TEAB (0.02 g, 0.1 mmol) were dissolved in 50 ml of anhydrous THF, and a solution of 4-hydroxybenzaldehyde (1.28 g, 10.5 mmol) in 50 ml of anhydrous THF was added dropwise causing hydrogen evolution. The mixture was stirred overnight at room temperature and filtered on a gooch, washing the filtered solid with THF. The solution was brought to dryness under

reduced pressure, and the solid thus obtained was washed with distilled water, filtered on a gooch, washed with diethyl ether and finally dried under vacuum.

Yield: 93% (2.67 g). Elemental analysis (theoretical values in parentheses): C 61.10 (61.22); H 3.43 (3.51); N 5.58 (5.64). FT-IR (KBr): 1703 cm^{-1} (ν C=O); 1177-1206 cm^{-1} (ν_{as} P=N); 973 cm^{-1} (ν P-O-Ph); 1500-1600 cm^{-1} (ν aromatic C=C). ^1H NMR (DMSO): 10.02 ppm (s, CHO); 8.12-7.17 ppm (m, aromatic). $\{^1\text{H}\}$ ^{31}P NMR (DMSO): δ 25.57 (d, $^2J_{\text{P,P}} = 93.4$ Hz, biphenoxy-substituted P); 9.34 (dd, $^2J_{\text{P,P}} = 91.1$ and 97.8 Hz, formylphenoxy-substituted P).

3.7.2. Synthesis of hexakis(4-formylphenoxy)cyclophosphazene (C-6-pCHO, MW=861.66)

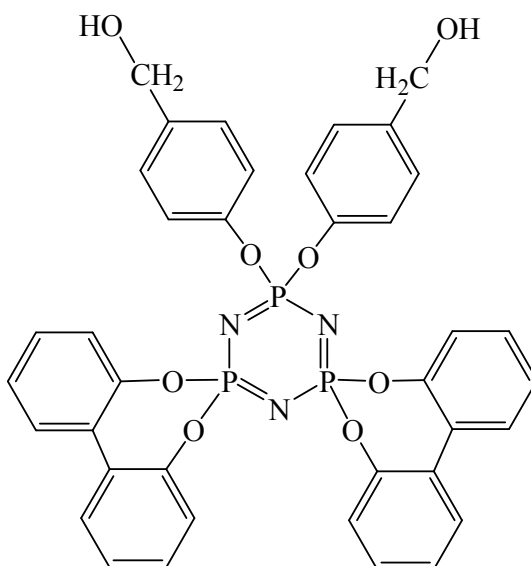


HCCP (2 g, 5.7 mmol), sodium hydride (60% dispersion in mineral oil, 1.52 g, 38.0 mmol) and TEAB (0.02 g, 0.1 mmol) were dissolved in 50 ml of anhydrous THF, and a solution of 4-hydroxybenzaldehyde (4.64 g, 38.0 mmol) in 50 ml of anhydrous THF was added dropwise causing hydrogen evolution. The mixture was stirred overnight at room temperature and filtered on a gooch, washing the filtered solid with THF. The solution was brought to dryness under reduced pressure, and the solid thus obtained was washed with distilled water, filtered on a gooch, washed with diethyl ether and finally dried under vacuum.

Yield: 91% (4.52 g). Elemental analysis (theoretical values in parentheses): C 58.10 (58.55); H 3.32 (3.51); N 4.70 (4.87). FT-IR (KBr): 1705 cm^{-1} (ν C=O); 1178 cm^{-1} (ν_{as} P=N); 962 cm^{-1} (ν P-O-Ph); 1500-1600 cm^{-1} (ν aromatic C=C). ^1H NMR (DMSO):

δ 9.93 (s, CHO); 7.82-7.16 (AA'BB' pattern, aromatic). $\{^1\text{H}\} \text{ } ^{31}\text{P}$ NMR (DMSO): δ 8.46 (s).

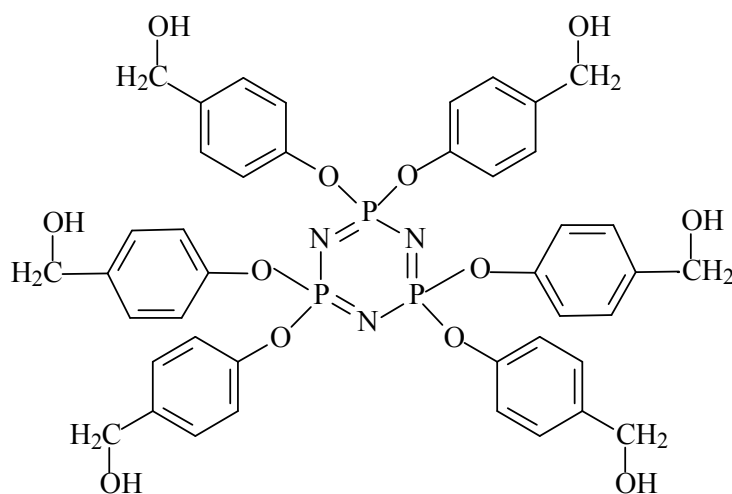
3.7.3. Synthesis of 2,2-bis(4-hydroxymethylenphenoxy)-4,4,6,6-bis[spyro(2',2''-dioxo-1',1''-biphenyl)]cyclotriphosphazene (C-2-pOH, MW = 749.58)



C-2-pCHO (2 g, 2.7 mmol; see section 3.7.1 for preparation) was dissolved in 150 ml of anhydrous THF, then a suspension of lithium borhydride (0.18 g, 8.3 mmol) in 30 ml of anhydrous THF was added dropwise. The mixture was stirred overnight at room temperature, then the solvent was evaporated under reduced pressure. The white solid thus obtained was treated with 50 ml of distilled water for an hour, filtered on a buchner, washed with distilled water and then with diethyl ether, and finally dried under vacuum.

Yield: 88% (1.60 g). Elemental analysis (theoretical values in parentheses): C 60.73 (60.89); H 4.00 (4.03); N 5.51 (5.61). FT-IR (KBr): 3374 cm^{-1} (ν OH); 1200-1168 cm^{-1} (ν_{as} P=N); 959 cm^{-1} (ν P-O-Ph). ^1H NMR (DMSO): 7.72-7.14 (m, aromatic); 5.29 (OH); 4.53 (CH_2). $\{^1\text{H}\} \text{ } ^{31}\text{P}$ NMR (DMSO): 26.26 ppm (d, $^2J_{\text{P,P}} = 93.4$ Hz; biphenoxy-substituted P); 10.87 ppm (dd, $^2J_{\text{P,P}} = 88.9$ e 94.3 Hz; hydroxymethylenphenoxy-substituted P).

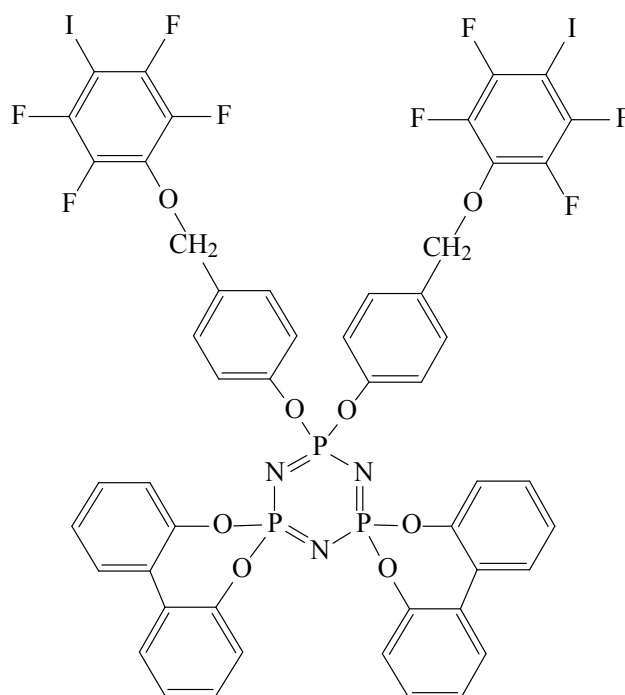
3.7.4. Synthesis of hexakis(4-hydroxymethylenphenoxy)cyclophosphazene (C-6-pOH, MW = 873.78)



C-6-pCHO (2 g, 2.3 mmol; see section 3.7.2 for preparation) was dissolved in 150 ml of anhydrous THF, then a suspension of lithium borhydride (0.50 g, 23 mmol) in 30 ml of anhydrous THF was added dropwise. The mixture was stirred overnight at room temperature, then the solvent was evaporated under reduced pressure. The white solid thus obtained was treated with 50 ml of distilled water for an hour, filtered on a buchner, washed with distilled water and then with diethyl ether, and finally dried under vacuum.

Yield: 95% (1.93 g). Elemental analysis (theoretical values in parentheses): C 57.43 (57.74); H 4.71 (4.85); N 4.68 (4.81). FT-IR (KBr): 3346 cm^{-1} (v OH); 1200-1168 cm^{-1} (v_{as} P=N); 959 cm^{-1} (v P-O-Ph). ^1H NMR (DMSO): δ 7.22-6.78 (AA'BB' pattern, aromatic); 5.23 (t, OH); 4.47 (CH_2). $\{^1\text{H}\}^{31}\text{P}$ NMR (DMSO): δ 9.79 (s).

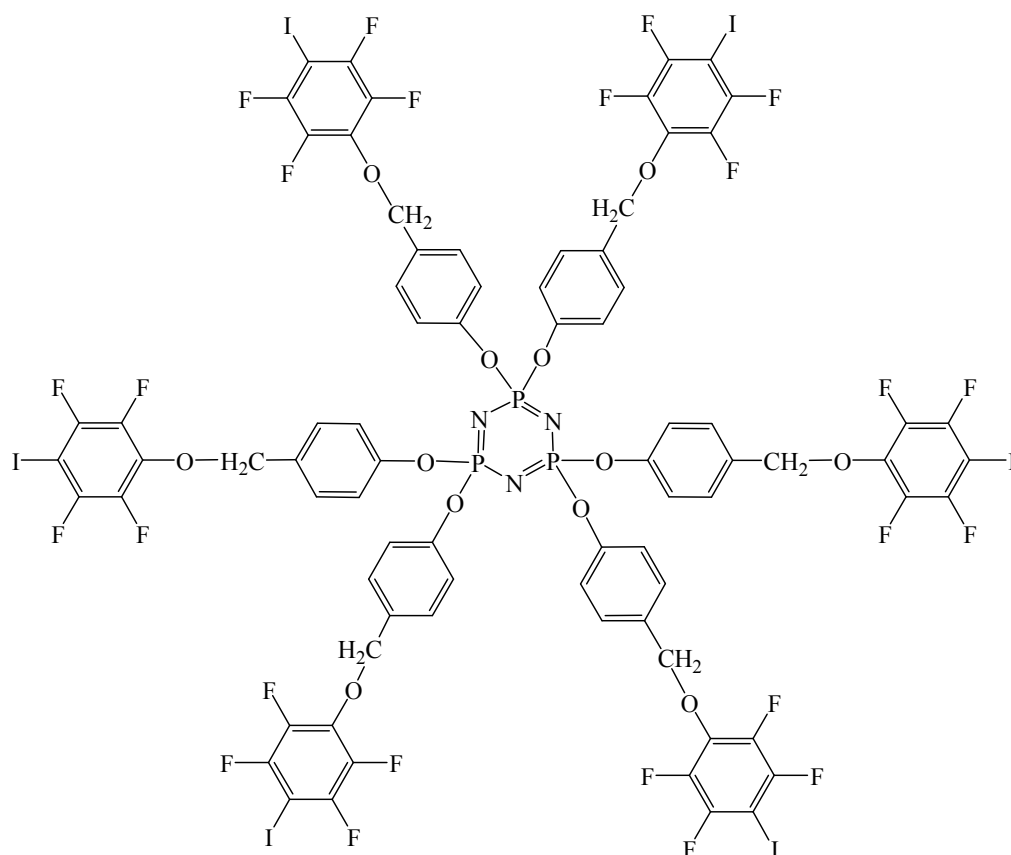
3.7.5. Synthesis of 2,2-bis[4-(2,3,5,6-tetrafluoro-4-iodophenoxymethylen)phenoxy]-4,4,6,6-bis[spiro(2',2''-dioxy-1',1''-biphenyl)]cyclophosphazene (C-2-ITFB, MW = 1297.49)



C-2-pOH (1.00 g, 1.3 mmol; see section 3.7.3 for preparation) and cesium carbonate (1.10 g, 3.4 mmol) were suspended in 4 ml (8.82 g, 30.0 mmol) of iodopentafluorobenzene, and the mixture was stirred at 150°C for 5.5 hours. Then it was filtered on a gooch and the solid was washed with diethyl ether. Evaporation to dryness of the iodopentafluorobenzene (in vacuo at 70°C) and of the diethyl ether used for washing (by means of a rotatory evaporator) yielded a colorless solid that was repeatedly washed with n-hexane and finally dried under vacuum.

Yield: 90%, 1.56 g. FT-IR (KBr): 2955-2884 (ν alkylic CH), 1608, 1508, 1483 cm^{-1} (ν aromatic C=C), 1230-1176 cm^{-1} (ν_{as} P=N), 1094 cm^{-1} (ν CF), 948 cm^{-1} (ν P-O-Ph). ^1H NMR (CDCl_3): δ 7.58-7.04 (m, aromatic CH); 5.28 (s, CH_2). $\{^1\text{H}\}^{31}\text{P}$ NMR (CDCl_3): δ 25.99 ppm (d, $^3J=93.8$ Hz, biphenyl-substituted P); 10.10 ppm (dd, $^3J=95.9$ and 90.1 Hz, phenol-substituted P). ^{19}F NMR (CDCl_3): -122.68 ppm (F in 3 and 5 positions: d, $^3J_{\text{F,F}}=53.5$ Hz); -154.82 ppm (F in 2 and 6 positions: d, $^3J_{\text{F,F}}=56.9$ Hz)

3.7.6. Synthesis of hexakis[4-(2,3,5,6-tetrafluoro-4-iodophenoxy)methylen]phenoxy-cyclophosphazene (C-6-ITFB, MW = 2517.47)



C-6-pOH (1.00 g, 1.1 mmol; see section 3.7.4 for preparation) and cesium carbonate (2.60 g, 8.0 mmol) were suspended in 5 ml (11.02 g, 37.5 mmol) of iodopentafluorobenzene, and the mixture was stirred at room temperature for 15 days. A white precipitate separated from the milk-like suspension. The mixture was brought to dryness obtaining a white solid, which was washed three times with 10 ml of n-hexane and dried under vacuum.

Yield: 92% (2.70g). FT-IR (KBr): 2950-2884 (ν alkylic CH), 1609, 1507, 1483 cm^{-1} (ν aromatic C=C), 1201-1180 cm^{-1} (ν_{as} P=N), 1095 cm^{-1} (ν CF), 955 cm^{-1} (ν P-O-Ph). ^1H NMR (CD_2Cl_2): δ 7.33, 7.29 and 6.97, 6.93 (AA'BB' pattern, aromatic), 5.19 (s, CH_2). $\{^1\text{H}\}^{31}\text{P}$ NMR (CD_2Cl_2): δ 9.29 ppm (s). ^{19}F NMR (CD_2Cl_2): δ -122.27 (d, $^3J_{\text{F,F}}=39$ Hz; CFCD); -155.66 (d, $^3J_{\text{F,F}}=20$ Hz; CF_2CO). $\{^1\text{H}\}^{13}\text{C}$ NMR (CD_2Cl_2): δ 150.74 (s, OC_{Ph}); 121.06 (s, $(\text{OCCH})_{\text{Ph}}$); 129.72 (s, $(\text{OCCHCH})_{\text{Ph}}$); 132.53 (s, $\text{CH}_2\text{C}_{\text{Ph}}$); 76.29 (s, CH_2); 137.48 (dd, $^2J_{\text{C,F}}=12$ Hz, $^3J_{\text{C,F}}=4$ Hz, OC_{ArF}); 140.84 (d, $^1J_{\text{C,F}}=263$ Hz, $(\text{OCCF})_{\text{ArF}}$); 147.32 (d, $^1J_{\text{C,F}}=245$ Hz, $(\text{OCCFCF})_{\text{ArF}}$); 64.41 (dd, $^2J_{\text{C,F}}=28$ Hz, $^3J_{\text{C,F}}=4$ Hz, IC_{ArF}).

3.7.7. Self-assembly

The vapor-liquid diffusion technique was used for the crystalization of complexes C1 and C2 (see Figure 76, section 4.6.3) Nearly saturated chloroform solutions of C-6-pITFB (20 mg, 0.008 mmol in 2 ml of CHCl_3) and of pyridine derivative DPy (3.8 mg, 0.024 mmol) or DPE (5.3 mg, 0.024 mmol) were mixed in a clear borosilicate vial. The opened vial was then closed in a cylindrical wide-mouth bottle containing carbon tetrachloride and the solvents were allowed to diffuse at room temperature until crystal formation occurred (3 days for C1, 6 days for C2) The crystals were filtered off the mother liquors (from which one to two further crystal fractions can be obtained in the same manner), washed with *n*-pentane and rapidly dried in the air at room temperature. Characterization is as follows.

a) C1 (with DPy)

Colourless crystal. Melting point: 170-173°C. FTIR (pure): 3043 cm^{-1} (ν C-H Py), 2958-2889 cm^{-1} (ν CH_2), 1590, 1533, 1474 cm^{-1} (ν aromatic C=C), 1200, 1177 (ν_{as} P=N), 1089 cm^{-1} (ν C-F), 994 cm^{-1} (Py ring wag), 951 cm^{-1} (P-O-C). ^1H NMR: δ 5.17 (s, CH_2 , 12H); 6.91, 6.95 and 7.27, 7.29 (AA'BB' pattern, Ph, 24H); 7.53, 7.55 and 8.73, 8.75 (AA'BB' pattern, Py, 24H). ^{19}F NMR: *conc.* 0.02 mol/l: δ -121.98 ($^3J_{\text{F,F}} = 20$ Hz, m, CFCl); -154.78 ($^3J_{\text{F,F}} = 20$ Hz, m, CFCO); *conc.* 0.01 mol/l: δ -121.97 ($^3J_{\text{F,F}} = 20$ Hz, m, CFCl); -154.77 ($^3J_{\text{F,F}} = 20$ Hz, m, CFCO).

b) C2 (with DPE)

Colourless crystal. Melting point: 190-193°C. FTIR (pure): 3030 cm^{-1} (ν C-H Py), 2952-2889 cm^{-1} (ν CH_2), 1596, 1474 cm^{-1} (ν aromatic C=C), 1202, 1178 cm^{-1} (ν_{as} P=N), 1092 cm^{-1} (ν C-F), 997 cm^{-1} (Py ring wag), 949 cm^{-1} (P-O-C). ^1H NMR: δ 5.17 (s, CH_2 , 12H); 6.91, 6.95 and 7.27, 7.29 (AA'BB' pattern, Ph, 24H); 7.19 (s, $\text{CH}=\text{CH}$, 12H); 7.36, 7.38 and 8.61, 8.63 (AA'BB' pattern, Py, 24H). ^{19}F NMR: *conc.* 0.02 mol/l: δ -121.99 ($^3J_{\text{F,F}} = 20$ Hz, m, CFCl); -154.78 ($^3J_{\text{F,F}} = 20$ Hz, m, CFCO); *conc.* 0.01 mol/l: δ -121.98 ($^3J_{\text{F,F}} = 20$ Hz, m, CFCl); -154.77 ($^3J_{\text{F,F}} = 20$ Hz, m, CFCO).

CHAPTER 4

RESULTS AND DISCUSSION

In the first part of this chapter (sections 4.1 to 4.4) we will present the results obtained during our investigations on the surface functionalization of silicon-based substrates (*i.e.* crystalline (100) silicon wafers, sodalime glasses and silica gel beads) and organic polymer plates (*i.e.* HDPE, PA6 and EVOH) using different experimental approaches. In the successive sections (4.5 and 4.6) of this chapter we will present two additional works carried out during this thesis aimed to obtain new phosphazene-based materials using chiral and non chiral oxazoline derivatives and supramolecular techniques.

4.1. SURFACE FUNCTIONALIZATION OF SODALIME GLASSES AND CRYSTALLINE SILICON (100) WAFERS WITH CHLOROPHOSPHAZENES: A THEORETICAL AND EXPERIMENTAL APPROACH

4.1.1. Preliminary considerations

The research on the surface functionalization of silicon-based materials with hexachlorocyclophosphazene was originated by the early observation that, during the thermally-induced ring-opening polymerization of HCCP to polydichlorophosphazene^{1,18}, the glass walls of the reactor play an important role in determining the final reproducibility of the overall process^{305,306}. This fact seems to suggest that a sort of interaction takes place between the chlorophosphazene and the surface of the sealed flask.

Starting from this point we carried out some simple preliminary experiments based on the immersion of carefully cleaned sodalime glasses into 0.1M HCCP solutions in anhydrous solvents to observe the deposition of cyclophosphazene-based films on the glass surface^{6,7,307}. Successive XPS analyses demonstrated the following important facts: *i*) HCCP on the glass surface can be analytically detected by XPS technique even at the high vacuum conditions prevailing during the analysis (3×10^{-8} Pa), while any attempt aimed at the determination of the XPS spectrum of neat HCCP under comparable conditions failed due to the high sublimation rate of this compound¹; this

fact seems to indicate that a genuine chemisorption takes place between the glass surface and the cyclophosphazene derivative instead of a simple physical adsorption process (physisorption); *ii*) the original elemental ratio of HCCP, *i.e.* Cl : P : N = 2 : 1 : 1, after the surface treatment of the sodalime glass slides, became close to 1 : 1 : 1; *iii*) carrying out the XPS characterizations long after the functionalization led to a significant decrease in the number of surface Cl atoms; in fact the initial Cl : P : N = 1 : 1 : 1 ratio rapidly declined to $x : 1 : 1$, where $x < 1$.

We then extended the same type of surface functionalization experiments to Si (100) wafers, to obtain results that were comparable to those presented above for the sodalime glasses.

On the basis of these preliminary findings, it may be hypothesized that putting HCCP in contact with the surface of silicon-based materials, a surface reaction takes place between the free hydroxyl groups existing on the surface of these substrates and HCCP. This may lead to the formation of P-O-Si bonds according to the simplified reaction scheme reported in Figure 22, in which three chlorines may react with surface hydroxylic groups to deliver the corresponding amount of hydrochloric acid and leaving unreacted the external chlorines of HCCP.

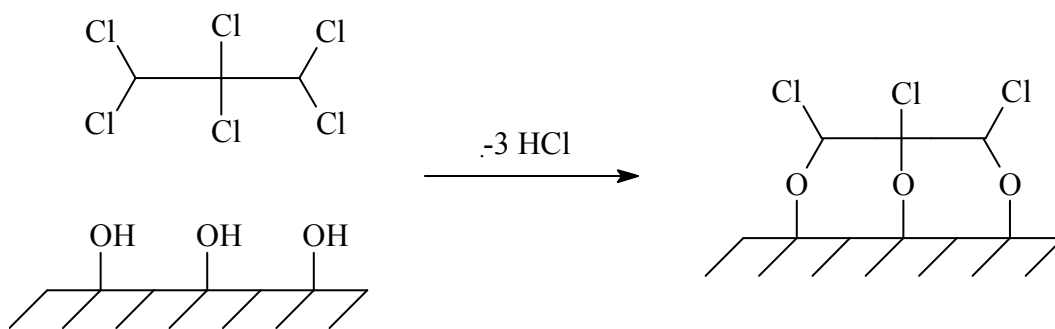


Figure 22. Hypothesis of reaction between HCCP and surface silanols based on our preliminary findings.

The driving force for this reaction may be provided by the cyclophosphazene itself present in the reaction mixture in a rather high concentration, because of the well known basicity features of this compound³⁰⁸. Given the documented reactivity of HCCP with water under a variety of experimental conditions^{199,309-312}, it is also plausible for water molecules adsorbed on the surface of silicon-based materials to influence the functionalization process. In addition, the variation of P : N : Cl ratios on the silicon-

based surfaces over time was attributed to surface hydrolysis of the residual chlorines induced by environmental moisture, to deliver HCl molecules and form P-OH groups, according to Figure 23.

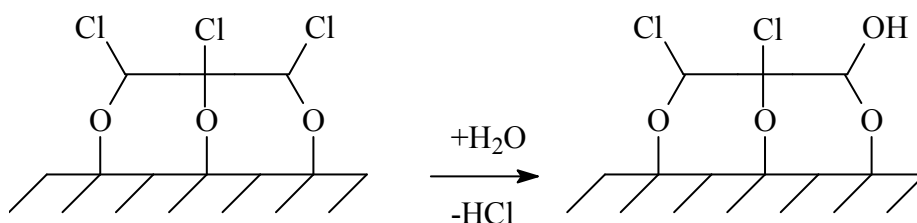


Figure 23. Hydrolysis of surface-bound HCCP derivative by the action of environmental moisture.

In spite of the fact that some aspects regarding the functionalization reaction of silicon-based surfaces with HCCP were still not fully understood (*e.g.* $\equiv\text{Si-OH}$ groups are reported to be not very much reactive towards P-Cl moieties³¹³, and the thickness of the HCCP layer deposited on the surface seemed to be not monomolecular, as it could be expected on the basis of the above reported Figure 22⁶), this process could be extremely important for the perspectives offered in the field of surface functionalization. In fact, an almost unlimited number of nucleophiles could be used to replace the residual chlorines present on the surface-grafted phosphazene derivative; furthermore, other phosphazene substrates (*e.g.* $\text{N}_4\text{P}_4\text{Cl}_8$, $\text{Cl}_2\text{NP(O)Cl}_3$, and $(\text{NPCl}_2)_n$) could be in principle exploited. These considerations prompted us to further investigate the subject, both by a theoretical simulation of the reaction of HCCP with a paradigmatic hydroxylated silicon-based surface, and by new experimental tests.

Semi-empirical quantum-mechanical PM3 methods^{314,315} have therefore been applied in order to qualitatively evaluate the interaction between HCCP and mono-hydroxyl $(\text{CH}_3)_3\text{Si}_4\text{O}_6\text{OH}$ or $(\text{CH}_3)_3\text{SiOH}$ species⁷. By starting with selected initial configurations and optimizing the system geometry, one can obtain useful information about the possibility of forming (cyclo)P-O-Si(cluster) bonds and can identify the most promising reaction pathways. Nevertheless, although semi-empirical methods allow to elucidate important qualitative properties at low computational costs, they are generally affected by severe limitations, since they are based on relevant simplifications and approximations (*e.g.* in the description of hypervalent S and P atoms, transition metals, nitro compounds, π - π interactions, induction attraction, lone pair interactions,

anisotropic short-range repulsion, ...) ³¹⁶. In order to get more accurate and reliable results, particularly concerning interaction energies, one has to adopt a non-empirical *ab initio* approach, which allows a quantum mechanical description (including electron correlation) of the electronic systems.

In this section we report first on such *ab initio* calculations, and subsequently on new surface functionalization experiences, carried on fused quartz samples and specifically conceived to provide a deeper insight into this not yet fully understood scientific issue.

4.1.2. Ab initio calculations

4.1.2.1. Structure of the HCCP molecule

In order to test the *ab initio* method here employed (see section 3.2.1), the structural properties of the free HCCP molecule were preliminarily calculated. A good agreement was found with available experimental results ^{317,318} and previous quantum-chemistry calculations ^{316,319-321} at the HF/6-31G*, HF/6-31G** and B3LYP/6-31G* theory level. These results are reported in Table 1.

Table 1. *Ab initio* calculated structural parameters of the free HCCP molecule, compared to previous theoretical estimates based on different methods (Hartree-Fock (HF) ^{316,319}, MP2 ^{316,321}), and experimental data ^{317,318} for the molecule in the crystalline phase.

| | our <i>ab initio</i> | Theory Level | | | | Experimental | |
|-------------------|----------------------|--------------------|-----------|-------|-------|--------------|--------|
| | | HF | DFT-B3LYP | MP2 | PM3 | Expt 1 | Expt 2 |
| <i>d</i> (P-N) Å | 1.598 | 1.577 | 1.619 | 1.600 | 1.640 | 1.59 | 1.581 |
| <i>d</i> (P-Cl) Å | 2.041 | 2.000 | 2.056 | 2.008 | 2.024 | 1.98 | 1.993 |
| ∠ P-N-P (deg) | 121.8 | 123.8 | 119.8 | 121.3 | 129.6 | 119.4 | 121.4 |
| ∠ N-P-N (deg) | 118.2 | 116.2 | 120.2 | 118.7 | 110.4 | 119.6 | 118.4 |
| ∠ Cl-P-Cl (deg) | 101.7 | 102.8 | 101.5 | 102.8 | 100.9 | 101.9 | 101.3 |
| ∠ N-P-N-P (deg) | 0.0 | | | | | | |
| ∠ P-N-P-Cl (deg) | 125.0 | 124.2 ^a | | | | | |

^a Reference ³²²

It should be noted that the computed values refer to the gas phase whereas the experimental data refer to the solid state, which always results in small deviations due to

lattice effects. In agreement with the information reported in literature^{316,322}, it was found that the planar arrangement (D_{3h} symmetry) represents a stable structure at all levels of theory and there are no non-planar stable configurations.

The *ab initio* calculations confirm that the HCCP molecule is highly polarized with a positive net charge on P and a negative net charge on N and Cl, respectively, so that a nucleophile should preferably attack the P atom.

4.1.2.2. Reaction between HCCP and hydroxylated silicon surface: thermodynamic data

In the hypothesis that a single HCCP molecule can interact with a hydroxylated-Si(100) surface leading to the formation of new P-O-Si bonds, with the consequent production of one or more HCl molecules, *ab initio* quantum mechanical calculations were performed.

In Table 2 are reported the most relevant energetic and structural data of different *chemisorbed* configurations, C1, C2, C3, and C4 shown in Fig. 24.

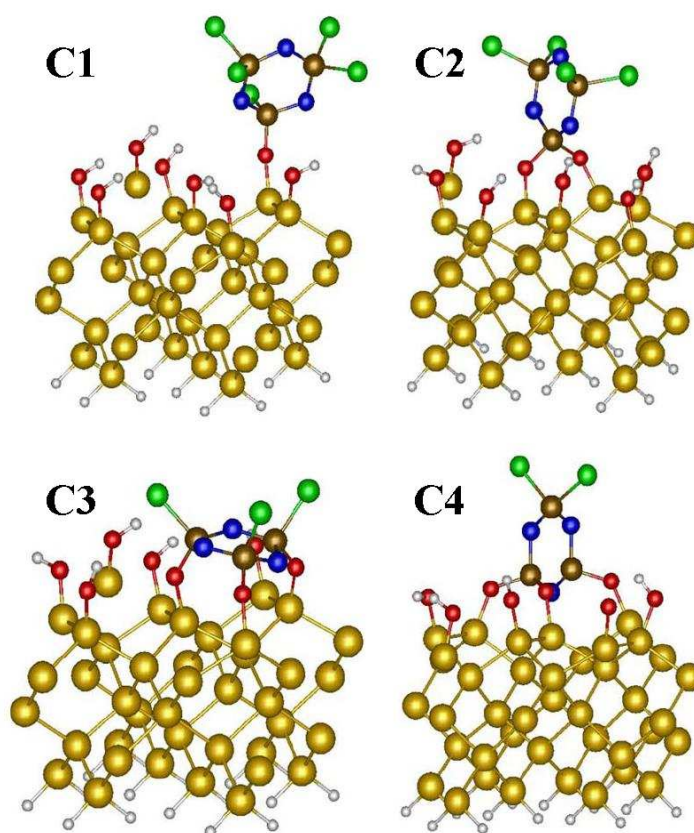


Figure 24. HCCP molecule chemisorbed on Si(100)-OH in different configurations (1 to 4 P-O-Si bonds formed). Orange, brown, green, blue, red and white balls denote Si, P, Cl, N, O, and H atoms, respectively.

Table 2. Binding energy, E_{bind} , and structural parameters of hexachlorocyclophosphazene (HCCP) molecule chemisorbed onto the OH-terminated Si(100) substrate. The different configurations, named C1, C2, C3 and C4, are characterized by the formation of 1, 2, 3 and 4 P-O bonds, respectively.

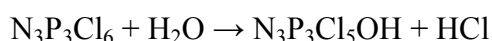
| | P^a-O (Å) | O-Si (Å) | P^a-Cl (Å) | Cl-P-Cl (deg) | N-P^a (Å) | N-P^a-N (deg) | P^a-N-P^a (deg) | torsional N-P-N-P (deg) | E_{bind} (kcal/mol) |
|---|-------------------------------|--------------------|--------------------------------|-------------------------|-------------------------------|-----------------------------------|---|---------------------------------------|---------------------------------------|
| P₃N₃Cl₆ | --- | --- | 2.041 | 101.7 | 1.598 | 118.2 | 121.8 | 0.0 | |
| C1 | 1.547 ^a | 1.741 | 2.032 | 100.6 | 1.597 | 116.3 ^a | 119.4 ^a | 14.2 ^a | 6.58 |
| | | | 2.041 | 101.8 | 1.599 | 118.2 | 120.3 ^a | | |
| | | | 2.051 | | 1.603 | 118.2 | 121.7 | | |
| | | | 2.054 | | 1.606 | | | | |
| | | | 2.066 ^a | | 1.606 ^a | | | | |
| | | | | | 1.624 ^a | | | | |
| C2 | 1.585 ^a | 1.734 | 2.043 | 100.4 | 1.586 | 115.5 ^a | 120.8 | 12.9 ^a | 9.27 |
| | 1.597 ^a | 1.736 | 2.048 | 101.7 | 1.591 | 118.7 | 121.5 ^a | | |
| | | | 2.053 | | 1.596 | 118.8 | 122.7 ^a | | |
| | | | 2.071 | | 1.602 | | | | |
| | | | | | 1.609 ^a | | | | |
| | | | | | 1.630 ^a | | | | |
| C3 | 1.573 ^a | 1.719 | 2.032 ^a | --- | 1.592 ^a | 115.0 ^a | 120.7 ^a | 17.8 ^a | 16.28 |
| | 1.579 ^a | 1.722 | 2.043 ^a | --- | 1.594 ^a | 115.0 ^a | 120.7 ^a | | |
| | 1.581 ^a | 1.725 | 2.058 ^a | | 1.599 ^a | 118.8 ^a | 122.4 ^a | | |
| | | | | | 1.602 ^a | | | | |
| | | | | | 1.624 ^a | | | | |
| | | | | | 1.625 ^a | | | | |
| C4 | 1.609 ^a | 1.717 | 2.057 | 100.3 | 1.587 | 117.1 ^a | 121.4 ^a | 2.0 ^a | 9.83 |
| | 1.613 ^a | 1.719 | 2.059 | | 1.595 | 117.5 ^a | 121.5 ^a | | |
| | 1.614 ^a | 1.720 | | | 1.596 ^a | 119.4 | 123.0 ^a | | |
| | 1.618 ^a | 1.729 | | | 1.600 ^a | | | | |
| | | | | | 1.601 ^a | | | | |
| | | | | | 1.604 ^a | | | | |

^a HCCP atoms involved in bonds with the Si(100)-OH surface

These configurations are based on the formation of 1, 2, 3, and 4 P-O-Si bonds respectively, with an equal number of HCl molecules as leaving groups (for the sake of

clarity these byproduct molecules have not been shown in Figure 24). In particular, C2 and C4 configurations are characterized by the substitution of geminal chlorines, while in C3 three non-geminal *cis* bonds are present. The binding energy, defined as the difference between the total energy of the whole system (after reaction, including the HCl leaving groups) and the total energy of the separated subsystems (before reaction), namely isolated Si(100)-OH surface and isolated HCCP molecule, gives us an insight of the energetically most stable configurations. From the inspection of Table 2 it is clear that the C3 structure, with its binding energy of 16.3 kcal/mol, is the most energetically favored, and, at the same time, in line with the predicted favored non-geminal substitution of the Cl atoms^{199,316}. So, the calculations show that chemisorption processes, with the formation of genuine chemical bonds (as can be inferred from the relatively large values of the binding energies), are certainly thermodynamically favored when HCCP interacts with the Si(100)-OH surface. The higher stability of the C3 configuration agrees with the elemental ratio (N : P : Cl = 1 : 1 : 1) found in earlier experiments^{6,7} and with the consequent microscopic mechanism proposed in Figure 22. Interestingly, the C3 structure turns out to be the less planar one, having the largest torsional N-P-N-P (14.2 deg) angle, whereas C4 is nearly planar (2.0 deg). In Table 2 the main structural data of C1-C4, compared with isolated HCCP, are also summarized.

More complex processes could occur, if the HCCP molecule undergoes chemical reactions prior to the interaction with the Si(100)-OH surface. For example, it could react with a H₂O molecule as follows^{309,310,323}:



so that the resulting mono-hydroxyl substituted HCCP (N₃P₃Cl₅OH) can be involved in consecutive interaction with the Si(100)-OH surface. As far as the binding energy is concerned, this reaction is energetically favored, giving products that are more stable than the starting reagents by 9.5 kcal/mol, in qualitative agreement with previous *ab initio* calculations³¹⁶, performed at the DFT-B3LYP level. Structural parameters are given later in Table 3, showing a configuration out of planarity with respect to HCCP. At this point N₃P₃Cl₅OH can interact with surface silanols *via* hydrogen bond formation. For instance, a physisorbed configuration (see Figure 25a), in which N₃P₃Cl₅OH forms a vertical H-bond with the substrate, is realized with a small binding energy of 1.4 kcal/mol.

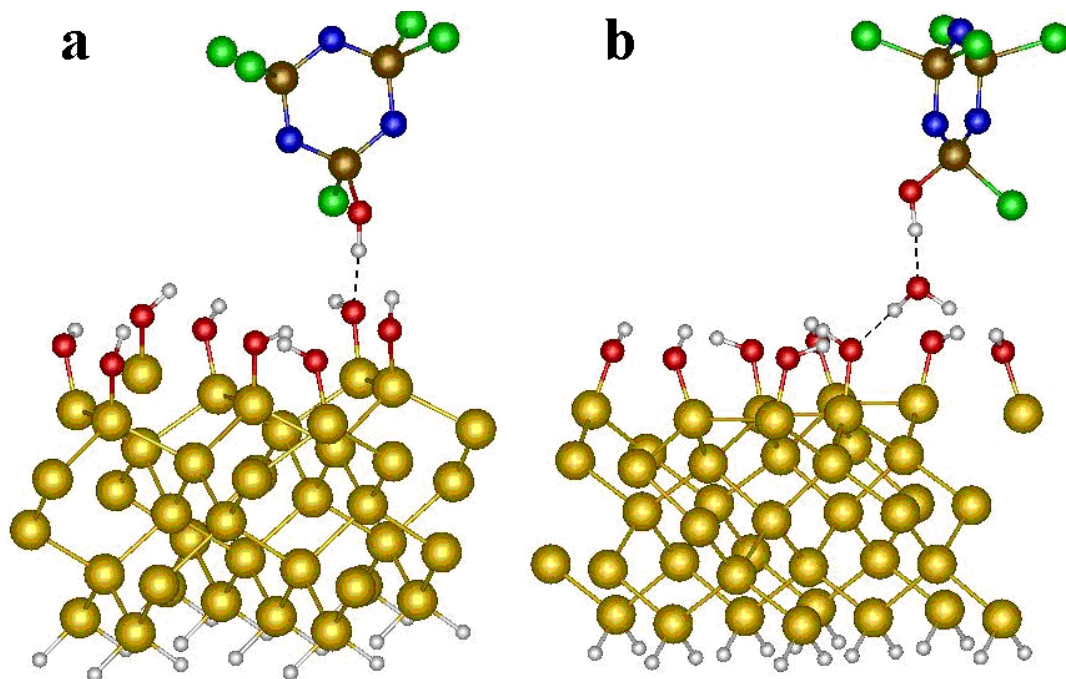
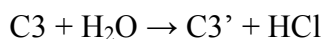


Figure 25. Hydrogen bonding interaction of $\text{N}_3\text{P}_3\text{Cl}_5\text{OH}$ with (a) the $\text{Si}(100)\text{-OH}$ surface, and (b) a physisorbed H_2O molecule

Eventually, $\text{N}_3\text{P}_3\text{Cl}_5\text{OH}$ and a surface silanol can give rise to a P-O-Si bond (similarly to configuration C1) with H_2O as a leaving group.

Again considering the water role, if a structure $\text{C3}'$ is realized from C3 *via* hydrolysis of residual chlorine,



it is energetically favored by 7.8 kcal/mol with respect to C3 . Subsequent reactions of the already chemisorbed molecule (for instance, with other water molecules) are also possible. In particular, by replacing, in the $\text{C3}'$ configuration, a second and a third Cl atom by an OH group ($\text{C3}''$ and $\text{C3}'''$), one obtains further gains in energy: in fact, the resulting structures are energetically more favored than C3 by 13.9 and 24.9 kcal/mol, respectively. Note that, while the N-P-N-P torsional angle (17.9 degrees) of the $\text{C3}'$ configuration is very close to that (17.8 degrees) of C3 , it increases substantially with the $\text{C3}''$ and $\text{C3}'''$ structures (being 28.2 and 34.2 degrees, respectively), thus leading to more and more non-planar (boat) configurations and suggesting the possibility of a ring-opening process. In Table 3 the energetic and structural data of $\text{C3}'$, $\text{C3}''$ and $\text{C3}'''$ configurations are summarized.

Table 3. Structural parameters of HCCP, $P_3N_3Cl_5OH$, $P_3N_3HCl_5(O)$, C3', C3'', C3''' and C3* configurations. The C3', C3'', C3''' and C3* binding energies, E_{bind} , are referred to C3.

| | P ^a -O (Å) | O-Si (Å) | P ^a -Cl (Å) | Cl-P-Cl (deg) | N-P ^a (Å) | N-P ^a -N (deg) | P ^a -N-P ^a (deg) | torsional N-P-N-P (deg) | E_{bind} (kcal/mol) |
|--|--------------------------|-------------|---------------------------|------------------|-------------------------|------------------------------|---|-------------------------------|--------------------------|
| $P_3N_3Cl_6$ | --- | --- | 2.041 | 101.7 | 1.598 | 118.2 | 121.8 | 0.0 | |
| $P_3N_3Cl_5OH$ | --- | --- | 2.037 | 101.2 | 1.594 | 116.3 | 121.1 | 4.9 | |
| | | | 2.045 | 101.3 | 1.595 | 118.4 | 122.2 | | |
| | | | 2.045 | | 1.598 | 118.5 | 122.3 | | |
| | | | 2.046 | | 1.599 | | | | |
| | | | 2.046 | | 1.605 | | | | |
| | | | 1.604 ^b | | 1.606 | | | | |
| [(N₂P₂Cl₄) [NH P(O)Cl] | --- | --- | 2.035 | 101.4 | 1.564 | 106.1 | 124.6 | 8.6 | |
| | | | 2.036 | 101.5 | 1.568 | 113.6 | 127.3 | | |
| | | | 2.037 | | 1.603 | 117.6 | 129.4 | | |
| | | | 2.044 | | 1.613 | | | | |
| | | | 2.078 | | 1.645 | | | | |
| | | | 1.469 ^c | | 1.765 | | | | |
| C3 | 1.573 ^a | 1.719 | 2.032* | --- | 1.592 ^a | 115.0 ^a | 120.7 ^a | 17.8 ^a | |
| | 1.579 ^a | 1.722 | 2.043* | --- | 1.594 ^a | 115.0 ^a | 120.7 ^a | | |
| | 1.581 ^a | 1.725 | 2.058* | | 1.599 ^a | 118.8 ^a | 122.4 ^a | | |
| | | | | | 1.602 ^a | | | | |
| | | | | | 1.624 ^a | | | | |
| | | | | | 1.625 ^a | | | | |
| C3' 1 P-OH external | 1.574 ^a | 1.711 | 2.042 ^a | --- | 1.592 ^a | 113.6 ^a | 120.3 ^a | 17.9 ^a | 7.8 |
| | 1.581 ^a | 1.720 | 2.070 ^a | --- | 1.598 ^a | 115.5 ^a | 121.6 ^a | | |
| | 1.583 ^a | 1.721 | | | 1.600 ^a | 118.6 ^a | 123.1 ^a | | |
| | | | | | 1.601 ^a | | | | |
| | | | | | 1.617 ^a | | | | |
| | | | | | 1.632 ^a | | | | |
| C3'' 2 P-OH external | 1.577 ^a | 1.706 | 2.044 ^a | --- | 1.599 ^a | 114.1 ^a | 120.1 ^a | 28.2 ^a | 13.9 |
| | 1.584 ^a | 1.708 | | --- | 1.600 ^a | 114.1 ^a | 120.3 ^a | | |
| | 1.584 ^a | 1.717 | | | 1.600 ^a | 118.2 ^a | 124.8 ^a | | |
| | | | | | 1.602 ^a | | | | |
| | | | | | 1.624 ^a | | | | |
| | | | | | 1.625 ^a | | | | |
| C3''' 3 P-OH external | 1.581 ^a | 1.708 | --- | --- | 1.597 ^a | 113.7 ^a | 119.9 ^a | 34.2 ^a | 24.9 |
| | 1.589 ^a | 1.710 | | --- | 1.600 ^a | 115.2 ^a | 120.5 ^a | | |
| | 1.594 ^a | 1.713 | | | 1.603 ^a | 117.0 ^a | 123.5 ^a | | |
| | | | | | 1.605 ^a | | | | |
| | | | | | 1.618 ^a | | | | |
| | | | | | 1.628 ^a | | | | |
| C3* 1 P-OPh external | 1.577 ^a | 1.706 | 2.046 ^a | --- | 1.591 ^a | 113.4 ^a | 120.5 ^a | 17.7 ^a | 2.8 |
| | 1.582 ^a | 1.716 | 2.061 ^a | --- | 1.596 ^a | 115.4 ^a | 122.0 ^a | | |
| | 1.584 ^a | 1.717 | | | 1.598 ^a | 118.8 ^a | 124.2 ^a | | |
| | | | | | 1.600 ^a | | | | |
| | | | | | 1.620 ^a | | | | |
| | | | | | 1.631 ^a | | | | |

^a atom involved in bonds with the Si(100)-OH surface

^b: P-OH

^c: P=O

If there are H₂O molecules already adsorbed (hydrogen bonded) on the Si(100)-OH surface, then the N₃P₃Cl₅OH can bond even more easily with the formation of an H bond: such a possible structure is shown in Figure 25b, and is characterized by a binding energy of 8.5 kcal/mol, that is of the same order of magnitude of typical H-bonds in water (4-5 kcal/mol).

The hydroxylated cyclophosphazene N₃P₃Cl₅OH, as resulting from (1), can rearrange proceeding by an intra-molecular mechanism^{312,324,325} that leads to H transfer from O to N with the formation of the *cyclophosphazane* [N₂P₂Cl₄][NHP(O)Cl] isomer, which turns out to be energetically slightly more favored than (parent) N₃P₃Cl₅OH by 1.8 kcal/mol (Table 3). If the same reaction takes place in N₃P₃(OH)₆, that is the HCCP molecule with all the Cl atoms replaced by OH groups, the resulting [N₂P₂(OH)₄][NHP(O)OH] molecule, having P=O and N-H groups, is energetically more favored than the initial one by 3.3 kcal/mol. Moreover, it has been found that the cyclophosphazane can interact more easily than cyclophosphazene with the Si(100)-OH substrate due to its much more reactive O atom; in particular it can form a weak or a strong H-bond with the surface (see Figure 26).

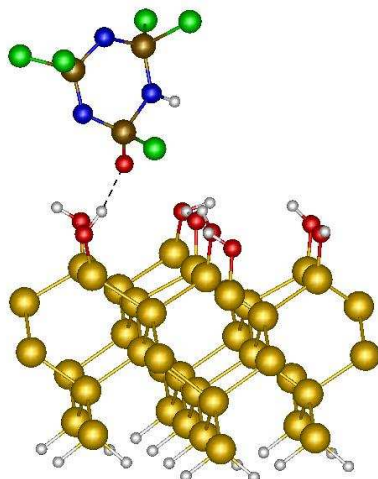
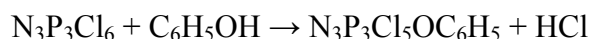


Figure 26. [N₂P₂ Cl₄][NHP(O)Cl] on Si(100)-OH surface (1 strong H-bond).

The calculated binding energies are 1.6 kcal/mol and 5.2 kcal/mol, respectively (note that, in the latter case, the binding energy is again that of typical H-bond in water). All these theoretical results give strong support to the hypothesis that water plays a crucial role in the processes of Si(100)-OH functionalization with HCCP. In addition, H₂O can interact with the cyclophosphazene-based film bound up with the Si(100)-OH surface, thus explaining the earlier experimental observation (see above,

C3', C3'' and C3''') of a relatively fast decrease in the portion of detected surface Cl atoms ($\text{Cl} : \text{P} : \text{N} = x : 1 : 1$, where $x < 1$). On this regard, it is also possible to suppose a hydrogen bonding interaction between P–OH groups and other P–OH or P=O ones of hydroxylated cyclophosphazenes and cyclophosphazanes, yielding a HCCP-based film with a thickness of more than one monolayer. Moreover, the formation of P–O–P bonds from condensation of two P–OH groups could occur, giving $(\text{N}_3\text{P}_3\text{Cl}_5)\text{-O-}(\text{N}_3\text{P}_3\text{Cl}_5)^{199,323}$.

Since glass surface functionalization by HCCP is actually performed using a suitable solvent (see sections 3.2.2.2 and 3.2.2.3), the HCCP molecule could also interact with molecules different from water (*vide supra*), before a direct interaction with the substrate takes place. For instance, if one considers the reaction of a HCCP molecule with a phenol group:



the resulting product is found to be more stable by 3.1 kcal/mol. Moreover, a chemisorbed structure, C3*, corresponding to the C3 one with a phenol group replacing a Cl atom, is found to be slightly favored by 2.8 kcal/mol with respect to C3 (see Table 3). However, at variance with the case of substitution by water molecules discussed above, in this case the substitution of Cl atoms by further phenol groups is energetically disfavored, due to steric hindrance reasons.

4.1.2.3. Reaction between HCCP and hydroxylated silicon surface: kinetic data

In order to predict the probability of the actual occurrence of a possible stable adsorption configuration it is important not only to evaluate its thermodynamic stability (*i.e.* the binding energy of selected configurations, as discussed in detail above), but also to take into account kinetic effects by estimating the energy barrier (if any) that the system must overcome to get to a given, final configuration. Therefore we have evaluated the energy barriers relative to different possible chemisorption mechanisms by the CI-NEB method. In particular, we find (see Figure 27) that the direct reaction between HCCP and the Si(100)-OH surface, to give the C1 configuration with one P–O–Si bond (Figure 24), is a substitutional process which requires an activation energy of 35 kcal/mol (Transition State). This is a rather substantial value but that does not prevent the possibility for the reaction to take place at the typical experimental conditions^{199,310}.

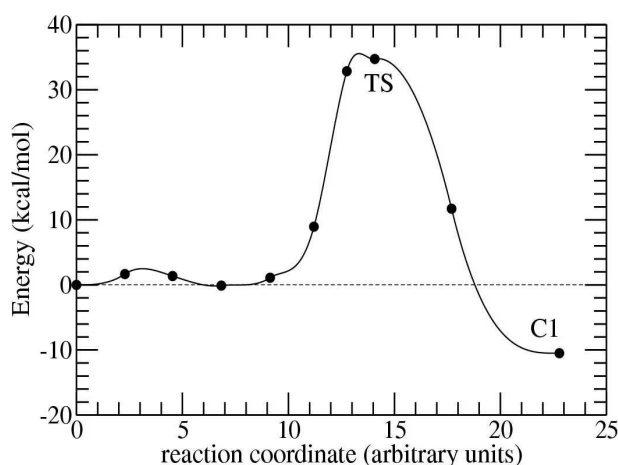


Figure 27. Energy barrier relative to the *chemisorption* mechanism leading to C1 configuration (TS: Transition State).

Figure 28 reports the reaction intermediate at the Transition State, showing the concurrent P–Cl bond elongation (3.398 Å), the silanol oxygen attack to phosphorus (SiO–P, 3.274 Å) and the formation of HCl as a leaving group.

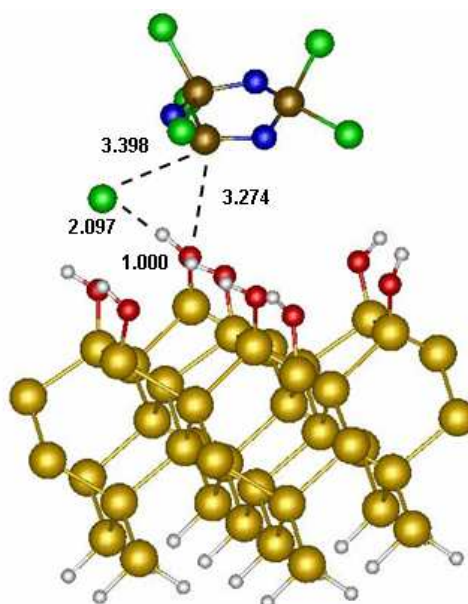


Figure 28. Reaction intermediate at the Transition State; distances are in Angstrom.

By proceeding with the investigation of possible reaction paths it was found that, for instance, the energy barrier separating the configuration C3 from C1 is even much larger, that is 108 kcal/mol. By itself this result seems to support the conclusion that, while C3 is thermodynamically more favored than C1, the opposite is true kinetically; however it should be pointed out that the transformation from C1 to C3 on the

Si(100)-OH surface is a relatively complex process, so that the possibility of finding a lower-energy reaction path cannot be ruled out; moreover the C1-C3 reaction, in actual experiments, could be made much more facile due to the presence of other substances such as water and/or the solvent.

Considering an effective water role, it would be possible to hypothesize that a water-mediated reaction occurs between HCCP and Si(100)-OH with the direct formation of P-O-Si bond (C1 configuration), lowering the activation energy, according to the reaction Scheme reported in Figure 29.

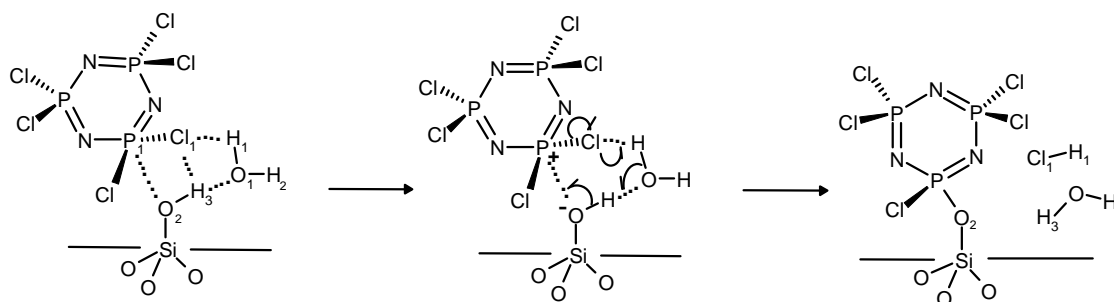


Figure 29. Possible H₂O-mediated concerted reaction between HCCP and Si(100)-OH, with P-O-Si formation.

This reaction, on the strength of a concerted mechanism depicted in the same Figure, would require a 6-member intermediate which rearranges to give P-O-Si bond, accompanied by H₂O and HCl as leaving groups.

The reaction of HCCP with a single water molecule (before interacting with the Si(100)-OH surface) is also characterized by a considerable energy barrier of 40 kcal/mol, similar to that found for the reaction between HCCP and the Si(100)-OH surface, leading to the C1 configuration. In this regard it is worth mentioning that some experimental evidences have been reported³⁰⁹⁻³¹¹ about the N₃P₃Cl_{6-x}(OH)_x formation under typical experimental conditions. In this case, the presence of surface silanols on which water is hydrogen bonded could favor the formation of N₃P₃Cl₅OH by a concerted reaction, thus lowering the activation energy, as shown in Figure 30.

Moreover, concerning the cyclophosphazene-cyclophosphazane transformation discussed above, an energy barrier was estimated of 30 kcal/mol, that is a value similar to that found for the reaction of HCCP with surface silanols. It is well known that actual phosphazene-phosphazane rearrangements are considerably facilitated by the presence of small quantities of alkyl halides acting as catalysts: in fact the presence of the catalyst is found to lower the activation energy even by a factor of 1.5-2³¹².

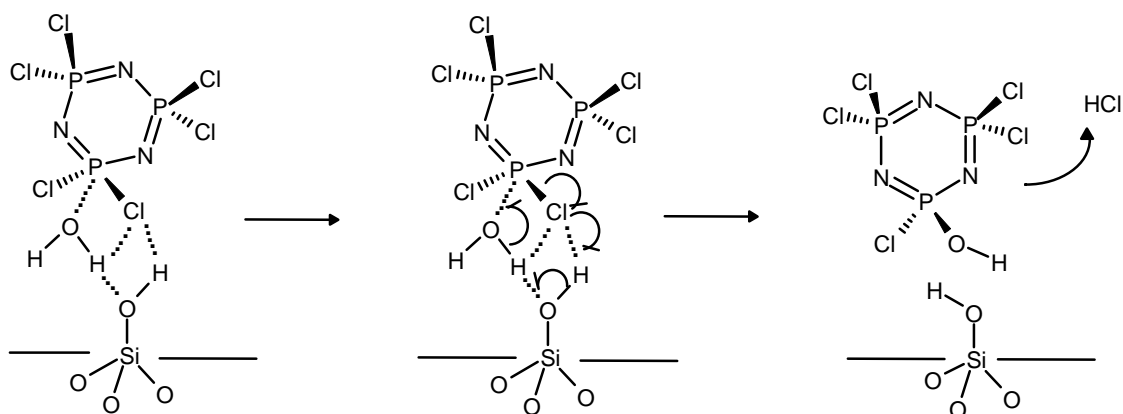


Figure 30. Possible water-mediated $\text{N}_3\text{P}_3\text{Cl}_5\text{OH}$ formation *via* a concerted mechanism involving HCCP, H_2O and $\text{Si}(100)\text{-OH}$

For completeness, the $\text{N}_3\text{P}_3(\text{OH})_6 \rightarrow [\text{N}_2\text{P}_2(\text{OH})_4][\text{NHP}(\text{O})\text{OH}]$ reaction is characterized by an energy barrier of 28 kcal/mol.

Since all the reactions and surface modifications here described are characterized by substantial energy barriers, it can be concluded that the choice of a suitable solvent, which could have a catalytic effect by lowering the energy barriers of the most relevant reactions, is probably crucial in real experiments. Therefore, even in this respect, these theoretical results are in line with the experimental evidence (see 4.1.3.1 below) of a key role played by the solvent in making the surface functionalization process efficient. Clearly, a full *ab initio* investigation of the reactions of HCCP and water, in presence of different possible solvents, would represent a formidable computational task. Hence concerning this important issue, only preliminary test simulations were carried out, which, although highly incomplete, nevertheless agree with the experimental observations. In particular, the much higher efficiency of *polar* THF ($\text{C}_4\text{H}_8\text{O}$) than *apolar* toluene (C_7H_8), when used as a solvent in the functionalization processes, can be partially rationalized by observing that a THF molecule is expected to be more reactive than toluene towards the hydroxylated surface, due to the presence of the lone-pair orbitals of its O atom. For instance, the *ab initio* calculations indicate that THF can give rise to a bound state with the $\text{Si}(100)\text{-OH}$ surface, by forming a weak H bond (binding energy is 1.2 kcal/mol), while this is not true for toluene.

4.1.3. Experimental approach

On the basis of the results of *ab initio* calculations, we decided to investigate in greater detail the surface functionalization reaction of silicon-based surfaces (*e.g.*

electrically fused quartz and sodalime glass) with hexachlorocyclophosphazene by using the XPS technique.

The experimental conditions were mainly based on the immersion of clean, HCl-activated sodalime and fused quartz glasses into a 0.1 M solution of HCCP in anhydrous THF to observe the deposition of cyclophosphazene-based films on the glass surface. Some samples were subject to a thermal dehydration treatment under vacuum before being plunged into the solution, to remove more or less extensively the H-bonded water on the surface of the samples³²⁶⁻³²⁸. After functionalization, most samples were washed with THF in order to extract the weakly bound HCCP from the glass surface, and in some cases a final drying was performed under vacuum at set temperatures.

Table 4 reports the most important features of the experimental procedures adopted for the deposition of cyclophosphazene-based films on the surface of the substrates.

Table 4. Preparative history of the samples. Note that “S” samples refer to sodalime glass substrates, while “Q” samples refer to fused quartz substrates.

| Sample | Previous vacuum drying | | HCCP Treatment | | THF washing | Final drying | |
|-----------|------------------------|----------|-----------------|-----------------|-------------|-----------------|------------------|
| | Temp. (°C) | Time (h) | Temp. (°C) | Time (h) | | Temp. (°C) | Time (h) |
| S1 | - | - | 23 ^a | 24 ^a | no | 23 | 8 |
| S2 | - | - | 23 | 24 | no | 23 | 8 |
| S3 | 23 | 6 | 23 | 24 | no | 23 | 15 |
| S4 | 70 | 6 | 23 | 24 | no | 23 | 15 |
| S5 | 120 | 6 | 23 | 24 | no | 23 | 15 |
| S6 | 170 | 6 | 23 | 24 | no | 23 | 15 |
| Q1 | - | - | 23 | 3 | no | 23 ^b | 0.2 ^b |
| Q2 | - | - | 23 ^c | - ^c | yes | 50 ^b | 0.5 ^b |
| Q3 | 70 | 1 | 64 | 0.5 | yes | 70 | 2.5 |
| Q4 | 70 | 1 | 64 | 1.5 | yes | 23 | 2.5 |
| Q5 | 70 | 1 | 64 | 3 | yes | 23 | 2.5 |
| Q6 | 190 | 1 | 64 | 1.5 | yes | 70 | 2.5 |

^a Functionalization reaction performed in toluene as a solvent, instead of THF

^b Drying performed in the air, instead of under vacuum

^c Prepared by droplet deposition method instead of immersion in solution

One dipping test was performed by using toluene as a solvent instead of THF in order to verify its efficiency towards HCCP deposition on glass surface with respect to THF.

Moreover, one sample was prepared by an alternative method, that is by simply letting one drop of 0.1M HCCP solution in anhydrous THF onto its surface instead of dipping the whole slide into the solution.

4.1.3.1. Influence of the solvent

Table 5 reports the XPS data for samples S1 and S2, both prepared by dipping into a 0.1 M solution of HCCP in anhydrous solvent at 23°C for 24h, where the solvent was toluene in the first case and tetrahydrofuran in the second. Both these samples were analyzed as prepared without post-washing in THF, thus leaving on the surface some weakly- or unbound HCCP, that is reported to sublime under high vacuum during the XPS analysis³²⁹⁻³³¹.

Table 5. XPS atomic percentages for sodalime glasses treated with HCCP solutions in THF and in toluene at room temperature. Alkaline and alkaline-earth metals of the sodalime glass have not been included for simplicity.

| Sample | Solvent | C | Si | O | P | N | Cl | N/P | Cl/P |
|--------|---------|------|------|------|------|------|-----|-----|------|
| S1 | toluene | 18.6 | 29.8 | 49.4 | 0.9 | 0.9 | 0.3 | 1.0 | 0.3 |
| S2 | THF | 20.1 | 16.9 | 31.6 | 11.5 | 12.5 | 7.4 | 1.1 | 0.6 |

The surface analyses point out the presence of chemisorbed HCCP in both samples, but in a higher amount for S2, *i. e.* when THF was used. This could be due to the higher polarity of THF, that may favor the reaction of the P-Cl groups of the phosphazene with the surface silanols of the samples. Moreover, the relative chlorine amount in the HCCP-derived film determines a higher Cl/P stoichiometric ratio in S2 to indicate, at least under these experimental conditions, a more limited hydrolysis of P-Cl bonds to P-OH. This could occur by reaction with water adsorbed on the sample surface³²⁶⁻³²⁸, or even with atmospheric moisture. In Table 5 the atomic percentages of silicon, oxygen and carbon are also reported; the first two are due to the SiO₂ network of sodalime glass, the third one to solvent residues and adventitious carbon.

Following these results, all subsequent surface functionalization experiments were carried out in THF as a solvent, rather than in toluene.

4.1.3.2. Influence of surface-adsorbed water

Table 6 reports the results of the XPS analysis for two fused quartz samples, one obtained by simple immersion into 0.1M solutions of HCCP in anhydrous THF at room temperature for three hours (Q1), and the second one prepared through the alternative method of droplet deposition (Q2) at 23°C under N₂ blanket, dried at 50°C, rinsed with freshly distilled anhydrous THF and finally dried for 0.5h at 50°C.

Table 6. Atomic percentages as revealed from XPS for fused quartz samples functionalized by immersion (Q1) and droplet deposition (Q2) methods at room temperature.

| Sample | C | Si | O | P | N | Cl | N/P | Cl/P |
|--------|------|------|------|-----|-----|-----|-----|------|
| Q1 | 9.3 | 33.1 | 51.8 | 2.0 | 2.0 | 1.8 | 1.0 | 0.9 |
| Q2 | 40.3 | 21.5 | 31.8 | 2.0 | 1.9 | 2.4 | 1.0 | 1.2 |

The diagnostic atomic percentage ratios of phosphorus, nitrogen and chlorine are close to 1 : 1 : 1 as reported in previous works⁵⁻⁷, suggesting that about 50% of the original chlorine atoms of HCCP undergo a substitution process during the functionalization procedure. Moreover, it should be underlined that these samples have been washed in THF, confirming that most HCCP is actually strongly adsorbed onto the silica surface.

The P_{2p} peak binding energy value is about 133.7 eV, lower than that of the pure HCCP trimer (134.5 eV)^{329,330}, which may suggest the vicinal substitution of a chlorine with oxygen to form a P-O bond³³⁰.

The N_{1s} peak profile analysis reveals, as shown in Figure 31, the presence of several N species. The decomposition of the peak, as indicated by the data reported in Table 7, points out the presence of at least three different chemical environments for the nitrogen. The first (**I**) component, about 398.0 eV, can be assigned to phosphazene-type nitrogen³²⁹⁻³³⁸, while the second (**II**) one, around 399.5 eV, may be attributed to a P-NH-P bond of a phosphazane-type nitrogen according to what was reported for phosphorus oxynitride species^{333,339,340}; finally, a third (**III**) component at about 402.3 eV is reasonably due to P-NH₂ groups and/or to the presence of N⁺-type nitrogen^{333,339,340}.

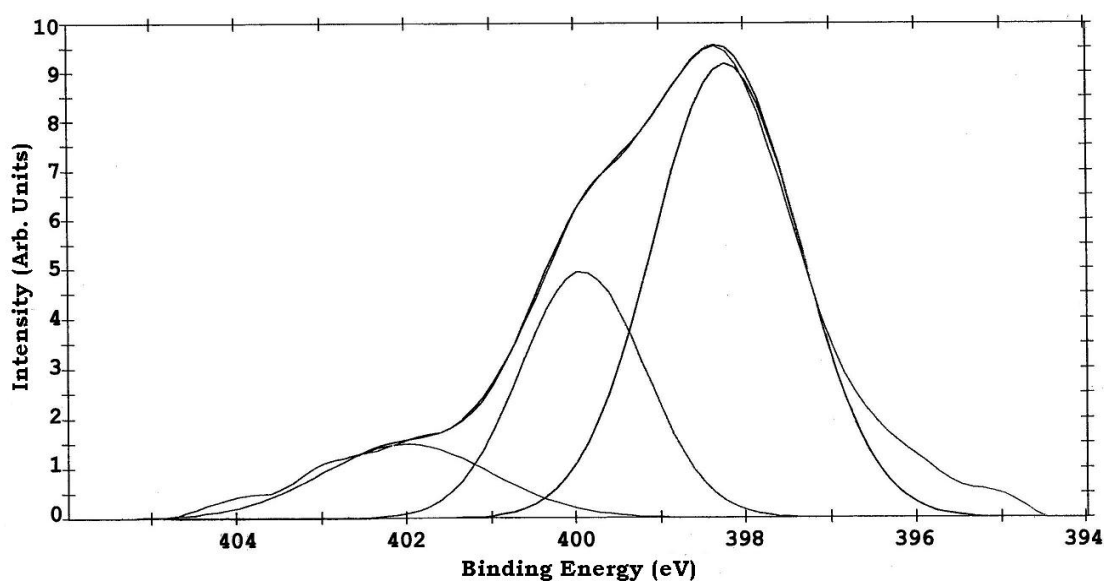


Figure 31. Deconvolution of the N_{1s} peak of sample Q1.

Table 7. Results of N_{1s} peak deconvolution of samples Q1 and Q2.

| Sample | BE (eV) | | | FWHM (eV) | | | Peak Area (%) | | |
|--------|---------|-------|-------|-----------|-----|-----|---------------|------|------|
| | I | II | III | I | II | III | I | II | III |
| Q1 | 398.1 | 399.7 | 402.2 | 1.7 | 2.1 | 2.5 | 45.0 | 44.0 | 11.0 |
| Q2 | 397.7 | 399.3 | - | 1.7 | 1.8 | - | 40.1 | 59.9 | - |

The presence of phosphazane segments could be explained, at a first level, by the reaction of HCCP with physisorbed water present on the surface of the substrates, that can result eventually in phosphazene-phosphazane rearrangement according to the pathway illustrated in Figure 32¹.

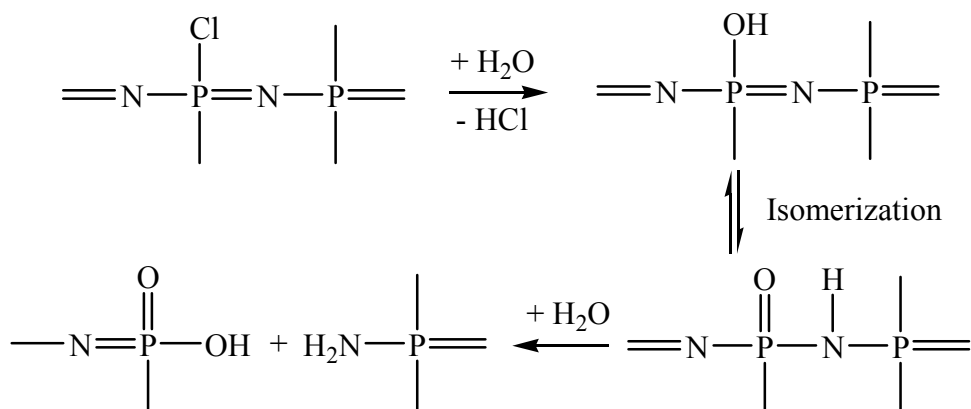


Figure 32. Schematic representation of chlorophosphazene hydrolysis, followed by phosphazene-phosphazane rearrangement and degradation of the phosphorus-nitrogen backbone.

This hypothesis is also supported by our previous theoretical calculations, that evidenced the crucial role that is likely to be played by water in the reaction with silanol-terminated surfaces, and in determining the bonding of cyclophosphazenes onto silanol-terminated surfaces by means of hydrogen or covalent bonds (P–OH \cdots HO–Si and P–O–Si).

In the same scheme one possible consequence of the process is illustrated, which is the cleavage of the original phosphazene backbone; this latter phenomenon could explain the presence of P–NH₂ segments and therefore the origin of the higher-energy nitrogen component in the XPS spectra.

In order to investigate the role of physisorbed water onto glass surface on the P : N : Cl stoichiometry of HCCP-based film, a set of sodalime glass samples was dried under vacuum for six hours at temperatures ranging from 23°C to 170°C, corresponding to different dehydration levels of the surface³²⁶⁻³²⁸. The glass surface functionalization was then carried out by immersion in the HCCP solution, using the same procedure exploited for the other experiences described so far (see Table 4). The results of XPS analysis for these samples are summarized in Table 8, together with those relative to sample S2, which had not undergone any previous drying process. The differences in the atomic concentrations between samples are mainly due to non-homogeneities in the deposited HCCP-based films.

Table 8. Atomic percentages as revealed from XPS for sodalime glass samples dehydrated at different temperatures and subsequently functionalized with HCCP at room temperature.

| Sample | Drying temp. (°C) | C | Si | O | P | N | Cl | N/P | Cl/P |
|--------|-------------------|------|------|------|------|------|------|-----|------|
| S2 | no drying | 20.1 | 16.9 | 31.6 | 11.5 | 12.5 | 7.4 | 1.1 | 0.6 |
| S3 | 23 | 29.4 | 22.1 | 31.0 | 5.7 | 7.1 | 4.7 | 1.2 | 0.8 |
| S4 | 70 | 30.0 | 13.1 | 21.3 | 12.9 | 12.8 | 10.1 | 1.0 | 0.8 |
| S5 | 120 | 31.8 | 7.3 | 16.3 | 16.6 | 15.9 | 11.9 | 1.0 | 0.7 |
| S6 | 170 | 27.6 | 18.2 | 26.2 | 9.8 | 9.9 | 8.2 | 1.0 | 0.8 |

Although the relative chlorine content does not seem to change remarkably between the different dried samples, it is nevertheless higher (about 30 %) when compared to the non-dried S2 sample. The results suggest that the previous dehydration treatment does actually reduce the hydrolysis of the chlorophosphazene, and that at least a drying

temperature of 70 °C is advisable to have a P : N : Cl ratio close to 1 : 1 : 1. It should also be remarked that a lower quantity of phosphazene is found on dried samples, again accounting for the influence of water on the overall process.

Moreover, when observing the N/P ratio, slight deviations from the expected value of 1 appear, which seem to be stronger when the previous vacuum treatment is performed at lower temperatures and therefore the sample surface is less extensively dehydrated. These N/P deviations from unity may suggest a possible change in the chemical structure of the original HCCP phosphorus – nitrogen backbone.

4.1.3.3. Influence of temperature and treatment duration

Based upon the preliminary results exposed above, a whole new series of functionalization experiments was devised, aimed at finding the best experimental conditions to obtain the grafting of HCCP onto the surface of silica-based substrates and at investigating the nature of the phosphazene layer deposited onto the surface of the substrates.

The treatments were carried out on fused quartz glass samples, all previously dehydrated by a one-hour vacuum treatment at 70°C or at 190°C and then functionalized by immersion in a 0.1M solution of HCCP in refluxing THF for different reaction times. All these samples were then rinsed with freshly distilled anhydrous THF after the functionalization treatment, to ensure the removal of unbound and weakly bound phosphazene molecules from the surface. As exposed more in detail in Table 4, different final drying temperatures before XPS analysis were also exploited.

The XPS results for the whole series of samples are shown in Table 9. In particular, for each sample the mean value of N/P and Cl/P stoichiometric ratio is reported.

Table 9. Atomic percentages as revealed from XPS for fused quartz samples functionalized with HCCP at THF reflux temperature for different treatment durations.

| Sample | Dehydration temp. (°C) | Reaction temp. (°C) | Reaction time (h) | Final Drying temp. (°C) | N/P | Cl/P |
|--------|------------------------|---------------------|-------------------|-------------------------|-----|------|
| Q1 | none | 23 | 3 | 23 | 1.0 | 0.9 |
| Q3 | 70 | 64 | 0.5 | 70 | 0.8 | 0.1 |
| Q4 | 70 | 64 | 1.5 | 23 | 0.6 | 0.3 |
| Q5 | 70 | 64 | 3.0 | 23 | 0.5 | 0.2 |
| Q6 | 190 | 64 | 1.5 | 70 | 0.6 | 0.1 |

It appears clearly from these data that these HCCP-derived films have a P : N : Cl stoichiometry quite different from what observed so far. In fact, both Cl/P and N/P ratio assume values sensitively lower than 1, as if an extensive degradation or an accelerated ageing occurred. So, these findings can be related firstly to the higher temperature selected for the treatment (64°C), secondly to the final drying temperature (70°C). As far as the preliminary vacuum dehydration temperature is concerned, its variation does not seem to have a great influence on the diagnostic N/P and Cl/P ratios, as already discussed above.

A common feature throughout the whole series seems to be the exceptionally low relative chlorine content of the samples, which would suggest an extensive hydrolysis of the original chlorophosphazene. This stands even when the previous vacuum treatment was performed at 190°C, a temperature at which the surface of silica is reported to be substantially dehydrated³²⁸. This could be due to the reaction temperature (*i.e.* about 64°C), which may favour the reaction with even traces of residual water present in the reaction environment. In fact, if the reaction is carried out at 23°C, as is the case for Q1 (see Tables 4 and 6), the atomic percentage ratios of phosphorus, nitrogen and chlorine are preserved and close to 1 : 1 : 1.

Besides the effect of water, P-OH groups may also be generated by the reaction of P-Cl with the silanols themselves, as reported by Zhivukhin³⁴¹, though in that case higher temperatures and less polar solvents were used (*i. e.* reflux in benzene, toluene and *o*-xylene).

Moreover, as the N/P atomic percentage ratio appears to be significantly lower than 1 in most cases, this reduction could be seen as a consequence of the extensive degradation of the cyclophosphazene. In fact, this process leads to the formation of phosphoric acid and ammonia as described by Allcock¹, and the latter byproduct is more volatile.

Dwight³⁴² studied the degradation of several differently substituted phosphazene homopolymers as an effect of long exposure to X-rays in an ESCA instrument, and found in those particular experimental conditions approximately twice as much phosphorus as nitrogen (N/P \approx 0.5).

Mochel^{324,343} reported the thermolysis of methoxy-substituted cyclo- and polyphosphazenes $[\text{NP}(\text{OCH}_3)_2]_x$ ($x = 3$ or n) according to a reaction pathway similar to the one illustrated in Figure 32, and proposed that the phosphazene-phosphazane

rearrangement could be initiated by the presence of P-OH or unsubstituted P-Cl sites; both groups are probably present in our deposited films.

In a general way, there seems to be a direct correlation between the lowering of the N/P ratio and the duration of the functionalization treatment. On the other side, when longer reaction times were employed, the final quantity of revealed phosphazene was generally higher. This suggests the conclusion that longer reaction times favour both the grafting and the degradation of the phosphazene compound.

A further insight can be attained by performing the deconvolution of the XPS N_{1s} peaks, whose results are given in Table 10. Figure 33 shows the deconvolution for sample Q3 as an example.

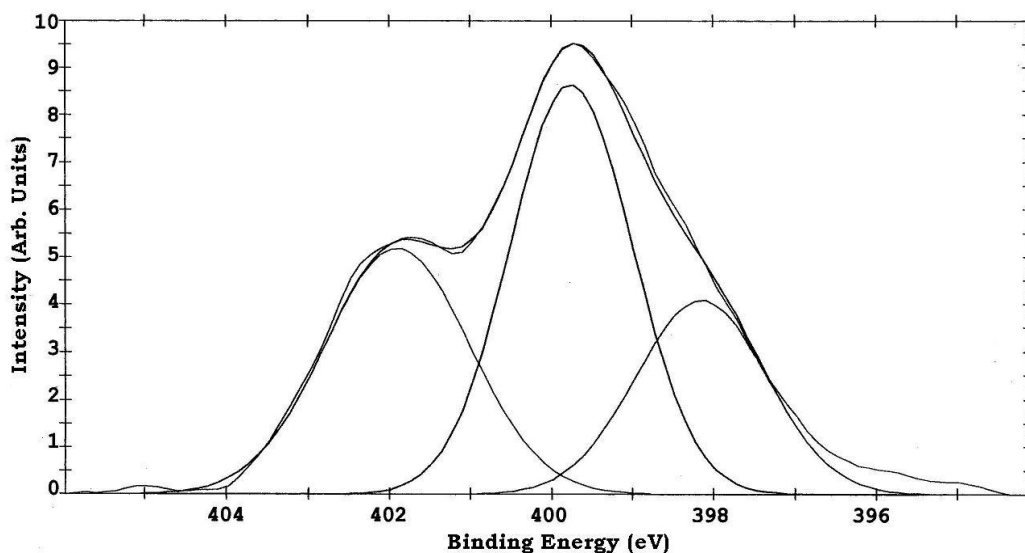


Figure 33. Deconvolution of the N_{1s} peak of sample Q3.

Table 10. Results of N_{1s} peak deconvolution of fused quartz samples functionalized with HCCP at THF reflux temperature for different treatment durations.

| Sample | Binding Energy (eV) | | | FWHM (eV) | | | Peak Area (%) | | |
|-----------|---------------------|-------|-------|-----------|-----|-----|---------------|------|------|
| | I | II | III | I | II | III | I | II | III |
| Q3 | 398.0 | 399.6 | 401.8 | 2.0 | 2.0 | 2.0 | 21.9 | 48.9 | 29.2 |
| Q4 | 397.5 | 399.0 | - | 2.1 | 2.0 | - | 51.2 | 48.8 | - |
| Q5 | 397.6 | 399.1 | - | 2.2 | 2.0 | - | 52.8 | 47.2 | - |
| Q6 | 398.0 | 399.5 | 401.7 | 1.9 | 1.9 | 2.0 | 19.9 | 46.8 | 33.2 |

The same three nitrogen components already described were found, approximately around 398.0, 399.5 and 401.8 eV, which are assignable to phosphazene (P=N=P), phosphazane (P-NH-P) and P-NH₂ groups. In the cited work by Dwight³⁴², a broadening in the N_{1s} peak of degraded polyphosphazenes was observed, and it was attributed to the formation of species consistent with the phosphazene – phosphazane rearrangement pathway already proposed by Mochel^{324,343}, and similar to the one shown above in Figure 32; this is in accordance with our attributions.

In addition, on the basis of the area percentages reported for the different N_{1s} components, it appears that the final drying temperature plays an important role. In fact, at higher temperatures the component assigned to phosphazenic (P=N) nitrogen decreases whereas the P-NH₂ type component increases, confirming an accelerated phosphazene-phosphazane rearrangement and degradation.

The relationship between the degree of chlorine substitution and the intensity of the N_{1s} components is plotted in Figure 34 for samples Q3 to Q6, together with sample S2 for a comparison, since the latter has a significantly higher Cl/P ratio.

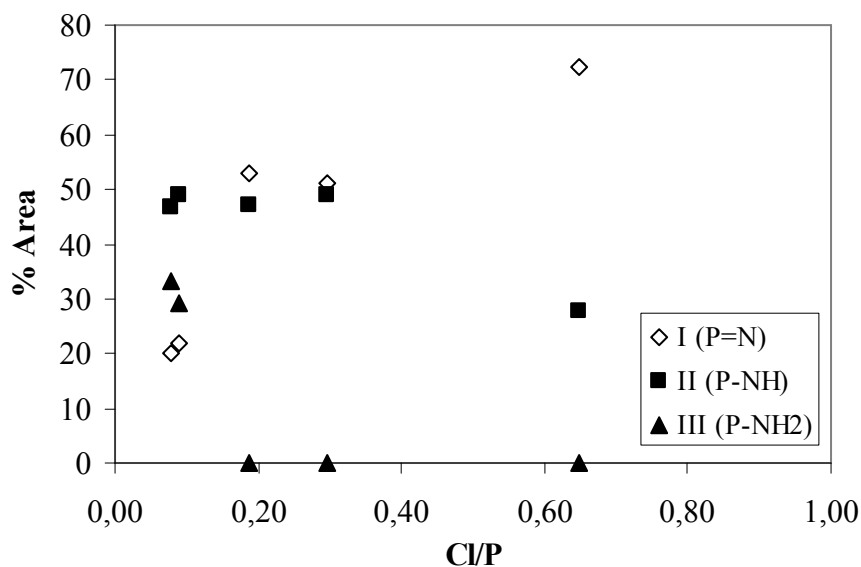


Figure 34. Plot of the relative intensities of the components of the N_{1s} XPS peak versus Cl/P atomic percentage ratio.

As the relative chlorine content diminishes, the original phosphazene component decreases to the benefit of the others. The third component, which we assigned to P-NH₂ segments generated by the backbone cleavage, appears only when the chlorine content is exceptionally low. These facts agree with the proposed interpretation of

degradative processes occurring *via* substitution of P-Cl with P-OH and subsequent phosphazane rearrangement.

4.1.4. Conclusions

The interaction of HCCP with the hydroxylated silicon-based surfaces has been studied by a combination of XPS experimental analysis and theoretical *ab initio* quantum mechanical calculations.

The calculated thermodynamic data indicated that multiple chemisorbed configurations of HCCP are possible. In this regard, the structural, energetic, and electronic properties of these configurations were investigated, and their relative activation energies were estimated by considering the more favorable reaction pathways.

The theoretical results suggested that surface functionalization reactions with HCCP are thermodynamically feasible, even if these reactions are characterized by remarkable kinetic energy barriers. In this regard, it should be noted that it is quite largely accepted that the phosphazene-phosphazane isomerization process takes place under typical experimental conditions³⁰⁹⁻³¹¹; as this reaction showed a calculated energy barrier comparable to that of HCCP chemisorption, it may be assumed that the surface functionalization of HCCP on Si(100)-OH is also feasible.

Moreover, theoretical calculations provided indications about the crucial role played by water in the process, although the presence of a suitable catalyst or solvent (*e.g.* THF) turned out to be also essential.

From the experimental point of view, the procedures described in this section allowed to obtain the deposition of thin phosphazene-based films derived from HCCP, which could be analytically detected by XPS even at the high vacuum conditions required by the technique and after sample washing in THF. This accounts for a strong interaction between the phosphazene and the silanol-terminated glass surface. The XPS analyses revealed a P : N : Cl stoichiometric ratio close to 1 : 1 : 1 when the functionalization was performed at 23°C, under controlled conditions including a previous thermal dehydration treatment of the substrate under vacuum.

Nevertheless, the deposited phosphazene films seemed to be subject to phosphazene – phosphazane isomerization processes, that could ultimately result in the cleavage of the phosphorus – nitrogen backbone of these compounds. In particular, the choice of

higher temperatures for the reaction and/or the final drying of the samples determined lower nitrogen- and chlorine-to-phosphorus percentage ratios to be found. This finding was accompanied by the appearance of new components in the N_{1s} XPS peak, which supported the hypothesis of degradative phenomena proceeding through a phosphazene-phosphazane rearrangement.

4.1.5. Acknowledgements

Theoretical calculations were performed by Prof. Pier Luigi Silvestrelli (Physics Department “G. Galilei”, University of Padova, Italy) and by Dr. Angelo Boscolo Boscoletto (Polimeri Europa – Tecnologia Chimica di Base, Porto Marghera, Italy). XPS measurements were performed by Dr. Laura Meda (Polimeri Europa, Istituto Donegani, Novara, Italy).

4.2. THIN PHOSPHAZENE FILMS DEPOSITION BY GLOW DISCHARGE-INDUCED SUBLIMATION (GDS)

4.2.1. Preliminary considerations

Deposition of phosphazene thin films on crystalline Si(100) was obtained by Glow Discharge-induced Sublimation (GDS) of HCCP. In some cases, silicon substrates had previously undergone activation by treatment with ion etching plasma in a mixed argon/oxygen atmosphere. Washing of the deposited samples with THF was performed, to check the stability of the films. Phosphazene-functionalized substrates were also used in substitution reactions with TFE and 4CNP, and the same treatment was performed on clean unfunctionalized silicon(100) wafers as “blank” samples.

The whole series of samples and the nomenclature employed for their designation are reported in Table 1 below.

Table 1. Obtained samples and their preparative history.

| Sample | Substrate activation | HCCP Deposition | THF washing | Reaction in solution/washing |
|------------------------|-----------------------------|------------------------|--------------------|-------------------------------------|
| AR PN 1 | No | 1 min | No | No |
| AR PN 2 | No | 2 min | No | No |
| ACT PN 1 | Yes | 1 min | No | No |
| ACT PN 2 | Yes | 2 min | No | No |
| AR PN 1 washed | No | 1 min | Yes | No |
| AR PN 2 washed | No | 2 min | Yes | No |
| ACT PN 1 washed | Yes | 1 min | Yes | No |
| ACT PN 2 washed | Yes | 2 min | Yes | No |
| ACT PN 2 CF3 | Yes | 2 min | No | Yes |
| Blank CF3 | No | No | No | Yes |
| ACT PN 1 CN | Yes | 1 min | No | Yes |
| ACT PN 2 CN | Yes | 2 min | No | Yes |
| Blank CN | No | No | No | Yes |

4.2.2. Deposition rate of HCCP derived thin films

HCCP-derived thin films were deposited by GDS technique and the film deposition rate was measured *in situ* by a quartz crystal microbalance.

In Figure 35 the deposition rate of the films vs. deposition time is reported, as obtained by placing the microbalance at a target-to-substrate distance of 12 cm.

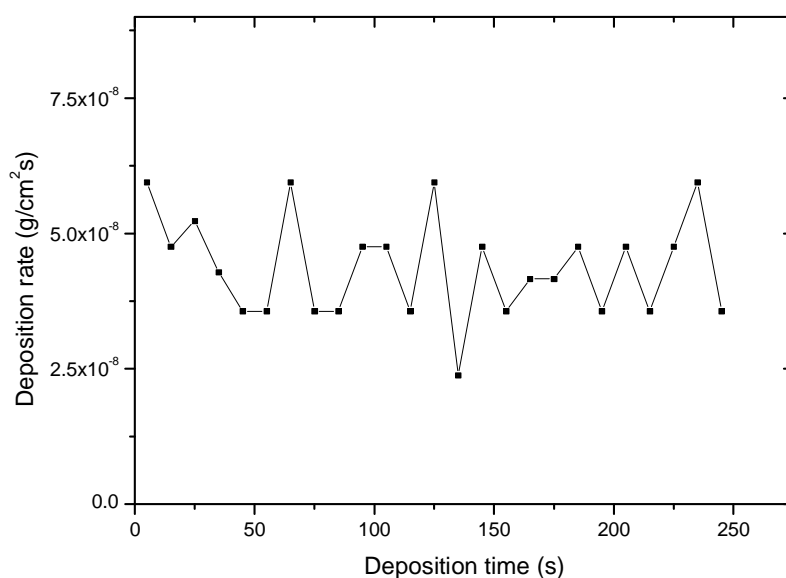


Figure 35. Deposition rate of HCCP-derived films vs deposition time (target-to-substrate distance = 12 cm)

The deposition rate is quite stable and its average value is $4.3 \cdot 10^{-8} \text{ g/cm}^2\text{s}$. The trend of the deposition rate appears quite different from that of other previously studied compounds such as polyimide precursor monomers³⁴⁴, where a monotonous decrease was observed as a function of deposition time. In that case, such a trend was explained as an effect of ion bombardment-induced formation of a damaged surface layer on the organic powder, which progressively hindered the sublimation of intact molecules.

The trend of HCCP deposition rate is quite similar to that previously reported for 2,4,6-trimethyl-*m*-phenylenediamine³⁴⁴, where the strong sublimation of undamaged molecules together with the emission of volatile fragments from the target delayed the formation of the damaged surface layer, which took as long as 500 s.

The main effect of the ion bombardment on the HCCP powder was therefore the gas phase emission of HCCP molecules and volatile molecular fragments, while the formation of non-volatile fragments on the target surface is very slow. This was as confirmed by the visual inspection of the powder at the end of the deposition, which revealed only a slight color change from white to light yellow.

4.2.3. Plasma composition by mass spectrometry

Plasma composition during film deposition was monitored by *in situ* mass spectrometry. In Figure 36 is reported the mass spectrum collected during HCCP deposition recorded by the electron ionizer.

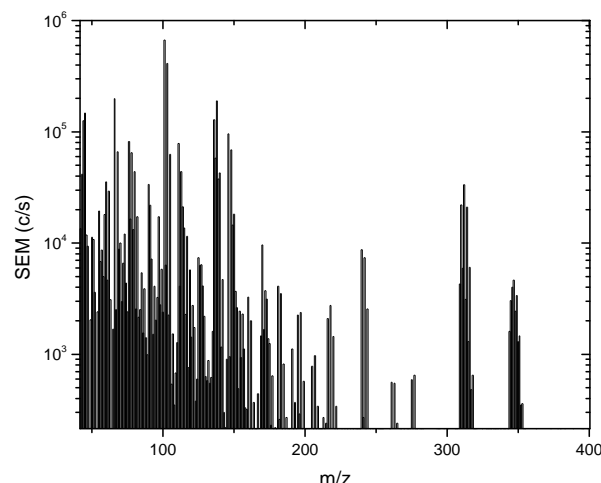


Figure 36. Mass spectrum collected during HCCP deposition (electron ionizer ON)

The comparison with literature data³⁴⁵ shows that all the typical fragmentation peaks of the HCCP molecule appear in the recorded spectrum. Besides the molecular ion peak ($[(\text{NPCl}_2)_3]^+$ at $m/z = 345$), the features due to fragmentation of the molecule appear at $m/z = 310$ ($[(\text{NPCl}_2)_3-\text{Cl}]^+$), $m/z = 240$ ($[(\text{NPCl}_2)_3-3\text{Cl}]^+$), $m/z = 146$ ($[\text{NP}_2\text{Cl}_2]^+$), $m/z = 111$ ($[\text{NP}_2\text{Cl}]^+$), and $m/z = 66$ ($[\text{PCl}]^+$).

In order to detect charged species only, the mass spectrum was collected also after switching off the ionizer of the spectrometer. In such a case no peaks appear, so it can be inferred that the amount of neutral HCCP molecules and molecular fragments is predominant with respect to that of ionized species.

In Figure 37 the plot of peak intensities of the main mass features recorded before and after plasma ignition as a function of time is reported.

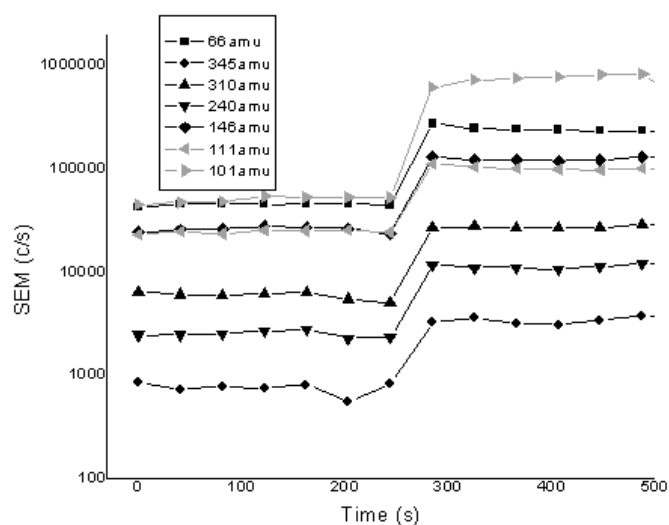


Figure 37. Intensities of the main mass peaks recorded before and after plasma ignition vs. time.

When the plasma is turned on ($t = 250$ s in Figure 37), a sudden increase in all the mass spectrum signals is recorded. The molecular fragmentation observed in mass spectra could arise in principle both from the spontaneous rearrangement of the molecular ion $[(\text{NPCl}_2)_3]^+$ inside the spectrometer and from the interaction between plasma and HCCP molecules in the deposition chamber. The relative intensities of the molecular fragment peaks observed after plasma ignition are nearly constant throughout the deposition with respect to the one of the molecular ion; this fact suggests that plasma-induced HCCP damage is independent on the deposition time, at least for the explored treatment duration.

In Table 11 are reported the average peak intensities of the main molecular fragments of the HCCP molecule, as obtained from Figure 37, before plasma ignition (I_{off}) and after plasma ignition (I_{on}). The values written as $\%I_{\text{off}}$ and $\%(I_{\text{on}} - I_{\text{off}})$ are the revealed intensity of the species already present before plasma ignition, and the increase in revealed intensity of the same species after plasma ignition, respectively; both these data are normalized against the corresponding value for the peak at $m/z = 310$. The last column of the table reports the ratio between these two quantities.

Table 11. Average peak intensities (counts per second) of the main molecular fragments of HCCP molecules, before plasma ignition (I_{off}) and after plasma ignition (I_{on}).

| m/z | Species | I_{off} (c/s) | I_{on} (c/s) | $I_{\text{on}} - I_{\text{off}}$ (c/s) | $\%I_{\text{off}}$ | $\%(I_{\text{on}} - I_{\text{off}})$ | $\frac{\%(I_{\text{on}} - I_{\text{off}})}{\%I_{\text{off}}}$ |
|-------|----------------------------------|---------------------------|--------------------------|---|--------------------|--------------------------------------|---|
| 345 | $(\text{NPCl}_2)_3$ | 800 | 3400 | 2600 | 13.8 | 12.3 | 0.90 |
| 310 | $(\text{NPCl}_2)_3 - \text{Cl}$ | 5800 | 26900 | 21100 | 100 | 100 | 1 |
| 240 | $(\text{NPCl}_2)_3 - 3\text{Cl}$ | 2480 | 11030 | 8550 | 42.7 | 40.5 | 0.95 |
| 146 | NP_2Cl_2 | 25400 | 122800 | 97400 | 438 | 462 | 1.05 |
| 111 | NP_2Cl | 25300 | 100000 | 74700 | 436 | 354 | 0.80 |
| 101 | PCl_2 | 52800 | 760000 | 707200 | 910 | 3352 | 3.70 |
| 66 | PCl | 45800 | 238000 | 192200 | 790 | 911 | 1.15 |

It must be observed that the presence of HCCP vapours in the deposition chamber before plasma ignition is expected, due to the low sublimation heat of HCCP, which gives rise to the sublimation of its molecules at the low pressure conditions of the deposition chamber (5 Pa) even without heating the phosphazene powder.

If the residual atmosphere in the mass spectrometer were completely contaminant-free, thus making experimental noise negligible, the spectrum collected before plasma ignition would then correspond to the fragmentation pattern of the HCCP molecule.

Unfortunately this is not the case, because of the presence of residual contaminants that can increase unpredictably the intensity of the peaks of HCCP molecular fragments. This uncertainty is avoided in the case of the spectrum collected after plasma ignition, by considering the difference between the peak intensity before and after plasma ignition ($I_{\text{on}} - I_{\text{off}}$) instead of the absolute intensity (I_{on}).

The data showed in Table 11 give some important information on the plasma-induced fragmentation of HCCP. The relative abundances of most molecular fragments do not strongly change after plasma ignition, since the difference is generally limited to a maximum of 20%; a strong increase is observed for the relative abundance of the PCl_2 fragment ($m/z = 101$) when plasma is turned on, as its value becomes almost four times as much. This increase indicates that the plasma induces damage on the HCCP molecules, with the production of molecular fragments that are not necessarily PCl_2 groups; in fact, these species can also arise from ionizer-induced fragmentation of higher molecular weight HCCP fragments in the mass spectrometer.

4.2.4. Characterization of HCCP-derived thin films

The typical FTIR spectrum of as-deposited phosphazene-derived thin film is represented in Figure 38.

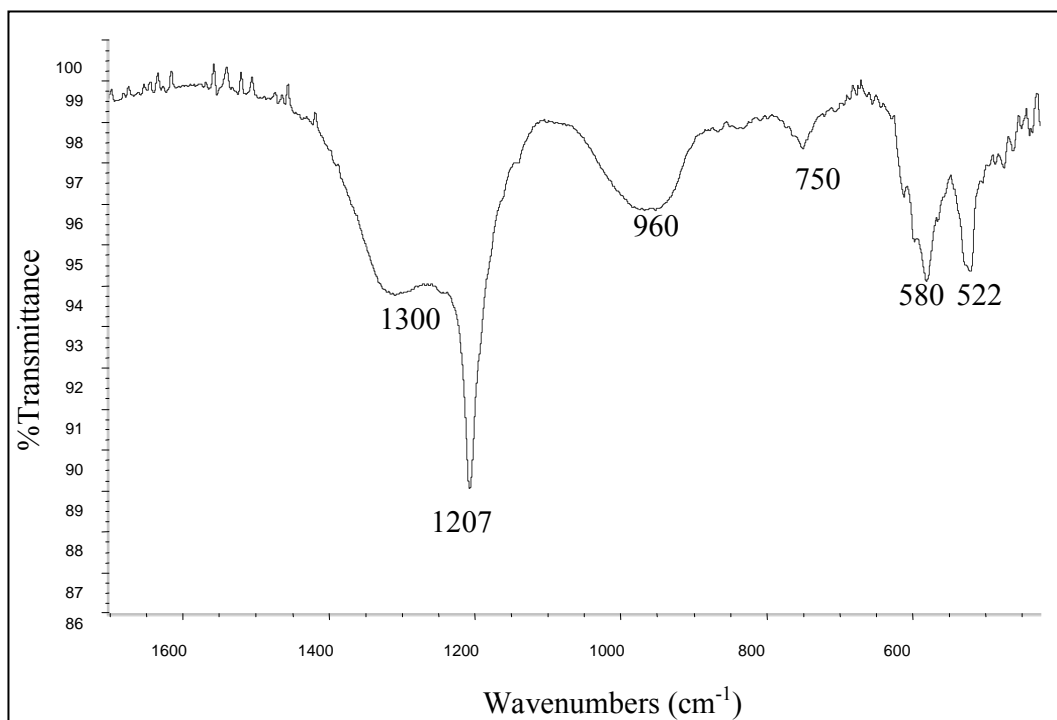


Figure 38. FTIR spectrum of as-obtained phosphazene-derived thin film.

In this spectrum the presence of phosphazenic material on the silicon surface is suggested by the intense absorption at 1207 cm^{-1} , accompanied by a broad shoulder about 1300 cm^{-1} ³⁴⁶, both assigned to the asymmetric stretching of -P=N- groups. The signal at 750 cm^{-1} is assigned to P-N stretching in linear polyphosphazenes³⁴⁶, and resonances at 580 and 522 cm^{-1} are attributable to the mixing of P-Cl and -P=N- vibrations in linear polyphosphazenes as well³⁴⁷. The diagnostic band related to cyclic phosphazene compounds, that is usually observed at 879 cm^{-1} ³²², is practically absent in the spectrum of Figure 4, even if small signals can be observed about $850\text{-}900\text{ cm}^{-1}$. This result suggests that phosphazene ring structure is almost completely lost in the deposited material, and linear $\text{-(N=PCl}_2\text{)}_n\text{-}$ chains are formed, as expected on the basis of previous literature^{348,349}.

The HCCP-derived thin films obtained are highly hydrophilic in nature, as assessed by the broad peak centred about 3250 cm^{-1} (not shown in figure) attributable to water molecules adsorbed on the surface of the coating. It is as well known that P-Cl functionality is hydrolytically unstable, especially in linear phosphazenes, and reacts with water to give P-OH groups and HCl, so the formation of P-OH groups can be also expected^{5,9}.

The broad peak centred about 960 cm^{-1} is probably due to the overlapping of two or more resonances, and can be attributed to vibrations involving wagging motions of PCl_2 groups in linear PDCP³⁴⁷, as well as vibrations of P-O bonds³¹³. It is noteworthy that P-O bonds could arise as a consequence of reaction with water and also due to the phosphazene covalent linkage to the substrate through P-O-Si bonds.

The XPS characterization allowed the surface composition and the BE of detected elements to be determined. In Table 12 are reported the atomic percentages obtained for samples ACT PN 2 and AR PN 2, deposited with or without preliminary surface activation treatment of the silicon substrate with Ar/O₂ plasma, respectively.

Table 12. XPS atomic percentages for selected samples.

| Sample | %O | % N | %Cl | %P | %Si | %F |
|-----------------|------|------|------|------|------|-----|
| AR PN 2 | 25.2 | 25.4 | 18.5 | 24.2 | -- | -- |
| ACT PN 2 | 22.8 | 24.9 | 21.5 | 23.4 | -- | -- |
| ACT PN 2 washed | 22.9 | 3.8 | 1.0 | 4.7 | 20.3 | -- |
| ACT PN 2 CF3 | 27.8 | 2.8 | 2.0 | 4.0 | 16.2 | 3.9 |

In both samples, the Cl : N : P atomic ratio results within the experimental uncertainties close to 1 : 1 : 1, which accounts for the loss of about 50% of chlorine atoms with respect to HCCP stoichiometry.

The detected BEs are in good agreement with those reported in literature for phosphazene compounds³²⁹. In particular, the BE of the P_{2p} peak ranges in the interval 133.5-134.4 eV. These values are close to the one found in (PNCl₂)₃, *i.e.* 134.6 eV. The same evidence has been found for the BE of the N_{1s} peak, ranging in the interval 398.6-398.7 eV, a value very close to that reported for HCCP.

The detected O_{1s} peak is due to the overlapping of two signals, centred respectively at 533.0 and 531.6 eV. The high amount of detected oxygen (22%-25%, see Table 13) can be ascribed both to adventitious contamination and to adsorbed water, as found by other XPS analyses of chlorophosphazene compounds³²⁹.

4.2.5. Behaviour of chlorophosphazene coatings towards washing

The behaviour of HCCP-derived coatings upon immersion in THF solvent has been studied. Selected samples, deposited with (ACT samples) or without (AR samples) preliminary ion etching of the substrates, were treated in anhydrous THF for 1 hour.

In Figure 39 are compared the FT-IR spectra of three different thin films, collected after washing in THF: samples AR PN 1 washed (Figure 39a), ACT PN 1 washed (Figure 39b) and ACT PN 2 washed (Figure 39c).

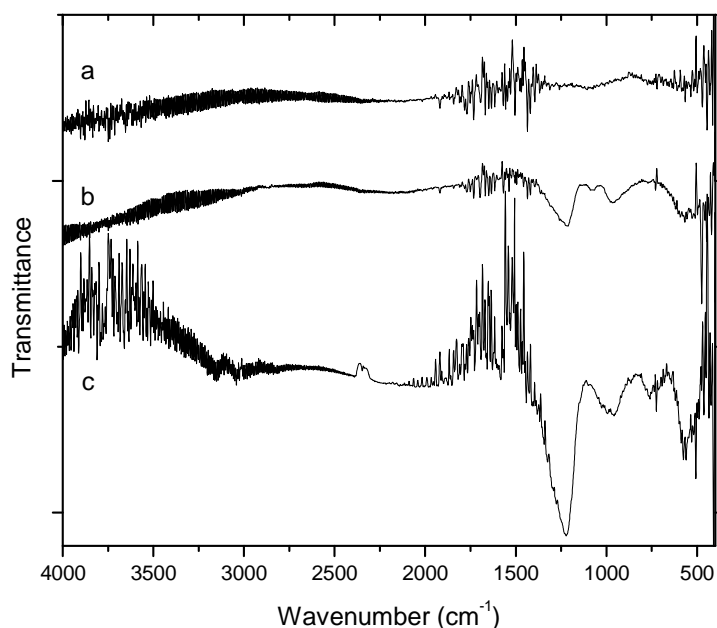


Figure 39. FTIR spectra collected after THF washing: samples (a) AR PN 1 washed, (b) ACT PN 1 washed and (c) ACT PN 2

Chlorophosphazene-derived coatings are almost completely removed by immersion and rinsing in anhydrous solvent, as already reported in previous literature on plasma-initiated HCCP polymerization^{348,349}. Nevertheless, the presence of broad signals in the regions about 1210, 900 and 500 cm^{-1} , suggests that ACT PN 1 and ACT PN 2 coatings are not fully cleaned-down, leaving an insoluble phosphazene-derived material on the sample. The presence of HCCP derivative attached onto the surface of THF-washed samples has been confirmed by XPS analysis, exclusively for deposits obtained on activated silicon substrates (see Table 12, sample ACT PN 2 washed).

4.2.6. Substitution reactions in solution

Surface functionalization of the HCCP-derived coating deposited on silicon wafers (ACT PN) was carried out by immersion of these materials in THF solutions containing an excess of TFE or 4CNP, in the presence of NaH as a base, and under a nitrogen blanket. After 1 h of treatment at room temperature, the functionalized samples (ACT CF3 and ACT CN, respectively) were rinsed in fresh THF, dried and characterized by FTIR spectroscopy and XPS analyses.

The IR spectrum of ACT CF3 is reported in Figure 40b, together with those of TFE (Figure 40c) and of the related blank material (Figure 40a, blank CF3).

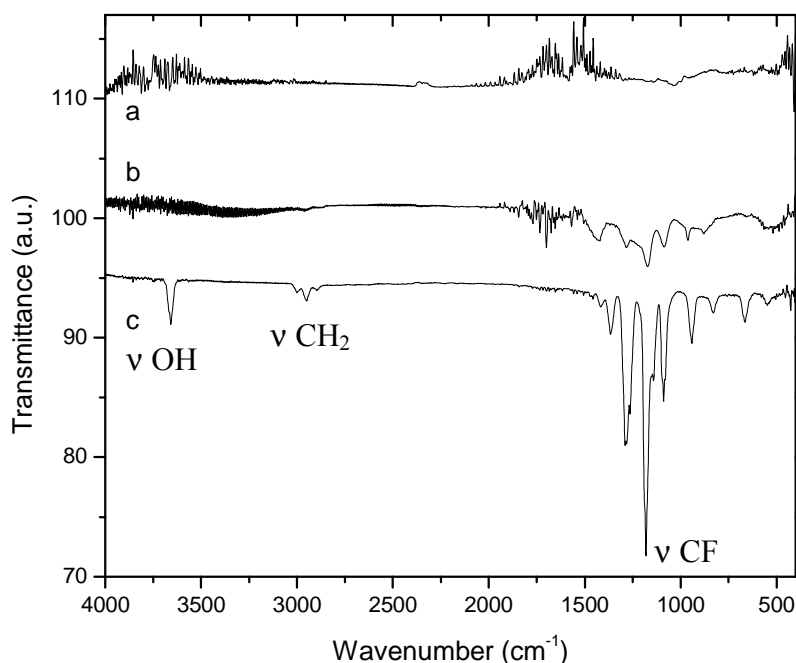


Figure 40. FTIR spectra of (a) blank CF3, (b) ACT PN CF3 and (c) liquid trifluoroethanol.

The presence of characteristic bands assigned to the $-\text{OCH}_2\text{CF}_3$ residue in the spectrum of sample ACT PN CF3 and the disappearance of the O-H stretching signal of TFE suggest that the alcohol reacted with the chlorophosphazene, leading to the formation of $\text{CF}_3\text{-CH}_2\text{-O-P}$ groups and NaCl. As a matter of fact, no absorption bands could be detected for silicon substrates treated only with TFE (sample blank CF3, Figure 40a) without previous phosphazene deposition. These findings could be confirmed by means of XPS analysis of phosphazene-functionalized thin films, which reveals the presence of fluorine (symmetric F_{1s} peak at 690.1 eV). The fluorine atomic percentage measured on ACT PN CF3 sample was 3.9% (see Table 12), suggesting that about one third of the remaining phosphorus atoms are substituted with one $-\text{OCH}_2\text{CF}_3$ group on average.

Similarly, the IR characterization of the HCCP coatings deposited on silicon wafers and functionalized with 4CNP (Figure 41) showed the presence of a typical band at 2232 cm^{-1} in ACT PN CN spectra (see Figures 41a, ACT PN 1 CN, and 41b, ACT PN 2 CN, respectively) attributed to the stretching of $-\text{CN}$ group. This signal is not appreciable on the surface of silicon substrates treated only with 4CNP (Figure 41c).

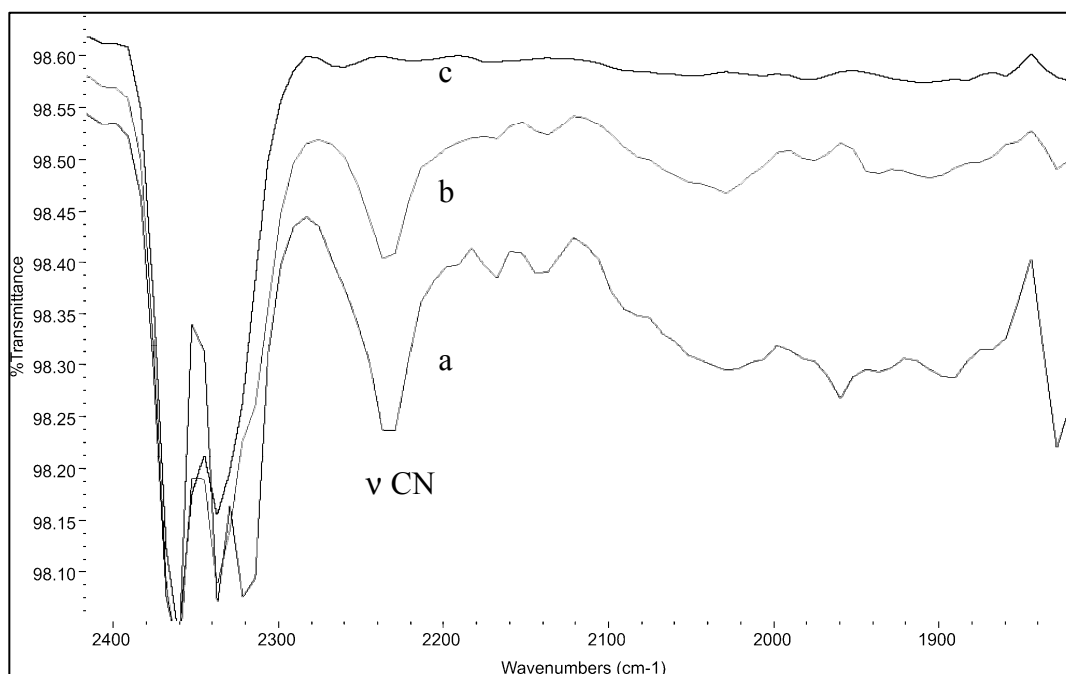


Figure 41. FTIR spectra of samples (a) ACT PN 1 CN, (b) ACT PN 2 CN and of (c) blank CN.

These results strongly indicate that the surface functionalization of silicon wafers with a fluorinated alcohol and a phenol group through the action of HCCP could be successfully achieved.

4.2.7. Conclusions

A new method for the modification of silicon surfaces with organic groups has been described, dealing with an HCCP derivative as coupling agent. The chlorophosphazene was employed in powder form as a target material for the deposition of thin films by Glow Discharge-induced Sublimation (GDS) technique.

Deposition rate measurements and mass spectrometry point out that during plasma deposition a strong sublimation of undamaged molecules together with the emission of volatile fragments from the target occur. Formation of a damaged surface layer on the target is then delayed for deposition times as long as 250 seconds.

The cyclic structure of HCCP is lost during plasma deposition, as shown by FT-IR spectroscopy, leading to linear oligomeric chlorinated phosphazene coatings on the silicon substrate.

Immersion and rinsing in anhydrous solvent leads to dissolution of the chlorophosphazene coating, unless the substrate was plasma-activated prior to deposition. In this case an insoluble phosphazene derivative is detectable on the sample, both by FT-IR and XPS analyses. As a consequence, a measurable extent of covalent bonding between deposited chlorophosphazene oligomers and surface Si-O groups is possibly obtained by activating silicon substrates by plasma ion etching.

Phosphazene coated silicon substrates have been reacted in solution with selected nucleophilic reagents, *i.e.* TFE and 4CNP, undergoing chlorine atom substitution that led to chemical modification of the silicon substrates.

Experimental results here reported can be envisaged as a starting point for the development of a general method for the immobilization of various molecules and macromolecules onto inorganic surfaces.

4.2.8. Acknowledgements

The deposition by GDS technique of thin phosphazene films was performed by Dr. Alessandro Sassi (Institute of Molecular Sciences and Technologies, ISTM, of the National Research Council, CNR, section of Padova, Italy) and by Dr. Gianluigi

Maggioni (University of Padova, Italy, c/o National Institute of Nuclear Physics, National Laboratories of Legnaro, Italy) at the LNL (National Laboratories of Legnaro, Italy, of the National Institute of Nuclear Physics). XPS measurements were performed by Dr. Silvia Gross (Institute of Molecular Sciences and Technologies, ISTM, of the National Research Council, CNR, section of Padova, Italy).

4.3. SURFACE FUNCTIONALIZATION OF POLYMERIC SUBSTRATES USING CHLORINATED PHOSPHAZENES AS COUPLING AGENTS

In this section we will describe the surface modification of three polymeric substrates of practical and industrial interest, *i.e.* HDPE, PA6 and EVOH, utilizing PDCP and HCCP as functionalization intermediates.

The overall process is illustrated in Figure 42.

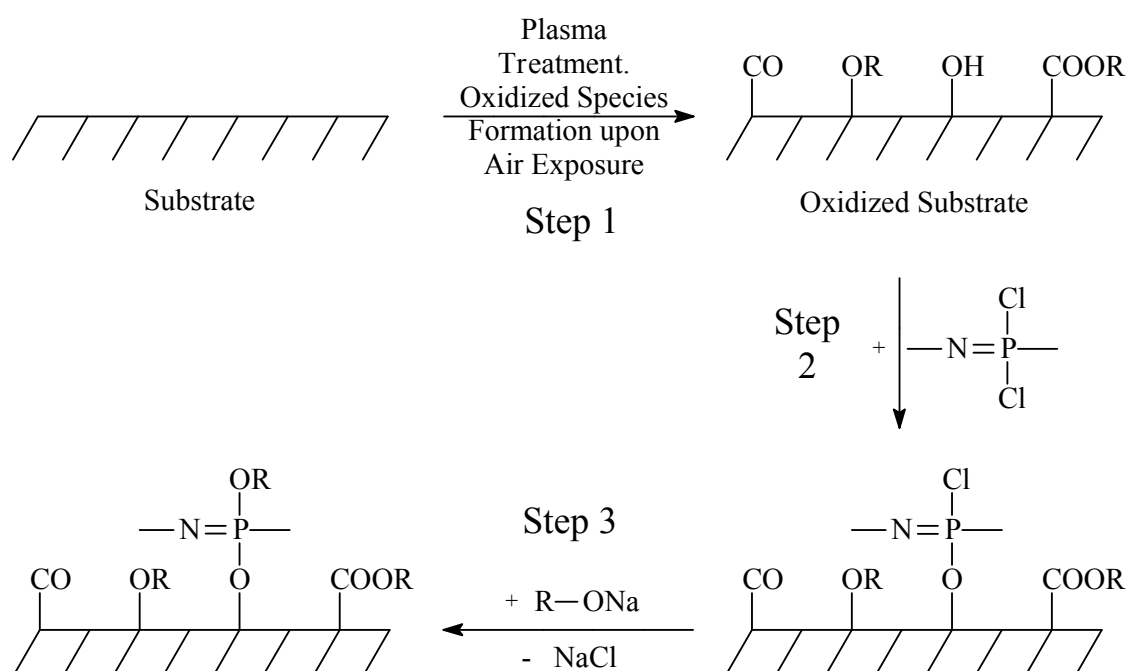


Figure 42. General scheme for the surface functionalization of polymeric plates with phosphazenes.

To make the grafting of the chlorophosphazenes possible, HDPE and PA6 were first treated with cold, low pressure plasma (step 1), so as to create hydroxyl functions on

their surfaces; these hydroxyls enable the bonding of the phosphazenes to the substrates through P-O-C covalent bonds (step 2). As hydroxyls are naturally present on the surface of EVOH, plasma treatment was not necessary for this polymer.

After grafting, HCCP and PDCP still maintain part of their P-Cl groups, which are therefore susceptible to undergo further substitution reactions with a great number of different nucleophiles, particularly alcohols, phenols and primary or secondary amines (step 3). The choice of such nucleophiles allows in principle to tailor the chemical and physical properties of the final substrate surface.

In this work we used three different nucleophiles for the surface functionalization of the polymeric samples, *i.e.*

- 1) TFE, because of its known and well explored reactivity towards chlorophosphazenes³⁴⁶, as it can be considered as a good marker in XPS analysis due to its fluorine content, and because of the potential biomedical applications of the corresponding poly[bis(2,2,2-trifluoroethoxy)phosphazene (PTFEP) for biocompatible and antithrombogenic coatings^{268-274,350-354},
- 2) HDFN, that may be considered as a good example for the introduction of longer fluorinated chains onto the surface of the substrates, possibly leading to major modifications of their surface energy and hydrophilicity;
- 3) AzB, a compound with known photochromic properties^{135,355,356} and a possible prototype for surface functionalization of polymeric substrates with NLO-active *push-pull* azobenzenic systems of similar chemical structure. This nucleophile was employed only for PA6 and EVOH substrates.

4.3.1. Step 1: Plasma treatment of HDPE and PA6

At a first stage of this work, preliminary investigations were carried out to determine the experimental conditions that enable the formation of the highest quantity of reactive hydroxyl functions on the surface of the substrates. This was done in order to improve phosphazene grafting and therefore the final modification of surface properties of the substrates. These preliminary researches were performed on HDPE substrates, and the experimental parameters thus individuated were also used for the surface activation of PA6 samples.

HDPE plates were first exposed to different cold low-pressure plasmas, allowing them to come into contact with the air immediately after. According to literature³⁵⁷⁻³⁶⁰,

this treatment brings about the cleaning of the polymer surface, the scission of the HDPE chains with volatilization of small polymer fragments, and the formation of surface radicals. This latest effect is responsible for the superficial reticulation of the polymer substrates and for the surface formation of polar species (*e.g.* carbonyl, carboxyl, ether groups, and hydroxylic functions) as soon as the samples are exposed to oxygen and moisture^{359,361}.

The samples obtained were characterized by contact angle measurement, and by FTIR-ATR and XPS Spectroscopy. All the measurements were carried out immediately after the treatment, due to the high mobility of the surface polymer chains; in fact, the polar chemical functions introduced by the plasma treatment, have the tendency to turn towards the polymer bulk over time to minimize the surface energy³⁶².

4.3.1.1. Contact angle study

Water contact angle measurements for plasma treated HDPE plates were used to individuate the appropriate experimental conditions for the surface modification of HDPE plates. As suitable plasma gases we exploited an argon/oxygen mixture and neat argon, using different plasma generator powers and exposure times. The corresponding results are reported in Figure 43 and in Table 13.

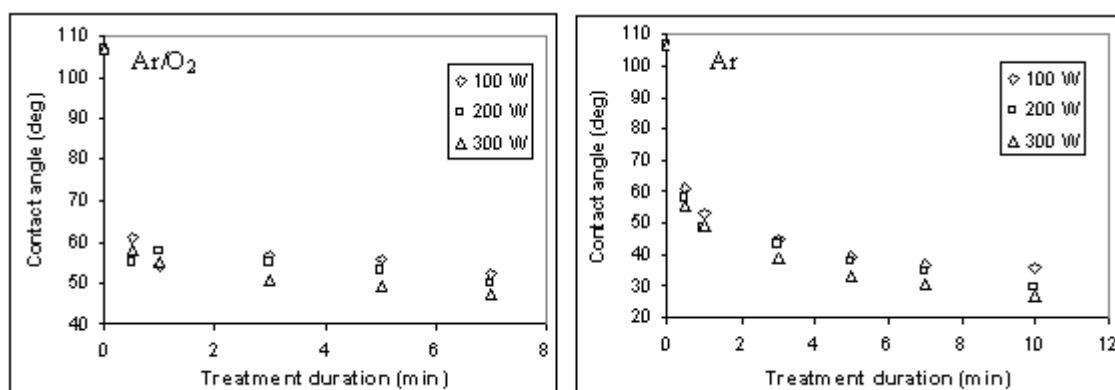


Figure 43. Contact angle measurements with water of HDPE surfaces treated with mixed Ar/O₂ plasma and with neat Ar plasma as a function of treatment duration.

Table 13. Contact angle with water of *HDPE* samples treated with Ar/O₂ (left) and with neat Ar (right) plasma treatments for different microwave powers and treatment durations (degrees).

| | Ar/O ₂ | | | Ar | | |
|------------|-------------------|-------|-------|-------|-------|-------|
| Time (min) | 100 W | 200 W | 300 W | 100 W | 200 W | 300 W |
| 0 | 106.7 | 106.7 | 106.7 | 106.7 | 106.7 | 106.7 |
| 0.5 | 53.9 | 55.1 | 57.9 | 61.2 | 57.8 | 55.8 |
| 1 | 54.1 | 57.2 | 55.0 | 53.2 | 48.2 | 48.7 |
| 3 | 56.5 | 55.0 | 50.4 | 45.0 | 43.1 | 38.8 |
| 5 | 55.7 | 53.1 | 49.3 | 39.5 | 38.1 | 33.1 |
| 7 | 52.6 | 49.6 | 47.2 | 36.7 | 34.5 | 30.4 |
| 10 | - | - | - | 36.0 | 29.4 | 26.7 |

As it can be seen from these data, the water contact angle of clean untreated HDPE surfaces is about 106°. As an effect of plasma treatment followed by air exposure, this value drops dramatically down to 47.2° (Ar/O₂ mixture) and to 26.7° (neat Ar), using the highest generator powers (300W) and longest treatment times (7 and 10 min, respectively). On the basis of these results, we kept the following experimental conditions as a standard for all the plasma treatments of HDPE and PA6 carried out in this work: neat argon plasma, power of 300W, treatment duration of 3 minutes, and gas flux of 0.30 dm³/min. This was estimated to be the best compromise between the formation of reactive functions on the surface of HDPE plates and the reduced damage of the polymer surface; in fact, such a damage would probably occur with more drastic experimental conditions³⁵⁹.

The application of the indicated treatment conditions to PA6 plates had a similar effect, lowering their contact angle with water from 76.5 to 43.3°. This result accounted for the formation of further polar species on the surface of this substrate, besides those that are naturally present in it.

4.3.1.2. Infrared study

In Figure 44 is shown the FTIR spectrum in Attenuated Total Reflectance (ATR) conditions of a HDPE sample treated with Ar plasma using the standard parameters. Note that the reported spectrum was obtained by subtraction of the virgin HDPE spectrum from the one of the functionalized sample.

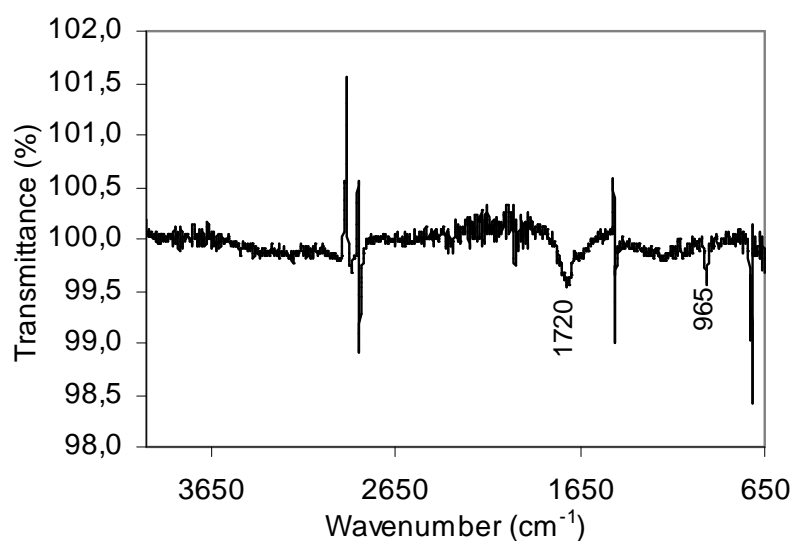


Figure 44. FTIR-ATR difference spectrum of HDPE treated with Ar plasma according to standard conditions with respect to untreated HDPE sample.

This Figure shows bands located at about 1720 cm^{-1} , assignable to C=O functions (possibly forming also hydrogen bonds, as indicated by the presence of a shoulder at lower wavenumbers), and at 965 cm^{-1} , assigned to C-O bonds³⁵⁷. Signals at about 2890 , 1460 and 730 cm^{-1} are also present, and they are attributed to imperfect subtractions of the polyethylene peaks. It is worth noting that no significant differences could be detected between the infrared spectra of the samples when analyzed 5 minutes, 1 hour or 3 hours after the plasma treatment; this suggests that the formation of polar functional groups on the surface took place immediately as soon as the treated HDPE plates were put in contact with the air.

4.3.1.3. XPS study

The XPS analysis of samples prepared according to the standard plasma conditions gave the results reported in Table 14.

Table 14. XPS atomic percentages for virgin HDPE and PA6 plates and for samples treated according to standard plasma activation procedure.

| Sample | C | O | N | O/C |
|--------------------------------------|------|------|------|------|
| <i>H1</i> - Virgin HDPE ^a | 93.4 | 4.4 | --- | 0.05 |
| <i>H2</i> - Ar plasma treated HDPE | 83.4 | 16.1 | 0.6 | 0.19 |
| <i>P1</i> - Virgin PA6 | 77.1 | 12.4 | 10.4 | 0.16 |
| <i>P2</i> - Ar plasma treated PA6 | 70.6 | 16.9 | 11.1 | 0.24 |

^a Presence of Si impurity (2.2%)

Although the virgin sample H1 seems to already contain some oxygen, perhaps due to a slight oxidation of the starting material, these data evidenced clearly the effect of the activation procedure. In fact, the O/C atomic percentage ratio grew from 0.05 to 0.19 for HDPE and from 0.16 to 0.24 for PA6 as a result of the plasma treatment. The introduction of a small quantity of nitrogen onto the sample surface appears to be a side effect, possibly coming from molecular nitrogen present as an impurity in the argon gas utilized. Curve fitting of the C_{1s} photopeak of sample H2 is illustrated in Figure 45.

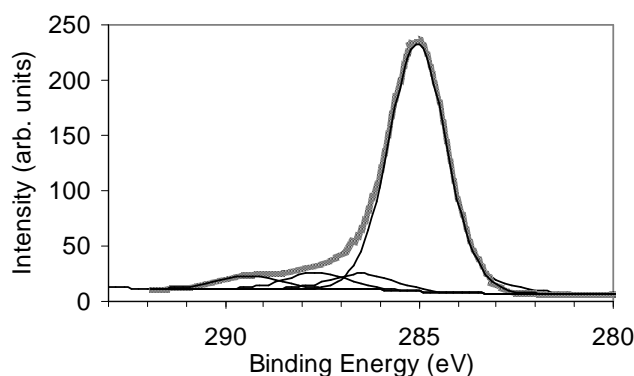


Figure 45. Deconvolution of XPS C_{1s} photopeak of sample H2 (plasma-treated HDPE).

Besides the main polyethylene carbon at 285.0 eV, the spectrum shows the presence of components assignable to carboxyl or ester (289.4 eV) functions and carbonyl (287.6 eV) groups as well as carbon single-bonded to one oxygen atom, that may come from alcoholic or ethereal moieties (286.5 eV)^{360,363,364}. All these additional features are substantially absent in the spectrum of untreated HDPE.

Similar considerations may be done by performing curve fitting of the C_{1s} photopeaks of polyamide samples P1 and P2, as illustrated in Figure 46a and 46b, respectively, and in Table 15.

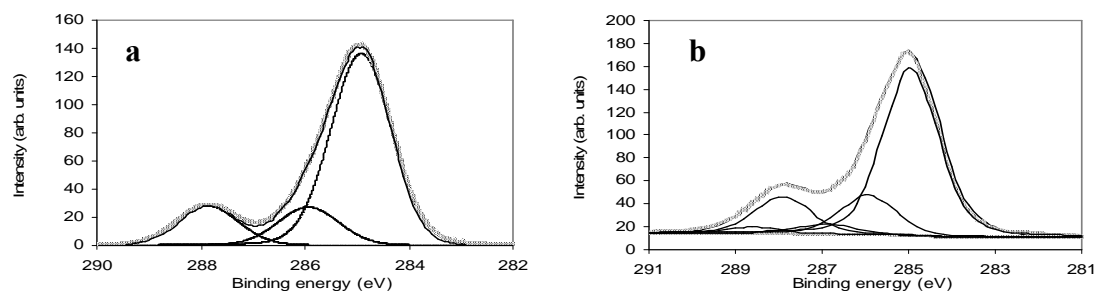


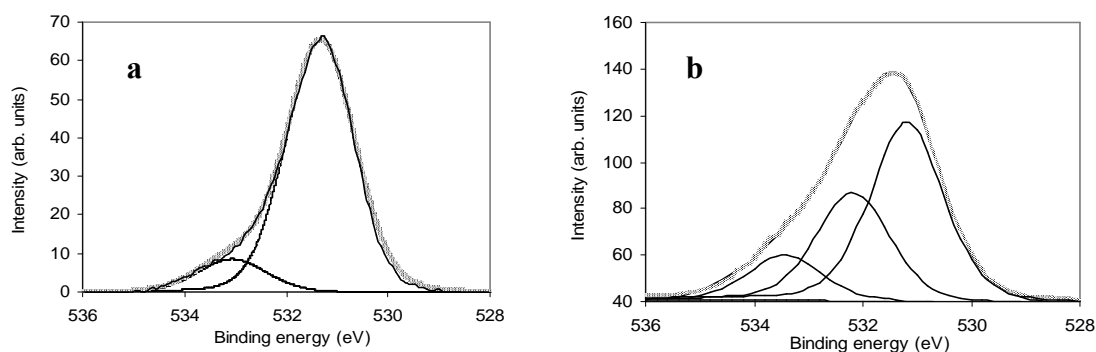
Figure 46. Curve fitting of XPS C_{1s} spectrum of (a) virgin and (b) plasma treated PA6.

Table 15. Curve fitting of XPS C_{1s} spectrum of virgin (P1) and plasma-treated (P2) PA6.

| C _{1s} , Sample <i>P1</i> | | | C _{1s} , Sample <i>P2</i> | | |
|------------------------------------|-------------|-----------|------------------------------------|-------------|-----------|
| Position (eV) | Area (a.u.) | FWHM (eV) | Position (eV) | Area (a.u.) | FWHM (eV) |
| 285.0 | 1.00 | 1.4 | 284.9 | 1.00 | 1.5 |
| 285.9 | 0.22 | 1.4 | 285.9 | 0.23 | 1.5 |
| | | | 286.9 | 0.06 | 1.5 |
| 287.9 | 0.22 | 1.4 | 287.9 | 0.22 | 1.5 |
| | | | 288.6 | 0.04 | 1.5 |

C_{1s} spectra of both samples present one major component at about 285.0 eV due to aliphatic CH₂ groups bonded only to other CH₂, and two other ones located at 285.9 and 287.9 eV that arise from nitrogen-bonded CH₂ and from amide groups, respectively. In the spectrum of sample P2, however, two minor components are present at 286.9 and 288.6 eV, the first of which can be assigned to alcoholic and/or ethereal moieties³⁶⁵, while the second one is probably due to carboxylic groups³⁶⁶.

The curve fitting of O_{1s} photopeaks of samples P1 and P2 yielded the results reported in Figures 47a and 47b, respectively, and in Table 16.

**Figure 47.** Curve fitting of XPS O_{1s} spectrum of (a) virgin and (b) plasma treated PA6.**Table 16.** Curve fitting of XPS O_{1s} spectrum of virgin (P1) and plasma-treated (P2) PA6.

| O _{1s} , Sample <i>P1</i> | | | O _{1s} , Sample <i>P2</i> | | |
|------------------------------------|-------------|-----------|------------------------------------|-------------|-----------|
| Position (eV) | Area (a.u.) | FWHM (eV) | Position (eV) | Area (a.u.) | FWHM (eV) |
| 531.3 | 1.00 | 1.6 | 531.2 | 1.00 | 1.6 |
| | | | 532.2 | 0.61 | 1.6 |
| 533.1 | 0.14 | 1.6 | 533.4 | 0.25 | 1.6 |

The components at about 531 and 533 eV are common to the two samples and are assigned to amide oxygen, free and engaged in hydrogen bonds, respectively³⁶⁷. In the plasma-treated sample a new component appears at 532.2 eV, attributed to the sum of different oxidized carbon species, such as oxygen double-bonded to carbon in

carboxylic groups and CH-bonded hydroxyl groups^{368,369}, confirming the observations already made for C_{1s} spectral simulations.

All these findings support the idea that cold argon plasma-treated HDPE and PA6 plates have their surface deeply modified under these conditions, and that the formation of oxidized species occurs, hydroxyl groups included.

4.3.2. Step 2: Grafting of chlorophosphazenes

Once functionalized by plasma treatments, the polymeric plates containing free hydroxyl groups on the surface were immersed in anhydrous THF or toluene solutions of HCCP and PDCP, in order to graft these molecules onto the surface of the substrates. In the case of HCCP the presence of anhydrous triethylamine was exploited.

The overall reaction, reported as Step 2 of Figure 42, makes it possible to attach both cyclic and polymeric phosphazenes onto the surface of HDPE plates, and leaves unreacted P-Cl groups potentially susceptible to undergo further functionalization reactions.

No characterization was attempted for the samples functionalized only with chlorophosphazenes (*i.e.*, between steps 2 and 3) because of the high hydrolytic instability of chlorophosphazenes grafted onto the surface of solid materials^{5,7}.

4.3.3. Step 3: Nucleophilic replacement of phosphazene residual chlorines

Substitution of residual chlorines present in the surface grafted phosphazenes with suitable nucleophiles brought about the final functionalization of the substrates. This process was carried out by immersing phosphazene-unctionalized samples in THF solutions of sodium trifluoroethoxide, heptadecafluorononoxide and 4-phenylazophenoxide, as obtained by treating the corresponding alcohols/phenols with metallic sodium, at room temperature and for several hours.

The substitution reaction that takes place in the phosphazene coupling agents is reported as Step 3 in Figure 42.

After treatment, the polymeric plates thus functionalized were characterized by FTIR-ATR and XPS spectroscopy, contact angle measurements, and also by UV-Vis spectroscopy in the case of azobenzene-functionalized samples.

4.3.3.1 Infrared characterization

Infrared characterization was actually possible only for HDPE samples because of the extremely low thickness of the deposited layer, and because the infrared spectra of PA6 and EVOH present strong peaks in the diagnostic regions of both the phosphazenes and the substituted nucleophiles. These factors made it difficult to clearly detect the diagnostic bands of the materials obtained, even when performing subtraction of the virgin polymer spectra.

The FTIR-ATR spectra of HDPE plates functionalized with phosphazenes and fluorinated alcohols were obtained as a difference between functionalized samples and virgin HDPE.

As reported in Figure 48, the FTIR-ATR spectrum of a HDPE sample with surface grafted HCCP and TFE shows a first series of bands located at 1230 cm^{-1} and at 1086 cm^{-1} , which are assignable to the asymmetric stretching of the P=N bond and to the P-O-C absorption of the phosphazene substrate, respectively. The presence of the TFE is proved by a signal at 1281 and 1169 cm^{-1} , assignable to the asymmetric and symmetric C-F stretching of the fluorinated alcohol.

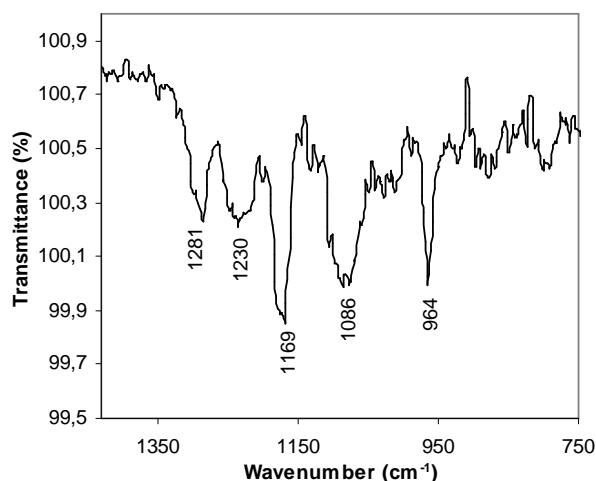


Figure 48. FTIR-ATR spectrum of HDPE functionalized with HCCP and TFE.

A similar IR pattern could be obtained for HDPE where HCCP and HDFN had been grafted, but the C-F symmetric stretch of this compound was found at about 1150 cm^{-1} . The narrow signal at 964 cm^{-1} present in the spectrum of Figure 48 has already been assigned in the preliminary study on HDPE surface activated by plasma (see 4.3.1.2).

4.3.3.2 Contact angle characterization

In Table 17 are reported the values of water contact angle ($\pm 2^\circ$) and the results of surface energy measurements for virgin, plasma-treated, and functionalized samples.

Table 17. Contact Angle values (± 2 deg) and Surface Energy for virgin, plasma-treated and functionalized HDPE, PA6 and EVOH samples.

| Sample | Contact angle w/H ₂ O (deg) | Free Surface Energy (mJ/m ²) | | | |
|------------------------------------|---|--|----------------|---------------------|----------|
| | | Total | Polar Comp. | Dispersive Comp. | Pol/Disp |
| H1 - Virgin HDPE | 106.7 | 33.2 | 0.0 | 33.2 | 0.00 |
| H2 - Ar plasma treated HDPE | 38.8 | 61.2 | 23.3 | 37.9 | 0.61 |
| H3 – HDPE,Ar+PDCP+TFE | 73.1 | 43.6 | 6.6 | 37.0 | 0.18 |
| H4 – HDPE,Ar+PDCP+HDFN | 118.9 | 10.8 | 0.3 | 10.5 | 0.03 |
| H5 – HDPE,Ar+HCCP+TFE | 91.9 | 25.5 | 3.2 | 22.3 | 0.14 |
| H6 – HDPE,Ar+HCCP+HDFN | 103.5 | 19.5 | 0.7 | 18.7 | 0.04 |
| P1 - Virgin PA6 | 76.5 | 39.6 | 5.2 | 34.4 | 0.15 |
| P2 - Ar plasma treated PA6 | 43.3 | 60.9 | 21.0 | 40.0 | 0.53 |
| P3 - PA6,Ar+PDCP+TFE | 103.1 | 15.3 | 3.0 | 12.3 | 0.24 |
| P4 - PA6,Ar+PDCP+HDFN | 123.2 | 7.1 | 1.0 | 6.2 | 0.16 |
| P5 - PA6,Ar+PDCP+AzB | 92.3 | 45.6 | 0.3 | 45.3 | 0.01 |
| P6 - PA6,Ar+HCCP+TFE | 99.0 | 36.4 | 0.2 | 36.2 | 0.01 |
| P7 - PA6,Ar+HCCP+HDFN | 99.7 | 23.8 | 0.8 | 23.0 | 0.03 |
| P8 - PA6,Ar+HCCP+AzB | 81.6 | 45.1 | 2.4 | 42.8 | 0.06 |
| E1 - Virgin EVOH | 75.6 | 44.5 | 5.1 | 39.4 | 0.13 |
| E2 – EVOH+PDCP+TFE | 84.9 | 38.6 | 2.6 | 36.1 | 0.07 |
| E3 – EVOH+PDCP+HDFN | 106.4 | 19.3 | 0.6 | 18.7 | 0.03 |
| E4 – EVOH+PDCP+AzB | 76.6 | 42.8 | 4.3 | 38.5 | 0.11 |
| E5 – EVOH+HCCP+TFE | 91.6 | 31.0 | 1.8 | 29.2 | 0.06 |
| E6 – EVOH+HCCP+HDFN | 110.2 | 10.5 | 1.6 | 8.9 | 0.18 |
| E7 – EVOH+HCCP+AzB | 88.6 | 39.9 | 1.0 | 39.0 | 0.03 |

Plasma treatment of HDPE and PA6 brought about a decrease in contact angle of the substrates, due to the formation of new polar species, as described in section 4.3.1.1. This is confirmed also by the higher value surface energy with respect to the virgin samples, and by the presence of polar components that were originally lower (PA6) or absent (HDPE) in the virgin polymers.

After phosphazene grafting and substitution with fluorinated alcohols, the contact angle with water grew for all tested substrates, even reaching values significantly higher than those of the virgin polymers. At the same time the ratio between polar and dispersive components dropped significantly, to suggest that the grafting of the

fluorinated alcohols did take place. As expected these effects are particularly evident in the case of HDFN, which presents a longer fluorinated chain; the enhanced hydrophobic character of the fluorinated surfaces was evidenced by their water contact angles, which resulted often higher than 100 degrees.

Similar considerations can be made for azobenzene-functionalized samples, but the modifications in contact angle and surface energy are weaker, as the azobenzene groups are less hydrophobic than the perfluorinated alkyl chains. All these findings strongly support the success of the surface functionalization of the substrates.

Interestingly, by comparison of the results obtained for PDCP- and HCCP-grafted samples, the introduction of the substituent molecules during the third functionalization step seems to have stronger effects for PA6 substrates when PDCP was used as a coupling agent, and for EVOH substrates when HCCP was employed. The behaviour observed for PA6 is not unexpected, both because the phosphazene polymer is more reactive than its trimeric homologue¹, and because a relatively smaller portion of available P-Cl groups are probably required to graft this polymer onto the surface; this would leave a greater quantity of reactive chlorines available for further nucleophilic substitution reactions.

In order to explain the opposite behaviour observed for EVOH samples one could invoke the consideration that these substrates probably still contained some physically adsorbed water when the phosphazene grafting process was performed, in spite of the preliminary overnight drying at 110°C. This would be due to the great number of polar hydroxyl functions naturally present both in the bulk and on the surface of the material. The water may induce hydrolysis phenomena on the phosphazene substrate and lead to the degradation of the -P=N- chain, as shown in Figure 48; the effects of such phenomena are expected to be more remarkable on PDCP-containing samples, because of the higher reactivity of the phosphazene polymer.

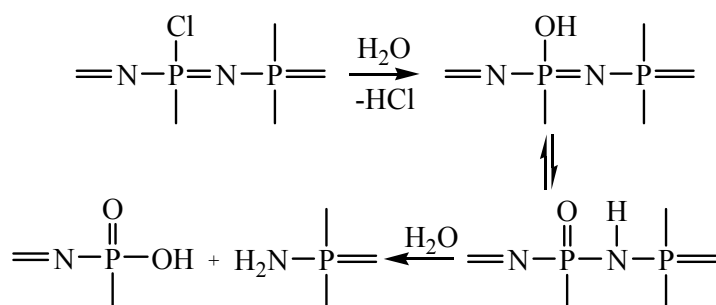


Figure 48. Phosphazene/phosphazane isomerization through hydrolysis of P-Cl groups, and subsequent chain or ring degradation.

4.3.3.3 XPS characterization

The results of XPS characterization are presented in Table 18, where the elemental atomic percentages are reported for the whole series of virgin, plasma-treated and final functionalized samples; the N/P and F/P atomic percentages ratios are also reported.

Table 18. Atomic percentages as revealed from XPS analysis for virgin, plasma-treated and functionalized HDPE, PA6 and EVOH samples.

| Sample | C | O | N | P | F | N/P | F/P |
|---|------|------|------|-----|------|------|-------|
| H1 - Virgin HDPE ^a | 93.4 | 4.4 | --- | --- | --- | --- | --- |
| H2 - Ar plasma treated HDPE | 83.3 | 16.1 | 0.6 | --- | --- | --- | --- |
| H3 – HDPE,Ar+PDCP+TFE | 84.1 | 12.5 | 0.9 | 0.7 | 1.8 | 1.32 | 2.59 |
| H4 – HDPE,Ar+PDCP+HDFN | 71.1 | 9.8 | 0.9 | 0.7 | 17.5 | 1.31 | 26.20 |
| H5 – HDPE,Ar+HCCP+TFE ^b | 69.5 | 13.0 | 2.6 | 2.3 | 7.8 | 1.14 | 3.41 |
| H6 – HDPE,Ar+HCCP+HDFN | 66.0 | 10.5 | 1.9 | 1.6 | 20.0 | 1.24 | 12.90 |
| P1 - Virgin PA6 | 77.1 | 12.4 | 10.4 | --- | --- | --- | --- |
| P2 - Ar plasma treated PA6 | 70.6 | 16.9 | 11.1 | --- | --- | --- | --- |
| P3 - PA6,Ar+PDCP+TFE | 58.6 | 14.6 | 10.3 | 2.2 | 14.3 | 4.68 | 6.50 |
| P4 - PA6,Ar+PDCP+HDFN | 49.6 | 8.2 | 6.0 | 1.3 | 34.8 | 4.61 | 26.76 |
| P5 - PA6,Ar+PDCP+AzB | 73.7 | 13.3 | 11.7 | 1.3 | --- | 9.0 | --- |
| P6 - PA6,Ar+HCCP+TFE | 67.5 | 14.0 | 11.1 | 1.5 | 5.8 | 7.40 | 3.86 |
| P7 - PA6,Ar+HCCP+HDFN | 59.6 | 14.3 | 8.9 | 2.1 | 15.1 | 4.23 | 7.19 |
| P8 - PA6,Ar+HCCP+AzB | 68.4 | 15.8 | 12.2 | 3.3 | --- | 3.69 | --- |
| E1 - Virgin EVOH | 86.0 | 11.6 | 2.4 | --- | --- | --- | --- |
| E2 – EVOH+PDCP+TFE | 73.6 | 20.9 | 0.7 | 0.8 | 4.0 | 0.82 | 4.79 |
| E3 – EVOH+PDCP+HDFN | 50.9 | 10.9 | 1.2 | 1.3 | 35.7 | 0.89 | 27.53 |
| E4 – EVOH+PDCP+AzB | 77.4 | 19.1 | 2.4 | 1.1 | --- | 2.10 | --- |
| E5 – EVOH+HCCP+TFE ^c | 50.7 | 18.4 | 5.5 | 6.4 | 17.7 | 0.87 | 2.78 |
| E6 – EVOH+HCCP+HDFN | 46.4 | 10.4 | 2.3 | 2.8 | 38.1 | 0.83 | 13.7 |
| E7 – EVOH+HCCP+AzB | 68.7 | 9.7 | 13.3 | 8.1 | 0.2 | 1.64 | 0.02 |

^a Si contamination (2.2%); ^b Si (2.6%), Cl (0.6%) and Na (1.6%) contaminations;

^c Si contamination (1.3%)

Nitrogen and phosphorus are present in the functionalized samples, and the N/P ratio is close to 1 (with obvious exceptions for PA6 substrates and AzB-containing samples), which accounts for the success of phosphazene grafting. The relatively low values of the atomic percentages revealed for these elements indicate that the grafted layer is extremely thin, possibly monomolecular. Phosphorus and nitrogen content was higher in HCCP-containing samples than in those where PDCP had been grafted; this is striking, if one considers the sizes of the two compounds and the fact that the linear phosphazene polymer is supposed to be more reactive than the corresponding trimer¹. These observations may in fact lead to expect higher phosphorus and nitrogen content

when PDCP is exploited, rather than HCCP. Different hypotheses can explain this finding, such as the differences in steric hindrance between the two phosphazene compounds, the different experimental conditions employed during grafting (the reaction with HCCP is performed for a longer time, at higher temperature and in the presence of triethylamine as a catalyst), or even the lack of complete substitution of the chlorine atoms during step 3; this last factor may lead to hydrolysis phenomena and chain degradation during the final washing of the samples, as already shown in section 4.3.3.2 and in Figure 48. This grafting difference between the two phosphazenes appeared particularly evident in EVOH samples, which is consistent with the observations made in section 4.3.3.2 while commenting on the contact angle results.

Moreover, a comparison between EVOH and plasma-treated HDPE– and PA6–functionalized surfaces showed that the phosphazene grafting reaction took place more efficiently on EVOH plates than on the other polymeric substrates. This is not unexpected since the ethylene/vinyl alcohol copolymer intrinsically contains a great quantity of hydroxyl functionalities, which are suitable for reaction with HCCP and PDCP. In fact, the atomic percentage of phosphorus was about 3% at the most for functionalized plasma-treated HDPE and PA6, while up to 8% was found for it in sample E7.

Further information can be inferred by the curve fitting of the N_{1s} spectra, whose results are reported in Table 19 for HDPE and EVOH functionalized with fluorinated alcohols. The N_{1s} spectrum of sample H5 is reported in Figure 49 as an example.

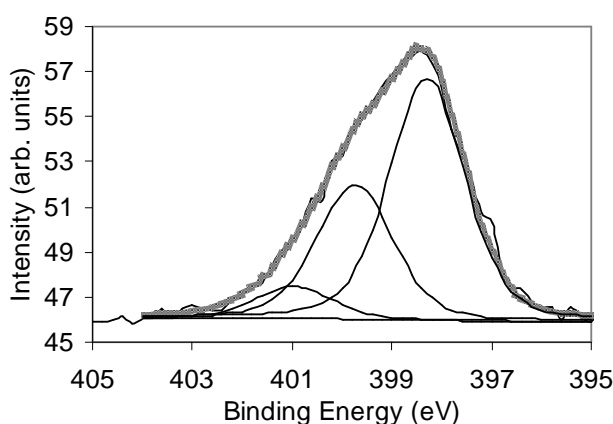


Figure 49. Deconvolution of XPS N_{1s} photopeak of sample H5.

Table 19. Results for deconvolution of XPS N_{1s} photopeaks of functionalized HDPE and EVOH samples. Peak areas of each sample are normalized against the component assigned to phosphazene backbone nitrogen.

| <i>Sample</i> | <i>Peak Position (eV)</i> | <i>Area Ratio</i> | <i>Assignment</i> |
|----------------------------|---------------------------|-------------------|-------------------------|
| H3 - HDPE+PDCP+TFE | 398.4 | 1.00 | PDCP chain |
| | 399.8 | 1.02 | 2 nd comp.* |
| | 401.5 | 0.14 | protonated N |
| H4 - HDPE+PDCP+HDFN | 398.8 | 1.00 | PDCP chain |
| | 400.1 | 0.84 | 2 nd comp. * |
| | 401.5 | 0.24 | protonated N |
| H5 - HDPE+HCCP+TFE | 398.3 | 1.00 | HCCP ring |
| | 399.8 | 0.56 | 2 nd comp. * |
| | 401.0 | 0.13 | protonated N |
| H6 - HDPE+HCCP+HDFN | 398.5 | 1.00 | HCCP ring |
| | 400.0 | 1.01 | 2 nd comp. * |
| | 401.3 | 0.20 | protonated N |
| E2 – EVOH+PDCP+TFE | 398.8 | 1.00 | HCCP ring |
| | 400.0 | 0.21 | 2 nd comp. * |
| | 400.9 | 0.02 | protonated N |
| E3 – EVOH+PDCP+HDFN | 398.6 | 1.00 | HCCP ring |
| | 400.0 | 0.42 | 2 nd comp. * |
| | 401.3 | 0.08 | protonated N |
| E5 – EVOH+HCCP+TFE | 398.4 | 1.00 | HCCP ring |
| | 399.9 | 0.23 | 2 nd comp. * |
| | 401.8 | 0.06 | protonated N |
| E6 – EVOH+HCCP+HDFN | 398.3 | 1.00 | HCCP ring |
| | 399.7 | 0.63 | 2 nd comp. * |
| | 401.8 | 0.04 | protonated N |

* See text for interpretation

In all the cases there is a first component that is assignable to the phosphazenic nitrogen³³⁰ around 398.5 eV, and a second one that is on average 1.4 eV higher in binding energy.

This second component, already highlighted in the case of poly[bis(2,2,2-trifluoroethoxy)phosphazene], was attributed by Fewell to branching in the polymer during the substitution reaction³⁷⁰. Other explanations could be the presence of phosphazane segments derived from hydrolysis phenomena¹, which may occur in spite of the care taken to keep the reaction environment anhydrous⁷⁵ or even during the final sample washing in the case of incomplete substitution reaction; another explanation may be the engagement of phosphazenic nitrogen atoms in electrostatic interactions with the polar moieties present on the substrates.

Finally, a third, weaker component is present around 401.3 eV, which can be tentatively assigned to protonated phosphazene nitrogens. This phenomenon could arise from the interaction with hydrochloric acid molecules that are evolved in step 2 of the functionalization process.

The presence of fluorine in TFE- and HDFN-functionalized samples indicates that substitution of chlorine atoms with the fluorinated alcohols actually occurs. Moreover, the curve fitting of the C_{1s} spectra of these samples reveals the appearance of new components around 293.2 eV (CF₃ groups) and 292.0 eV (CF₂ groups, present in HDFN-containing samples only). It is less straightforward to make analogous considerations for the samples where substitution was performed with AzB, but better evidence of the presence of the azobenzene system comes from the results of UV-Vis absorption analyses, which are reported later in this section (see section 4.3.3.4). It suffices here to remark that the nucleophilic substitution in step 3 with AzB generally yields higher carbon contents and N/P ratios than those of analogous samples where fluorinated alcohols were used.

The effectiveness of chlorine atom substitution in the final step of the procedure can be estimated through the diagnostic ratios F/P for samples functionalized with fluorinated alcohols, and N/P for HDPE and EVOH samples functionalized with AzB. If the chlorophosphazenes underwent quantitative nucleophilic substitution in solution, the ratios would be F/P = 6 for the substitution with TFE, F/P = 34 for HDFN, and N/P = 5 in the case of AzB. The experimental values were generally significantly lower, which accounts for the exploitation of a relevant part of the P-Cl groups in covalent bonds with the surface of the substrate (and thus their unavailability for substitution in step 3), or for the incompleteness of the substitution reaction. It is noteworthy that the values of such diagnostic ratios on HCCP-containing samples are generally lower than those obtained with PDCP and the same nucleophilic substituents, to suggest that a higher portion of the P-Cl groups present in the starting chlorophosphazene was exploited for bonding with the substrate surface in the case of the trimer. This is intuitive when considering that HCCP is formed by an almost planar, six-membered ring with the six reactive chlorines uniformly distributed on the two sides of the ring plane^{318,322,371}, while PDCP consists of a long, flexible, linear polymer chain, mostly in a *cis-trans* planar configuration^{372,373}, which could easily fold between two successive “anchoring points” with the substrate. Moreover, looking at Tables 18 and 19 it appears

that another factor influencing the diagnostic ratios could be the presence of the species associated with the second N_{1s} component in the XPS spectra. Observing the data relative to HDPE and EVOH samples substituted with fluorinated alcohols, it appears that in most cases, the higher the area of the second N_{1s} component (at about 399.9 eV), the lower the relative quantity of grafted fluorinated alcohols.

Finally, an interesting observation came from comparison of the C_{1s} curve fittings of the virgin EVOH copolymer and of the functionalized samples. It is always possible to identify one component at about 285.0 eV due to CH_2 groups in ethylene and vinyl alcohol sequences, and another one around 286.4 eV that can be assigned to carbon single-bonded to oxygen in vinyl alcohol units. Positions and relative areas of these components for several samples are summarized in Table 20, while the C_{1s} curve fitting for samples E1 and E3 are reported as an illustration in Figure 50a and 50b, respectively.

Table 20. Comparison of revealed CH_2 and C-O components of virgin and fluorinated alcohol-functionalized EVOH samples from XPS analysis.

| Sample | Ethylene/vinyl CH_2 position (eV) | Vinyl C-O position (eV) | (C-O)/(CH_2) peak area ratio | FWHM ^a |
|-----------------------------|--|----------------------------|-------------------------------------|-------------------|
| E1 - Virgin EVOH | 284.9 | 286.3 | 0.17 | 1.4 |
| E2 - EVOH+PDCCP+TFE | 285.0 | 286.5 | 0.39 | 1.5 |
| E3 - EVOH+PDCCP+HDFN | 285.0 | 286.5 | 0.35 | 1.5 |
| E5 - EVOH+HCCP+TFE | 284.9 | 286.4 | 0.36 | 1.5 |
| E6 - EVOH+HCCP+HDFN | 285.0 | 286.6 | 0.35 | 1.6 |

^a FWHM was kept fixed for all components of the same sample's C_{1s} spectrum

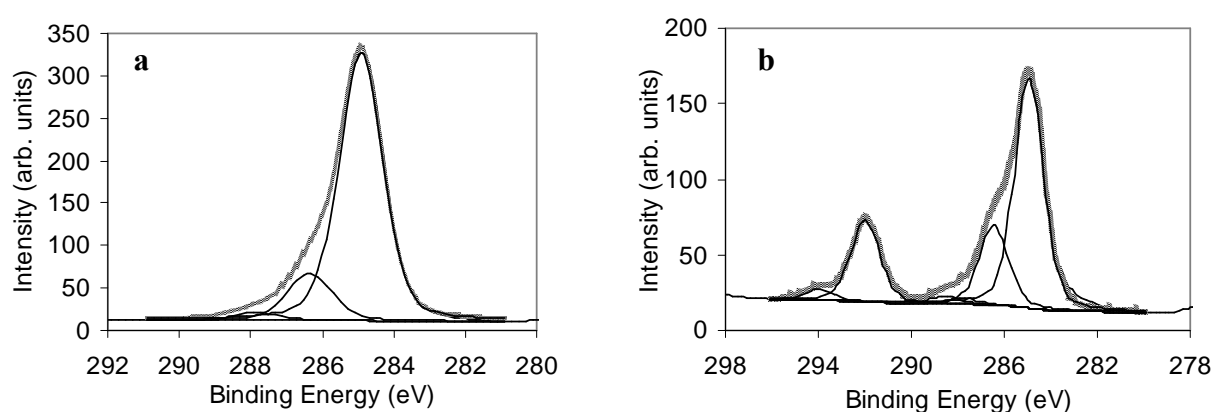


Figure 50. Deconvolution of C_{1s} XPS photopeak of samples (a) E1 and (b) E3.

A stronger contribution from vinyl alcohol sequences is revealed on the functionalized samples, which could be explained by the tendency of the virgin copolymer to minimize surface energy by preferentially exposing apolar ethylene sequences at the interface with air³⁶². In fact, the ratio between the areas of C-O and CH₂ spectrum components for sample E1 is 0.17, while it should be 0.39 for homogeneous EVOH containing 44% of ethylene units. Phosphazene grafting appears therefore to stabilize the vinyl alcohol units on the outermost layer of the substrate.

The other observable components in Figure 50b are located around 288.5, 292.0 and 293.6 eV, assigned respectively to CH₂, CF₂ and CF₃ carbons from HDFN, together with a minor component at 287.8 eV, present also in virgin EVOH and coming from impurity oxidized units, probably containing carbonyl moieties.

4.3.3.4. UV-Vis characterization

Reflectance UV-Vis spectra were collected in the case of azobenzene-functionalized PA6 and EVOH samples to verify both the functionalization with the optically active molecule and the photochromic properties of the materials obtained. This was achieved through exposition of the samples to 365 nm radiation, collecting spectra at different irradiation times. After light exposure, a thermal relaxation treatment in an oven at 60°C was performed to thermally reverse the photochemically induced isomerization process. The spectrum of sample E7 (EVOH functionalized with HCCP and AzB) is reported in Figure 51.

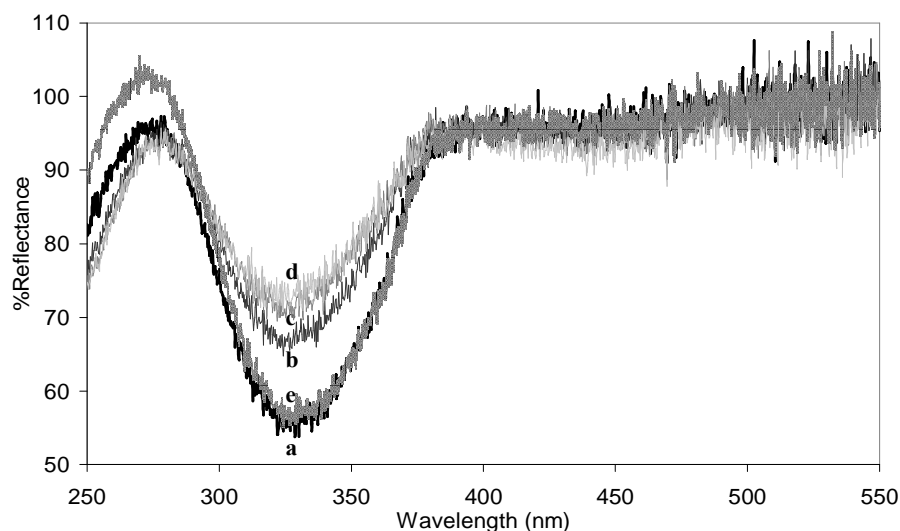


Figure 51. UV-Vis reflectance spectra of sample E7 (a) as prepared; after irradiation with 365 nm light for (b) 15 min, (c) 1h, (d) 18h; and (e) after final thermal relaxation at 60°C for 24h.

The neat azobenzene molecule can exist in a *trans* and in a *cis* form, which are characterized by two different absorptions in the UV (330 nm) and in the visible (430 nm) range of the spectrum. Interconversion between the two isomers can occur both photochemically (*trans*→*cis* and *cis*→*trans*) and thermally (*cis*→*trans*)^{135,355,356}, according to the scheme in Figure 52.

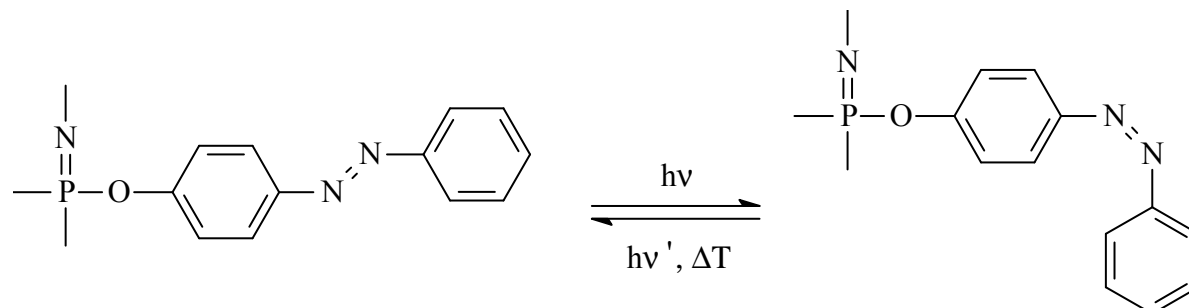


Figure 52. Photoinduced *trans-cis* isomerization and photochemical/thermal relaxation of azobenzene moieties bonded to phosphazene substrates.

The reported spectrum does present both these bands, as expected. When the samples are irradiated with 365 nm light, the *trans* band becomes less intense and the *cis* band grows, though in a less remarkable way because of the spectral noise and of the lower absorption cross section of the corresponding isomer; this phenomenon accounts for the isomerization of the azobenzene moieties from the *trans* to the *cis* form. As far as the reversibility of the process is concerned, the curve (e), which represents the reflectance spectrum of sample E7 after 18 hours of UV light irradiation followed by thermal relaxation at 60°C in an oven for 24 hours, shows that the photochromic transition in this system is almost completely reversible.

4.3.4. Conclusions

In this section we presented a new method to functionalize the surface of different industrially important organic polymers, *i.e.* HDPE, PA6 and EVOH, with fluorinated alcohols and azobenzene using cyclic (NPCl₂)₃ and polymeric (NPCl₂)_n chlorinated phosphazenes as coupling agents.

In the first step of this process, HDPE and PA6 undergo a surface treatment with cold, low pressure argon plasma, which introduces a variety of polar groups on their surfaces, including free hydroxyl functionalities. These moieties were reacted in a second step with the chlorophosphazenes to graft these derivatives onto the surface of the substrates through the formation of strong covalent P-O-C(substrate) bonds. The

residual chlorines were eventually substituted in a third step with the above mentioned nucleophiles, thus changing the surface properties of the polymer plates.

The functionalized samples were characterized by a variety of surface techniques, *i.e.* contact angle measurement, FTIR-ATR and XPS spectroscopy, and UV-Vis absorption. All the results were consistent with the effectiveness of the designed synthetic strategy to achieve surface functionalization of the materials employed, revealing a remarkable decrease of surface energy and hydrophilicity in the samples functionalized with fluorinated alcohols, and the appearance of reversible photochromic features in the azobenzene-functionalized polymer plates.

The results also pointed out that surface modification appeared to be more effective on EVOH substrates, and when HCCP was used instead of PDCP. This latest effect could be due to several reasons, such as a more efficient grafting reaction under the exploited experimental conditions and/or higher stability of the phosphazene trimer towards possible hydrolysis phenomena.

It should be pointed out that the surface functionalization technique here presented is completely general and could be applied in principle to modify the surfaces of many polymeric materials with an almost infinite number of nucleophiles having different features, thanks to the versatility of phosphazene chemistry⁴.

4.3.5. Acknowledgements

XPS measurements were performed by Dr. Leon Gengembre and Dr. Martine Frere (Unity of Catalysis and Solid Chemistry, University of Sciences and Technologies of Lille I, France).

The work presented in this section was performed at the Laboratory of Infrared and Raman Spectrochemistry (LASIR) of the University of Sciences and Technologies of Lille I, Villeneuve d'Ascq, France, under the direction of Prof. Ahmed Mazzah. Prof. Roger De Jaeger from LASIR and Dr. Charafeddine Jama from PERF Laboratory of Lille are also gratefully acknowledged for their scientific support throughout the project.

4.4. CYCLOPHOSPHAZENES PARTIALLY SUBSTITUTED WITH TRIALKOXY-SILANE DERIVATIVES FOR THE SURFACE FUNCTIONALIZATION OF SILICON-BASED SUBSTRATES AND FOR THE PREPARATION OF NEW BULK MATERIALS AND THIN FILMS

4.4.1. Preliminary considerations

The general strategy adopted to functionalize the surface of silica gel beads, Si(100) wafers and silica glass slides, and for the preparation of new bulk materials and thin films by sol-gel technique in the presence of TEOS or by self-condensation processes, is reported in Path B of Figure 1. This approach is based on the preliminary preparation of cyclophosphazenes containing about 50% by mole of selected organic substituents, able to grant specific surface properties to the final functionalized substrates, while the residual 50% of the reactive sites are substituted with trialkoxysilane groups.

This was obtained by treating HCCP first with 4CNP, PEG-750-ME, TFP or AzB, and saturating successively the residual P-Cl groups in the trimer with APTES. The whole synthetic procedure is illustrated more in detail in Figure 53.

The nucleophilic substituents exploited in these researches were selected for the following reasons:

- 1) 4CNP, because of the possibility to act as a marker for characterization, due to the presence in its IR spectrum of a characteristic band at about 2230 cm^{-1} attributed to the stretching of the $\text{-C}\equiv\text{N}$ group³⁷⁴;
- 2) PEG-750-ME, because of its well known features as an ionic conductor¹⁵⁵, its biomedical characteristics³⁷⁵ and its intrinsic skeletal flexibility, in principle able to modify the mechanical properties of the bulk materials obtained by sol-gel technique;
- 3) TFP, as it may influence the optical properties (*i.e.* the refractive index) and the surface wettability of the corresponding functionalized materials, and as it is a good prototype for the functionalization of silicon-based materials with fluorinated alcohols having longer $\text{-CF}_2\text{-}$ chains;
- 4) AzB, because it is a molecule showing photochromic properties^{135,355,356}.

4.4.2. Synthesis of cyclophosphazenes

4.4.2.1 Preliminary synthesis of hexakis(4CNP)cyclophosphazene (C-6-pCN)

The synthetic work started with the preparation of hexakis(4CNP)cyclophosphazene, $[\text{NP}(\text{OC}_6\text{H}_4\text{-}p\text{-CN})_2]_3$ to obtain its complete spectroscopic characterization. The cyclophosphazene was synthesized by reacting HCCP with the stoichiometric amount of 4CNP in dry acetone and in the presence of Cs_2CO_3 as a base, following the procedure reported by G.A.Carriedo²⁹⁹ (see Figure 54).

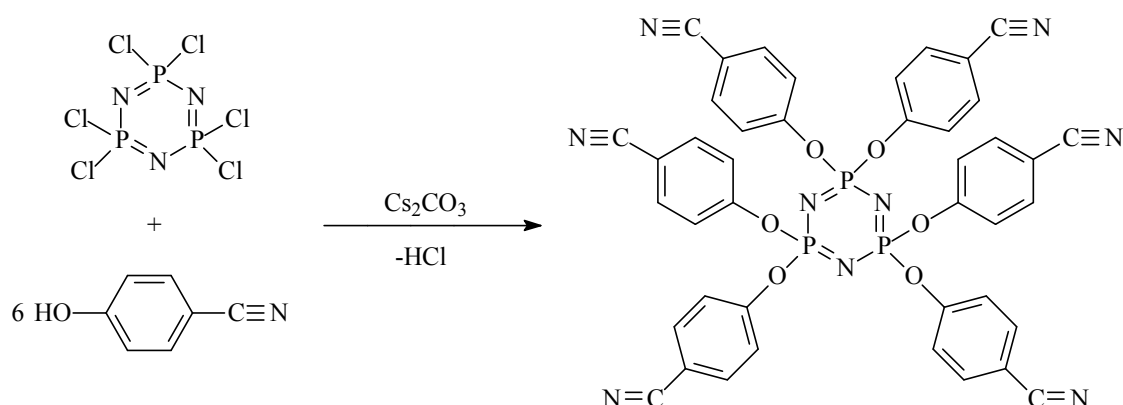


Figure 54. Synthesis of hexakis(4CNP)cyclophosphazene.

As expected, the IR spectroscopic characterization of the product showed the presence of a strong band at 2225 cm^{-1} which is an indication of the presence of the $\text{-C}\equiv\text{N}$ group in this material.

4.4.2.2. First reaction step: partial substitution of HCCP with nucleophiles

Tris(4CNP)tris(chloro)cyclophosphazene was prepared by reaction of HCCP with three equivalents of 4CNP in hot toluene and TEA as a base, according to the following Scheme (Figure 55).

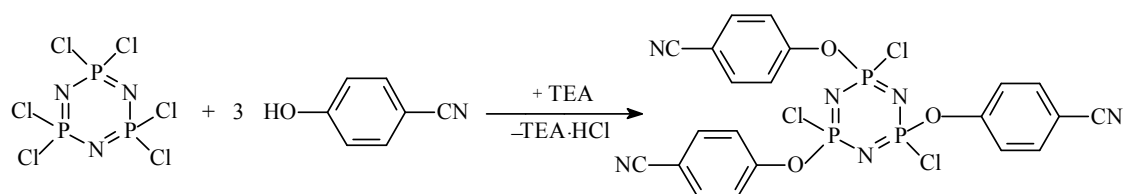


Figure 55. Partial substitution of HCCP with 4CNP.

The reaction took place in a quantitative way, as it could be demonstrated by weighing the triethylammonium chloride formed during the process. This cyclophosphazene was characterized by IR and ^{31}P NMR spectroscopy.

The infrared spectrum showed several series of signals, at 2230, 1599 and 1496, 1201 and 1187, and at 944 cm^{-1} , attributed to the stretching of the $\text{C}\equiv\text{N}$ function, to the breathing of the $\text{C}=\text{C}$ bonds of the aromatic ring, to the asymmetric stretching of the $\text{P}=\text{N}$ group of the cyclophosphazene ring, and to the vibration of the $\text{P}-\text{O}-\text{Ph}$ moiety, respectively.

The presence of these signals confirms that the substitution of the 4-cyanophenol in the cyclophosphazene took place without modification of the $-\text{P}=\text{N}-$ inorganic ring.

The ^{31}P NMR spectrum of the compound is reported in Figure 56 below.

As it can be seen from this spectrum, the original singlet of HCCP located at $\delta = 21.3$ (Part a) was completely absent in the second spectrum (Part b), to indicate that the original HCCP was consumed during the synthesis. In the rather complex ^{31}P NMR spectrum of the reaction products, one can distinguish three different series of multiplets located at $\delta 29 \div 25$, $20 \div 14$, and $7 \div -2$, respectively, that are indicative of the presence of a mixture of several (4-cyanophenoxy)-substituted cyclophosphazenes of variable structure, possibly bi-, tri- (as the main product), and tetra- substituted, and also having *cis* or *trans* configurations¹.

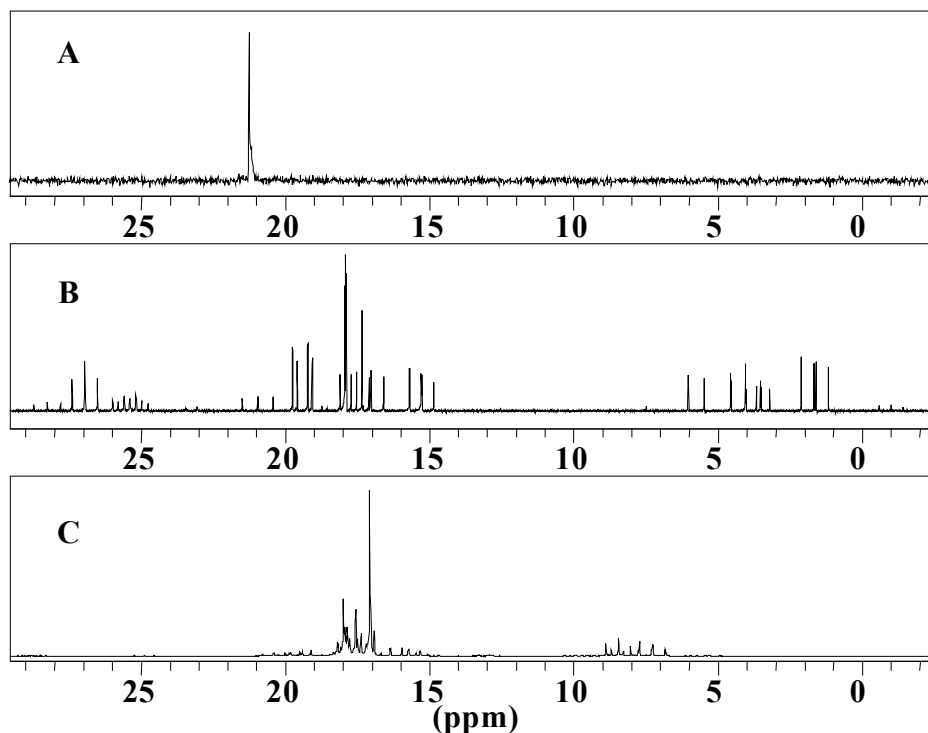


Figure 56. $\{^1\text{H}\}^{31}\text{P}$ NMR spectra of (a) HCCP, (b) tris(4CNP)tris(chloro)-cyclophosphazene and (c) tris(4CNP)tris(APTES)cyclophosphazene.

Following our previous experience with the 4CNP substituent, we assumed that in the first step the substitution reactions of HCCP with PEG-750-ME, TFP and AzB are (almost) quantitative, and that the products are based on mixtures of different cyclophosphazene isomers, as discussed above. This is supported by the rather complex ^{31}P NMR spectra measured for the other cyclophosphazenes isolated after the first step, which are similar to the one shown in part b of Figure 56.

4.4.2.3. Second step: residual chlorines substitution with APTES

The first reaction step described above was immediately followed by the saturation of the residual reactive sites in the cyclophosphazenes with APTES, as shown in Figure 53 above. This reaction was carried out at room temperature by adding the appropriate quantity of APTES to the partially substituted cyclophosphazenes, in the presence of an excess of TEA and for time periods varying between 24 and 72 h.

In accordance with literature^{301,376}, this substitution reaction was not quantitative, as it could be confirmed by determining the amount of triethylammonium chloride delivered during the synthesis (about 70% yield). This suggests that the cyclophosphazene mixture produced in this process always contained molecules having the structure described in Figure 57 below, where R has the same meaning as in Figure 53, and in which residual unreacted chlorines are still present in the cyclophosphazene structure. The presence of these compounds should not interfere with the surface modification reaction, and therefore the reaction mixture was used without further purification.

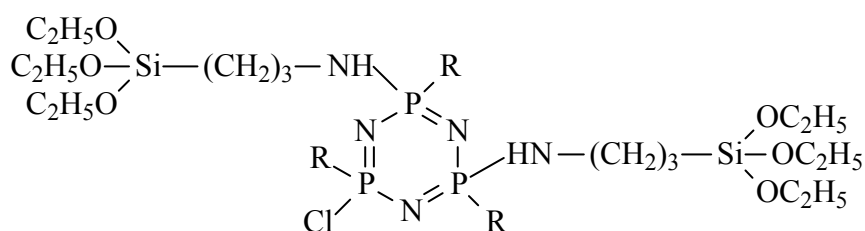


Figure 57. Product of incomplete reaction of tris(4-cyanophenoxy)-tris(chloro)cyclophosphazene with γ -APTES. The product shown is one of the possible isomers.

The FTIR characterization of these compounds was not performed due to the intrinsic hydrolytic instability of the trialkoxysilane moieties, that hydrolyze rapidly upon exposure to the atmosphere and bring about reticulation of the cyclophosphazenes.

The general IR features of these substrates were inferred by examining the IR spectra of the monoliths or thin films produced by sol-gel technique (see 4.4.4.2).

The ^{31}P NMR spectra of the products described above remained rather complicated, as illustrated in part C of Figure 56, where the spectrum of the cyclophosphazene containing 4CNP and APTES groups is shown as an example.

4.4.3. Surface functionalization of silica gel

The surface of silica gel beads exploited in this work was preliminarily activated by the hydrolysis of Si-O-Si bonds of this material, as obtained by the action of hot, concentrated (37%) hydrochloric acid solution, according to the procedure reported by Fritz²⁸⁰.

After this initial step, activated SiO_2 beads were heated at 80°C under vacuum for 1 h, treated with anhydrous THF solutions of cyclophosphazenes containing APTES and 4CNP, PEG-750-ME, TFP or AzB. After filtration under nitrogen and washing with anhydrous THF (common to all products), silica gel beads functionalized with PEG-750-ME, TFP and AzB were washed with distilled water and diethyl ether before drying. The overall reaction Scheme is illustrated in Figure 58, where R has the same meaning as in Figure 53.

The FTIR characterization of the functionalized SiO_2 beads showed typical phosphazene bands in the spectral range of $1230\text{--}1170\text{ cm}^{-1}$ (asymmetric ν of the $-\text{P}=\text{N}-$ units) and at 950 cm^{-1} (P-O-C vibration of the phosphazene substituents), together with other absorptions between $2980\text{--}2880\text{ cm}^{-1}$ (ν of alkyl residues of APTES, PEG-750-ME, and TFP), at 2228 cm^{-1} ($\nu\text{ C}\equiv\text{N}$ of the 4CNP-containing product) and at about 1600 and 1500 cm^{-1} ($\text{C}=\text{C}$ vibrations of the 4CNP and AzB aromatic rings). These bands unequivocally indicated that the cyclophosphazenes substituted with the four nucleophiles were present on the surfaces of the functionalized SiO_2 gels. The FTIR spectrum of silica gel functionalized with the 4CNP-containing cyclophosphazene is reported in Figure 59 as an illustration.

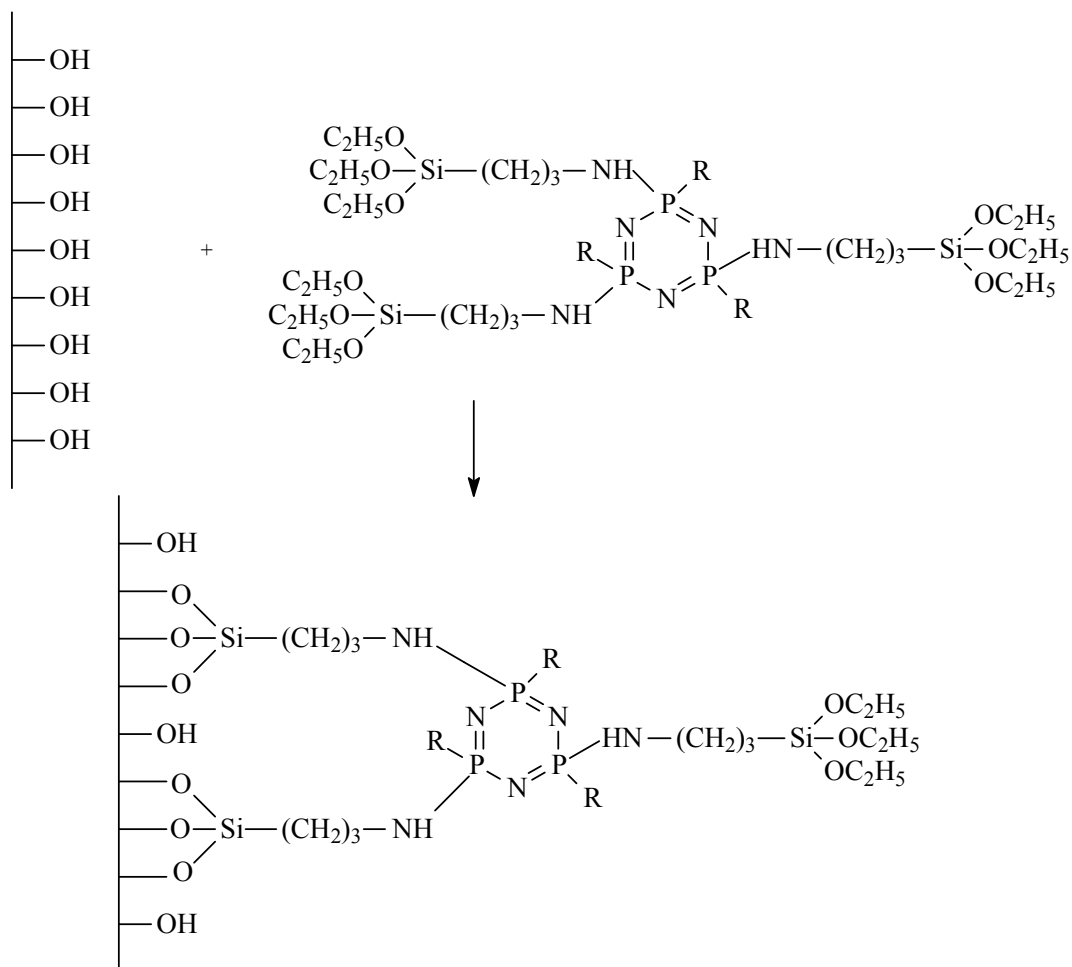


Figure 58. Surface functionalization of silica gel with tris(4CNP, PEG-750-ME, TFP or AzB)tris(γ -APTES)cyclophosphazenes.

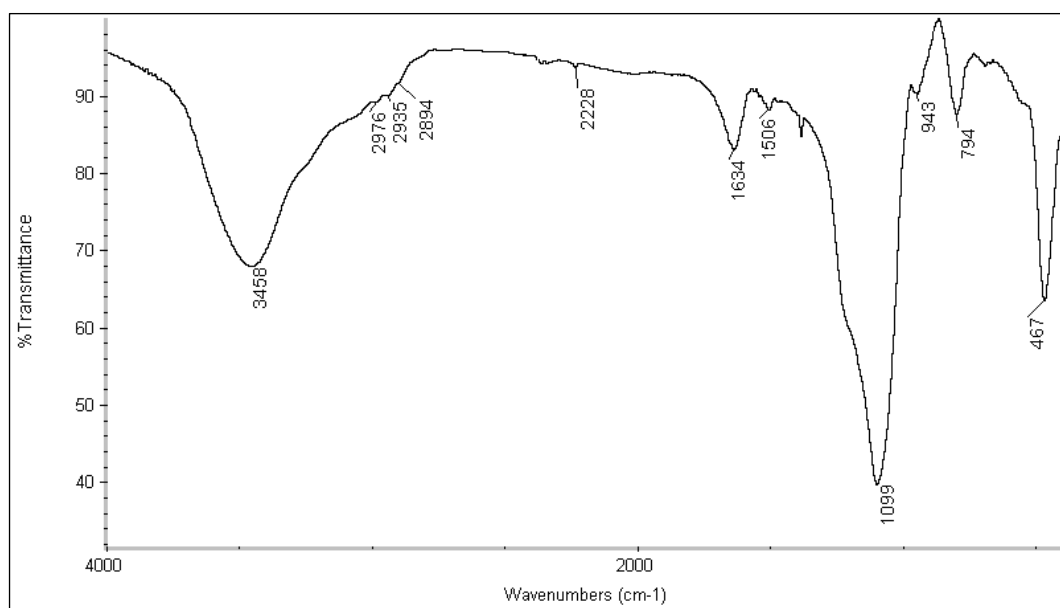


Figure 59. FTIR spectrum of silica gel surface-functionalized with tris(4CNP)tris(γ -APTES)cyclophosphazene.

As far as the solid state NMR characterization is concerned, the ^{31}P SPE NMR spectra of silica gel beads functionalized with 4CNP, PEG-750-ME, TFP and AzB groups show two non-resolved bands at δ 18÷20 and 6÷12, which suggested that the phosphazene unit was present in all products. Moreover, these chemical shifts are similar to those observed in solution for the corresponding substituted cyclophosphazenes. This result confirmed that the cyclophosphazene ring was preserved during the functionalization process, and that it was present on the surface of these products.

The ^{13}C CP MAS NMR spectrum of 4CNP-functionalized silica gel is reported in Figure 60. The presence of both APTES and 4CNP moieties was clearly assessed by signals at δ 8.7, 21.1, 42.5, 107.7, 121.8, 133.6 and 154.5. The three signals attributed to the silane *n*-propyl chain (δ 8.7, 21.1 and 42.5) were characterized by the same broad peak width (about 220 Hz at half maximum) and the same intensity. In previous literature on trialkoxysilane-based sol-gel materials³⁷⁷⁻³⁷⁹, ^{13}C CP MAS NMR band width and intensity are related to the silane molecular dynamics. On this basis we concluded that in the 4CNP-containing cyclophosphazene mixture, the silane mobility was restricted by covalent bonds at both chain ends ($-\text{NH}-\text{CH}_2\text{CH}_2\text{CH}_2-\text{Si}\equiv$). Furthermore, alkoxysilane hydrolysis-condensation reactions were not complete, as indicated by the presence of resonances at about δ 58 and 16 attributed to $\text{Si}-\text{O}-\underline{\text{C}}\text{H}_2-\text{CH}_3$ and $\text{Si}-\text{O}-\text{CH}_2-\underline{\text{C}}\text{H}_3$ groups, respectively. The $\underline{\text{C}}\text{H}_2-\text{Si}$ carbon atom has a chemical shift of δ 8.7, in agreement with silicon low degree of condensation³⁷⁹.

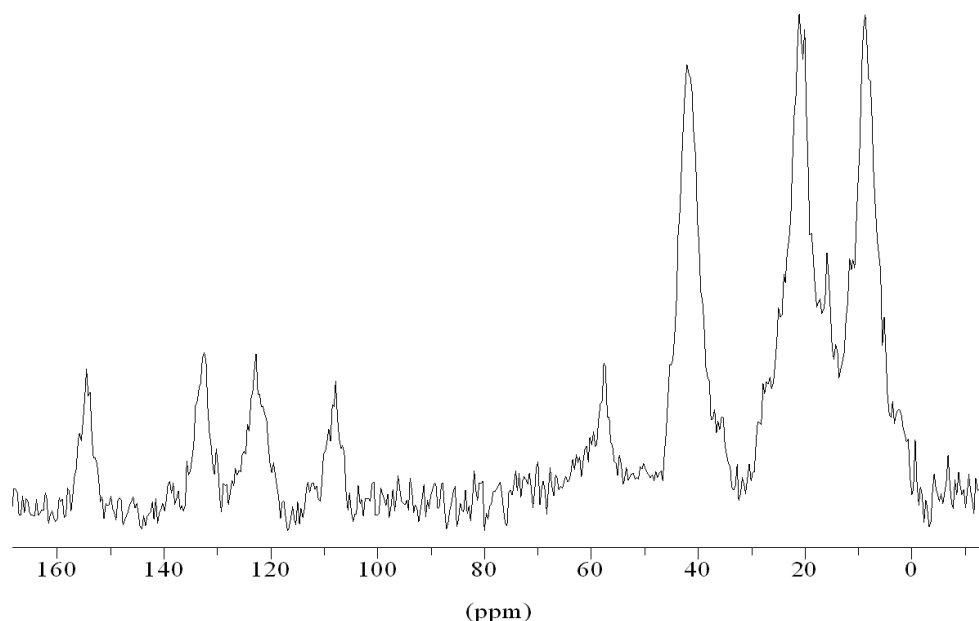


Figure 60. ^{13}C CP MAS NMR spectrum of silica gel functionalized with tris(4CNP)tris(γ -APTES)cyclophosphazene.

The ^{13}C CPMAS spectra of the other functionalized gels (containing PEG-750-ME, TFP or AzB) were essentially similar, and showed both the presence of APTES and the low mobility of the propyl chain ends, but with the important difference that the signals from the ethoxy groups of the silane moieties were not present any more, as it can be seen in Figure 61 that presents the spectrum of PEG-750-ME-functionalized silica gel.

This effect could be achieved by washing the samples with water, which led to completion of the hydrolysis of alkoxy moieties. Moreover, these samples exhibit $\text{CH}_2\text{-Si}$ chemical shifts around δ 9.5–10.0, indicating a good degree of condensation of the alkoxysilane with the formation of siloxane bonds (Si-O-Si).

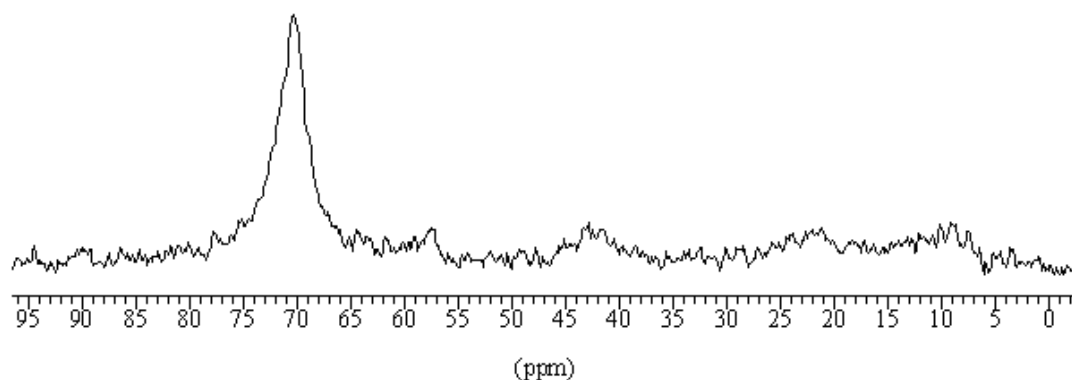


Figure 61. ^{13}C CPMAS spectrum of PEG-750-ME-functionalized silica gel.

In the recorded spectra were equally recognizable bands due to the presence of the nucleophiles introduced in the first step of the reaction. In particular, the PEG-750-ME residue could be detected at δ 57.7 ($\text{H}_3\text{C}\text{OCH}_2\text{-}$), 61.2 ($\text{-CH}_2\text{-O-P}$) and 70.3 ($\text{-O-CH}_2\text{-CH}_2\text{-O-}$), and the tetrafluoropropoxy group at δ 61.7 ($\text{CF}_2\text{-CH}_2\text{-O-P}$) and 107–116 ($\text{H-CF}_2\text{-CF}_2\text{-}$); finally, the 4-phenylazophenoxy pendant yielded signals at δ 121.6 (aromatic C2, C3, C5, C6, C2', C6', see legenda in paragraph 3.5.2.4 for numeration), 128.4 (aromatic C3', C4', C5'), and 152.8 (aromatic C1, C4, C1').

^{29}Si CP MAS NMR spectra provide a better insight into the reaction between the alkoxysilane and the substrate. In Figure 62 are reported the relative spectra for 4CNP-functionalized silica gel (part A) and silica gel activated by HCl (part b).

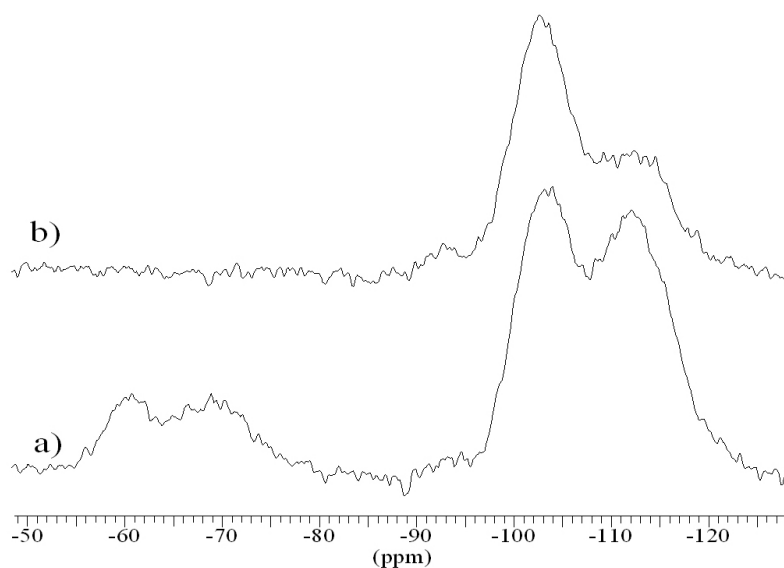


Figure 62. ^{29}Si CP MAS NMR spectra for (a) 4CNP-functionalized silica gel and (b) activated silica gel.

The presence of T^2 and T^3 trialkoxysilane units (*i.e.* engaged in two or three siloxanic bridges) was revealed by two non resolved peaks centered about δ -60 and -69, respectively, whereas resonances about δ -103 and -112 arised from the silica gel and were attributed to Q^3 and Q^4 (*i.e.* engaged in three or four siloxane bridges) units, respectively. The grafting process was achieved by condensation with the surface silanol groups of the silica gel, as evidenced by the increase of the relative intensity of the Q^4 unit resonance with respect to the activated silica gel prior to the functionalization process. Through the deconvolution of the ^{29}Si CP MAS NMR spectra, an estimation of the Actual Functionality (AF) for Q^n and T^n units could be made. The silica gel condensation degree increased from 80% (AF found on activated silica gel) to 88-91% (see 3.5.3.2.) by surface reaction with trialkoxysilane moieties. Notably, the AF relative to T^n silicon units was about 86% for the 4CNP-functionalized gel and 91-92% for the others, in agreement with the higher condensation degree of PEG-, TFP- and AzB-functionalized gels already indicated by ^{13}C CPMAS spectra above, which was due to the performed water washing of these materials.

Even though ^{29}Si CP MAS NMR spectra cannot be exploited for quantitative analysis, a rough estimation of the relative amount of silane bonded onto the silica surface has been done by integration of T^n and Q^n resonances. The results showed that the grafting yield was highly dependent on the particular organic substituent pending from the cyclophosphazene ring, *i.e.* 4CNP ($\text{T}^n/\text{Q}^n=0.23$), PEG-750-ME ($\text{T}^n/\text{Q}^n=0.33$),

TFP ($T^n/Q^n=0.61$) and AzB ($T^n/Q^n=0.26$), though it should be noted that grafting of the AzB-containing compound was performed at a lower temperature.

4.4.4. Monoliths and thin films preparation

The preparation of monoliths and thin film coatings on crystalline silicon (100) wafers starting from the above described cyclophosphazenes could be obtained by sol-gel technique using two different procedures, *i.e.*, by acid-catalyzed self-condensation processes and by acid-catalyzed condensation reactions carried out in the presence of an excess of TEOS.

4.4.4.1. Self-condensation processes

This procedure was exploited only for the 4CNP-cosubstituted cyclophosphazene. A THF solution of tris(4CNP)tris(APTES)cyclophosphazene was hydrolyzed under acidic conditions using a stoichiometric ratio $H_2O/Si=3/1$.

The hydrolysis reactions led to products similar to that reported in Figure 63.

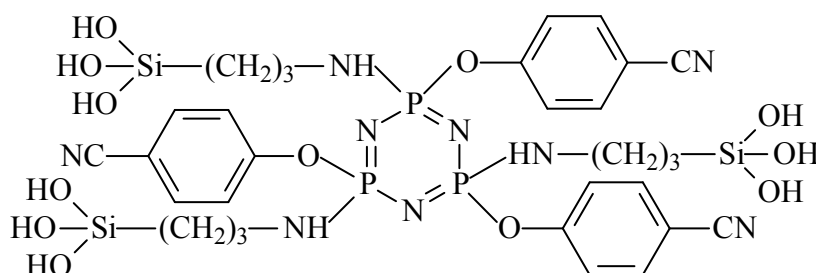


Figure 63. Product of the hydrolysis of tris(4CNP)tris(APTES)cyclophosphazene. One of the possible isomers is shown.

The solution was aged under stirring for 24 h and then used for the preparation of both monoliths and thin films.

4.4.4.2. Monolith preparation from self-condensation processes

APTES-functionalized cyclophosphazene monoliths were obtained by pouring the above described solution in polyethylene test tubes (1 cm diameter) and heating it at 45°C in an oven for 60 h. A schematic representation of the processes occurring in these materials is reported in Figure 64, in which the monoliths are formed due to the

condensation of the silanol groups present in the hydrolyzed cyclophosphazene, which led to the formation of Si-O-Si bonds.

The prepared materials were characterized by IR and solid state NMR spectroscopy and their thermal stability was tested.

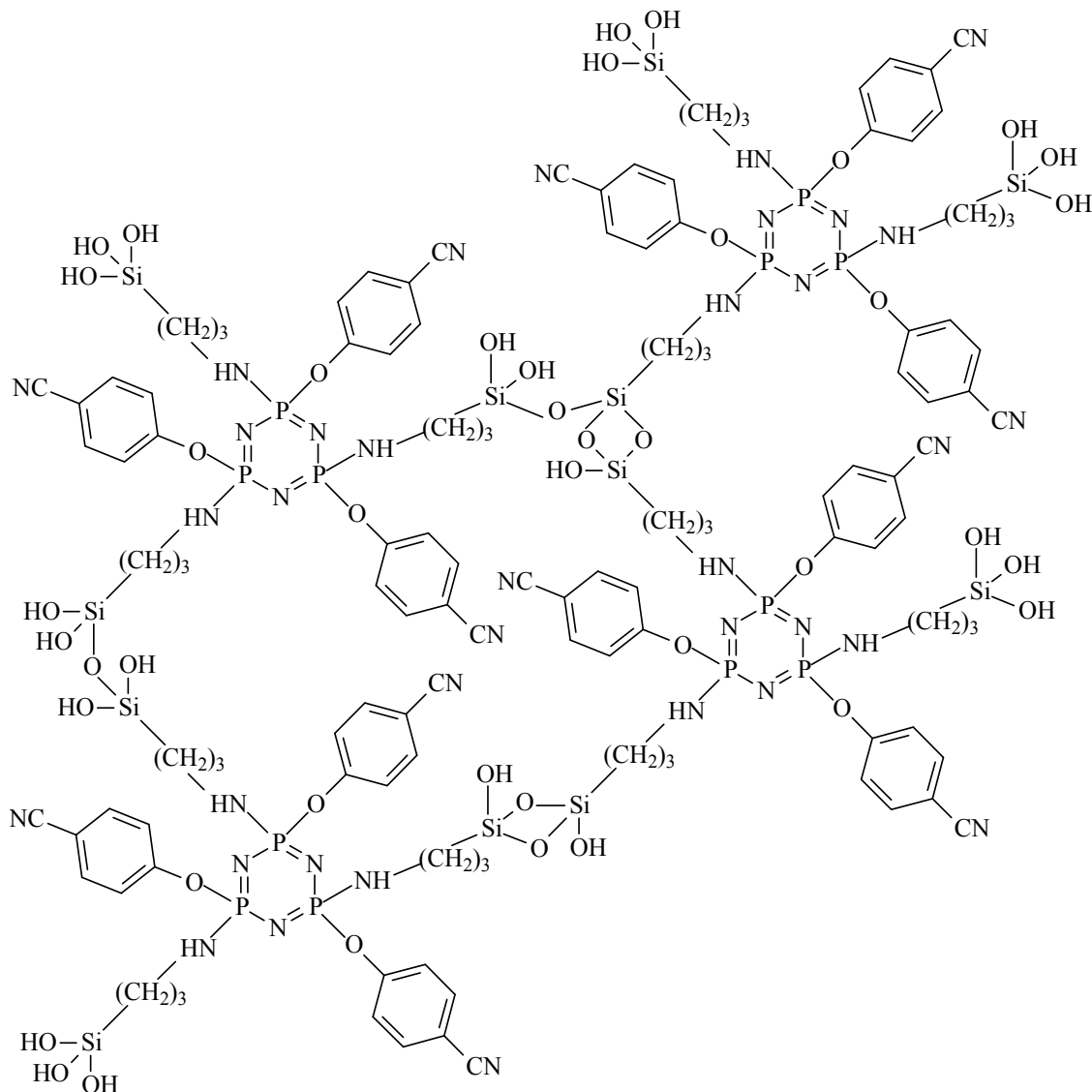


Figure 64. Schematic representation of the condensation of hydrolyzed phosphazenic compound.

The FTIR spectrum of grinded monoliths dispersed in KBr matrices, carried out after sample drying at 50°C overnight, is reported in Figure 65.

The presence of bands located at 2230 cm^{-1} (stretching of the $\text{C}\equiv\text{N}$ groups), 1600 and 1500 cm^{-1} (breathing of the aromatic ring), 1200 and 1187 cm^{-1} (asymmetric stretching of the $-\text{P}=\text{N}-$ group), 1100 cm^{-1} and 1050 cm^{-1} (asymmetric stretching of the Si-O-Si bonds originated by the condensation reactions), and at 950 cm^{-1} (stretching of the

P-O-Ph groups) clearly indicated that the monoliths are formed by cyclophosphazenes functionalized with phenols bearing cyano units in their chemical structure.

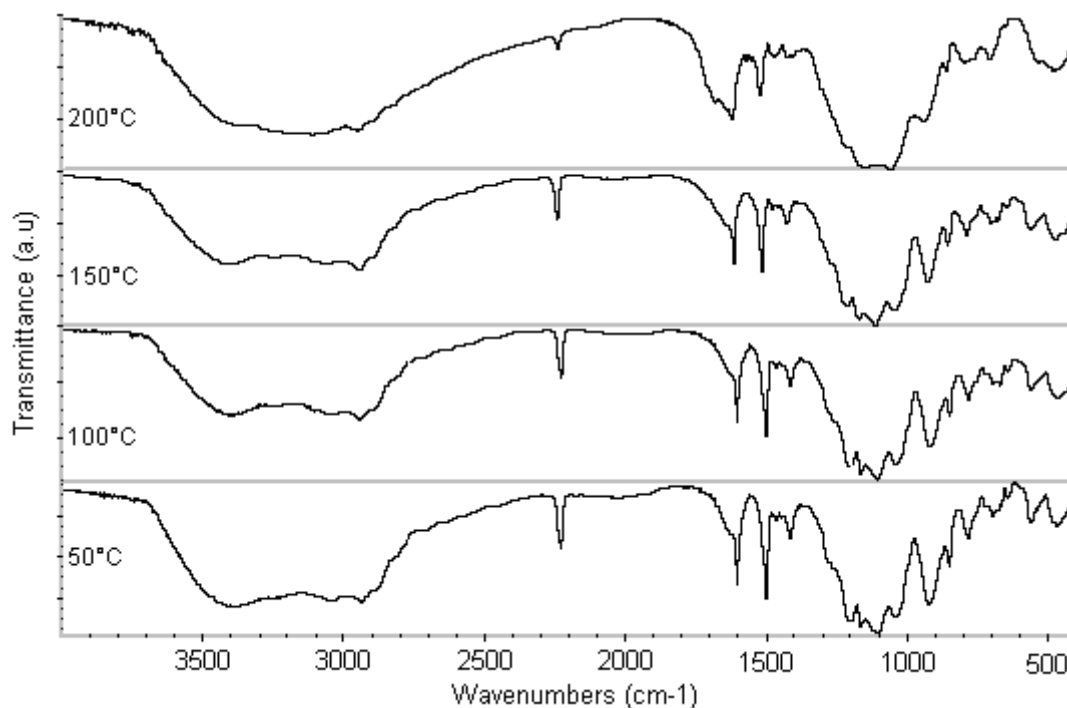


Figure 65. FTIR spectra of monoliths obtained by self-condensation of tris(4CNP)tris(APTES)cyclophosphazene and subsequently annealed at different temperatures.

The monoliths obtained were heated successively at increasingly higher temperatures (100°C, 150°C and 200°C) to check their thermal stability. As expected, the thermal treatment induced a volume decrease of the materials. The products appeared to be thermally stable up to 150°C, also maintaining the general appearance of the spectrum. At 200°C however modifications in the FTIR spectrum appeared, mostly based on the decrease of the band at 2230 cm^{-1} and on the onset of a new shoulder at 1700 and 1750 cm^{-1} ; these changes were possibly due to the hydrolysis of the cyano groups to form amide or carboxylic functions. In general, a broadening of the whole series of bands of the spectrum occurred, possibly due to enhanced matrix rigidity.

Solid state NMR characterization of the self-condensed tris(4CNP)tris(APTES)-cyclophosphazene-based material confirmed the maintenance of precursor structure through the sol-gel processing. In detail, the ^{13}C CP MAS NMR spectrum (not shown here) suggested that 4CNP and APTES moieties are actually linked to the phosphazene ring, thanks to the signals at δ 154.5, 108.7 and 43.2, which are relative to the two

quaternary aromatic carbons C1 and C4, and to the γ carbon of the propyl silane chain, respectively. In fact, the corresponding chemical shifts for free 4CNP and APTES are about δ 161, 101 and 45, respectively³⁸⁰. The observed ^{31}P chemical shifts (δ 18.8, 12.2, and 4.9) are consistent with the preservation of the cyclic phosphazene structure, whereas the formation of silicon-based network is well assessed by ^{29}Si CP MAS NMR (Actual Functionality = 82%).

From these observations the general conclusion can be drawn that the molecular structure of the synthesized tris(4CNP)tris(APTES)cyclophosphazene precursor was maintained in the monoliths prepared by sol-gel technique. Upon heating in air, these materials appear to be thermally stable until 150-200°C, while above these temperatures degradative and hydrolytic phenomena become observable.

4.4.4.3. Thin film coating deposition from self-condensation processes

The same sol used for the preparation of cyclophosphazene-based monoliths was concurrently used to prepare surface coatings on crystalline (100) silicon wafers using the dipping technique. After immersion of Si wafers in the solution for 1 min, the materials were dried for 15 minutes at room temperature and for 16 h at 110°C. They were successively characterized by FTIR spectroscopy, that showed the presence in the thin phosphazene films of the whole series of bands described above for tris(4CNP)tris(APTES)-cyclophosphazene-derived monoliths, with also the same thermal stability and good adhesion features.

4.4.4.4. Condensation processes in the presence of TEOS

The preparation of monoliths and thin film coatings deposited on the surface of crystalline (100) silicon wafers could be achieved by sol-gel technique using the tris(4CNP, PEG-750-ME, TFP, or AzB)tris(APTES)cyclophosphazenes by acid (HCl)-catalyzed condensation processes also in the presence of an excess of TEOS. Thus an acid solution of TEOS in anhydrous THF was reacted with an excess of water at room temperature for 1 h, and then added to the solution of the appropriately functionalized cyclophosphazene, to yield a mixture with the stoichiometric ratios TEOS / distilled water / hydrochloric acid / substituted cyclophosphazene equal to 1 / 4 / 0.01 / 0.03. The resulting mixture was stirred for 5 days at room temperature and then used for the following processes.

4.4.4.5. Monolith Preparation from condensation processes in the presence of TEOS

The general procedure for the preparation of cyclophosphazene-containing monoliths consisted of pouring portions of the precursor solution prepared as described above in polypropylene sample-tubes, and then of evaporating the solvent at different temperatures, times and rates. The monoliths, obtained as cylindrical bars, were grinded for FTIR and solid state NMR (^{13}C , ^{29}Si and ^{31}P) characterization.

The IR characterization showed bands at about 1200 cm^{-1} (asymmetric ν of $-\text{P}=\text{N}-$) and in the spectral range of $960\text{-}940\text{ cm}^{-1}$ (ν P-O-C of the phosphorus/substituent system) to indicate the presence of cyclophosphazene units. Additional bands were present at $2980\text{-}2850\text{ cm}^{-1}$ (ν of the CH_2 groups in APTES, PEG-750-ME or in TFP), 2233 cm^{-1} (4CNP-substituted sample, CN stretching) and at about 1600 and 1500 cm^{-1} (4CNP- and AzB-moiety containing samples, assigned to the breathing of the aromatic rings). These findings provided evidence of the presence of 4CNP, PEG-750-ME, TFP and AzB groups to indicate the presence of both the phosphazene cycle and of the appropriate substituents in the materials obtained.

Additional evidence came from solid state NMR analysis and thermal characterization.

The ^{13}C CP MAS NMR spectra of the cyclophosphazene/TEOS derived materials once more confirmed the substantial preservation of the phosphazene-based molecular precursor through the sol-gel processing, through signals arising from both the *n*-propylsilane moiety and from the other organic pendants. Even though the observed ^{31}P NMR chemical shifts were in good agreement with the substantial preservation of the phosphazene ring structure, PEG and TFP bearing materials exhibited a minor ^{31}P component of the spectrum centered about -8 ppm , which suggested that a small part of the cyclic trimer may be opened^{1,381,382}, to form linear phosphazene oligomers. Fitting of the spectra allowed to quantify the linear phosphazene content in PEG-750-ME and TFP containing materials, which resulted about 8 and 4%, respectively.

The ^{29}Si CP MAS NMR characterization showed that the trialkoxysilane moieties are almost fully condensed ($\text{AF}^{\text{Tn}} = 90\text{-}93\%$) in the Q^{n} -based network ($\text{AF}^{\text{Qn}} = 79\text{-}86\%$).

Thermal characterization³⁸³ was performed both as Differential Scanning Calorimetry (DSC) and as Dynamical Mechanical Thermal Analysis (DMTA). The DSC spectra reported in Figure 66 evidenced the presence of various transitions of organic phosphazene substituents between -70 and 40°C . Moreover, above this

temperature some endothermal peaks revealed the evolution of volatile species, corresponding to a mass loss of about 12%.

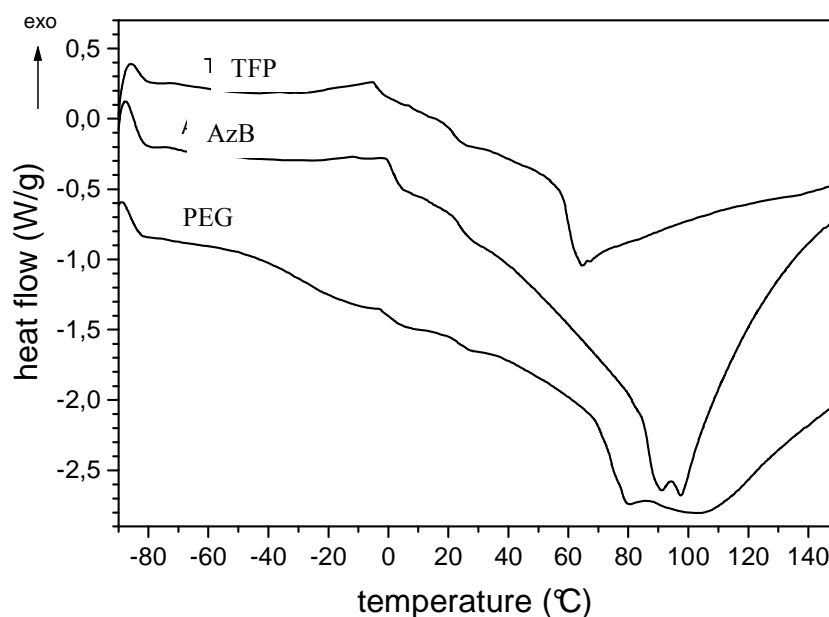


Figure 66. DSC thermograms of tris(PEG, TFP or AzB)tris(APTES)cyclophosphazene/TEOS derived materials (first scan). Evaluation data are reported in Table 1.

Various glass transition signals could be distinguished for each cyclophosphazene/TEOS derived material, whose position (T_g) and intensity (ΔC_p) depended on the nature of the organic pendant, as summarized in Table 21 below. In the same Table are also reported the values of endothermal peak temperature (T_p) and enthalpy (ΔH_p) of tris(PEG, TFP or AzB)tris(APTES) cyclophosphazene/TEOS derived monolith materials. The presence of several T_g signals, detected by the high sensitivity calorimeter, may be related to the presence of isomeric cyclophosphazenes coming after random chlorine substitution on the $(\text{NPCl}_2)_3$ ring, and/or to the diversity of the surrounding APTES/TEOS material after sol/gel reactions.

Concerning the nature of the organic substituents, as expected the most intense and lowest glass transition temperature was found in the case of tris(PEG)tris(APTES) cyclophosphazene/TEOS, located at -28°C ($\Delta C_p = 0.22$), well in agreement with the long flexible chain of PEG. On the other hand, two main transitions with $\Delta C_p = 0.15/0.20$ could be observed at about 0°C and 22°C for both $R = \text{TFP}$ or $R = \text{AzB}$. A second DSC scan of the same sample after 5 days exhibited similar thermal signals, as shown in Table 21.

Table 21. Glass transition temperatures (T_g), variation of specific heat at the glass transition (ΔC_p), endothermal peak temperature (T_p) and enthalpy (ΔH_p) of tris(PEG, TFP or AzB)tris(APTES) cyclophosphazene/TEOS derived materials measured in differential scanning calorimetry.

| | 1st scan | | | | 2nd scan ^a | | | |
|-----|------------------|----------------------------|------------------|--------------------------|-----------------------|----------------------------|------------------|--------------------------|
| | T_{g1} (°C) | ΔC_{p1} (J/g K) | T_{p1} (°C) | ΔH_{p1} (J/g) | T_{g2} (°C) | ΔC_{p2} (J/g K) | T_{p2} (°C) | ΔH_{p2} (J/g) |
| PEG | -69 | 0.01 | 102 | 41 | -71 | 0.02 | 98 | 8 |
| | -28 | 0.22 | | | -31 | 0.10 | | |
| | -2 | 0.08 | | | -3 | 0.03 | | |
| | 23 | 0.07 | | | 26 | 0.05 | | |
| | | | | | 54 | 0.28 | | |
| TFP | -66 | 0.02 | 64 | 28 | -69 | 0.03 | 77 | 18 |
| | -5 | 0.15 | | | -7 | 0.13 | | |
| | 21 | 0.18 | | | 19 | 0.16 | | |
| | 41 | 0.13 | | | 61 | 0.29 | | |
| AzB | -69 | 0.03 | 98 | 75 | -69 | 0.03 | 66 | 64 |
| | 1 | 0.20 | | | 4 | 0.17 | | |
| | 24 | 0.15 | | | 28 | 0.31 | | |
| | | | | | 51 | 0.22 | | |

^aThe second scan was performed after five days from the first one.

The higher damping effect of the long PEG-750-ME chain has been also confirmed by DMTA analysis³⁸⁴. The resulting thermogram (Figure 67) evidenced the main peak of the loss factor (or $\tan\delta$) centered at -5°C with some minor shoulders.

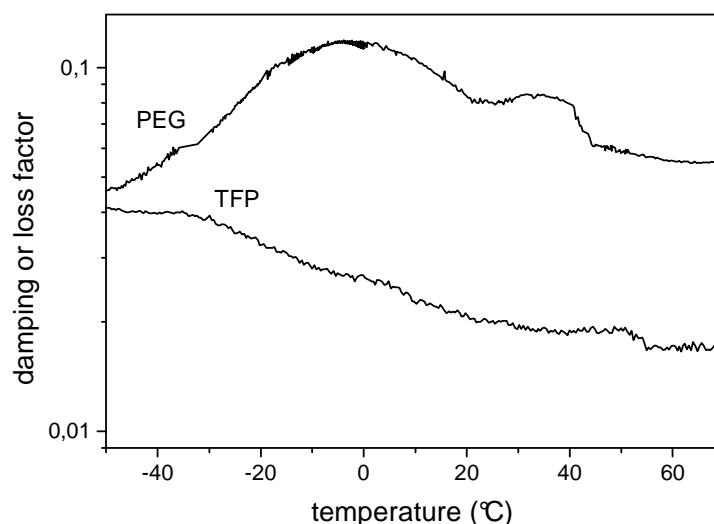


Figure 67. Damping factor of tris(PEG or TFP)tris(APTES)cyclophosphazene/TEOS derived materials.

The height of the peak is related to amorphous phase content, and the longer the chain, the higher the mobility, the higher the damping (in the range 0.05-0.12 for the

PEG-containing material). In the case of R = TFP, the damping ranged between 0.015 and 0.04, due to the higher rigidity of tris(TFP)tris(APTES)cyclophosphazene/TEOS. A much higher rigidity and brittleness was exhibited by tris(AzB)tris(APTES)cyclophosphazene/TEOS, and no DMTA could be successfully performed with this material.

Thermal characterization analyses demonstrated that the final mechanical properties of cyclophosphazene/TEOS monoliths could be, to a certain extent, tailored depending on the exploited cyclophosphazene substituent.

4.4.4.6. Thin films deposition from condensation processes in the presence of TEOS

Si(100) crystalline silicon wafers or clean sodalime glass slides were dipped for 1 min in the appropriate precursor solution, and subsequently dried first at room temperature for 15 min and then at 50°C for 16 h. The samples obtained were successively characterized by FTIR and UV-visible transmission spectroscopy.

The IR spectrum of the cyclophosphazene-functionalized thin films on crystalline (100) silicon wafers evidenced the same series of bands reported above for the monoliths (see 4.4.5), to indicate that both the phosphazene cycle and the appropriate substituents are present in these materials.

Additional support to the occurrence of the functionalization reaction came from the UV-visible spectroscopic analysis of clean sodalime glass slides functionalized with tris(AzB)tris(APTES)cyclophosphazene. The UV-visible spectrum of this film is reported in Figure 68 below.

Curve 1 refers to the film as deposited. The other curves refer to the sample after 365 nm light irradiation for different times, and after post-irradiation relaxation in an oven at 50°C for 23 hours. All curves show two absorption maxima at 330 and 430 nm which are attributed to the *trans* and *cis* form of the azobenzene substituents present in the cyclophosphazene, respectively.

These two isomers are interconvertible both photochemically (*trans*→*cis* and *cis*→*trans*) and thermally (*cis*→*trans*)^{135,355,356}, according to the equilibrium reaction reported in Figure 52 (see 4.3.3.4), and are characterized by different absorption maxima, geometries and polarities^{355,356}.

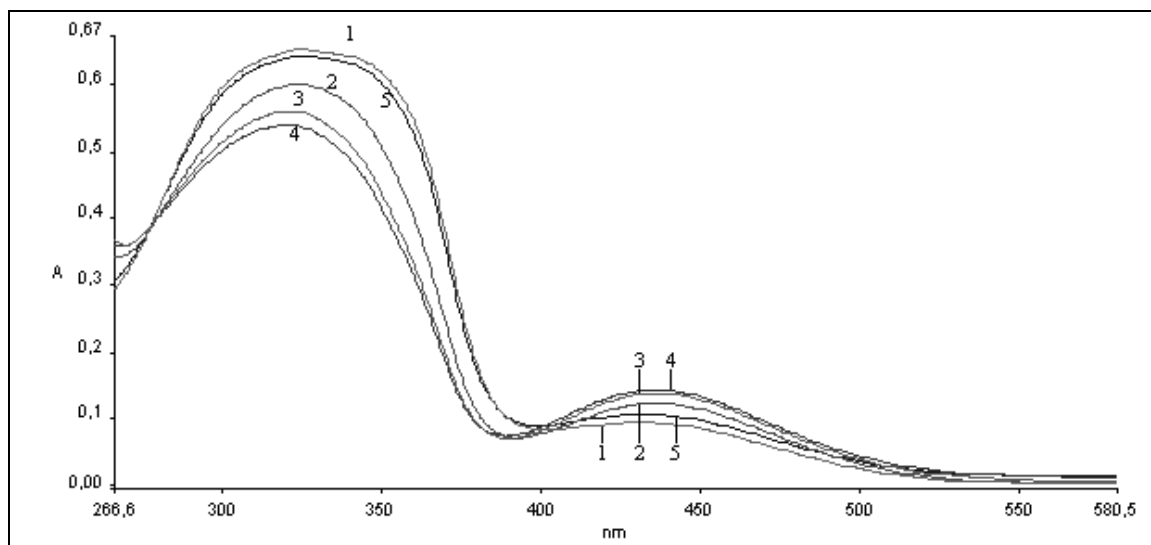


Figure 68. Photochromism of tris(AzB)tris(APTES)cyclophosphazene. Excitation wavelength is 365 nm. (1) original film; (2) 15' irradiation; (3) 60' irradiation; (4) 11h irradiation; (5) post irradiation relaxation at 50°C for 23 h.

The irradiation of the AzB-containing sample with an excitation light of 365 nm brought about a decrease in the band at 330 nm (trans isomer) and a simultaneous increase in the band at 430 nm (cis isomer) as reported in Figure 68, to indicate that light-induced isomerization of the AzB moieties took place. This process could be easily reversed by thermal treatment of the coatings by heating the deposited films at 50°C for 23 h. The cycle was repeated twice, showing an almost complete recovery of the photochromic properties.

4.4.5. Conclusions

In this chapter we described the synthesis and the characterization of new materials based on the surface functionalization of crystalline (100) silicon wafers and sodalime glass slides and on the formation of cyclophosphazene monoliths through the sol-gel technique.

This goal could be achieved through the synthesis of cyclophosphazenes formally containing three APTES substituents, while the three additional positions in the cyclophosphazene were saturated by 4CNP, PEG-750-ME, TFP or AzB substituents, respectively.

In this way the multifunctionality of the cyclophosphazenes has been used to deposit on the surface of suitable supports, or to insert in the sol-gel monoliths, molecules granting them different physico/chemical properties.

The materials obtained have been fully characterized by standard spectroscopic (FTIR, UV-visible, solution and solid state NMR) techniques and thermal (DSC and DMTA) analyses to assess their chemical structure and their physical properties. Possible applications as photochromic substrates or as products of modulated mechanical features could be envisaged.

It may be useful to stress that this method is completely general and that it can be in principle exploited to functionalize the surface of silicon-based substrates with any nucleophile that can be attached to the phosphazene ring.

4.4.6. Acknowledgements

The work here presented was performed at the Department of Chemical Processes of the Engineering (DPCI) of the University of Padova, Italy, in collaboration with Dr. Alessandro Sassi of DPCI for solid state NMR, Dr. Alfonso Venzo from the Institute of Molecular Sciences and Technologies (ISTM) of the National Research Council (CNR), Padova, Italy, for solution NMR, and Prof. Luca Fambri from the Department of Materials Engineering of the University of Trento, Italy, for thermal analyses.

4.5. CYCLOPHOSPHAZENES SUBSTITUTED WITH 2-OXAZOLINE GROUPS AS STARTING PRODUCTS FOR THE PREPARATION OF NEW MATERIALS

4.5.1. Preliminary considerations

Among highly reactive chemical functions commonly used in organic chemistry, 2-oxazoline groups occupy an important position³⁸⁵⁻³⁹¹.

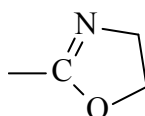


Figure 69. General structure of 2-oxazoline (OXA) moieties.

In fact, a large number of scientific papers^{302,392-397}, review articles³⁸⁵⁻³⁹¹ and industrial patents³⁹⁸⁻⁴⁰² reported the practical utilization of oxazoline derivatives as starting materials for polymerization processes^{390,403,404}, synthetic intermediates⁴⁰⁵, protecting groups for carboxylic functions⁴⁰⁶, chain extenders^{407,408}, core molecules for dendrimer preparation^{409,410}, active functionalities for blending processes⁴¹¹⁻⁴¹³, and products suitable to favour recycling of organic macromolecules^{396,398,399}.

The combination between 2-oxazoline and phosphazene derivatives was first attempted by J.Y.Chang⁴¹⁴⁻⁴¹⁶ who used phosphazenes substituted with bromomethylenephenoxy groups to induce the polymerization of 2-methyl-2-oxazoline to obtain star polymers with a cyclophosphazene core⁴¹⁴ or to prepare poly[bis(4-methylphenoxy)phosphazene]-g-poly-2-methyl-2-oxazoline grafted copolymers^{415,416}.

Expanding upon this research, a series of compounds was recently proposed in which the 2-oxazoline moiety was directly inserted into the phosphazene substrates by thermally-induced grafting reactions^{15,78,80,81,417} to favor the formation of blends among polyphosphazenes and commercial macromolecules, or by reacting 2-(4-hydroxyphenyl)-2-oxazoline³⁰² with HCCP^{15,80,81,304,418-420}, and/or with 2,2-dichloro-4,4,6,6-bis[spiro(2',2''-dioxo-1',1''-biphenyl)]cyclophosphazene^{15,303,420,421}, C-2-Cl, to prepare C-6-OXA and C-2-OXA, *i.e.* cyclophosphazenes containing six and two 2-oxazoline units, respectively. These products were used as chain-extendors for polyesters^{15,80,303,304,419} and as compatibilizing agents for polyamide/polycarbonate⁴¹⁸ and high density polyethylene/polyamide-6 blends⁴²¹.

Considering the cyclophosphazenes described above, it may be realized that only 2-(4-hydroxyphenyl)-2-oxazoline was used for their preparation. According to literature³⁰², this compound was synthesized by reacting methyl-4-hydroxybenzoate with 2-aminoethanol to produce first an amidic intermediate that is successively cyclized to form the 2-oxazoline ring by the action of thionyl chloride. It may be reasoned that using 1-amino-2-propanol (that is commercially available as chiral R-(-), S-(+), and as racemic (±) derivatives), then it would be easy to prepare chiral and racemic 2-(4-hydroxyphenyl)-5-methyl-2-oxazoline derivatives from which cyclophosphazenes showing optical activity could be eventually obtained. This could be extremely interesting, given the low number of chiral cyclophosphazenes synthesized and characterized up to now⁴²².

4.5.2. Synthesis and characterization of the oxazoline-containing phosphazenes

During this work cyclophosphazene derivatives were systematically combined with molecules containing 2-oxazoline groups, as a preliminary part of a research project aimed at the preparation of a new class of chiral cyclophosphazenes suitable to favor blending processes and for the preparation of chiral phases for the chromatographic separation of enantiomeric species⁴²³. Furthermore, this type of cyclophosphazenes can act as monomers for the synthesis of cycloliner and cyclomatrix phosphazene macromolecules³⁰³.

The synthesis of the 2-(4-hydroxyphenyl)-2-oxazolines was carried out according to the procedure put forward by Saegusa³⁰², in which methyl-4-hydroxybenzoate was reacted with an excess of 2-aminoethanol, or with chiral R-(-), S-(+) and racemic (\pm) 1-amino-2-propanol to prepare the corresponding hydroxybenzamides (I-IV), according to the scheme in Figure 70 below. These compounds were then cyclized to 2-(4-hydroxyphenyl)-2-oxazolines (a-d) by the action of thionyl chloride, as reported in the same scheme.

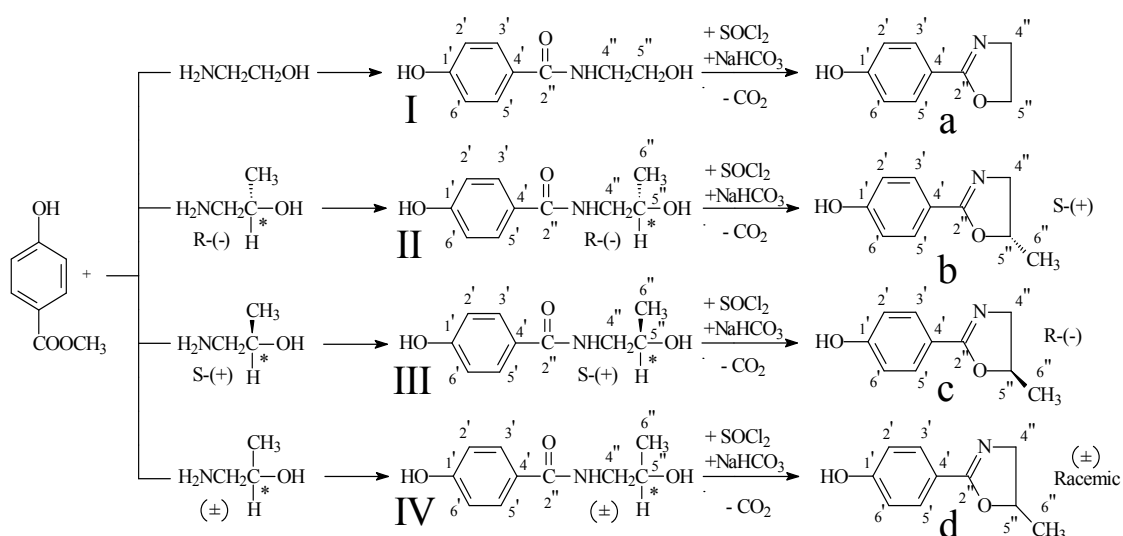


Figure 70. Synthesis of 2-(4-hydroxyphenyl)-2-oxazoline (a), and of 2-(4-hydroxyphenyl)-5-methyl-2-oxazolines (b-d)

The mechanism of this reaction is of importance because it could be proved^{424,425} that the first step to hydroxybenzamides takes place maintaining the steric configuration of the asymmetric carbon, while the cyclization reaction of the hydroxybenzamide species to hydroxyphenyl-2-oxazolines occurs following a classical $\text{S}_{\text{N}}2$ mechanism with the

complete inversion of this configuration. These facts are described in detail in Figure 71, for the synthesis of S-(+)-2-(4-hydroxyphenyl)-5-methyl-2-oxazoline.

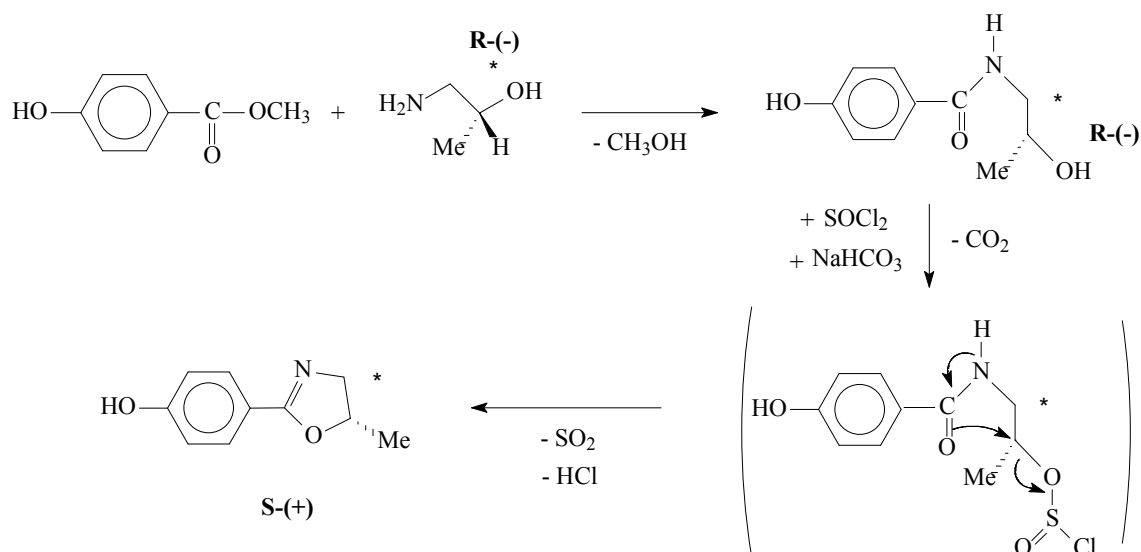


Figure 71. Inversion of the Chiral Configuration during the synthesis of S-(+)-2-(4-hydroxymethyl)-5-methyl-2-oxazoline.

Products (b) and (c) (see Figure 70) are chiral derivatives due to the presence of a carbon atom in the oxazoline ring containing four different chemical substituents, while products (a) and (d) do not show any optical activity because of the lack of chiral carbons (a), or because a racemic mixture as in the case of product (d).

The chemical characterization of the products, carried out by elemental analysis, optical activity measurement, IR, UV, and by ^1H and ^{13}C NMR spectroscopy is consistent with the structure described in Figure 70.

The 2-(4-hydroxyphenyl)-2-oxazolines described above were successively reacted with the three different cyclophosphazenes reported in Figure 72, according to the classical nucleophilic substitutive reaction of chlorinated cyclophosphazenes¹.

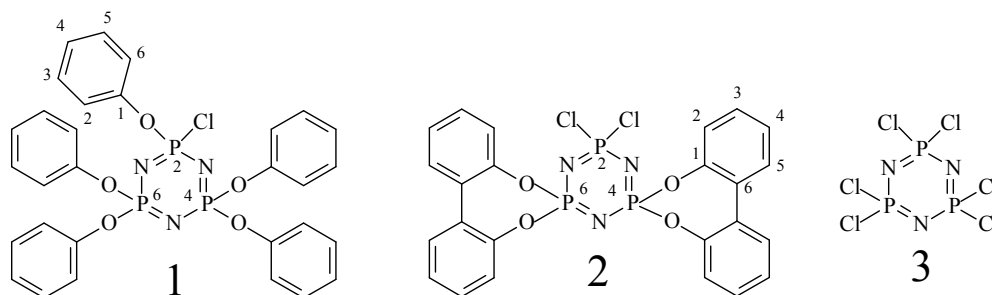


Figure 72. Pentakis(phenoxy)-monochlorocyclophosphazene (1), 2,2-dichloro-4,4,6,6-bis[spiro(2',2'')-dioxo-1',1'']-biphenyl]cyclophosphazene (2) and HCCP (3).

These compounds contain one (pentakis(phenoxy)monochlorocyclophosphazene, C-1-Cl), two (2,2-dichloro-4,4,6,6-bis[spiro(2',2'')-dioxo-1',1'']-biphenyl)cyclophosphazene, C-2-Cl) and six (HCCP) reactive chlorines in their chemical structure, respectively. The whole series of chiral and non chiral cyclophosphazenes reported in Table 22 at the end of this section was prepared in this way.

The IR spectra of the whole series of compounds presented bands localized in the ranges $3071 \div 3059 \text{ cm}^{-1}$ (ν aromatic C-H); $2976 \div 2864 \text{ cm}^{-1}$ (ν aliphatic C-H); $1608 \div 1587 \text{ cm}^{-1}$, and $1505 \div 1482 \text{ cm}^{-1}$ attributed to the breathing modes of the aromatic ring; $1648 \div 1645 \text{ cm}^{-1}$ (ν C=N of the oxazoline group); $1272 \div 1151 \text{ cm}^{-1}$ (ν asymmetric -P=N-); and $947 \div 930 \text{ cm}^{-1}$ (ν of the P-O-Ph group).

As far as the ^1H NMR spectra of compounds 1a-3d are concerned, two series of peaks were found. One of them was located between δ 8 and 6.5 and was attributed to the aromatic protons of the phenoxy or 2,2'-biphenyldioxy systems, and a second one was located between δ 5 and 1.5 and was assigned to the 2-oxazoline (two triplets at δ 4.9 and 4.05 due to the protons in the position 5'' and 4'', respectively), and 5-methyl-2-oxazoline (a doublet at δ 1.38 assigned to the methyl group in 6'' position; two doublets of doublets roughly at a δ of 4.1 and 3.5, assigned to the protons in the position 4''; and a multiplet at δ 4.8 attributed to the proton in the 5'' position) residues.

Similarly, in the ^{31}P NMR spectra, cyclophosphazenes hexasubstituted with equivalent groups exhibited a sharp singlet in the range between δ 7.88 for 3a, and at δ 9.32 for the other three cyclophosphazenes. Conversely, multiplets were observed for cyclophosphazenes substituted with a single 2-oxazoline group, due to the small influence on the phosphorus atom δ 's of the 2-oxazoline ring present in the para position of the phenoxy substituent. This fact makes the peaks of the ABC system in these compounds almost indistinguishable (δ about 9.45).

A more complicated structure was presented by the ^{31}P NMR spectra of cyclophosphazenes containing two 2-oxazoline substituent groups.

The resonance of the ^{31}P nucleus bonded to the oxazolinophenoxy groups, P2, appeared in the range of δ 11 \div 13 as a doublet of doublets because of the different $^2J_{\text{P,P}}$ coupling constants with the two other phosphorus nuclei (see 3.6.3.7 to 3.6.3.10). The two other phosphorus atoms, P4 and P6, bonded to the 2,2'-diphenyldioxy moieties,

exhibited slightly different chemical shift values and appeared as two doublets in the range of δ 27 \div 24.

All given chemical shift values are compatible with the structures assigned to these compounds and reported in Table 22.

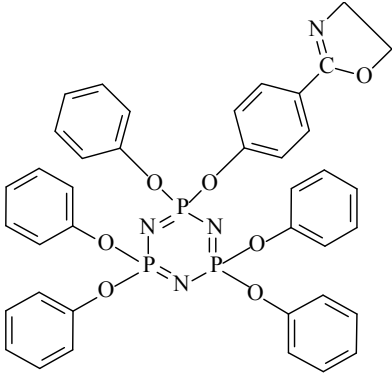
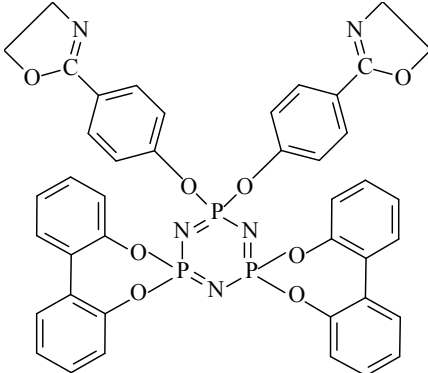
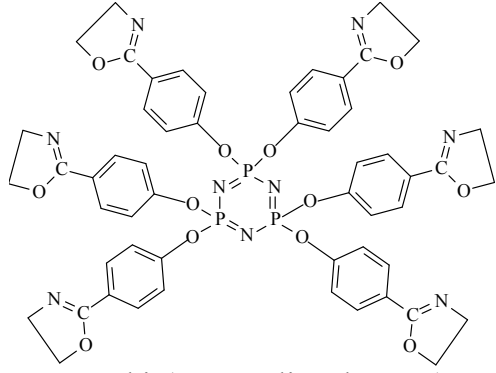
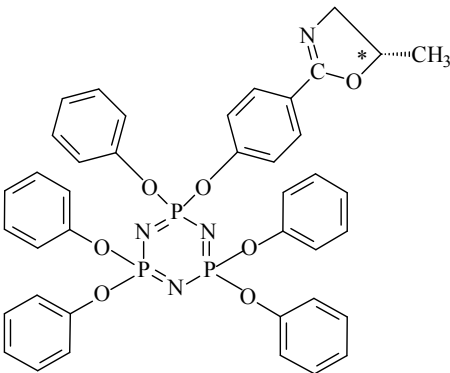
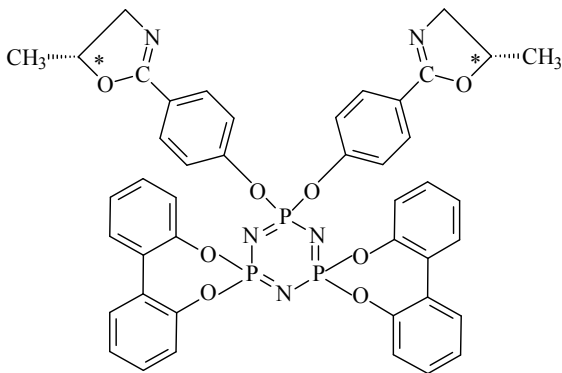
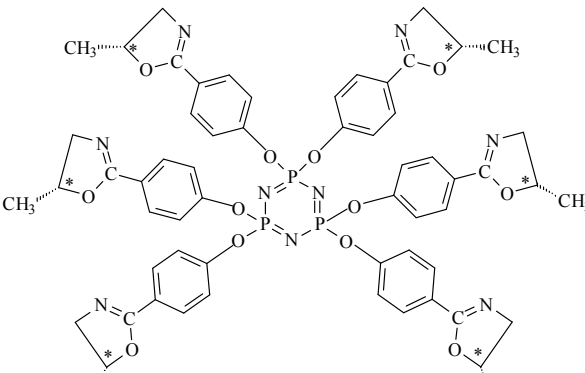
4.5.3. Conclusions

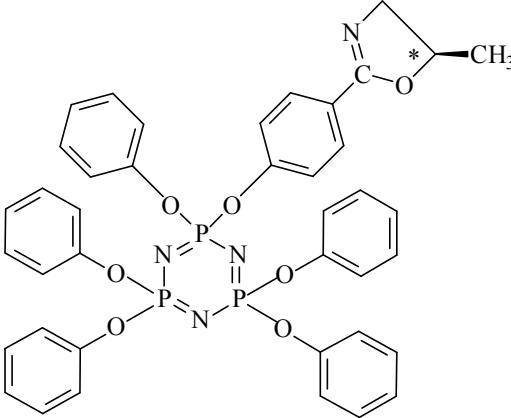
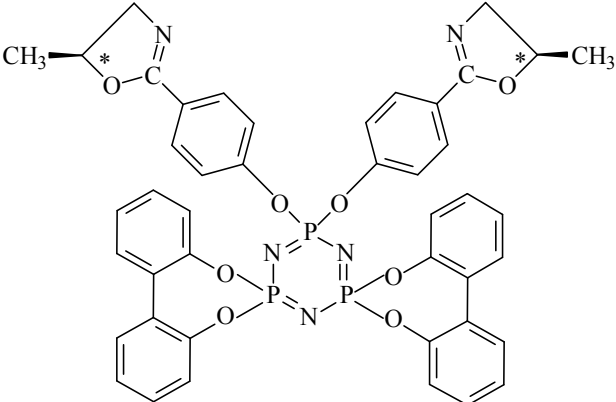
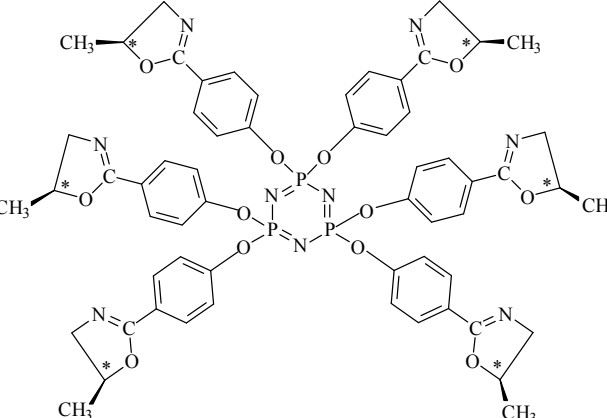
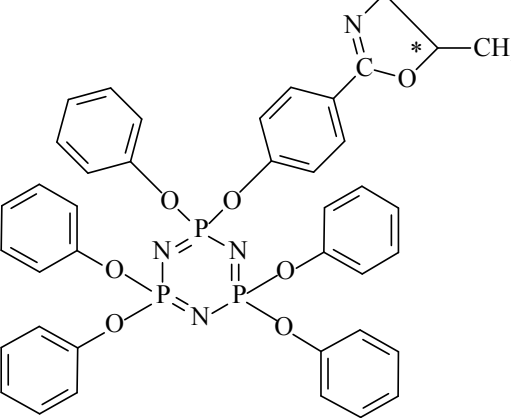
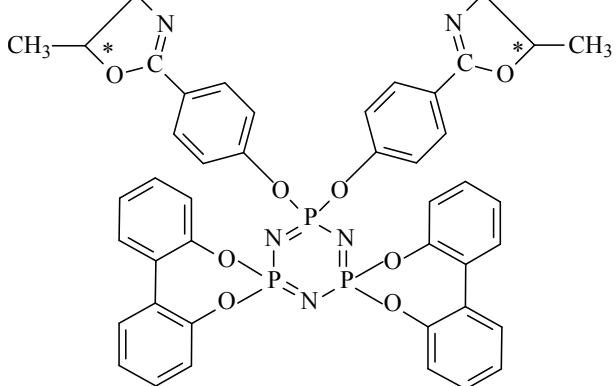
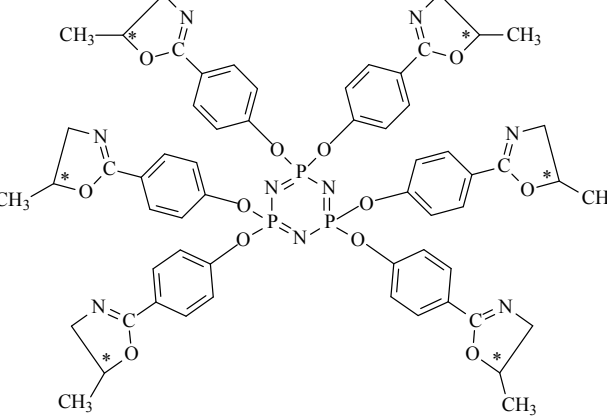
In this section the synthesis of twelve different cyclophosphazenes substituted with 2-oxazoline derivatives was reported, together with the preparation of the corresponding 2-oxazolines. The characterization of these compounds was carried out by elemental analysis, optical activity measurements, FTIR and ^1H , ^{13}C and ^{31}P NMR spectroscopy. These compounds have possible applications for the preparation of cyclolinear, cyclomatrix and star polymers, as compatibilizing agents for blends of organic macromolecules, and as chain extenders for commercial plastics.

4.5.4. Acknowledgements

The work here presented was mostly performed at the Department of Chemical Processes of the Engineering (DPCI) of the University of Padova, Italy, in collaboration with Dr. Luisa Fiocca (ENI SpA – Refining and Marketing Division, Research Center of Novara, Italy) who performed the synthesis of the oxazolinic compounds **a - d** and of their amidic precursors, and with Dr. Alfonso Venzo from the Institute of Molecular Sciences and Technologies (ISTM) of the National Research Council (CNR), Padova, Italy, who performed NMR analyses.

Table 22. Chemical Structure of cyclophosphazenes containing 2-oxazoline groups

| | | |
|--|---|---|
| <p style="text-align: center;">1a</p>  <p style="text-align: center;">Pentakisphenoxy-mono-(4-oxazolinophenoxy)cyclophosphazene</p> | <p style="text-align: center;">2a</p>  <p style="text-align: center;">2,2-bis(4-oxazolinophenoxy)-4,4,6,6-bis[spyro(2',2''-dioxo-1',1''-biphenyl)]cyclophosphazene</p> | <p style="text-align: center;">3a</p>  <p style="text-align: center;">Hexakis(4-oxazolinophenoxy)cyclophosphazene</p> |
| <p style="text-align: center;">1b</p>  <p style="text-align: center;">Pentakisphenoxy-mono[4-(5-methyl)-oxazolinophenoxy]cyclophosphazene S-(+)</p> | <p style="text-align: center;">2b</p>  <p style="text-align: center;">2,2-bis[4-(5-methyl)-oxazolinophenoxy]-4,4,6,6-bis[spyro(2',2''-dioxo-1',1''-biphenyl)]cyclophosphazene S-(+)</p> | <p style="text-align: center;">3b</p>  <p style="text-align: center;">Hexakis[4-(5-methyl)-oxazolinophenoxy]cyclophosphazene S-(+)</p> |

| | | |
|--|--|--|
| <p>1c</p>  <p>Pentakisphenoxy-mono[4-(5-methyl)-oxazolinophenoxy]cyclophosphazene R(-)</p> | <p>2c</p>  <p>2,2-bis[4-(5-methyl)-oxazolinophenoxy]-4,4,6,6-bis-[spyro(2',2''-dioxo-1',1''-biphenyl)]cyclophosphazene R(-)</p> | <p>3c</p>  <p>Hexakis[4-(5-methyl)-oxazolinophenoxy]-cyclophosphazene R(-)</p> |
| <p>1d</p>  <p>Pentakisphenoxy-mono[4-(5-methyl)-oxazolinophenoxy]cyclophosphazene (±)</p> | <p>2d</p>  <p>2,2-bis[4-(5-methyl)-oxazolinophenoxy]-4,4,6,6-bis-[spyro(2',2''-dioxo-1',1''-biphenyl)]cyclophosphazene (±)</p> | <p>3d</p>  <p>Hexakis[4-(5-methyl)-oxazolinophenoxy]cyclophosphazene (±)</p> |

4.6. SUPRAMOLECULAR RODS VIA HALOGEN BONDING-BASED SELF-ASSEMBLY OF FLUORINATED PHOSPHAZENE NANOPILLARS

4.6.1. Preliminary considerations

Halogen bonding is defined as any non-covalent interaction involving halogens as electron density acceptors⁴²⁶⁻⁴²⁹. It is recently emerging as a reliable tool in crystal engineering as, thanks to its strength and directionality, it allows complex supramolecular architectures to be designed and assembled with a high degree of predictability. Bromo- and iodo-perfluorocarbons are particularly robust electron acceptors (halogen bonding donors) and their halogen-bonding mediated self-assembly with nitrogen substituted hydrocarbons, working as electron donors (halogen bonding acceptors), proved to be an efficient and reliable strategy in affording new and structurally different perfluorocarbon-hydrocarbon hybrid materials.

Numerous examples are available in literature showing that when bidentate halogen bonding donors self-assemble with bidentate halogen bonding acceptors, infinite chains are formed where one donor module and one acceptor module alternate along the chains, their shape depending on the structure of the starting compounds. Linear modules afford linear infinite chains, *e.g.* α,ω -diiodoperfluoroalkanes or 1,4-diiodotetrafluorobenzene interacting with α,ω -dicyanoalkanes or 4,4'-dipyridines⁴³⁰⁻⁴³², while angular modules afford zigzag chains, with the angulation depending on the one of the starting modules; for example, the chains obtained from 1,2-dibromotetrafluorobenzene are more angulated than those obtained from 1,3-dibromotetrafluorobenzene^{433,434}.

A pentaerythritol derivative bearing four iodotetrafluorobenzene residues adopts a conformation where the four arms point two by two to the opposite sides. Upon interaction with dinitrogen hydrocarbons, supramolecular architectures are formed in the shape of infinite ribbons wherein one pentaerythritol module and two dinitrogen hydrocarbons alternate along the ribbon⁴³⁵.

Recently the first halogen bonded supramolecular array employing a cyclophosphazene module has been reported, which employs 1,4-diiodotetrafluorobenzene and a cyclophosphazene substituted with two 4-pyridinoxy groups⁴³⁶⁻⁴³⁸.

Within this thesis, we worked on the second example of this kind of system, by synthesizing a cyclophosphazene containing six iodotetrafluorophenyl residues and challenging it with 4,4'-dipyridyl (DPy) and 1,2-di(4-pyridyl)ethylene (DPE) to form supramolecular self-assemblies.

4.6.2. Synthesis and characterization of the phosphazene precursor

Hexakis[4-(2,3,5,6-tetrafluoro-4-iodophenoxy)methylen]phenoxy]cyclotriphosphazene (C-6-ITFB) was prepared in three steps from HCCP, as shown in Figure 73 below.

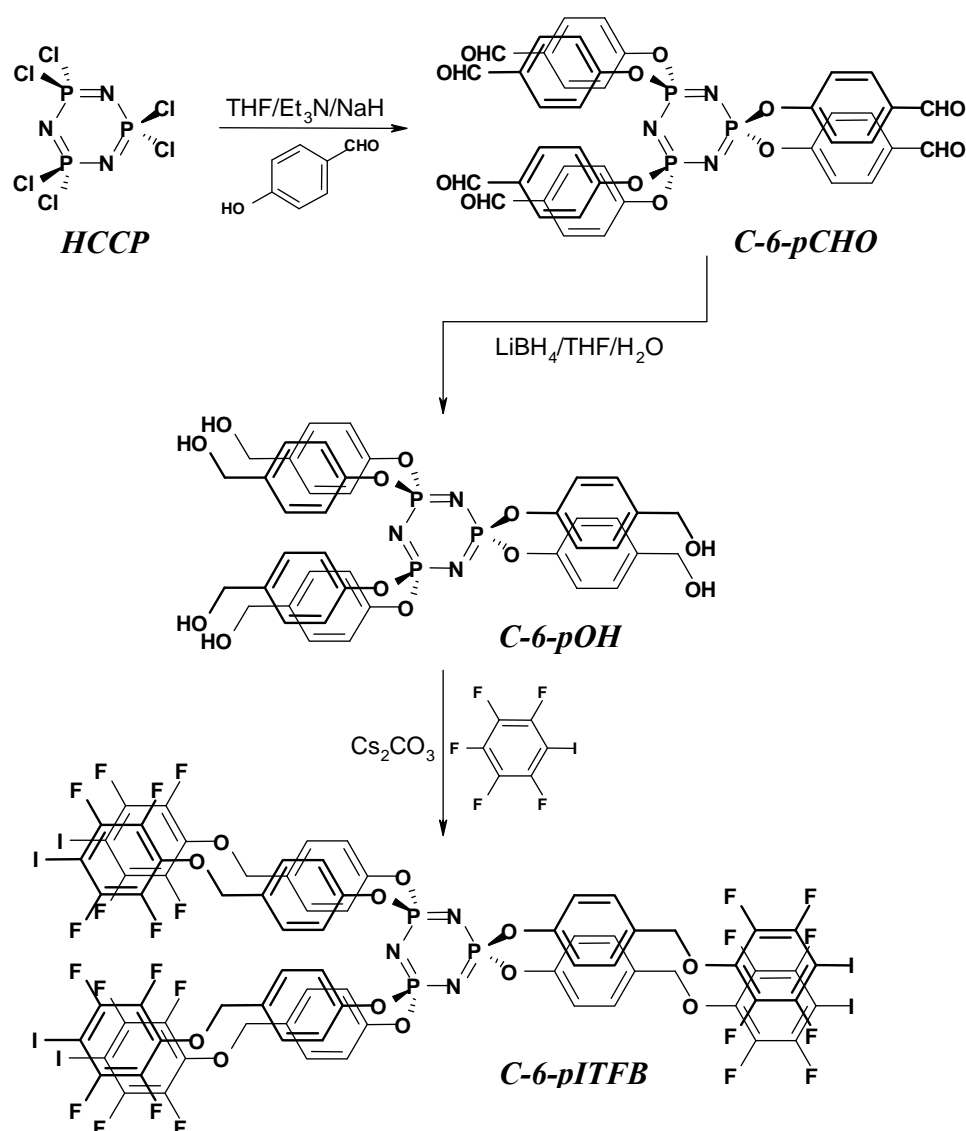


Figure 73. Synthesis of hexakis[4-(2,3,5,6-tetrafluoro-4-iodophenoxy)methylen]phenoxy]cyclotriphosphazene.

In the presence of a base, the nucleophilic attack of 4-hydroxybenzaldehyde on HCCP afforded hexakis(4-formylphenoxy)cyclotriphosphazene (C-6-pCHO) in high yields⁴³⁹, and the reduction of the formyl moieties to -CH₂OH groups was performed by using LiBH₄ at room temperature. This optimized procedure⁴⁴⁰ afforded hexakis (4-hydroxymethylenephenoxy)cyclotriphosphazene (C-6-pOH), again in high yield, after an easy purification from side products.

Finally, peretherification was performed via S_NAr of the alcoholic oxygen atoms of C-6-pOH on iodopentafluorobenzene (IPFB)⁴⁴¹. The reaction occurs with very high regioselectivity on the fluorine atom *para* to the iodine. When it is performed at room temperature, no brown side products are formed (as is the case when high temperature is used) and the final product C-6-pITFB is purified from the excess IPFB and isolated in high yield.

The FTIR spectrum of the compound, reported in Figure 74, showed all expected components, with signals at 1201, 1180 and 1166 cm⁻¹ (asymmetric v P=N), 955 cm⁻¹ (v P-O-C), 1609, 1507 and 1483 cm⁻¹ (aromatic C=C breathing), 2950 and 2884 cm⁻¹ (v CH₂), and 1095 cm⁻¹ (v C-F).

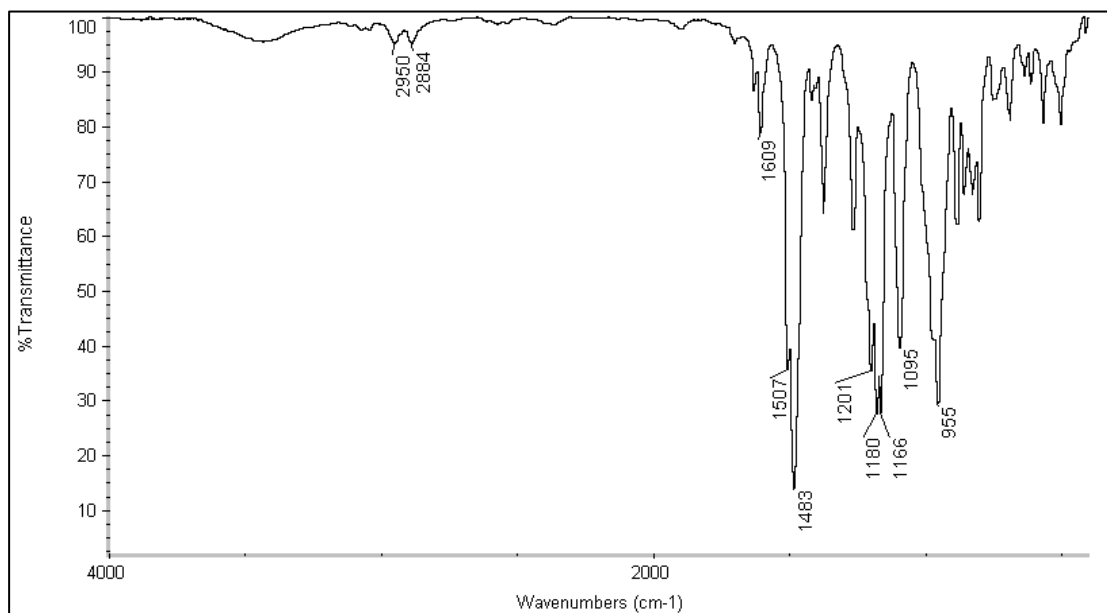


Figure 74. FTIR spectrum of hexakis[4-(2,3,5,6-tetrafluoro-4-iodophenoxy)methyl]phenoxy]cyclotriphosphazene.

NMR characterization was consistent with the expected compound structure as well. The {¹H}³¹P NMR spectrum showed one singlet at δ 9.19, accounting for the peretherification of all six alcoholic pendants of C-6-pOH.

In the ^1H NMR spectrum of C-6-pITFB, two doublets were due to the benzyl protons at δ 7.31 and 6.95. The CH_2 moiety, that in C-6-pOH yields a doublet at δ 4.47, was shifted downfield to δ 5.19 and became a singlet as an effect of the substitution of the hydroxyl proton with the iodopentafluorobenzene ring.

Finally the ^{19}F NMR spectrum of the compound, reported in Figure 75, gave further evidence of the presence of the iodotetrafluorobenzene ring.

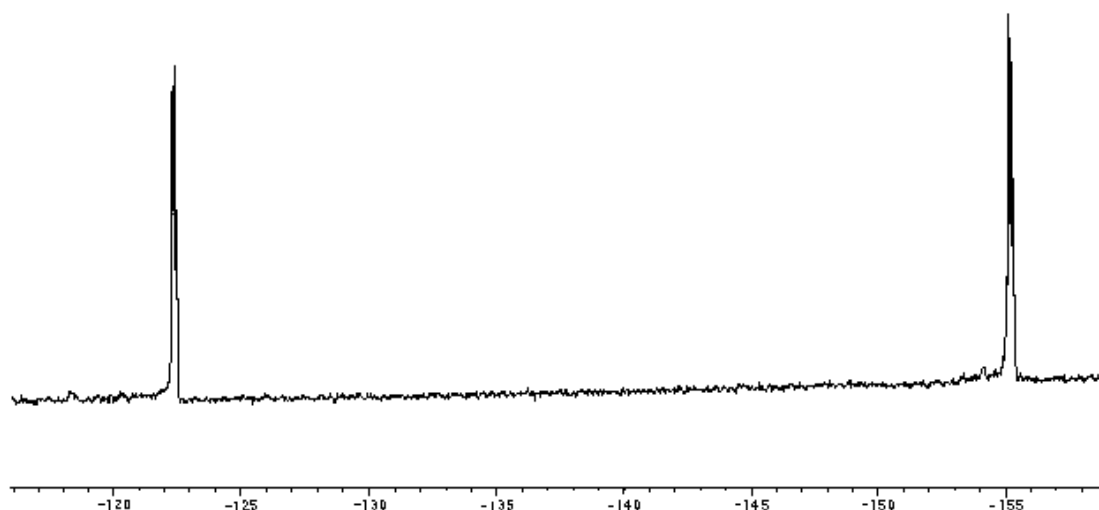


Figure 75. ^{19}F NMR spectrum of hexakis[4-(2,3,5,6-tetrafluoro-4-iodophenoxy)methyl]cyclophosphazene.

The fact that only two doublets were found, at δ -122.58 (CF in *meta* position with respect to the benzyl moiety) and -155.30 (CF in *ortho* position with respect to the benzyl moiety) accounts for the regioselectivity of the peretherification reaction, that involves the fluorine atom in *para* to the iodine atom of IPFB.

4.6.3. Formation of supramolecular assemblies

By allowing slow diffusion of CCl_4 into chloroform solutions of C-6-pITFB and either DPy or DPE, precipitation of the molecular complexes C1 and C2 as crystalline solids occurred, respectively (see Figure 76 below).

In these adducts, the cyclophosphazene derivative works as a hexadentate electron acceptor and the starting modules are present in a stoichiometric ratio of one C-6-pITFB per three DPy or DPE, as it could be confirmed by integration of the ^1H NMR spectra of C1 and C2.

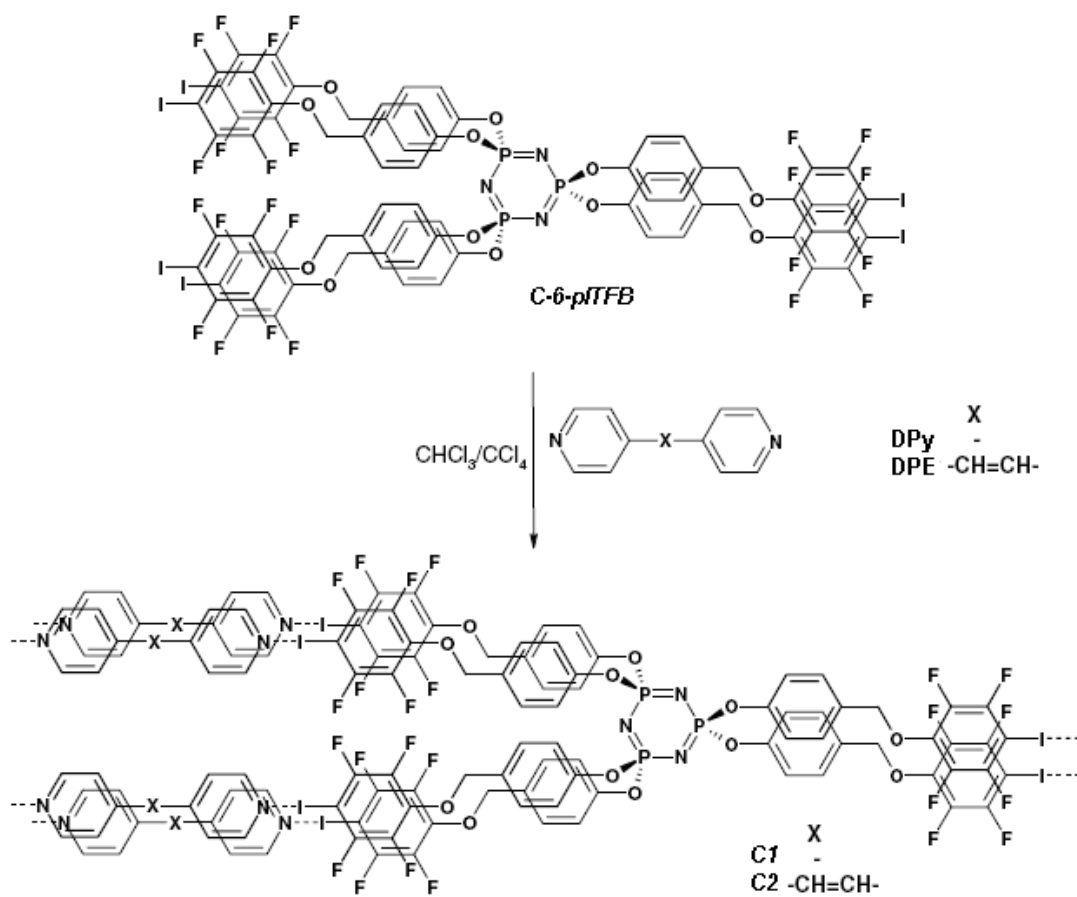


Figure 76. Halogen bonding driven self assembly of C-6-pITFB with DPy and DPE to give the supramolecular complexes C1 and C2.

In the ^{19}F NMR spectra of the complexes, $\text{I}-\text{C}=\text{C}-\text{F}$ and $\text{O}-\text{C}=\text{C}-\text{F}$ signals showed small and very small upfield shifts respectively, when compared to pure C-6-pITFB. The shifts decreased when diluting the adducts solutions, as it is typically observed when iodoperfluoroarenes are halogen bonded to pyridine derivatives^{426-429,432,434,442,443}.

DSC analysis gave a reliable proof that these solids are well-defined crystalline species rather than mechanical mixtures of the starting modules. A solid mixture of two compounds that does not form a structurally defined adduct commonly melts lower than the pure starting components, while a melting point increase is a strong indication that a specific crystalline complex is formed. As shown in Table 23, the melting points of C1 and C2 are higher than those of their precursors; moreover, the melting endotherms of the source compounds were missing in the thermographs of the adducts.

Table 23. Thermal features of C1, C2 and their precursors

| Compound | Melting Point (°C) | Starting modules mean melting points (°C) | Δ Melting point ^a |
|------------------|--------------------|--|-------------------------------------|
| <i>C-6-pITFB</i> | 142-144 | | |
| <i>DPy</i> | 109-112 | | |
| <i>DPE</i> | 150-151 | | |
| <i>C1</i> | 170-173 | 125-128 | + 45 |
| <i>C2</i> | 190-193 | 146-147 | + 44 |

^a Difference between the melting point of the complex and the mean value of the melting points of corresponding starting modules

The observed increases are non-minor, thus accounting for the strength of halogen bonding between the modules.

N \cdots I interactions are weaker than covalent or ionic bonds^{430,442,444,445}, it is therefore reasonable to discuss the vibrational spectra of complexes C1 and C2 in terms of modified modes of starting materials. FTIR spectra of the complexes showed the bands of both phosphazene and pyridine derivatives, but the frequency shifts and intensity changes of some bands are diagnostic of halogen bonding occurrence^{426-429,446}. For instance, the pyridine ν_{C-H} stretching modes were shifted to higher frequencies and decreased their intensities in the complexes with respect to the pure components, *e.g.* the band at 3025 cm⁻¹ in DPy moves to 3043 cm⁻¹ in C1. These changes can be correlated with the decreased electron density on pyridine protons in formed complexes, due to the $n \rightarrow \sigma^*$ electron donation from nitrogen to iodine atoms. Moreover, the pyridine ring absorptions at 989 and 990 cm⁻¹, in DPy and DPE respectively, were blue shifted to 994 and 997 cm⁻¹ in C1 and C2. Similar shifts have already been observed in the FTIR spectra of related pyridine derivatives when the nitrogen atom is involved in either halogen or hydrogen bonding^{426,427,429,446-448}.

Single crystal X-ray diffraction analysis of C1 and C2 gave details about the supramolecular organization of the modules in the two complexes. Crystallographic data are reported in Table 24.

The closest intermolecular contacts are by far those involving tetrafluorobenzene iodines and pyridine nitrogens. As expected, these nitrogens are better electron donors than those of the phosphazene and ether oxygens^{17,426-429,449,450}. The N \cdots I distances varied in the range 2.741-2.979 Å in C1 and 2.813-2.870 Å in C2. These distances are substantially longer than the N–I covalent bond (2.07 Å)⁴⁵¹.

Table 24. Crystallographic data for the supramolecular complexes

| | <i>C1</i> | <i>C2</i> |
|--|---|--|
| Empirical Formula | C ₇₈ H ₃₆ F ₂₄ I ₆ N ₃ P ₃ ·3(C ₁₀ H ₈ N ₂) | C ₇₈ H ₃₆ F ₂₄ I ₆ N ₃ P ₃ ·3(C ₁₂ H ₁₀ N ₂) |
| M (g mol ⁻¹) | 2985.96 | 3064.07 |
| Crystal System | monoclinic | monoclinic |
| Space group | <i>P</i> 21/ <i>c</i> | <i>P</i> 21/ <i>c</i> |
| <i>a</i> (Å) | 16.032(2) | 26.052(4) |
| <i>b</i> (Å) | 38.986(5) | 14.830(2) |
| <i>c</i> (Å) | 16.812(2) | 28.692(5) |
| β (°) | 90.84(3) | 98.93(3) |
| <i>V</i> (Å ³) | 10507(2) | 10951(3) |
| <i>Z</i> | 4 | 4 |
| ρ_{calc} (g cm ⁻³) | 1.888 | 1.858 |
| μ (Mo K α) (mm ⁻¹) | 1.930 | 1.854 |
| Total reflections | 148359 | 13782 |
| Unique reflections | 21961 | 19263 |
| Data [<i>I</i> > 2 σ (<i>I</i>)] | 18456 | 16507 |
| <i>R</i> _{int} | 0.0339 | 0.0350 |
| Parameters | 1459 | 1513 |
| <i>R</i> ₁ (all, observed) | 0.0723, 0.0591 | 0.0585, 0.0462 |
| <i>wR</i> ₂ (all, observed) | 0.1325, 0.1272 | 0.1071, 0.1014 |
| Goodness-of-fit | 1.253 | 1.149 |
| $\Delta\rho_{\text{min}}$ | -0.49 | -0.78 |
| $\Delta\rho_{\text{max}}$ | 1.69 | 0.83 |

The C-6-pITFB module adopted a pillar-like conformation where the six 4-iodotetrafluorophenyl substituted arms are nearly parallel to each other and almost perpendicular above and below the roughly planar phosphazene ring, as shown in Figure 77 that illustrates the ball-and-stick model for the complex C2.

Different N···I–C angles are present in the two structures but, consistently with the $n \rightarrow \sigma^*$ character of halogen bonding, they are invariably close to 180° (171.4–178.3° in C1, 173.9–178.9° in C2). This directionality of the interactions translates the alignment of C-6-pITFB's arms into the dipyrindyl modules alignment within the obtained complexes, and the pillar-like conformation of the phosphazene derivative is translated into the rod-like shape of the infinite chains present in the adducts.

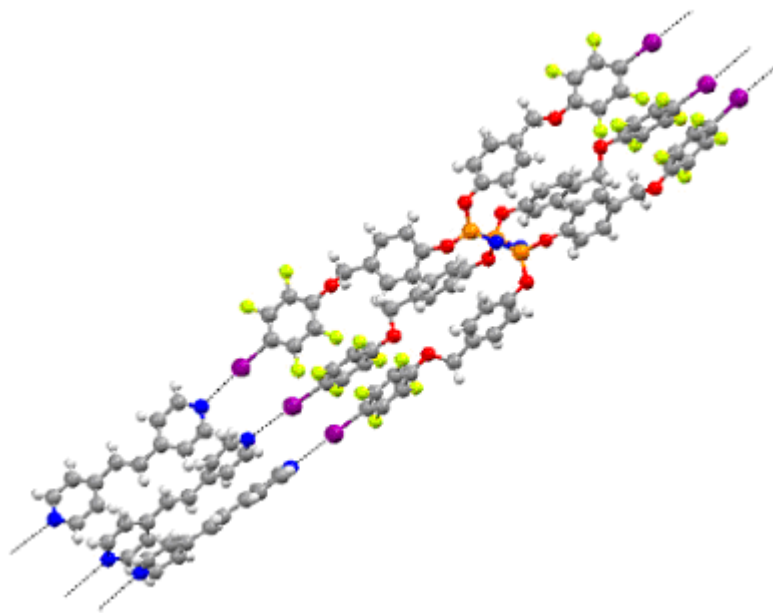


Figure 77. Ball and stick view of the supramolecular complex C2 showing how the six phosphazene arms, and the halogen bonded dipyriddyethylene are perpendicular to the phosphazene ring. Colors are as follows: carbon, gray; hydrogen, light gray; oxygen, red; nitrogen, blue; phosphorus, orange; iodine, violet. $N\cdots I$ halogen bondings are dotted black lines.

In these supramolecular rods, one phosphazene module and three dipyriddy modules alternate along the rod, confirming the stoichiometry already indicated by ^1H NMR analysis (see above).

Figure 78 compares the shapes of the rods in C1 (top) and C2 (bottom), adopting the same color scheme as Figure 77.

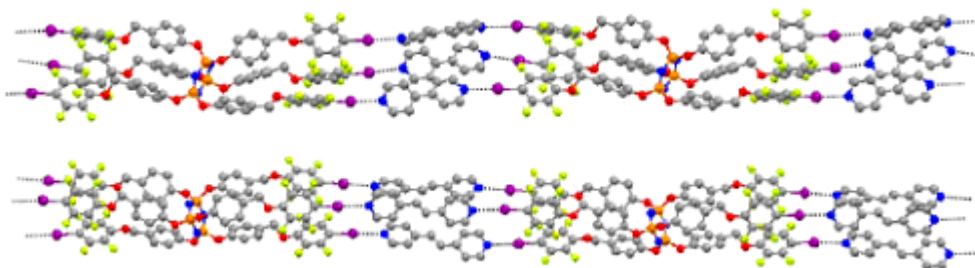


Figure 78. A comparison between one of the supramolecular rods in the complexes C1 (top) and C2 (bottom). Colors are as in Figure 77. $N\cdots I$ halogen bonds are dotted black lines

The similarities between the two architectures are evident and confirm the reliability of the $N\cdots I$ halogen bond as a tool in crystal engineering, as well as the robustness of the phosphazene pillar as a polydentate halogen bonding donor.

Alongside nitrogen-iodine halogen bonding, the only other short-range interactions present in the two complexes are a network of weak hydrogen bonds, mostly involving fluorine and hydrogen atoms with bond lengths in the range 2.24÷2.57 Å (C1) and 2.36÷2.59 Å (C2), which stabilize the overall crystal packing in both structures.

Halogen bonding is therefore responsible for the self-assembly of starting modules into the supramolecular rods, which are parallel to [010] in C1 and to [10 $\bar{1}$] in C2, while the hydrogen bonds link together these rods into the observed crystal matrix.

At the molecular level, the main difference between the two complexes was the greater length of DPE with respect to DPy, which resulted at the supramolecular level into a pitch difference, *i.e.* that of C2 is 2.65 Å longer.

4.6.4. Conclusions

In this section we have described the synthesis and characterization of a cyclotriphosphazene derivative containing six iodotetrafluorobenzene residues and its utilization in the formation of supramolecular self-assemblies from it in the presence of linear dipyridyl derivatives by means of halogen bonding.

The iodotetrafluorobenzene moieties point three by three to the opposite sides of the phosphazene ring and, as an effect of the directionality of the N \cdots I interaction, this molecular piece of information is translated into the self-assembly of infinite rods wherein one phosphazene module and three dipyridyl derivatives alternate along the supramolecular rods, whose pitch can be engineered by careful choice of a suitable spacer between the pyridyl groups.

The effectiveness of the N \cdots I halogen bonding in crystal engineering was already shown in literature thanks to the formation of one- and two-dimensional objects (infinite chains⁴³⁰⁻⁴³² and ribbons⁴³⁵) and it is here extended to the formation of three-dimensional cylindrical rods.

Finally, the cyclotriphosphazene moiety proved to be a particularly effective scaffold to preorganize various halogen bonding donor sites in order to determine the structure and geometry of the supramolecular architecture formed in the presence of convenient halogen bonding acceptors. Remarkably, the C-6-pITFB cyclophosphazene described in this chapter constitutes the first example of hexadentate halogen bonding donor.

The behaviour of other phosphazene scaffolds (*e.g.* a cyclotriphosphazene containing two iodotetrafluorobenzene residues, synthesized from the two-chlorine containing C-2-Cl phosphazene compound as described in sections 3.7.1, 3.7.3 and 3.7.5) is currently under study.

4.6.5. Acknowledgements

The synthesis and characterization of the phosphazenic compounds were performed at the Department of Chemical Processes of the Engineering (DPCI) of the University of Padova, Italy.

Assembling and characterization of the supramolecular architectures were performed at the NFMLab of the *Politecnico* University of Milan, Italy, by the *équipe* of Prof. Giuseppe Resnati: Dr. Fanny Chaux, Prof. Pierangelo Metrangolo, Dr. Tullio Pilati, and Dr. Maurizio Sansotera.

CHAPTER 5

CONCLUSIONS

The research project described in this thesis was based on two main areas: the use of chlorinated phosphazenes as coupling agents for the surface functionalization of solid substrates and the synthesis of phosphazenic compounds for the production of new materials and of supramolecular structures.

The surface functionalization of inorganic siliceous substrates has been first handled by means of theoretical *ab initio* calculations, that demonstrated the feasibility from the thermodynamic point of view of the grafting of HCCP onto these substrates. From the kinetic point of view, remarkable energy barriers were found, but they can reasonably be lowered by the choice of a suitable solvent for the reaction. The experimental tests carried out on sodalime and fused quartz glass by dipping in HCCP solutions, revealed by XPS analysis that the phosphazene does bind strongly onto the surface of the substrates, but it is prone to hydrolytic degradation phenomena.

More stable HCCP-based films were obtained by Glow Discharge-induced Sublimation technique on crystalline Si(100) wafers, though the FTIR characterization reported that the cyclic structure of the precursor is mainly lost during the deposition. Subsequent substitution reactions with TFE and 4CNP allowed the introduction of such functional groups onto the surface of the samples, that were characterized by FTIR and XPS techniques.

HCCP and PDCP could be successfully used as coupling agents for the surface functionalization of polymeric substrates, and we could introduce fluorinated alcohols of different lengths and azobenzene moieties onto the surfaces of EVOH and of Ar plasma-treated HDPE and PA6 plates. These were characterized by means of FTIR-ATR, contact angle, UV-Vis and XPS analyses, which confirmed the modification of their surface energy and wettability, and the introduction of photochromic features in the case of the *azo* compound.

Furthermore, several HCCP derivatives evenly substituted with APTES and different organic pendants (4CNP, PEG-750-ME, TFP, AzB) have been prepared, which were characterized by NMR spectroscopy. These compounds have been both grafted on the surface of silica gel particles, and employed in sol-gel processes for the deposition of thin films on sodalime glass and silicon and for the production of hybrid organic-inorganic bulk materials. The analyses performed by FTIR, solid state NMR,

UV-Vis and thermal (DSC and DMTA) techniques confirmed that the products thus obtained have different physico-chemical features depending on the nature of the pendant groups on the cyclophosphazene ring.

It should be stressed that the proposed functionalization procedure has a general character, and can in principle be extended to the surface modification of different solid substrates with an enormous range of organic compounds, thanks to the synthetic versatility of phosphazene chemistry.

As far as the synthesis of compounds for the production of new materials is concerned, a series of twelve cyclophosphazenes containing 2-oxazoline groups of chiral, non chiral or racemic nature has been prepared and characterized by FTIR, NMR, elemental analysis and measurements of the optical rotatory power; the analyses confirmed that all the compounds presented the expected structure. Possible applications of these molecules include the synthesis of cyclomatrix crosslinked polymers for the chromatographic separation of enantiomeric species, and the utilization as chain extenders for the recycling of polymeric materials .

Finally, cyclophosphazenes containing two or six iodotetrafluorophenoxy moieties were prepared and characterized by FTIR and NMR spectroscopy. The hexasubstituted compound was employed in the presence of dipyridyl compounds to form three-dimensional self-assembled nanostructures, generated by supramolecular halogen bonding interactions. These structures were characterized by FTIR, NMR and DSC techniques, and by X-ray diffraction. Remarkably, the synthesized cyclophosphazene containing six iodotetrafluorophenoxy moieties represents the first example of hexadentate halogen bonding donor.

REFERENCES

- (1) Allcock, H. R. *Phosphorus-Nitrogen Compounds. Cyclic, Linear, and High Polymeric Systems*; Academic Press: New York, USA, 1972.
- (2) Allcock, H. R. *Synthesis and Applications of Poly(organophosphazenes)*; Wiley: New York, USA, 2003.
- (3) *Phosphazenes. A Worldwide Insight*; Gleria, M.; De Jaeger, R., Eds.; NOVA Science Publishers: Hauppauge, USA, 2004.
- (4) Gleria, M.; De Jaeger, R. *Topics in Current Chemistry* **2005**, *250*, 165.
- (5) Silvestrelli, P.; Gleria, M.; Milani, R.; Boscolo-Boscoletto, A. *J. Inorg. Organomet. Polym. Mater.* **2006**, *16*, 327.
- (6) Djanic, G., *Master Thesis*, University of Padova, Italy, (2001).
- (7) Milani, R., *Master Thesis*, University of Padova, Italy, (2003).
- (8) Boscolo-Boscoletto, A.; Gleria, M.; Milani, R.; Meda, L.; Bertani, R. *J. Inorg. Organomet. Polym. Mater.* **2008**, manuscript in preparation.
- (9) Sassi, A.; Maggioni, G.; Della Mea, G.; Milani, R.; Gleria, M. *Surf. Coat. Technol.* **2007**, *201*, 5829.
- (10) Milani, R.; Gleria, M.; Gross, S.; De Jaeger, R.; Mazzah, A.; Gengembre, L.; Frere, M.; Jama, C. *J. Inorg. Organomet. Polym. Mater.* **2008**, submitted.
- (11) Milani, R.; Gleria, M.; Sassi, A.; De Jaeger, R.; Mazzah, A.; Gengembre, L.; Frere, M.; Jama, C. *Chem. Mater.* **2007**, *19*, 4975.
- (12) De Jaeger, R.; Mazzah, A.; Gengembre, L.; Frere, M.; Jama, C.; Milani, R.; Bertani, R.; Gleria, M. *J. Appl. Polym. Sci.* **2008**, in press.
- (13) Sassi, A.; Milani, R.; Venzo, A.; Gleria, M. *Design. Monomers Polym.* **2006**, *9*, 627.
- (14) Milani, R.; Sassi, A.; Venzo, A.; Bertani, R.; Gleria, M. *Design. Monomers Polym.* **2007**, *19*, 555.
- (15) Gleria, M.; Po, R.; Giannotta, G.; Fiocca, L.; Bertani, R.; Fambri, L.; La Mantia, F. P.; Scaffaro, R. *Macromolecular Symposia* **2003**, *196 (Metal- and Metalloid-Containing Macromolecules)*, 249.
- (16) Fiocca, L.; Po', R.; Giannotta, G.; Gleria, M.; Venzo, A.; Milani, R.; De Paoli, G. *Design. Monomers Polym.* **2008**, in press.
- (17) Bertani, R.; Chaux, F.; Gleria, M.; Metrangolo, P.; Milani, R.; Pilati, T.; Resnati, G.; Sansotera, M.; Venzo, A. *Inorg. Chim. Acta* **2007**, *360*, 1191.

- (18) De Jaeger, R.; Gleria, M. *Prog. Polym. Sci.* **1998**, *23*, 179.
- (19) Rose, S. H. *J. Polym. Sci., Part B* **1968**, *6*, 837.
- (20) Gleria, M.; Minto, F.; Bertani, R.; Facchin, G.; Tondello, E. *Gazz. Chim. Ital.* **1997**, *127*, 343.
- (21) Allcock, H. R.; Kugel, R. L. *J. Am. Chem. Soc.* **1965**, *87*, 4216.
- (22) Allcock, H. R.; Kugel, R. L. *Inorg. Chem.* **1966**, *5*, 1716.
- (23) Stewart, F. F.; Peterson, E. S. In *Inorganic Polymers*; De Jaeger, R., Gleria, M., Eds.; NOVA Science Publishers: Hauppauge, 2007, p 481.
- (24) De Jaeger, R.; Gleria, M. In *Inorganic Polymers*; De Jaeger, R., Gleria, M., Eds.; NOVA Science Publishers: Hauppauge, 2007, p 515.
- (25) Carenza, M.; Lora, S. In *Inorganic Polymers*; De Jaeger, R., Gleria, M., Eds.; NOVA Science Publishers: Hauppauge, 2007, p 583.
- (26) Carriedo, G. A.; Alonso, F. J. G. In *Synthesis and Characterizations of Poly(organophosphazenes)*; Gleria, M., De Jaeger, R., Eds.; Nova Science Publishers, Inc.: Hauppauge, 2004, p 171.
- (27) Allcock, H. R.; Fuller, T. J. *Macromolecules* **1980**, *13*, 1338.
- (28) Gleria, M.; Bertani, R.; De Jaeger, R. *J. Inorg. Organomet. Polym.* **2004**, *14*, 1.
- (29) Minto, F.; Gleria, M.; Pegoretti, A.; Fambri, L. *Macromolecules* **2000**, *33*, 1173.
- (30) Gleria, M.; Vitulli, G.; Pertici, P.; Facchin, G.; Bertani, R. In *Inorganic Polymers*; De Jaeger, R., Gleria, M., Eds.; NOVA Science Publishers: Hauppauge, 2007, p 609.
- (31) Pertici, P.; Vitulli, G.; Gleria, M.; Facchin, G.; Milani, R.; Bertani, R. *Macromol. Symp.* **2006**, *235*, 98.
- (32) Gleria, M.; Minto, F.; Galeazzi, A.; Scoponi, M. Italian Patent, 1,302,510 (2000), assigned to Consiglio Nazionale delle Ricerche.
- (33) Singler, R. E.; Bierberich, M. J., In *Synthetic Lubricants and High Performance Functional Fluids*; Shubkin, R. L., Ed.; Marcel Dekker: New York, USA, 1993; Chap. 10; p 215.
- (34) Singler, R. E.; Gomba, F. J. In *Synthetic Lubricants and High-Performance Functional Fluids*; Rudnick, L. R., Shubkin, R. L., Eds.; Marcel Dekker, Inc.: New York, USA, 1999; Chapt. 13, Vol. 77, p 297.

- (35) Tonei, D. M.; Bertani, R.; De Jaeger, R.; Gleria, M. In *Phosphazenes: A Worldwide Insight*; Gleria, M., De Jaeger, R., Eds.; Nova Science Publishers: Hauppauge, USA, 2004; Chapt. 28, p 669.
- (36) Allcock, H. R.; Fuller, T. J.; Matsumura, K. US Patent, 4,239,755 (1980), assigned to USA Department of Health, Education and Welfare.
- (37) Allcock, H. R.; Fuller, T. J.; Matsumura, K. *J. Org. Chem.* **1981**, *46*, 13.
- (38) Labarre, J. F. *Top. Curr. Sci.* **1982**, *102*, 1.
- (39) Labarre, J. F. *Top. Curr. Sci.* **1985**, *129*, 173.
- (40) Vogel, A. I. *A Textbook of Practical Organic Chemistry*; Longman: London, 1970.
- (41) Smith, M. B.; March, J. *March's Advanced Organic Chemistry. Reactions, Mechanisms, and Structure*; John Wiley & sons: New York, USA, 2001.
- (42) Montoneri, E.; Gleria, M.; Ricca, G.; Pappalardo, G. C. *Makromol. Chem.* **1989**, *190*, 191.
- (43) Montoneri, E.; Gleria, M.; Ricca, G.; Pappalardo, G. C. *J. Macromol. Sci., Chem.* **1989**, *A26*, 645.
- (44) Montoneri, E.; Ricca, G.; Gleria, M.; Gallazzi, M. C. *Inorg. Chem.* **1991**, *30*, 150.
- (45) Allcock, H. R.; Fitzpatrick, R. J.; Salvati, L. *Chem. Mater.* **1991**, *3*, 1120.
- (46) Allcock, H. R.; Klingerberg, E. H.; Welker, M. F. *Macromolecules* **1993**, *26*, 5512.
- (47) Allcock, H. R.; Klingenberg, E. H.; Weller, M. P. U.S. US, 5,548,060 (1996), Chem. Abstr. 125, 248884e (1996), assigned to Penn State Research Foundation.
- (48) Montoneri, E.; Casciola, M. *J. Inorg. Organomet. Polym.* **1996**, *6*, 301.
- (49) Montoneri, E.; Boffa, V. In *Inorganic Polymers*; De Jaeger, R., Gleria, M., Eds.; NOVA Science Publishers: Hauppauge, 2007, p 767.
- (50) Allcock, H. R.; Kwon, S. *Macromolecules* **1986**, *19*, 1502.
- (51) Jenkins, A. D.; Ledwith, A. *Reactivity, Mechanism and Structure in Polymer Chemistry*; J. Wiley: London, 1974.
- (52) Austin, P. E.; Riding, G. H.; Allcock, H. R. *Macromolecules* **1983**, *16*, 719.
- (53) Blonsky, P. M.; Shriver, D. F.; Austin, P. E.; Allcock, H. R. *J. Am. Chem. Soc.* **1984**, *106*, 6854.

- (54) Allcock, H. R.; Austin, P. E.; Neenan, T. X.; Sisko, J. T.; Blonsky, P. M.; Shriver, D. F. *Macromolecules* **1986**, *19*, 1508.
- (55) Facchin, G.; Minto, F.; Gleria, M.; Bertani, R.; Bortolus, P. *J. Inorg. Organomet. Polym.* **1991**, *1*, 389.
- (56) Fambri, L.; Minto, F.; Gleria, M. *J. Inorg. Organomet. Polym.* **1996**, *6*, 195.
- (57) Minto, F.; Fontana, G.; Bertani, R.; Facchin, G.; Gleria, M. *J. Inorg. Organomet. Polym.* **1996**, *6*, 367.
- (58) Fontana, G.; Minto, F.; Gleria, M.; Facchin, G.; Bertani, R.; Favero, G. *Eur. Polym. J.* **1996**, *32*, 1273.
- (59) Minto, F.; Fambri, L.; Gleria, M. *Macromol. Chem. Phys.* **1996**, *197*, 3099.
- (60) Caminiti, R.; Gleria, M.; Lipkowitz, K. B.; Lombardo, G. M.; Pappalardo, G. C. *J. Am. Chem. Soc.* **1997**, *119*, 2196.
- (61) Minto, F.; Gleria, M.; Favero, G. *J. Macromol. Sci., Pure Appl. Chem.* **1997**, *A34*, 2177.
- (62) Gleria, M.; Minto, F.; Fontana, G.; Bertani, R.; Facchin, G. *Macromolecules* **1995**, *28*, 4399.
- (63) Gleria, M.; Minto, F.; Doriguzzi, F.; Bertani, R.; Facchin, G.; Tondello, E. *Macromolecules* **1997**, *30*, 4310.
- (64) Gleria, M.; Bolognesi, A.; Porzio, W.; Catellani, M.; Destri, S.; Audisio, G. *Macromolecules* **1987**, *20*, 469.
- (65) Meille, S. V.; Porzio, W.; Bolognesi, A.; Gleria, M. *Makromol. Chem., Rapid Commun.* **1987**, *8*, 43.
- (66) Gleria, M.; Minto, F.; Bortolus, P.; Porzio, W.; Bolognesi, A. *Eur. Polym. J.* **1989**, *25*, 1039.
- (67) Minto, F.; Gleria, M.; Bortolus, P.; Daolio, S.; Facchin, B.; Pagura, C.; Bolognesi, A. *Eur. Polym. J.* **1989**, *25*, 49.
- (68) Gleria, M.; Minto, F.; Bortolus, P.; Porzio, W.; Meille, S. V. *Eur. Polym. J.* **1990**, *26*, 315.
- (69) Gleria, M.; Minto, F.; Flamigni, L.; Bortolus, P. *J. Inorg. Organomet. Polym.* **1992**, *2*, 329.
- (70) Minto, F.; Scoconi, M.; Fambri, L.; Gleria, M.; Bortolus, P.; Pradella, F. *Eur. Polym. J.* **1992**, *28*, 167.

- (71) Minto, F.; Scoponi, M.; Gleria, M.; Pradella, F.; Bortolus, P. *Eur. Polym. J.* **1994**, *30*, 375.
- (72) Gleria, M.; Minto, F.; Scoponi, M.; Pradella, F.; Carassiti, V. *Chem. Mater.* **1992**, *4*, 1027.
- (73) Zeldin, M.; Jo, W. H.; Pearce, E. M. *J. Polym. Sci., Polym. Chem. Ed.* **1981**, *19*, 917.
- (74) Carriedo, G. A.; Fernandez-Catuxo, L.; Garcia-Alonso, F.; Gomez-Elipse, P. *J. Organometallic Chem.* **1995**, *503*, 59.
- (75) Carriedo, G. A.; Fernandez-Catuxo, L.; Garcia Alonso, F. J.; Elipse, P. G.; Gonzalez, P. A.; Sanchez, G. *J. Appl. Polym. Sci.* **1996**, *59*, 1879.
- (76) Gomez, M. A.; Marco, C.; Gomez Fatou, J. M.; Carriedo, G. A.; Garcia Alonso, F. J.; Gomez Elipse, P. *Eur. Polym. J.* **1996**, *32*, 717.
- (77) Carriedo, G. A.; Garcia Alonso, F. J.; Gonzales, P. A. *Macromol. Rapid Commun.* **1997**, *18*, 371.
- (78) Gleria, M.; Minto, F.; Po', R.; Cardi, N.; Fiocca, L.; Spera, S. *Macromol. Chem. Phys.* **1998**, *199*, 2477.
- (79) Fiocca, L.; Po', R.; Lucchelli, E.; Giannotta, G.; Cardi, N.; Minto, F.; Tiso, B.; Bertani, R.; Gleria, M., *Proceedings of the XIV Italian Meeting on Macromolecular Science and Technology*, Salerno, Italy, September 13-16, 1999, p 501.
- (80) Gleria, M.; Minto, F.; Bertani, R.; Tiso, B.; Po', R.; Fiocca, L.; Lucchelli, E.; Giannotta, G.; Cardi, N. *Phosphorus Res. Bull.* **1999**, *10*, 730.
- (81) Gleria, M.; Minto, F.; Galeazzi, A.; Po', R.; Cardi, N.; Fiocca, L.; Spera, S. *Phosphorus, Sulfur and Silicon Relat. Elem.* **1999**, *144-146*, 201.
- (82) Medici, A.; Fantin, G.; Pedrini, P.; Gleria, M.; Minto, F. *Macromolecules* **1992**, *25*, 2569.
- (83) Allcock, H. R.; Kwon, S. *Macromolecules* **1989**, *22*, 75.
- (84) Allcock, H. R. In *Phosphazenes. A Worldwide Insight*; Gleria, M., De Jaeger, R., Eds.; Nova Science Publishers: Hauppauge, 2004; Chapt. 1, p 1.
- (85) Tate, D. P. *J. Polym. Sci., Polym. Symp.* **1974**, *48*, 33.
- (86) Tate, D. P. *Rubber World* **1975**, 41.
- (87) Tate, D. P.; Lohr, D. F. *ACS Polym. Prep.* **1984**, *25(1)*, 283.
- (88) Kyker, G. S.; Antkowiak, T. A. *Rubber Chem. Technol.* **1974**, *47*, 32.

- (89) Critchley, J. P.; Knight, G. J.; Wright, M. M. *Heat-Resistant Polymers*; Plenum Press: New York, 1983, Chapt. 8, p 389.
- (90) Penton, H. R. In *Inorganic and Organometallic Polymers*; Zeldin, M., Wynne, K. J., Allcock, H. R., Eds.; ACS Symposium Series: Washington, DC, USA, 1988; Chapt. 21, Vol. 360, p 277.
- (91) Potin, P.; De Jaeger, R. *Eur. Polym. J.* **1991**, *27*, 341.
- (92) Quinn, E. J.; Dieck, R. L. *J. Fire & Flammability* **1976**, *7*, 5.
- (93) Quinn, E. J.; Dieck, R. L. *J. Fire & Flammability* **1976**, *7*, 358.
- (94) DeEdwardo, A. H.; Zitomer, F.; Stuetz, D.; Singler, R. E.; Macaione, D. *Org. Coat. Prep.* **1976**, *36*, 737.
- (95) DeEdwardo, A. H.; Zitomer, F.; Stackman, R. W.; Kramer, C. E. US Patent, 4,042,561 (1977), Chem. Abstr. 87, 118861f (1977), assigned to Celanese Corp.
- (96) Thompson, J. E.; Reynard, K. A. *J. Appl. Polym. Sci.* **1977**, *21*, 2575.
- (97) Mueller, W. B. *J. Cellular Plastics* **1986**, *22*, 53.
- (98) Allen, C. W. *J. Fire Sci.* **1993**, *11*, 320.
- (99) Allen, C. W.; Hernandez-Rubio, D. In *Phosphazenes. A Worldwide Insight*; Gleria, M., De Jaeger, R., Eds.; Nova Science Publishers, Inc.: Hauppauge, 2004, p 485.
- (100) Quinn, E. J.; Althouse, B. M.; Potin, P., *Proceedings of the Symp. Chem. Comb., Toxicity, MARM*, Millerville, PA., 1988.
- (101) Allcock, H. R. *Phosphorus-Nitrogen Compounds. Cyclic, Linear, and High Polymeric Systems*; Academic Press: New York, 1972, p 358.
- (102) Allcock, H. R. In *Biodegradable Polymers as Drug Delivery Systems*; Chasin, M., Langer, R., Eds.; Marcel Dekker: New York, 1990; Chapt. 5, p 163.
- (103) Scopelianos, A. G., In *Biomed. Polym.*; Shalaby, S. W., Ed.; Hanser: Munich, 1994; p 153.
- (104) Heyde, M.; Schacht, E. In *Phosphazenes: A Worldwide Insight*; Gleria, M., De Jaeger, R., Eds.; Nova Science Publishers, Inc.. Hauppauge, N.Y., 2004; Chapt. 15, p 367.
- (105) Gettleman, L. In *Phosphazenes. A Worldwide Insight*; Gleria, M., De Jaeger, R., Eds.; NOVA Science Publishers: Hauppauge, 2004; Chapt. 16, p 399.

- (106) Gleria, M.; Bortolus, P.; Minto, F.; Flamigni, L., In *Inorganic and Organometallic Polymers with Special Properties*; Laine, R. M., Ed.; Nato ASI Series E: Applied Sciences, 1992; Vol. 206; p 375.
- (107) Bortolus, P.; Gleria, M. *J. Inorg. Organomet. Polym.* **1994**, 4, 1.
- (108) Bortolus, P.; Gleria, M. *J. Inorg. Organomet. Polym.* **1994**, 4, 95.
- (109) Bortolus, P.; Gleria, M. *J. Inorg. Organomet. Polym.* **1994**, 4, 205.
- (110) Gleria, M.; Bortolus, P.; Minto, F. In *Phosphazenes: A Worldwide Insight*; Gleria, M., De Jaeger, R., Eds.; Nova Science Publishers, Inc.. Hauppauge, N.Y., 2004; Chapt. 17, p 415.
- (111) Allcock, H. R. *ACS Polym. Prep.* **1993**, 34(1), 261.
- (112) Hiraoka, H.; Chiong, K. N. *J. Vac. Sci. Technol.* **1987**, B5, 386.
- (113) Stannett, V. T.; Chern, R. T.; Grune, G. L.; Harada, J. *ACS Polym. Prep.* **1991**, 32(2), 34.
- (114) Welker, M. F.; Allcock, H. R.; Grune, G. L.; Chern, R. T.; Stannett, V. T. *Polym. Mater. Sci. Eng.* **1992**, 66, 259.
- (115) Ahn, D. K.; Kang, J. H.; Kim, S. J.; Park, B. S.; Park, C. E.; Park, C. G. *J. Photopolym. Sci. Technol.* **1992**, 5, 67.
- (116) Grune, G. L.; Greer, R. W.; Chern, R. T.; Stannett, V. T., *Proceedings of the Radtech Asia '93 UV/EB Conf. Expo., Conf. Proc.*, Tokyo, Japan, November 10-13, 1993, p 396.
- (117) Welker, M. F.; Allcock, H. R.; Grune, G. L.; Chern, R. T.; Stannett, V. T. *ACS Symp. Ser.* **1994**, 537, 293.
- (118) Grune, G. L.; Greer, R. W.; Chern, R. T.; Stannett, V. T. *J. Macromol. Sci., Pure Appl. Chem.* **1994**, A31, 1193.
- (119) Allcock, H. R.; Desorcie, J. L.; Riding, G. H. *Polyhedron* **1987**, 6, 119.
- (120) Chandrasekhar, V.; Justin Thomas, K. R. *Appl. Organometallic Chem.* **1993**, 7, 1.
- (121) Chandrasekhar, V.; Justin Thomas, K. R. In *Structure and Bonding. Structures and Biological Effects*; Clarke, M. J., Goodenough, J. B., Ibers, J. A., Jørgensen, C. K., Mingos, D. M. P., Neilands, J. B., Palmer, G. A., Reinen, D., Sadler, P. J., Weiss, R., Williams, R. J. P., Eds.; Springer-Verlag: Berlin, Germany, 1993, Vol. 81, p 41.

- (122) Chandrasekhar, V.; Krishnan, V. In *Phosphazenes: A Worldwide Insight*; Gleria, M., De Jaeger, R., Eds.; Nova Science Publishers, Inc.: Hauppauge, N.Y., 2004; Chapt. 34, p 827.
- (123) Golemme, G.; Drioli, E. *J. Inorg. Organomet. Polym.* **1996**, *6*, 341.
- (124) Golemme, G.; Drioli, E. In *Phosphazenes. A Worldwide Insight*; Gleria, M., De Jaeger, R., Eds.; Nova Science Publishers, Inc.: Hauppauge, 2004, p 555.
- (125) Kim, C.; Allcock, H. R. *Macromolecules* **1987**, *20*, 1726.
- (126) Singler, R. E.; Willingham, R. A.; Lenz, R. W.; Furukawa, A.; Finkelman, H. *Macromolecules* **1987**, *20*, 1727.
- (127) Allcock, H. R.; Kim, C. *Macromolecules* **1989**, *22*, 2596.
- (128) Platé, N. A.; Antipov, E. M.; Kulitchikhin, V. G. *Makromol. Chem. Macromol. Symp.* **1990**, *33*, 65.
- (129) Singler, R. E.; Willingham, R. A.; Noel, C.; Friedrich, C.; Bosio, L.; Atkins, E. D. T.; Lenz, R. W. In *Liquid-Crystalline Polymers*; Weiss, R. A., Ober, C. K., Eds.; ACS Symposium Series: Washington, USA, 1990; Chapt. 14, Vol. 435, p 185.
- (130) Allcock, H. R.; Kim, C. *Macromolecules* **1990**, *23*, 3881.
- (131) Singler, R. E.; Willingham, R. A.; Noel, C.; Friedrich, C.; Bosio, L.; Atkins, E. *Macromolecules* **1991**, *24*, 510.
- (132) Dembek, A. A.; Kim, C.; Allcock, H. R.; Devine, R. L. S.; Steier, W. H.; Spangler, C. W. *Chem. Mater.* **1990**, *2*, 97.
- (133) Allcock, H. R.; Dembek, A. A.; Kim, C.; Devine, R. L. S.; Shi, Y.; Steier, W. H.; Spangler, C. W. *Macromolecules* **1991**, *24*, 1000.
- (134) Dembek, A. A.; Allcock, H. R.; Kim, C. H.; Devine, R. L. S.; Steier, W. H.; Shi, Y. Q.; Spangler, C. W. *ACS Symp.Ser.* **1991**, *455*, 258.
- (135) Gleria, M.; Minto, F. Italian Patent, 1,240,644 (1993), assigned to Consiglio Nazionale delle Ricerche.
- (136) Allcock, H. R.; Kim, C. *Macromolecules* **1991**, *24*, 2846.
- (137) Allcock, H. R.; Lavin, K. D.; Tollefson, N. M.; Evans, T. L. *Organometallics* **1983**, *2*, 267.
- (138) Bonsignore, L.; Corda, L.; Maccioni, E.; Podda, G.; Gleria, M. *Gazz. Chim. Ital.* **1991**, *121*, 341.

- (139) Valter, B.; Masar, B.; Janout, V.; Hrudkova, H.; Cefelin, P.; Tur, D. R.; Vinogradova, C. V. *Makromol. Chem.* **1991**, *192*, 1549.
- (140) Blonsky, P. M.; Shriver, D. F.; Austin, P. E.; Allcock, H. R. *Polym. Mater. Sci. Eng.* **1985**, *53*, 118.
- (141) Shriver, D. F.; Farrington, G. C. *Chem. Eng. News* **1985**, *63*, 42.
- (142) Allcock, H. R.; Neenan, X. T. *Macromolecules* **1986**, *19*, 1495.
- (143) Blonsky, P. M.; Shriver, D. F.; Austin, P. E.; Allcock, H. R. *Solid State Ionics* **1986**, *18/19*, 258.
- (144) Tonge, K. M.; Shriver, D. F. *J. Electrochem. Soc.* **1987**, *134*, 269.
- (145) Abraham, K. M.; Alagmir, M.; Perrotti, S. J. *J. Electrochem. Soc.* **1988**, *135*, 535.
- (146) Ratner, M. A.; Shriver, D. F. *Chem. Rev.* **1988**, *88*, 109.
- (147) Bennett, J. L.; Dembek, A. A.; Allcock, H. R.; Heyen, B. J.; Shriver, D. F. *Chem. Mater.* **1989**, *1*, 14.
- (148) Inoue, K.; Kinoshita, K.; Nakahara, H.; Tanigaki, T. *Macromolecules* **1990**, *23*, 1227.
- (149) Abraham, K. M.; Alagmir, M. *Chem. Mater.* **1991**, *3*, 339.
- (150) Allcock, H. R.; Dodge, J. A.; Van Dyke, L. S.; Martin, C. R. *Chem. Mater.* **1992**, *4*, 780.
- (151) Tada, Y.; Sato, M.; Takeno, N.; Kameshima, T.; Nakacho, Y.; Shigehara, K. *Macromol. Chem. Phys.* **1994**, *195*, 571.
- (152) Selvaraj, I. I.; Chaklanobis, S.; Chandrasekhar, V. *J. Electrochem. Soc.* **1995**, *142*, 3434.
- (153) Allcock, H. R.; Napierala, M. E.; Cameron, C. G.; O'Connors, S. J. M. *Macromolecules* **1996**, *29*, 1951.
- (154) Allcock, H. R.; Kuharcik, S. E.; Reed, C. S.; Napierala, M. E. *Macromolecules* **1996**, *29*, 3384.
- (155) Chandrasekhar, V. *Adv. Polym. Sci.* **1998**, *135*, 139.
- (156) Kulkarni, A. R. *Solid State Ionics* **2000**, *136-136*, 549.
- (157) Chen-Yang, Y. W.; Chen, H. C.; Lin, F. L. *ACS Polym. Prep.* **2001**, *42(2)*, 46.
- (158) Allcock, H. R.; Kellam, E. C.; Morford, R. V. U.S. US, 14,616 (2002), Chem. Abstr. 136, 86257 (2002), assigned to The Penn State Research Foundation, USA.

- (159) Urquidi-Macdonald, M.; Castaneda, H.; Cannon, A. M. *Electrochim. Acta* **2002**, *47*, 2495.
- (160) Harrup, M. K.; Wertsching, A. K.; Stewart, F. F. U.S. US, 6,544,690 (2003), Chem. Abstr. 138, 274124 (2003), assigned to United States of America.
- (161) Inoue, K. In *Phosphazenes. A Worldwide Insight*; Gleria, M., De Jaeger, R., Eds.; NOVA Science Publishers: Hauppauge, 2004; Chapt. 22, p 535.
- (162) Coltrain, B. K.; Ferrar, W. T.; Landry, C. J. T.; Molaire, T. R.; Zumbulyadis, N. *Chem. Mater.* **1992**, *4*, 358.
- (163) Facchin, G.; Fantin, G.; Gleria, M.; Guglielmi, M.; Spizzo, F. *ACS Polym. Prep.* **1993**, *34(1)*, 322.
- (164) Guglielmi, M.; Colombo, P.; Brusatin, G.; Facchin, G.; Gleria, M. *J. Sol-Gel Sci. Technol.* **1994**, *2*, 109.
- (165) Facchin, G.; Gleria, M.; Minto, F.; Bertani, R.; Guglielmi, M.; Brusatin, G. *Macromol. Rapid Commun.* **1995**, *16*, 211.
- (166) Brusatin, G.; Guglielmi, M.; De Jaeger, R.; Facchin, G.; Gleria, M.; Musiani, M. *J. Mater. Sci.* **1997**, *32*, 4415.
- (167) Guglielmi, M.; Brusatin, G.; Facchin, G.; Gleria, M. *J. Mater. Res.* **1996**, *11*, 2029.
- (168) Pivin, J. C.; Brusatin, G.; Zalczer, G. *Thin Solid Films* **1996**, *287*, 65.
- (169) Pivin, J. C.; Brusatin, G.; Guglielmi, M.; Facchin, G.; Gleria, M. *Nucl. Instr. and Meth. B* **1996**, *112*, 294.
- (170) Guglielmi, M.; Brusatin, G.; Facchin, G.; Gleria, M.; De Jaeger, R.; Musiani, M. *J. Inorg. Organomet. Polym.* **1996**, *6*, 221.
- (171) Guglielmi, M.; Brusatin, G.; Facchin, G.; Gleria, M. *Appl. Organometallic Chem.* **1999**, *13*, 339.
- (172) Brusatin, G.; Gleria, M.; Dirè, S.; Facchin, G.; Guglielmi, M. In *Phosphazenes. A Worldwide Insight*; Gleria, M., De Jaeger, R., Eds.; NOVA Science Publishers: Hauppauge, 2004; Chapt. 19, p 467.
- (173) Allcock, H. R.; Brennan, D. J.; Allen, R. W. *Macromolecules* **1985**, *18*, 139.
- (174) Allcock, H. R.; Brennan, D. J.; Graaskamp, J. M.; Parvez, M. *Organometallics* **1986**, *5*, 2434.
- (175) Allcock, H. R.; Brennan, D. J.; Graaskamp, J. N. *Macromolecules* **1988**, *21*, 1.

- (176) Allcock, H. R.; Brennan, D. J.; Dunn, B. S.; Parvez, M. *Inorg. Chem.* **1988**, 27, 3226.
- (177) Allcock, H. R.; Brennan, D. J. *J. Organometallic Chem.* **1988**, 341, 231.
- (178) Allcock, H. R.; Brennan, D. J.; Dunn, B. S. *Macromolecules* **1989**, 22, 1534.
- (179) Allcock, H. R.; Coggio, W. D.; Archibald, R. S.; Brennan, D. J. *Macromolecules* **1989**, 22, 3571.
- (180) Wisian-Neilson, P.; Islam, M. S. *Macromolecules* **1989**, 22, 2026.
- (181) Brennan, D. J.; Graaskamp, J. M.; Dunn, B. S.; Allcock, H. R., In *Inorg. Synth.*; Allcock, H. R., Ed.; Wiley: New York, USA, 1989; Vol. 25; p 60.
- (182) Allcock, H. R.; Kuharcik, S. E. *J. Inorg. Organomet. Polym.* **1995**, 5, 307.
- (183) Allcock, H. R. In *Ultrastructure Processing of Advanced Ceramics*; MacKenzie, J. D., Ulrich, D. R., Eds.; Wiley Interscience: New York, 1988; Chapt. 53, p 705.
- (184) Allcock, H. R.; Welker, M. F.; Parvez, M. *Chem. Mater.* **1992**, 4, 296.
- (185) Kotaka, T.; Adachi, K. U.S. US, 4,933,479 (1990), Chem. Abstr. **113**, 222935z (1990), assigned to Idemitsu Petrochemical Co., Ltd.
- (186) Ouyang, M.; Gong, K. *Gaofenzi Tongbao* **1993**, 90, 105, Chem. Abstr. 122, 51179g (1995).
- (187) Maruyama, I.; Fujiwara, H.; Ito, Z.; Shigematsu, H. Jpn. Kokai Tokkyo Koho JP, 02 45,534 [90 45,534] (1990), Chem. Abstr. 113, 116130y (1990), assigned to Maruzen Petrochemical Co., Ltd.
- (188) Riesel, L., unpublished results.
- (189) Allcock, H. R.; Allen, R. W.; O'Brien, J. P. *J. Am. Chem. Soc.* **1977**, 99, 3984.
- (190) Allcock, H. R.; Allen, R. W.; O'Brien, J. P. US Patent, 4,151,185 (1979), Chem. Abstr. 91, 39646u (1979), assigned to Research Corp.
- (191) Alix, A. J. P.; Manfait, M.; Labarre, J. F. *J. Chim. Phys.* **1982**, 79, 129.
- (192) Labarre, J. F.; Guerch, G.; Sournies, F.; Spreafico, F.; Filippeschi, S. *J. Mol. Struc.* **1984**, 117, 59.
- (193) Brandt, K.; Jedlinski, Z. *Makromol. Chem. Suppl.* **1985**, 9, 169.
- (194) Labarre, J. F.; Guerch, G.; Levy, G.; Sournies, F. U.S. US, 4,595,682 (1986).
- (195) Allen, C. W. In *The Chemistry of Inorganic Homo- and Hetero-Cycles*; Haiduc, I., Sowerby, D. B., Eds.; Academic Press: London, 1987; Chapt. 20, Vol. 2, p 501.

- (196) Labarre, J. F.; Sournies, F. Eur. Pat. Appl. EP, 240,392 (1987), assigned to Centre National de la Recherche Scientifique (CNRS).
- (197) Ouassini, A.; De Jaeger, R.; Hilali, S.; Fournier, C.; Hecquet, B. *Eur. J. Med. Chem.* **1988**, 23, 347.
- (198) Labarre, J. F.; Sournies, F.; Guerch, G.; El Bakili, A.; Bonnet, J. P.; Castera, P.; Faucher, J. P.; Graffeuil, M. *Phosphorus, Sulfur and Silicon Relat. Elem.* **1989**, 41, 167.
- (199) Van de Grampel, J. C. *Coord. Chem. Rev.* **1992**, 112, 247.
- (200) Baek, H.; Cho, Y.; Lee, C. O.; Sohn, Y. S. *Anti-Cancer Drugs* **2000**, 11, 715.
- (201) Sohn, Y. S.; Song, S. C.; Lee, S. B. U.S. US, 6,333,422 (2001), assigned to Korea Institute of Science and Technology.
- (202) *Chem. Week* **1962**, Dec. 14, 83.
- (203) Krishnamurthy, S. S.; Sau, A. C. *Adv. Inorg. Chem. Radiochem.* **1978**, 21, 41.
- (204) Haiduc, I. *The Chemistry of the Inorganic Ring Systems*; Wiley-Interscience: London, 1970; Vol. 2, Chapt. 5, p 623.
- (205) Vanek, W. *Angew. Chem. Int. Ed. Engl.* **1969**, 8, 617.
- (206) Conesa, A. P.; Albagnac, G.; Brun, G. *C.R. Acad. Agric. Fr.* **1973**, 59, 1457.
- (207) Conesa, A. P. *C.R. Acad. Agric. Fr.* **1974**, 60, 1353.
- (208) Barel, D.; Black, C. A. *Agron. J.* **1979**, 71, 15.
- (209) Calancea, L.; Chiriac, M. *Isotopenpraxis Environ. Health Stud.* **1993**, 29, 357.
- (210) Allcock, H. R. *Acc. Chem. Res.* **1978**, 11, 81.
- (211) Allcock, H. R. In *Inclusion Compounds*; Atwood, J. L., Davies, J. D. E., MacNicol, D. D., Eds.; Academic Press: London, UK, 1984; Chapt. 8, Vol. 1, p 351.
- (212) Chandrasekhar, V.; Muralidhara, M. G. R.; Selvaraj, I. I. *Heterocycles* **1990**, 31, 2231.
- (213) Ripmeester, J. A.; Ratcliffe, C. I. In *Inclusion compounds*; Atwood, J. L., Davies, J. E. D., MacNicol, D. D., Eds.; Oxford University Press: Oxford, UK, 1991, Vol. 5, p 37.
- (214) Allcock, H. R.; Silverberg, E. N.; Dudley, G. K. *Macromolecules* **1994**, 27, 1033.

- (215) Kobayashi, T.; Isoda, S.; Kubono, K. In *Comprehensive Supramolecular Chemistry*; MacNicol, D. D., Toda, F., Bishop, R., Eds.; Pergamon, UK, 1996; Chapt. 13, Vol. 6, p 399.
- (216) Sozzani, P.; Comotti, A.; Simonutti, R.; Bracco, S. In *Phosphazenes: A Worldwide Insight*; Gleria, M., De Jaeger, R., Eds.; Nova Science Publishers, Inc.. Hauppauge, N.Y., 2004; Chapt. 37, p 909.
- (217) Corda, L.; Anchisi, C.; Podda, G.; Traldi, P.; Gleria, M. *Heterocycles* **1986**, *24*, 2821.
- (218) Podda, G. *Gazz. Chim. Ital.* **1988**, *118*, 397.
- (219) Landini, D.; Maia, A.; Podda, G.; Secci, D.; Yan, Y. M. *J. Chem. Soc. Dalton Trans.* **1992**, 1721.
- (220) Bullitta, M. P.; Maccioni, E.; Corda, L.; Podda, G. *J. Heterocyclic Chem.* **1993**, *30*, 93.
- (221) Varnek, A. A.; Maia, A.; Landini, D.; Gamba, A.; Morosi, G.; Podda, G. *J. Phys. Org. Chem.* **1993**, *6*, 113.
- (222) Scheidecker, S.; Semenzin, D.; Etemad-Moghadam, G.; Sournies, F.; Koenig, M.; Labarre, J. F. *Phosphorus, Sulfur, and Silicon* **1993**, *80*, 85.
- (223) Zanin, B.; Scheidecker, S.; Sournies, F.; Labarre, J. F. *J. Mol. Struct.* **1991**, *246*, 133.
- (224) Valerio, C.; Labarre, M. C.; Labarre, J. F. *J. Mol. Struct.* **1993**, *299*, 171.
- (225) Segues, B.; Sournies, F.; Crasnier, F.; Labarre, J. F. *Phosphorus, Sulfur, and Silicon* **1994**, *88*, 123.
- (226) Gleria, M.; Minto, F. Italian Patent, 1,205,540 (1989), assigned to Consiglio Nazionale delle Ricerche.
- (227) Fantin, G.; Medici, A.; Fogagnolo, M.; Gleria, M.; Minto, F. Italian Patent, 1,265,090 (1996), assigned to Consiglio Nazionale delle Ricerche.
- (228) Gleria, M.; Facchin, G.; Bertani, R.; Minto, F. Italian, 1,270,949 (1997), assigned to The National Research Council of Italy.
- (229) Pond, D. M.; Wang, R. S. H. U.S., 3,936,418 (1976), Chem. Abstr. 84, 151551r (1976), assigned to Eastman Kodak Co.
- (230) Gleria, M.; Paolucci, G.; Minto, F.; Lora, S. *Chem. Ind. (Milan)* **1982**, *64*, 479.
- (231) Wiezer, H. Europ. Pat. Appl. EP, 64 752 (1982), Chem. Abstr. 98, 108403w (1983), assigned to Hoechst A.-G.

- (232) Gleria, M.; Minto, F.; Bortolus, P.; Lora, S. Italian, 1,176,618 (1987), assigned to The National Research Council of Italy.
- (233) Bortolus, P.; Busulini, L.; Lora, S.; Minto, F.; Pezzin, G. Italian Patent, 1,196,213 (1988), assigned to Consiglio Nazionale delle Ricerche.
- (234) Inoue, K.; Takahata, H.; Tanigaki, T. *J. Appl. Polym. Sci.* **1993**, *50*, 1857.
- (235) Inoue, K. Jpn. Kokai Tokkyo Koho JP, 06 135,977 [94 135,977] (1994), Chem. Abstr. 121, 179870a (1994), assigned to Nippon Shoe.
- (236) Wang, R. H. S.; Irick, G. US Patent, 4,080,361 (1978), Chem. Abstr. 89, 111121x (1978), assigned to Eastman Kodak.
- (237) Goins, D. E.; Li, H. M. U.S. US, 5,105,001 (1992), Chem. Abstr. 117, 61662y (1992), assigned to Ethyl Corp.
- (238) Sournies, F.; Labrousse, L.; Graffeuil, M.; Crasnier, F.; Faucher, J. P.; Labarre, M. C.; Labarre, F. *Phosphorus, Sulfur, and Silicon* **1994**, *89*, 47.
- (239) Sournies, F.; Fouga, C.; Graffeuil, M.; Faucher, J. P.; Crasnier, F.; Labarre, M. C.; Labarre, J. F. *Phosphorus, Sulfur, and Silicon* **1994**, *90*, 159.
- (240) Sournies, F.; Crasnier, F.; Graffeuil, M.; Faucher, J. P.; Lahana, R.; Labarre, M. C.; Labarre, F. *Angew. Chem. Int. Ed. Engl.* **1995**, *34*, 578.
- (241) Caminade, A. M.; Majoral, J. P. In *Phosphazenes: A Worldwide Insight*; Gleria, M., De Jaeger, R., Eds.; Nova Science Publishers: Hauppauge, USA, 2004; Chapt. 30, p 713.
- (242) Caminade, A. M.; Majoral, J. P. In *Inorganic Polymers*; Nova Science Publishers: Hauppauge, USA, 2007, p 809.
- (243) Exarhos, G. J. *NTIS Special Publ.* **1990**, *801*, 324.
- (244) Fewell, L. L. *ACS Polym. Prep.* **1991**, *32(1)*, 134.
- (245) Neenan, T. X.; Allcock, H. R. *Biomaterials* **1982**, *3*, 78.
- (246) Allcock, H. R.; Fitzpatrick, R. J.; Salvati, L. *Chem. Mater.* **1992**, *4*, 769.
- (247) Allcock, H. R.; Morrissey, C. T.; Way, W. K.; Winograd, N. *Chem. Mater.* **1996**, *8*, 2730.
- (248) Allcock, H. R.; Smith, D. E. *Chem. Mater.* **1995**, *7*, 1469.
- (249) Ohkawa, K.; Matsuki, T.; Saiki, N. U.S. US, 4,959,442 (1990), Chem. Abstr. 114, 83683y (1991), assigned to Teijin Ltd.
- (250) Lora, S.; Palma, G.; Bozio, R.; Caliceti, P.; Pezzin, G. *Biomaterials* **1993**, *14*, 430.

- (251) Kolich, C. H.; Klobucar, W. D.; Books, J. T. U.S. US, 4,945,139 (1990), Chem. Abstr. 113, 154152q (1990), assigned to Ethyl Corp.
- (252) Allcock, H. R.; Fitzpatrick, R. J.; Salvati, L. *Chem. Mater.* **1991**, 3, 450.
- (253) Matsuki, T.; Saiki, N.; Emi, S. Eur. Pat. Appl. EP, 425,268 (1991), Chem. Abstr. 115, 227837v (1991), assigned to Teijin Limited.
- (254) Matsuki, T.; Saiki, N.; Emi, S. U.S. US, 5,380,658 (1995), Chem. Abstr. 115, 227837 (1991), assigned to Teijin Ltd.
- (255) Matsuki, T.; Saiki, N.; Emi, S. U.S. US, 5,268,287 (1993), Chem. Abstr. 115, 227837 (1991), assigned to Teijin Ltd.
- (256) Allcock, H. R.; Rutt, J. S.; Fitzpatrick, R. J. *Chem. Mater.* **1991**, 3, 442.
- (257) Allcock, H. R.; Silverberg, E. N.; Nelson, C. J.; Coggio, W. D. *Chem. Mater.* **1993**, 5, 1307.
- (258) Spitaleri, A.; Pertici, P.; Scalera, N.; Vitulli, G.; Hoang, M.; Turney, T. W.; Gleria, M. *Inorg. Chim. Acta* **2003**, 352, 61.
- (259) Pertici, P.; Vitulli, G.; Salvatori, P.; Pitzalis, E.; Gleria, M. In *Phosphazenes: A Worldwide Insight*; Gleria, M., De Jaeger, R., Eds.; Nova Science Publishers, Inc.. Hauppauge, N.Y., 2004; Chapt. 26, p 621.
- (260) Adams, B. E.; Hansel, R. D.; Quinn, E. J. US Patent, 4,145,479 (1979), Chem. Abstr. 90, 206024c (1979), assigned to Armstrong Cork Co.
- (261) Adams, E. B.; Quinn, E. J.; Rodger, W. R. Brit. UK Pat. Appl. GB, 2,046,627 (1980), assigned to Armstrong Cork Co.
- (262) Dez, I.; De Jaeger, R. *J. Appl. Polym. Sci.* **2003**, 89, 1925.
- (263) Allcock, H. R.; Fitzpatrick, R. J.; Visscher, K.; Salvati, L. *Chem. Mater.* **1992**, 4, 775.
- (264) Pemberton, L.; De Jaeger, R. *Chem. Mater.* **1996**, 8, 1391.
- (265) Dez, I.; De Jaeger, R. *Macromolecules* **1997**, 30, 8262.
- (266) Pemberton, L.; De Jaeger, R.; Gengembre, L. *J. Appl. Polym. Sci.* **1998**, 69, 1965.
- (267) Tsubokawa, N.; Tsuchida, H. *J. Macromol. Sci., Chem.* **1992**, A29, 311.
- (268) Grunze, M.; Welle, A. PCT Int. Appl. WO, 99 16,477 (1999), Chem. Abstr. 130, 272061h (1999), assigned to Universität Heilderberg.
- (269) Grunze, M. PCT Int. Appl. WO, 01 70,296 (2001), Chem. Abstr. 135, 262311 (2001), assigned to Polyzenix GmbH, Germany.

- (270) Grunze, M.; Gries, C. PTC Int. Appl. WO, 01 80919 (2001), assigned to Universität Hidelberg.
- (271) Grunze, M.; Welle, A. U.S. US, 2002 54851 (2002).
- (272) Grunze, M. PTC Int. Appl. WO, 02 64,666 (2002).
- (273) Grunze, M.; Tur, D. R.; Pertsin, A. Ger. Offen. DE, 10,113,971 (2002).
- (274) Grunze, M.; Tur, D.; Pertsin, A. PCT Int. Appl. WO, 2002 77,073 (2002), Chem. Abstr. 137, 264178 (2002), assigned to Polyzenix GmbH, Germany.
- (275) Perrin, D. D.; Armarego, W. L. F.; Perrin, D. R. *Purification of Laboratory Chemicals*; Pergamon Press: Oxford, UK, 1980.
- (276) Helioui, M.; De Jaeger, R.; Puskaric, E.; Heubel, J. *Makromol. Chem.* **1982**, *183*, 1137.
- (277) D'Halluin, G.; De Jaeger, R.; Chambrette, J. P.; Potin, P. *Macromolecules* **1992**, *25*, 1254.
- (278) De Jaeger, R.; Potin, P. In *Phosphazenes. A Worldwide Insight*; Gleria, M., De Jaeger, R., Eds.; Nova Science Publishers: Hauppauge., 2004; Chapt. 2, p 25.
- (279) De Jaeger, R.; Lacherai, A.; Potin, P. Fr. Demande FR, 2,697,008 (1994), Chem. Abstr. 121, 60735v (1994), assigned to Elf Atochem S.A.
- (280) Fritz, J. S.; King, J. N. *Anal. Chem.* **1976**, *48*, 570.
- (281) Davies, J. A.; Sylvain, D.; Pikerton, A. A. *Inorg. Chem.* **1991**, *30*, 2380.
- (282) Frye, J. S.; Maciel, G. E. *J. Magn. Resonance* **1982**, *48*, 125.
- (283) *Handbook of XPS*; Moulder, J. F.; Stickle, W. F.; Sobol, P. E.; Bomben, K. D., Eds.; Perkin-Elmer Corp.: Eden Prairie, MN, USA, 1992.
- (284) **1998**, Bruker, SMART 5.0 and SAINT 4.0 for Windows NT, Area Detector Control and Integration Software, Bruker Analytical X-ray System Inc., Madison, WI.
- (285) Sheldrick, G. M. **1996**, SADABS: Program for Empirical Absorption Correction of Area Detector Data, University of Göttingen, Göttingen, Germany.
- (286) Burla, M. C.; Camalli, M.; Carrozzini, B.; Cascarano, G. L.; Giacovazzo, C.; Polidori, G.; Spagna, R. *J. Appl. Crystallogr.* **2003**, *36*, 1103.
- (287) Sheldrick, G. M. **1997**, SHELXL-97: Program for Refinement of Crystal Structures, University of Göttingen, Göttingen, Germany.

- (288) Car, R.; Parrinello, M. *Phys. Rev. Lett.* **1985**, *55*, 2471, we have used the code CPMD, developed by Hutter J. *et al.* at MPI für Festkörperforschung and IBM Research Laboratory (see <http://www.cpmc.org>).
- (289) Becke, A. D. *Phys. Rev. A* **1998**, *38*, 3098.
- (290) Lee, C.; Yang, W.; Parr, R. C. *Phys. Rev. B* **1988**, *37*, 785.
- (291) Costanzo, F.; C., S.; Silvestrelli, P. L.; Ancillotto, F. *J. Phys. Chem. B* **2003**, *107*, 10209.
- (292) Costanzo, F.; Silvestrelli, P. L.; Ancillotto, F. *J. Phys. Chem. B* **2005**, *109*, 819.
- (293) Sorescu, D. C.; Jordan, K. D. *J. Phys. Chem. B* **2000**, *104*, 8259.
- (294) Troullier, N.; Martins, J. *Phys. Rev. B* **1991**, *43*, 1993.
- (295) Hutter, J.; Luthi, H. P.; Parrinello, M. *Comp. Mater. Sci.* **1994**, *2*, 244.
- (296) Henkelman, G.; Uberuaga, B. P.; Jonsson, H. *J. Chem. Phys.* **2000**, *113*, 9901.
- (297) <http://www.sissa.it/sbraccia/gNEB.d/>.
- (298) <http://www.sissa.it/cm/thesis/2005/sbraccia.pdf>.
- (299) Carriedo, G. A.; Fernandez-Catuxo, L.; Garcia Alonso, F. J.; Gomez-Elipse, P.; Gonzalez, P. A. *Macromolecules* **1996**, *29*, 5320.
- (300) Dez, I.; Levalois-Mitjaville, J.; Grützmacher, H.; Gramlich, V.; De Jaeger, R. *Eur. J. Inorg. Chem.* **1999**, 1673.
- (301) Schneider, A.; Kairies, S.; Rose, K. *Monatsch. Chem.* **1999**, *130*, 89.
- (302) Kobayashi, S.; Mizutani, T.; Saegusa, T. *Makromol. Chem.* **1984**, *185*, 441.
- (303) Bertani, R.; Fambri, L.; Fiocca, L.; Giannotta, G.; Gleria, M.; Po', R.; Scalabrin, S.; Tondello, E.; Venzo, A. *J. Inorg. Organomet. Polym. Mater.* **2007**, *17*, 387.
- (304) Gleria, M.; Minto, F.; Tiso, B.; Bertani, R.; Tondello, E.; Po, R.; Fiocca, L.; Lucchelli, E.; Giannotta, G.; Cardi, N. *Design. Monomers Polym.* **2001**, *4*, 219.
- (305) Gimblett, F. G. R. *Plast. Inst. (London) Trans. J.* **1960**, *28*, 65.
- (306) Emsley, J.; Udy, P. B. *Polymer* **1972**, *13*, 593.
- (307) Barreca, D.; Djanic, G.; Tondello, E.; Bertani, R.; Gleria, M. Italian Patent, PD 000242 (2002).
- (308) Feakins, D.; Last, W. A.; Neemuchwala, N.; Shaw, R. A. *Chem. Ind. (London)* **1963**, 164.
- (309) Pollard, F. H.; Nickless, G.; Warrender, R. W. *J. Chromatogr.* **1962**, *9*, 485.
- (310) Allcock, H. R.; Gardner, J. E.; Smeltz, K. M. *Macromolecules* **1975**, *8*, 36.

- (311) De Ruiter, B.; Winter, H.; Wilting, T.; Van de Grampel, J. C. *J. Chem. Soc. Dalton Trans.* **1984**, 1207.
- (312) Alekseiko, L. N.; Gorchakov, V. V.; Ivanov, Y. V.; Murashov, D. A.; Rozanov, I. A. *Zh. Neorg. Chim.* **1989**, 34, 1958, Russ. J. Inorg. Chem. 1989, 34, 1113, Chem. Abstr. 112, 43485k (1990).
- (313) Allcock, H. R.; Brennan, D. J.; Whittle, R. R. *Heteroatom Chem.* **1996**, 7, 67.
- (314) Dewar, M. J. D.; Zoeibisch, E. G.; Healey, E. F.; Stewart, J. P. *J. Am. Chem. Soc.* **1985**, 107, 3902.
- (315) Stewart, J. P. *Journal of Computational Chemistry* **1989**, 10, 209.
- (316) Schulz, A.; Thormählen, M.; Müller, H. C. *Internet Electron. J. Mol. Des.* **2003**, 2, 653.
- (317) Wilson, A.; Carrol, D. F. *J. Chem. Soc.* **1960**, 2548.
- (318) Bullen, G. J. *J. Chem. Soc. A* **1971**, 1450.
- (319) Luaña, V.; Pendas, A. M.; Costales, A.; Carriedo, G. A.; Garcia Alonso, F. J. *J. Phys. Chem. A* **2001**, 105, 5280.
- (320) Moller, C.; Plesset, M. S. *Phys. Rev.* **1934**, 46, 618.
- (321) Bartlett, R. J. *Ann. Rev. Phys. Chem.* **1981**, 32, 359.
- (322) Elaiss, A.; Vergoten, G.; Dhamelinourt, P.; Becquet, R. *Electr. J. Theor. Chem.* **1997**, 2, 11.
- (323) Gabler, D. G.; Haw, J. F. *Inorg. Chem.* **1990**, 29, 4018.
- (324) Mochel, V. D.; Cheng, T. C. *Macromolecules* **1978**, 11, 176.
- (325) Shaw, R. A. *Phosphorus and Sulfur* **1978**, 4, 101.
- (326) Iler, R. K. *The Chemistry of Silica*; J. Wiley & Sons: New York, USA, 1979.
- (327) Brinker, C. J.; Scherer, G. W. *Sol-Gel Science. The Physics and Chemistry of Sol-Gel Processing*; Wiley: New York, USA, 1990.
- (328) Zhuravlev, L. T. *Colloid Surface* **2000**, A 173, 1.
- (329) Vassileva, P.; Krastev, V.; Lakov, L.; Peshev, O. *Journal of Materials Science* **2004**, 39, 3201.
- (330) Dake, L. S.; Baer, D. R.; Ferris, K. F.; Friedrich, D. M. *Journal of Electron Spectroscopy* **1990**, 51, 439.
- (331) Green, B.; Ridley, D. C.; Sherwood, P. M. A. *J. Chem. Soc. Dalton Trans.* **1973**, 1042.

- (332) Pelavin, M.; Hendrickson, D. N.; Hollander, J. M.; Jolly, W. L. *J. Phys. Chem.* **1970**, *74*, 1116.
- (333) Brow, R. K.; Peng, Y. B.; Day, D. E. *J. Non-Cryst. Solids* **1990**, *126*, 231.
- (334) Muñoz, F.; Pascual, L.; Durán, A.; Montagne, L.; Palavit, G.; Berojan, R.; Marchand, R. *J. Non-Cryst. Solids* **2003**, *324*, 142.
- (335) Wang, B.; B.S., K.; Sales, B. C.; Bates, J. B. *J. Non-Cryst. Solids* **1995**, *183*, 297.
- (336) Day, D. E. *J. Non-Cryst. Solids* **1989**, *112*, 7.
- (337) Marchand, R.; Agliz, D.; Boukbir, L.; Quemerais, A. *J. Non-Cryst. Solids* **1988**, *103*, 35.
- (338) Hendrickson, D. N.; Hollander, J. M.; W.L., J. *Inorg. Chem.* **1969**, *8*, 2642.
- (339) Zhu, W. M.; Weil, E. D.; Mukhopadhyay, S. *J. Appl. Polym. Sci.* **1996**, *62*, 2267.
- (340) Weil, E. D.; Zhu, W. M.; Patel, N.; Mukhopadhyay, S. M. *Polym. Degrad. Stab.* **1996**, *54*, 125.
- (341) Zhivukhin, S. M.; Tolstoguzov, V. B.; Ivanov, A. I. *Russ. J. Inorg. Chem.* **1962**, *7*, 1134.
- (342) Dwight, D. W.; McGrath, J. E.; Beck, A. R.; Riffle, J. S. *ACS Polym. Prep.* **1979**, *20(1)*, 702.
- (343) Cheng, T. C.; Mochel, V. D.; Adams, H. E.; Longo, T. F. *Macromolecules* **1980**, *13*, 158.
- (344) Maggioni, G.; Quaranta, A.; Negro, E.; Carturan, S.; Della Mea, G. *Chem. Mater.* **2004**, *16*, 2394.
- (345) Gleria, M.; Audisio, G.; Daolio, S.; Traldi, P.; Vecchi, E. *Macromolecules* **1984**, *17*, 1230.
- (346) Allcock, H. R.; Kugel, R. L.; Valan, K. J. *Inorg. Chem.* **1966**, *5*, 1709.
- (347) Dumont, D.; Bougeard, D. *Comput. Theor. Polymer Sci.* **1999**, *9*, 89.
- (348) Osada, Y.; Hashidzume, M.; Tsuchida, E.; Bell, A. T. *Nature* **1980**, *286*, 693.
- (349) Klein, A. J.; Bell, A. T.; Soong, D. S. *Macromolecules* **1987**, *20*, 782.
- (350) Grunze, M.; Schrenk, M. G. Ger. Offen. DE, 19,613,048 (1996), Chem. Abstr. 125, 285036a (1996).
- (351) Welle, A.; Grunze, M. *Proc. 19th Annu. Meet. Adhes. Soc.* **1996**, 432, Chem. Abstr. 127, 140507 (1997).

- (352) Grunze, M.; Welle, A.; Tur, D. R. *Annu. Tech. Conf. - Soc. Plast. Eng.* **1998**, 56 (Vol. 3), 2713.
- (353) Welle, A.; Grunze, M.; Tur, D. *Mater. Res. Soc. Symp. Proc.* **1998**, 489, 139.
- (354) Schuessler, A.; Grunze, M.; Denk, R. PCT Int. Appl. WO, 2003 15,719 (2003), Chem. Abstr. 138, 193324 (2003), assigned to Polyzenix G.m.b.H.; Euroflex Schuessler G.m.b.H., Germany.
- (355) *Photochromism. Molecules and Systems*; Dürr, H.; Bouas-Laurent, H., Eds.; Elsevier: Amsterdam, 1990.
- (356) Irie, M. *Pure Appl. Chem.* **1990**, 62, 1495.
- (357) Nitschke, M.; Hollander, A.; Mehdorn, F.; Behnisch, J.; Meichsner, J. *J. Appl. Polym. Sci.* **1996**, 59, 119.
- (358) Hegemann, D.; Brunner, H.; Oehr, C. *Nucl. Instrum. Methods Phys. Res., Sect. B* **2003**, 208, 281.
- (359) Guruvenket, S.; Mohan Rao, G.; Komath, M.; Raichur, A. M. *Applied Surface Science* **2004**, 236, 278.
- (360) Tajima, S.; Komvopoulos, K. *J. Phys. Chem. B* **2005**, 109, 17623.
- (361) France, R. M.; Short, R. D. *Langmuir* **1998**, 14, 4827.
- (362) Atkins, P. W. *Physical Chemistry*; Oxford University Press: Oxford, UK, 1998.
- (363) Martin, A. R.; Manolache, S.; Denes, F. S.; Mattoso, L. H. C. *J. Appl. Polym. Sci.* **2002**, 85, 2145.
- (364) Wickson, B. M.; Brash, J. L. *Colloid Surface A* **1999**, 156, 201].
- (365) Yip, J.; Chan, K.; Sin, K. M.; Lau, K. S. *J. Appl. Surf. Sci.* **2003**, 205, 151.
- (366) Davies, M. C.; Lynn, R. A. P.; Hearn, J.; Paul, A. J.; Vickerman, J. C.; Watts, J. F. *Langmuir* **1996**, 12, 3866.
- (367) Ariza, M. J.; Castellon, E. R.; Rico, R.; Benavente, J.; Munoz, M.; Oleinikova, M. J. *Colloid Interface Sci.* **2000**, 226, 151.
- (368) Seto, F.; Muraoka, Y.; Sakamoto, N.; Kishida, A.; Akashi, M. *Angew. Makromol. Chem.* **1999**, 266, 56.
- (369) Suh, T. S.; Joo, C. K.; Kim, J. C.; Lee, M. S.; Lee, H. K.; Choe, B. J. H. *J. Appl. Polym. Sci.* **2002**, 85, 2361.
- (370) Fewell, L. L. *J. Appl. Polym. Sci.* **1990**, 41, 391.
- (371) Boyd, R. H.; Kesner, L. *J. Am. Chem. Soc.* **1977**, 99, 4248.
- (372) Giglio, E.; Pompa, F.; Ripamonti, A. *J. Polym. Sci.* **1962**, 59, 293.

- (373) Allcock, H. R.; Arcus, R. A. *Macromolecules* **1979**, *12*, 1130.
- (374) Silverstein, R. M.; Webster, F. X. *Spectrometric Identification of Organic Compounds*; John Wiley & Sons Inc.: New York, 1998.
- (375) *Poly(ethylene glycol): Chemistry and Biological Applications*; Harris, J. M.; Zalipsky, S., Eds.; Oxford University Press: Oxford, UK, 1999.
- (376) Christova, D.; Ivanova, S. D.; Velichkova, R. S.; Tzvetkova, P.; Mihailova, P.; Lakov, L.; Peshev, O. *Design. Monomers Polym.* **2001**, *4*, 329.
- (377) Innocenzi, P.; Brusatin, G.; Guglielmi, M.; Bertani, R. *Chem. Mater.* **1999**, *11*, 1672.
- (378) Innocenzi, P.; Brusatin, G.; Babonneau, F. *Chem. Mater.* **2000**, *12*, 3726.
- (379) Innocenzi, P.; Sassi, A.; Brusatin, G.; Guglielmi, M.; Favretto, D.; Bertani, R.; Venzo, A.; Babonneau, F. *Chem. Mater.* **2001**, *13*, 3635.
- (380) Spectral Database for Organic Compounds SDBS, <http://www.aist.go.jp/RIODB/SDBS/>.
- (381) Krishnamurthy, S. S.; Woods, M. *Annu. Rep. NMR Spectrosc.* **1987**, *19*, 175.
- (382) Allen, C. W. In *Phosphorus - 31 NMR Spectral Properties in Compound Characterization and Structural Analysis*; Quin, L. D., Verkade, J. G., Eds.; V C H Publishers: 220 E 23RD St/Suite 909/New York/NY 10010, 1994, p 103.
- (383) Turi, E. A. *Thermal Characterization of Polymeric Materials*; Academic Press: San Diego CA, USA, 1997.
- (384) Nielsen, L. E.; Landel, R. F. *Mechanical Properties of Polymers and Composites*; Marcel Dekker: New York, USA, 1994.
- (385) Frump, J. A. *Chem. Rev.* **1971**, *71*, 483.
- (386) Litt, M.; Levy, A.; Herz, J. *J. Macromol. Sci., Chem.* **1975**, *A9*, 703.
- (387) Percec, V.; Nava, H.; Rodriguez-Parada, J. M. In *Advances in Polymer Synthesis*; Culberstone, B. M., McGrath, J. E., Eds.; Plenum Press: New York, 1985, p 235.
- (388) Kobayashi, S. *Prog. Polym. Sci.* **1990**, *15*, 751.
- (389) Gant, T. G.; Meyers, A. I. *Tetrahedron* **1994**, *50*, 2297.
- (390) Aoi, K.; Okada, M. *Prog. Polym. Sci.* **1996**, *21*, 151.
- (391) Culberstone, B. M. *Prog. Polym. Sci.* **2002**, *27*, 579.
- (392) Inata, H.; Matsumura, S. *J. Appl. Polym. Sci.* **1985**, *30*, 3325.
- (393) Inata, H.; Matsumura, S. *J. Appl. Polym. Sci.* **1986**, *32*, 5193.

- (394) Inata, H.; Matsumura, S. *J. Appl. Polym. Sci.* **1987**, *33*, 3069.
- (395) Sano, Y. *J. Polym. Sci., Polym. Chem. Ed.* **1989**, *27*, 2749.
- (396) Cardi, N.; Po', R.; Giannotta, G.; Occhiello, E.; Garbassi, F.; Messina, G. *J. Appl. Polym. Sci.* **1993**, *50*, 1501.
- (397) Po', R.; Abis, L.; Fiocca, L.; Mansani, R. *Macromolecules* **1995**, *28*, 5699.
- (398) Po', R.; Cardi, N.; Gennaro, A.; Giannotta, G.; Occhiello, E. Eur. Pat. Appl. EP, 583,807 (1993), assigned to Enichem S.p.A.
- (399) Po', R.; Cardi, N.; Fiocca, L.; Gennaro, A.; Giannotta, G.; Occhiello, E. U.S. US, 5,331,065 (1994), assigned to Enichem S.p.A.
- (400) Schuetz, J. D.; Meridith, B. C.; Hohlfeld, R. W. In *PCT WO Appl.*, 1985.
- (401) Chum, P. W. S.; Barger, M. A.; Dixit, T. P.; Schuetz, J. E. In *Eur. Pat. Appl. EP*, 1986.
- (402) Chum, P. W. S.; Barger, M. A.; Dixit, T. P.; Schuetz, J. E. In *U.S. US*, 1987.
- (403) Gunatillake, P. A.; Odian, G.; Tomalia, D. A. *Macromolecules* **1988**, *21*, 1556.
- (404) Jordan, R.; Ulman, A. *J. Am. Chem. Soc.* **1998**, *120*, 243.
- (405) Müller, P.; Wörner, C.; Mülhaupt, R. *Macromol. Chem. Phys.* **1995**, *196*, 1917.
- (406) Meyers, A. I.; Temple, D. L. *J. Am. Chem. Soc.* **1970**, *92*, 6644.
- (407) Loontjens, T.; Belt, W.; Stanssens, D.; Weerts, P. *Polym. Bull.* **1993**, *30*, 13.
- (408) Loontjens, T.; Belt, W.; Stanssens, D.; Weerts, P. *Macromol. Chem., Macromol. Symp.* **1993**, *75*, 211.
- (409) Lach, C.; Hanselmann, R.; Frey, H.; Mülhaupt, R. *Macromol. Rapid Commun.* **1998**, *19*, 461.
- (410) Lach, C.; Müller, P.; Frey, H.; Mülhaupt, R. *Macromol. Rapid Commun.* **1997**, *18*, 253.
- (411) Baker, W. E.; Saleem, M. *Polymer* **1987**, *28*, 2057.
- (412) Vainio, T.; Hu, G. H.; Lambla, M.; Seppälä, J. *J. Appl. Polym. Sci.* **1996**, *61*, 843.
- (413) Vocke, C.; Anttila, U.; Heino, M.; Hietaoja, P.; Seppälä, J. *J. Appl. Polym. Sci.* **1998**, *70*, 1923.
- (414) Chang, J. Y.; Ji, H. J.; Han, M. J.; Rhee, S. B.; Cheong, S.; Yoon, M. *Macromolecules* **1994**, *27*, 1376.
- (415) Chang, J. Y.; Park, P. J.; Han, M. J.; Chang, T. *Phosphorus Sulfur Silicon Relat. Elem.* **1999**, *144-146*, 197.

- (416) Chang, J. Y.; Park, P. J.; Han, M. J. *Macromolecules* **2000**, *33*, 321.
- (417) Canova, L.; Fiocca, L.; Giannotta, G.; Po', R.; Gleria, M. In *Phosphazenes. A Worldwide Insight*; Gleria, M., De Jaeger, R., Eds.; Nova Science Publishers, Inc.: Hauppauge, 2004, p 505.
- (418) Giannotta, G.; Po, R.; Fiocca, L.; Cardi, N.; Lucchelli, E.; Braglia, R.; Fambri, L.; Pegoretti, A.; Minto, F.; Gleria, M. *Phosphorus, Sulfur Silicon Relat. Elem.* **2001**, *168-169*, 587.
- (419) Po, R.; Fiocca, L.; Giannotta, G.; Lucchelli, E.; Cardi, N.; Minto, F.; Fambri, L.; Gleria, M. *Phosphorus, Sulfur Silicon Relat. Elem.* **2001**, *168-169*, 269.
- (420) Gleria, M.; Bertani, R.; Po, R.; Giannotta, G.; Fiocca, L.; Fambri, L.; La Mantia, F. P.; Scaffaro, R.; Resnati, G. *Phosphorus Sulfur Silicon Relat. Elem.* **2004**, *179*, 827.
- (421) Scaffaro, R.; Mistretta, M. C.; La Mantia, F. P.; Gleria, M.; Bertani, R.; Samperi, F.; Puglisi, C. *Macromol. Chem. Phys.* **2006**, *207*, 1986.
- (422) Carriedo, G. A.; Garcia Alonso, F. J. In *Inorganic Polymers*; De Jaeger, R., Gleria, M., Eds.; NOVA Science Publishers: Hauppauge, 2007, p 787.
- (423) Scalabrin, S., *Master Thesis*, University of Padova, Italy, (2001).
- (424) Fisher, P. M.; Sandosham, J. *Tetrahedron Lett.* **1995**, *36*, 5409.
- (425) Wong, G. S. K.; Wu, W. X., In *The Chemistry of Heterocyclic Compounds*; Palmer, D. C., Ed.; John Wiley & Sons, 2004; Chap. 8; Vol. 60; p 331.
- (426) Metrangolo, P.; Resnati, G. *Chem. Eur. J.* **2001**, *7*, 2511.
- (427) Metrangolo, P.; Pilati, T.; Resnati, G.; Stevenazzi, A. *Curr. Opin. Colloid Interface Sci.* **2003**, *8*, 215.
- (428) Fox, B. D.; Liantonio, R.; Metrangolo, P.; Pilati, T.; Resnati, G. *J. Fluor. Chem.* **2004**, *125*, 271.
- (429) Metrangolo, O.; Neukirk, H.; Pilati, T.; Resnati, G. *Acc. Chem. Res.* **2005**, *38*, 386.
- (430) Walsh, R. B.; Padgett, C. W.; Metrangolo, P.; Resnati, G.; Hanks, T. W.; Pennington, W. T. *Cryst. Growth Des.* **2001**, *1*, 165.
- (431) Messina, M. T.; Metrangolo, P.; Panzeri, W.; Pilati, T.; Resnati, G. *Tetrahedron* **2001**, *57*, 8543.
- (432) Liantonio, R.; Metrangolo, P.; Pilati, T.; Resnati, G.; Stevenazzi, A. *Cryst. Growth Des.* **2003**, *3*, 799.

- (433) Liantonio, R.; Luzzati, S.; Metrangolo, P.; Pilati, T.; Resnati, G. *Tetrahedron* **2002**, *58*, 4023.
- (434) De Santis, A.; Forni, A.; Liantonio, R.; Metrangolo, P.; Pilati, T.; Resnati, G. *Chem. Eur. J.* **2003**, *9*, 3974.
- (435) Caronna, T.; Liantonio, R.; Logothetis, T. A.; Metrangolo, P.; Pilati, T.; Resnati, G. *J. Am. Chem. Soc.* **2004**, *126*, 4500.
- (436) Farina, A.; Meille, S. V.; Messina, M. T.; Metrangolo, P.; Resnati, G. *Angew. Chem.* **1999**, *111*, 2585.
- (437) Gleria, M.; Bertani, R.; Po', R.; Giannotta, G.; Fiocca, L.; Fambri, L.; La Mantia, F. P.; Scaffaro, R.; Resnati, G. *Phosphorus, Sulfur and Silicon Relat. Elem.* **2004**, *179*, 827.
- (438) Bertani, R.; Ghedini, E.; Gleria, M.; Liantonio, R.; Marras, G.; Metrangolo, P.; Meyer, F.; Pilati, T.; Resnati, G. *Crystengcomm* **2005**, *7*, 511.
- (439) Gleria, M.; Lora, S.; Minto, F.; Busulini, L.; Paolucci, G. *Chem. Ind. (Milan)* **1981**, *63*, 719.
- (440) Cui, Y.; Ma, X.; Tang, X.; Luo, Y. *Eur. Polym. J.* **2004**, *40*, 299.
- (441) Liantonio, R.; Mele, M. L.; Metrangolo, P.; Pilati, T.; Resnati, G. *Supramol. Chem.* **2003**, *15*, 177.
- (442) Amati, M.; Lelj, F.; Liantonio, R.; Metrangolo, P.; Luzzati, S.; Pilati, T.; Resnati, G. *J. Fluor. Chem.* **2004**, *125*, 629.
- (443) Neukirch, H.; Liantonio, R.; Guido, E.; Pilati, T.; Metrangolo, P.; Resnati, G. *Chem. Commun.* **2005**, *12*, 1536.
- (444) Valerio, G.; Raos, G.; Meille, S. V.; Metrangolo, P.; Resnati, G. *J. Phys. Chem. A* **2000**, *104*, 1617.
- (445) Zou, J. W.; Jiang, Y. J.; Guo, M.; Hu, G. X.; Zhang, B.; Liu, H. C.; Yu, Q. S. *Chem. Eur. J.* **2005**, *11*, 740.
- (446) Messina, M. T.; Metrangolo, P.; Navarrini, W.; Radice, S.; Resnati, G.; Zerbi, G. *J. Mol. Struc.* **2000**, *524*, 87.
- (447) Roukolainen, J.; Tanner, J. R.; ten Brinke, G.; Thomas, E. L.; Ikkala, O. *Macromolecules* **1998**, *31*, 3532.
- (448) Roukolainen, J.; Saariaho, M.; Serimaa, R.; ten Brinke, G.; Thomas, E. L.; Ikkala, O. *Macromolecules* **1999**, *32*, 1152.

- (449) Shaw, R. A.; Nabi, S. N., In *Phosphorus Chemistry*; Quin, L. D., Ed.; ACS Sym. Ser.: Washington DC, USA, 1984; Vol. 64; p 307.
- (450) Shaw, R. A. *Phosphorus and Sulfur* **1986**, 28, 99.
- (451) Padmanabhan, K.; Paul, I. E.; Curtin, D. Y. *Acta Crystallogr., Sect. C: Cryst. Struct. Commun.* **1990**, 46, 88.
- (452) Briggs, D.; Seah, M. P. *Practical Surface Analysis*; J.Wiley & Sons: Chichester, UK, 1983.
- (453) Ertl, G.; Küppers, J. *Low Energy Electrons and Surface Chemistry*; VCH: Weinheim, Germany, 1985.
- (454) Fadley, C. S. *Electron Spectroscopy, Theory, Techniques and Applications*; Pergamon Press: New York, USA, 1978.
- (455) Feldman, L. C.; Mayer, J. W. *Fundamentals of Surface and Thin Film Analysis*; Elsevier Science: New York, USA, 1986.
- (456) Owens, D. K.; Wendt, R. C. *J. Appl. Polym. Sci.* **1969**, 13, 1741.
- (457) Fowkes, F. M. *Ind. Eng. Chem.* **1964**, 56, 40.
- (458) Mirabella, F. M., In *Principles, Theory and Practice of Internal Reflection Spectroscopy*; Mirabella, F. M., Ed.; Marcel Dekker, Inc.: New York, 1993.
- (459) Skourlis, T. P.; McCullough, R. L. *J. Appl. Polym. Sci.* **1994**, 52, 1241.
- (460) Harrick, N. J.; du Pre, F. K. *Applied Optics* **1966**, 5, 1739.
- (461) Maggioni, G.; Carturan, S.; Rigato, V.; Della Mea, G. *Surf. Coat. Technol.* **2001**, 142-144, 156.
- (462) Maggioni, G.; Carturan, S.; Quaranta, A.; Patelli, A.; Della Mea, G.; Rigato, V. *Surf. Coat. Technol.* **2003**, 174-175, 1151.
- (463) Maggioni, G.; Carturan, S.; Quaranta, A.; Patelli, A.; Della Mea, G. *Chem. Mater.* **2002**, 14, 4790.
- (464) Maggioni, G., *PhD Thesis*, Università di Trento, Italy, (2006).
- (465) Biersack, J. P.; Haggmark, L. G. *Nucl. Instr. Meth.* **1980**, 174, 257.

APPENDICES

A1. Characterization techniques

A1.1. X-ray Photoelectron spectroscopy (XPS)

The XPS technique^{452,453} is a powerful tool to obtain qualitative and quantitative information on the chemical composition of the surface of a solid system.

Irradiation of a material by sufficiently energetic radiation causes electron emission (photoelectric effect), as described by Einstein's law

$$h\nu = BE + KE + \phi_s$$

where KE is the Kinetic Energy of the emitted photoelectron, $h\nu$ is the energy of the incoming photon, BE is the Binding Energy of the electron as referred to the vacuum level, and ϕ_s is the work function of the solid, defined as the energy difference between the Fermi level and the vacuum level.

Photoelectronic emission leads to the formation of a *core* hole, that subsequently evolves towards energetically favoured states according to two different competing mechanisms (see figure 79):

1. X-ray fluorescence, with emission of exceeding energy as photons (radiative process);
2. The Auger process, in which exceeding energy is ceased to an electron (Auger electron) that is subsequently expelled (non radiative process).

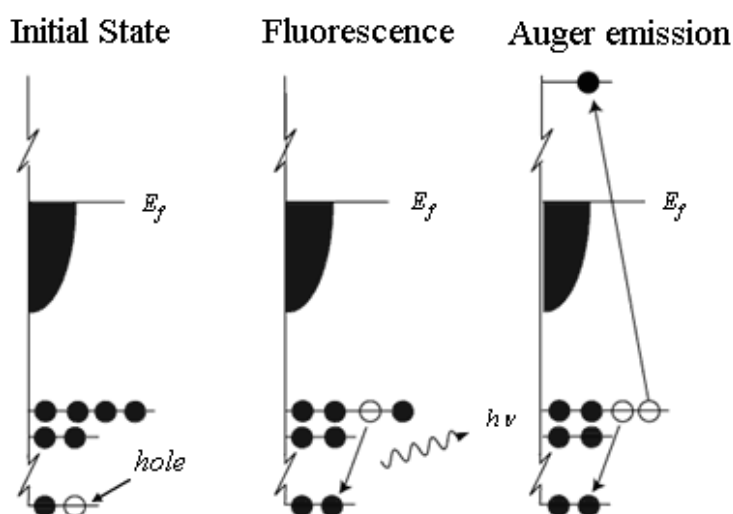


Figure 79. Possible decay paths for a hole generated in a core level.

Fluorescence becomes more and more likely as the atomic number grows, while the Auger process prevails for lighter atoms ($Z \leq 35$). The latter causes the appearance in XPS spectra of the so-called Auger peaks, normally studied in AES spectroscopy. As the kinetic energy of an Auger peak is related to energy level differences, it does not depend on the energy of the ionizing radiation.

Outgoing electrons can undergo inelastic scattering, and therefore have their kinetic energy lowered; such electrons do not contribute to photoelectronic peaks and cause an increase in spectral noise. Inelastic scattering limits the depth from which an emitted electron can be subsequently revealed, and grants XPS and AES high surface sensitivity. The probed sample depth depends on the electronic mean free path Λ_e , which in turn depends on the kinetic energy of the photoelectron itself.

Figure 80 shows the general dependence of Λ_e on kinetic energy in the typical photoelectronic spectroscopy range (5–1500 eV); the mean free path is lower than 50 Å.

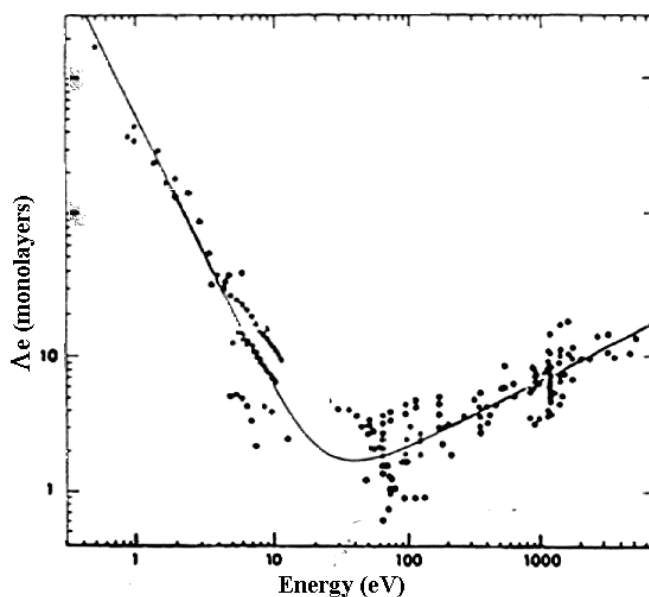


Figure 80. Photoelectron mean free path in function of their kinetic energy.

An XPS spectrum measures the number of emitted electrons in function of their BE , and is characterized by the presence of peaks that are typical of the emitting atoms. It is possible to distinguish in it a primary and a secondary structure. The primary structure comprises peaks due to core and valence electrons and to Auger peaks, while the secondary includes low intensity peaks that are due to the radiation source (satellite peaks caused by imperfect monochromaticity, and ghost peaks, caused by contaminations from the source itself) or to multielectronic processes (*shakeup* and

shakeoff)^{454,455}. The latter are characteristic of a specific oxidation state of the emitting element, and give valuable chemical information.

Core electron *BE*'s are specific of a given orbital in a given atom and depend on its effective nuclear charge. As the surrounding chemical environment varies, so changes the strength of the bond between the nucleus and its core electrons; this reflects into a peak shift to higher or lower *BE*'s (*chemical shift*). This phenomenon allows to determine whether a given element is present in different compounds or reticular sites, and whether the same atom is present in different chemical states in a compound⁴⁵⁴. Auger peaks also exhibit chemical shifts, but their interpretation is more complex because several electronic levels are involved.

An important diagnostic help is given by the Auger parameter α , defined as the sum of the kinetic energy of an Auger peak and of the *BE* of a photoelectric peak relative to the same element⁴⁵²:

$$\alpha = BE (XPS) + KE (Auger)$$

The α parameter has a characteristic value for each oxidation state of a given chemical species and is used as *finger print* in the qualitative analysis of a material when the chemical shift of photoelectronic peaks is too low to be accurately determined.

The area of the photoelectronic bands of a sample gives quantitative information on its composition, according to the simplified formula

$$C_i = 100 \frac{A_i}{S_i} \left(\sum_j \frac{A_j}{S_j} \right)^{-1}$$

where C_i is the relative concentration of a species i , A_i is the area of its photopeak, and S_i is a suitable sensitivity factor for that species.

A1.2. Contact angle and surface energy measurement

The surface energy of a solid can be determined from the measurement of the contact angle between a liquid with a known surface tension and the solid surface itself, by using the Young equation

$$\gamma_{SV} = \gamma_{SL} + \gamma_{LV} \cdot \cos \theta$$

where γ_{SV} is the surface tension of the solid in the presence of the liquid vapour, γ_{SL} is the interfacial tension between the solid and the liquid, γ_{LV} is the surface tension of the

liquid in the presence of its vapour, and θ is the contact angle between the solid and the liquid, as shown in Figure 81.

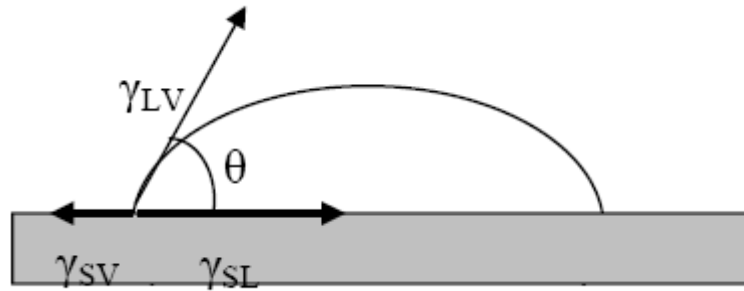


Figure 81. Schematic representation of the parameters involved in Young's equation.

The Owens-Wendt model⁴⁵⁶ has been used in this thesis to determine the surface energy of surface-modified polymeric materials. In this model the surface energy of the liquid and of the solid are considered as the sum of their respective polar and dispersive components, and the adhesion work W_{SL} between the solid and the liquid is defined as follows:

$$W_{SL} = 2\sqrt{\gamma_L^d \cdot \gamma_S^d} + 2\sqrt{\gamma_L^p \cdot \gamma_S^p} = \gamma_L(1 + \cos \theta)$$

where γ_L^d , γ_S^d , γ_L^p and γ_S^p are the polar (p) and dispersive (s) components of the surface energy of the liquid (L) and of the solid (S), and the last member is derived from the Young equation (note that it has been imposed $\gamma_L = \gamma_{LV}$ and $\gamma_S = \gamma_{SV}$)

Since γ_L^d and γ_L^p are known for many common liquids⁴⁵⁷, it is theoretically enough to measure the contact angles of the solid with two different liquids to calculate γ_S^d and γ_S^p , and therefore the solid's free surface energy. Higher precision can be obtained though by rewriting the above expression as

$$\frac{\gamma_L(1 + \cos \theta)}{2\sqrt{\gamma_L^d}} = \sqrt{\gamma_S^d} + \sqrt{\gamma_S^p} \frac{\sqrt{\gamma_L^p}}{\sqrt{\gamma_L^d}}$$

and plotting the first member of the equation as a function of $[(\gamma_L^p)^{1/2}/(\gamma_L^d)^{1/2}]$. Performing the linear regression with the data obtained from measurements obtained with different liquids, yields γ_S^d and γ_S^p . In this thesis, contact angles were always measured with water, formamide and diiodomethane.

A1.3. Fourier Transform Infrared Spectroscopy in Attenuated Total Reflection mode (FTIR-ATR)

The FTIR-ATR spectroscopy is based on the phenomenon of internal total reflection and the concept of evanescent wave^{458,459}.

Radiation propagating from a medium 1 of refractive index n_1 to another medium 2 of lower refractive index n_2 undergoes total internal reflection, provided the incidence angle θ is higher than a critical value named $\theta_c = n_2 / n_1$, as depicted in Figure 82 for an ideal non-absorbing system.

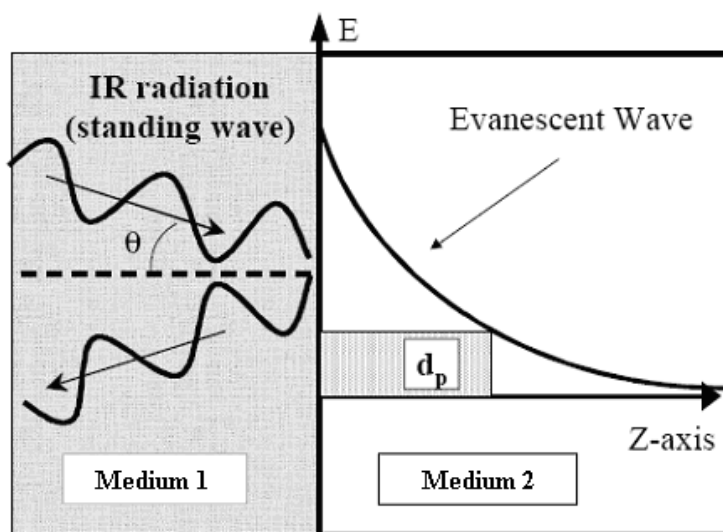


Figure 82. Illustration of the internal total reflection phenomenon and of an evanescent wave

Even though the incident wave is totally reflected without energy loss, the electromagnetic field intensity in medium 2 (lower refractive index) is not zero, as there is an instantaneous normal component of energy flow into medium 2 whose time average is zero. This electric field in medium 2, associated with a so-called *evanescent wave*, decays exponentially as it penetrates into the lower-refractive index medium. This behaviour can be described by the following expression:

$$E = E_0 \exp\left(\frac{-2\pi}{\lambda} \sqrt{\sin^2 \theta - n_{21}^2} \cdot z\right)$$

where E_0 is the incident field amplitude, λ is the wavelength of the radiation, $n_{21} = (n_2/n_1)$ and z is the coordinate describing the penetration depth into medium 2.

In a FTIR-ATR analysis, the sampling surface is pressed into intimate contact with the top surface of a high refractive index crystal such as diamond, ZnSe or Ge. The IR radiation from the spectrometer is reflected several times at the crystal boundaries, and

at the same time it penetrates into the sample *via* the evanescent wave with each reflection occurring at the crystal – sample interface; absorption phenomena thus occur at the characteristic wavelengths for the examined sample. At the output end of the crystal, the beam is directed back into the normal beam path of the spectrometer, as in Figure 83.

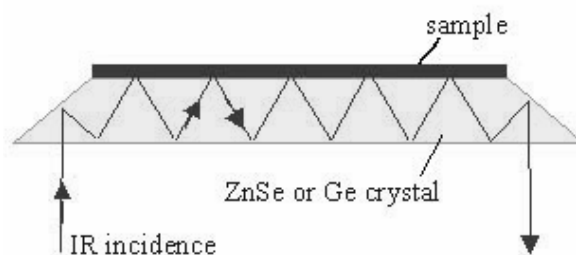


Figure 83. Schematic representation of the path of the IR radiation in an FTIR-ATR measurement.

The penetration depth of the evanescent wave, d , is defined as the distance from the crystal-sample interface at which the intensity of the evanescent wave decays to $1/e$ (37%) of its original value⁴⁶⁰. It can be given by:

$$d = \frac{\lambda}{2\pi n_1 \sqrt{\sin^2 \theta - n_{21}^2}}$$

and is generally around the micron order of magnitude, which makes FTIR-ATR a surface-specific analytical technique, though not as much as XPS. The depth of penetration and the total number of reflections along the crystal can be controlled either by varying the angle of incidence of the beam or by the selection of the crystal.

Another factor influencing the measurement is the clamping pressure of the sample onto the crystal, as it is necessary for the contact between the crystal and the sample to be as intimate as possible. Higher clamping pressure ensures better contact and therefore more intense absorption spectra.

Finally it is important to note that, as it can be seen from the expression of the penetration depth, d depends on the wavelength of the radiation. This means that in FTIR-ATR spectra, the absorption bands at lower wavenumbers are relatively more intense.

A2. Experimental techniques

A2.1. Glow Discharge-induced Sublimation (GDS)

Glow discharge-induced sublimation (GDS) is a solvent-free technique for the deposition of thin organic films on solid substrates⁴⁶¹⁻⁴⁶⁴. In a standard magnetron sputtering equipment, an organic powder is bombarded by low energy ($E < 1$ keV) noble gas ions, which are obtained by the use of radio frequency radiation. By the effect of momentum transfer phenomena, the ions dissipate their energy causing target heating and sublimation of the bombarded organic molecules. In common magnetron sputtering treatments this effect is considered detrimental because it can induce demagnetization of permanent magnets or even target melting and therefore the target is cooled, while in GDS this heating effect is exploited to create vapours that subsequently condense onto the surface of a solid substrate and form thin coatings on it.

The typical GDS procedure can be schematized as follows (Figure 84):

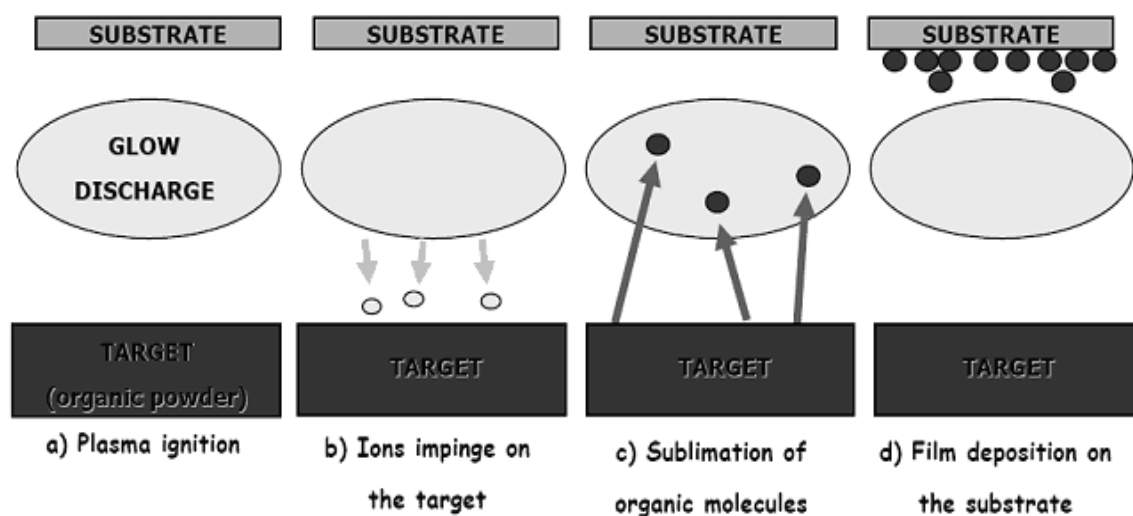


Figure 84. Schematic representation of Glow-Discharge-induced Sublimation technique.

(a) the organic compound to be sublimed is put on the target, and a weakly ionized plasma is ignited; (b) low energy (< 1 keV) noble gas ions impinge on the target; (c) energy transfer induces sublimation of the organic compound; (d) sublimated molecules condense onto the substrate yielding film deposition.

In comparison to other classical chemical procedures for the deposition of thin organic films such as spin coating or dip coating, GDS has the advantages of solvent

absence, precise control of film thickness and homogeneity, and high reproducibility; on the other hand, the necessity of a vacuum chamber makes it more costly.

In comparison to vacuum evaporation, where plasma is not used, the deposition rate can be up to one - two orders of magnitude higher, and the plasma, which is a highly reactive environment, can be used to tailor the properties of the deposited films; nevertheless, damage of the target compound can occur by scission of intramolecular chemical bonds, with production of both volatile and non-volatile fragments and therefore reduction of the number of integer molecules able to reach the substrate. Moreover, the volatile fragments can interfere in the ionization and excitation processes of the plasma and can be incorporated in the deposited film, while non-volatile fragments can give rise to surface layers on the target that hinder the sublimation process.

Finally, it should be taken into account that sublimated molecules can have interactions with plasma ions and electrons before reaching the substrate to be coated, *e.g.* ionization or protonation. Such interactions can be studied by *in situ* mass spectrometry, using particular filters to select neutral or charged species^{344,462,463}. The acquisition of a charge can influence the deposition of sublimed molecules, as the presence of strong electric fields in the region next to the substrate can affect both the trajectory and the energy of the species.

Some precautions can be adopted to reduce the undesired side effects of GDS: (1) utilization of a powder as a target rather than pressed pellets favours sublimation, because of the weakness of intermolecular bonds, high surface area and presence of numerous voids; (2) previous drying of the powder permits to avoid the presence of water, that can interfere by formation of hydrogen bonds or even by performing chemical reactions in plasma environment; (3) utilization of low molecular weight gases for plasma reduces damaging effects on the target organic compounds; (4) minimization of ion energy and maximization of ion current density reduce molecular damage as well; (5) utilization of short deposition times, as it has been demonstrated by TRIM (TRansport of Ions in Matter) calculations⁴⁶⁵ that sublimation prevails over fragmentation in the early stages of the GDS deposition process.

The apparatus for GDS deposition consists basically of a standard radio frequency magnetron sputtering chamber, with a stainless steel six-way vacuum chamber equipped with six DN200CF vacuum flanges (see Figure 85).

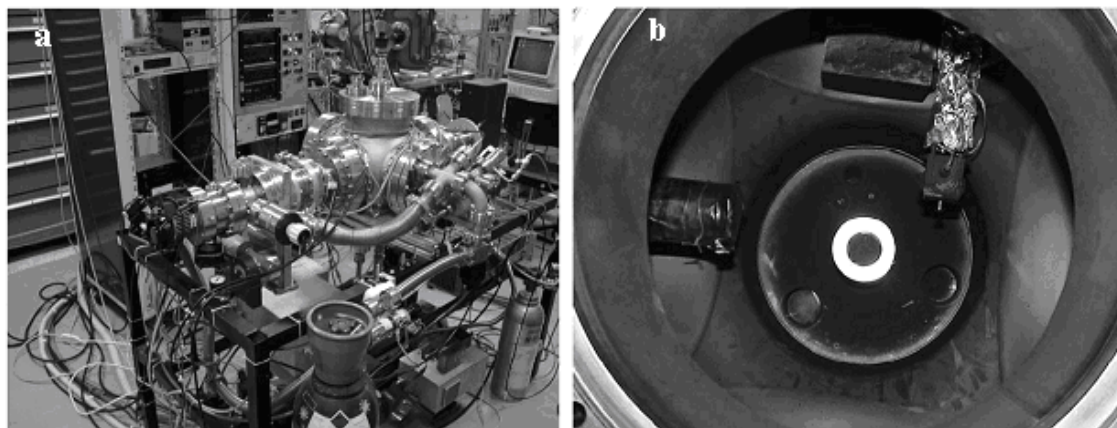


Figure 85. (a) Experimental apparatus for GDS deposition; (b) Top view of the cylindrical sputtering source and of the quartz crystal microbalance, inside the chamber

The bottom flange carries the magnetron sputtering source, where the organic compound target is put. The upper flange carries the stainless steel sample holder for the substrate, whose distance from the target can be varied in order to change the thickness and the homogeneity of the deposited coating. Below the target, a ring of permanent magnets generates the magnetic field above the target surface. The source is electrically connected to a radio frequency power generator through a matching box, which has the function to match the impedances of the power generator and of the plasma in order to maximize the power consumed in the plasma itself.

The pumping system, consisting of a turbomolecular pump and of a rotary pump, is connected to the chamber through one of the side flanges. The turbomolecular pump evacuates the chamber down to 10^{-4} Pa and is used to keep the desired working pressure during the deposition, which is monitored by three gauges.

Another side flange is occupied by a quartz crystal microbalance, that is used to monitor the deposition rate. It consists basically of a quartz crystal disc which oscillates at a fixed frequency; when a coating is deposited onto it, the oscillation frequency changes in a way that can be related to the mass of the deposited coating.

The gas used for the deposition is supplied to the chamber by means of a pressure reducer, connected through stainless steel tubes to a leak valve allowing fine gas flow regulation.

A2.2. Sol-gel technique

The sol-gel process³²⁷ can be obtained from two classes of precursors, that is inorganic (chlorides, nitrates, sulfates, etc.) and alkoxylic precursors.

In this process, an inorganic, highly-reticulated polymer is formed by means of hydrolysis and condensation reactions. In the case of an alkoxy silane precursor, the sol-gel process can be illustrated by the following reactions:

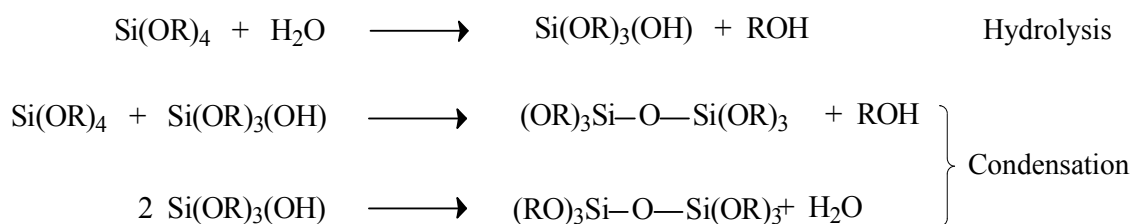
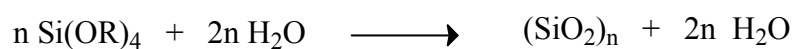


Figure 86. Schematic illustration of the sol-gel process.

The overall reaction can be described as follows:



The hydrolysis of a tetralkoxysilane solution in an organic solvent, such as ethyl alcohol, yields the formation of compounds containing siloxanic functions (-SiOH). The hydrolyzed compounds undergo successive condensation reactions to form a colloidal dispersion of particles called a *sol*. As the condensation proceeds, a three-dimensional, continual, liquid-containing solid network is finally formed, which is called *gel*. Gels can successively undergo further aging, as condensation proceeds causing the contraction of the solid and the expulsion of liquid from the network; a *xerogel* is thus formed, characterized by high porosity and surface area.

It should be noted that even small changes of the experimental conditions (temperature, solvent, concentration, catalysis, solvent evaporation rate) can lead to dramatic changes in the morphology of the solid obtained (surface area, pores dimension and distribution, density, etc.)

The hydrolysis reaction, in the first step of the process, involves a nucleophilic attack of the water molecule on the silicon atom, but its exact mechanism depends on the type of catalyst used. Three catalysis mechanisms can be employed: acid, basic and nucleophilic, as described below.

Acid Catalysis

The first step is the reversible protonation of the alkoxylic group, which makes it a better leaving group; then, nucleophilic substitution by water (or by another silanol) occurs through a pentacoordinate intermediate, and the catalyst is regenerated.

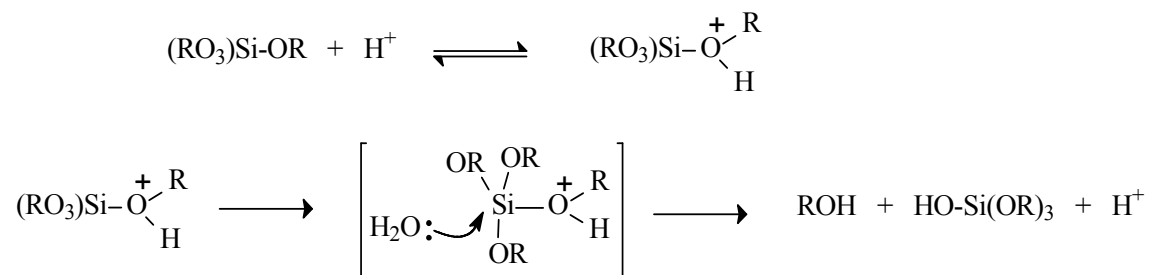


Figure 87. Hydrolysis of alkoxysilanes by acid catalysis.

Basic catalysis

The nucleophilic OH^- ion reacts with the alkoxysilane to form a pentacoordinate intermediate, and an RO^- alkoxylic ion is the leaving group. The hydroxide ion is then regenerated by reaction of the alkoxide with a molecule of water.

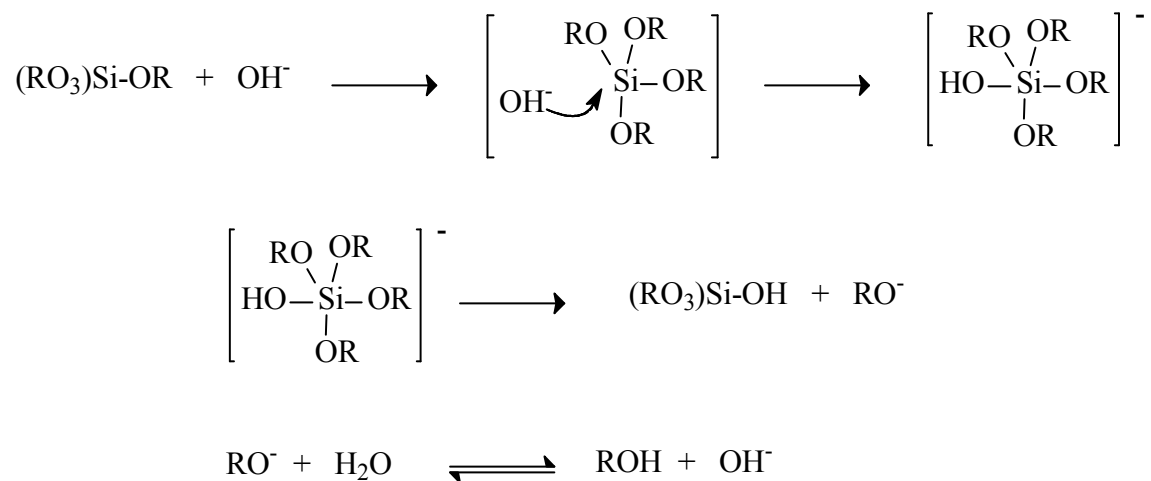


Figure 88. Hydrolysis of alkoxysilanes by basic catalysis.

Nucleophilic catalysis

The nucleophile (F^- , N-methylimidazole, N,N'-dimethylaminopyridine, etc.) coordinates with the alkoxy silane, giving rise to a pentacoordinate intermediate that is more reactive towards substitution reactions with water or silanols. A hexacoordinate species is thus formed, that ultimately leads to the formation of alcohol and of a silanol group, and to the regeneration of the catalyst.

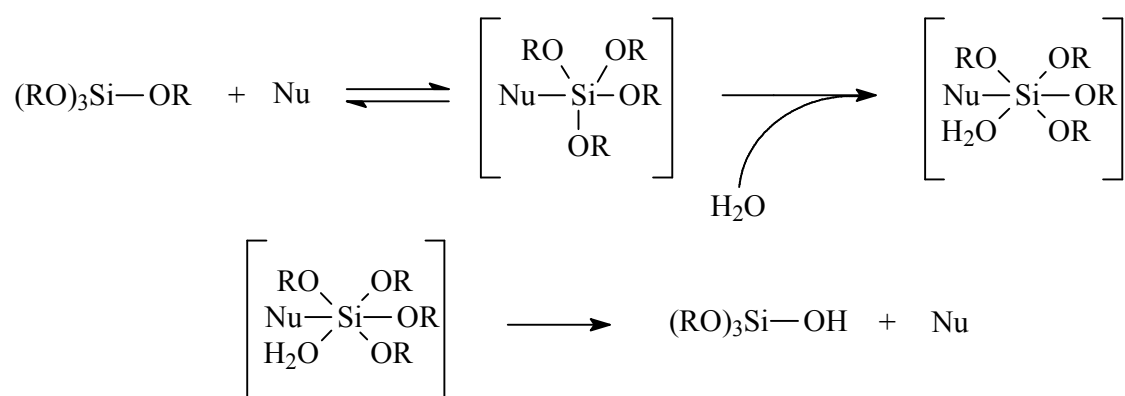


Figure 89. Hydrolysis of alkoxy silanes by nucleophilic catalysis.

LIST OF PUBLICATIONS

Journal Articles

- (1) Pertici, P.; Vitulli, G.; Gleria, M.; Facchin, G.; Milani, R.; Bertani, R. *Macromolecular Symposium* **2006**, 235, 98.
- (2) Sassi, A.; Milani, R.; Venzo, A.; Gleria, M. *Designed Monomers and Polymers* **2006**, 9, 627.
- (3) Silvestrelli, P.; Gleria, M.; Milani, R.; Boscolo-Boscoletto, A. *Journal of Inorganic and Organometallic Polymers and Materials* **2006**, 16, 327.
- (4) Milani, R.; Gleria, M.; Sassi, A.; De Jaeger, R.; Mazzah, A.; Gengembre, L.; Frere, M.; Jama, C. *Chemistry of Materials* **2007**, 19, 4975.
- (5) Milani, R.; Sassi, A.; Venzo, A.; Bertani, R.; Gleria, M. *Designed Monomers and Polymers* **2007**, 19, 555.
- (6) De Jaeger, R.; Mazzah, A.; Gengembre, L.; Frere, M.; Jama, C.; Milani, R.; Bertani, R.; Gleria, M. *Journal of Applied Polymer Science* **2008**, in press.
- (7) Milani, R.; Gleria, M.; Gross, S.; De Jaeger, R.; Mazzah, A.; Gengembre, L.; Frere, M.; Jama, C. *Journal of Inorganic and Organometallic Polymers and Materials* **2008**, submitted.
- (8) Sassi, A.; Maggioni, G.; Milani, R.; Carturan, S.; Gleria, M.; Della Mea, G. *Surface and Coating Technology* **2007**, 201, 5829.
- (9) Bertani, R.; Chaux, F.; Gleria, M.; Metrangolo, P.; Milani, R.; Pilati, T.; Resnati, G.; Sansotera, M.; Venzo, A. *Inorganica Chimica Acta* **2007**, 360, 1191.
- (10) Fiocca, L.; Po', R.; Giannotta, G.; Gleria, M.; Venzo, A.; Milani, R.; De Paoli, G. *Designed Monomers and Polymers* **2008**, in press.
- (11) Milani, R.; Gleria, M.; Sassi, A.; De Jaeger, R.; Mazzah, A.; Jama, C.; Gengembre, L. *Molecular Crystals Liquid Crystals* **2008**, in press.
- (12) Milani, R.; Gleria, M.; Sassi, A.; De Jaeger, R.; Mazzah, A.; Jama, C.; Gengembre, L. *Pure Applied Chemistry* **2008**, submitted.
- (13) Boscolo-Boscoletto, A.; Gleria, M.; Milani, R.; Meda, L.; Bertani, R. *Journal of Inorganic and Organometallic Polymers and Materials* **2008**, manuscript in preparation.

- (14) Gleria, M.; Milani, R.; Bertani, R.; Boscolo-Boscoletto, A.; De Jaeger, R., In *Biomedical Applications of Polyphosphazenes*; Andrianov, A. K., Ed.; Wiley: New York, USA, **2008**, submitted.

Congress Communications

- (15) Sassi, A.; Maggioni, G.; Milani, R.; Carturan, S.; Gleria, M.; Della Mea, G., *INFN Annual Report*, Legnaro, Padova, Italy, 2006, p 102.
- (16) Sassi, A.; Della Mea, G.; Gleria, M.; S., C.; Milani, R.; Maggioni, G., *Tenth International Conference on Plasma Surface Engineering*, Garmisch-Partenkirchen, Germany, September 10-15, 2006, p 571, Poster No. 4093.
- (17) Milani, R.; Gleria, M.; Sassi, A.; De Jaeger, R.; Mazzah, A.; Jama, C.; Gengembre, L., *Proceedings of the 18th International Symposium on Plasma Chemistry*, Kyoto, Japan, August 26-31, 2007, submitted.
- (18) Milani, R.; Gleria, M.; Sassi, A.; De Jaeger, R.; Mazzah, A.; Jama, C.; Gengembre, L., *IX International Conference on Frontiers of Polymers and Advanced Materials*, Krakow, Poland, July 8-12, 2007, p 301.
- (19) Milani, R.; Gleria, M.; Bertani, R.; De Jaeger, R.; Mazzah, A.; Jama, C.; Frere, M.; Gengembre, L., *Syntheses and Methodologies in Inorganic Chemistry. From Molecules to Nanosystems*, Bressanone (Bolzano), Italy, December 2-6, 2007, Poster No. 11.
- (20) Gleria, M.; Milani, R.; Bertani, R.; Sassi, A.; Venzo, A.; Fambri, L.; De Jaeger, R.; Mazzah, A.; Jama, C.; Frere, M.; Gengembre, L., *TICME, Trento Innovation Conferences in Materials Engineering*, Trento, Italy, December 16-19, 2007, p 107, Poster No. P25.

ACKNOWLEDGEMENTS

As I went over these two hundred pages of thesis over and over again with a red pen in my hand, I came to realize something little by little. All this work made me get in touch with a deal of different people, more or less frequently, more or less directly, but it did nonetheless. And if it's true that every person you meet enriches you somehow, then there's a lot of thanks to give here. Perhaps as I was thinking about this, something made it past the red pen. So much. It was worth.

I will start off by thanking those who contributed directly to this thesis. I will do it in English, because I feel these lines should be understandable by all of them.

- My Supervisor in Italy, Dr. Mario Gleria, Institute of Molecular Sciences and Technologies (ISTM) of the National Research Council (CNR) in Padova, for the simplest of reasons: because I owe him so much, that I have to make it simple by just saying that I owe him so much;
- My Supervisor in France, Prof. Ahmed Mazzah, Laboratory of Infrared and Raman Spectrochemistry (LASIR), University of Sciences and Technologies of Lille, for giving me the opportunity of a precious work experience in a pleasant and stimulating environment; and for the help in both scientific and everyday issues during my stay in Lille;
- Prof. Roberta Bertani, Prof. Rino Antonio Michelin and the staff of the Department of Chemical Processes of the Engineering (DPCI), University of Padova, for their scientific hospitality, without which this thesis could not have been done;
- Prof. Roger De Jaeger from the LASIR, for his constant and precious scientific support during my work in France, and for the patience he demonstrated in being my first French language teacher. He was a reference point throughout my stay in Lille;
- Dr. Charafeddine Jama, PERF Laboratory of the National Superior Chemistry School of Lille (ENSCL), for his scientific contribution and logistic support regarding my stay in France, both of which proved to be very important and greatly appreciated;
- Dr. Leon Gengembre, Catalysis and Solid State Chemistry Unit, University of Sciences and Technologies of Lille, for his invaluable contribution in the discussion of the XPS data;

- Dr. Martine Frere, Catalysis and Solid State Chemistry Unit, University of Sciences and Technologies of Lille, for the great (both in quantity and quality!) work done at the XPS back in France, and for all those second coffees of the day. Her presence alone was enough to make both morning work and French coffee pleasant;
- all the staff of the LASIR in Lille, for their kindness and hospitality (even after the 9th of July... now *that's* being hospitable!);
- Dr. Alessandro Sassi, ISTM-CNR in Padova, for all that relates to GDS, and for every solid state NMR in this thesis. Working with him proved once again to be a pleasure;
- Dr. Gianluigi Maggioni, National Laboratories of Legnaro of the National Institute of Nuclear Physics (INFN), for performing the GDS depositions;
- Dr. Silvia Gross, ISTM-CNR in Padova, for performing the XPS analyses of the films deposited by GDS technique;
- Dr. Alfonso Venzo, ISTM-CNR in Padova, for his presence is behind almost every single solution NMR of this thesis, be it to perform or to comment it;
- Prof. Giovanni Depaoli, University of Padova, for his logistic support to the researches described in this thesis;
- Prof. Pierluigi Silvestrelli, University of Padova, for performing the *ab initio* theoretical calculations about the functionalization of siliceous substrates;
- Dr. Angelo Boscolo Boscoletto, ENI-Polimeri Europa, Marghera, for his unflagging contribution to the sections concerning the theoretical calculations and the functionalization of inorganic substrates;
- Dr. Laura Meda, ENI-Polimeri Europa, Novara, for the great helpfulness and the even greater patience she demonstrated while performing the XPS analyses concerning the functionalization of inorganic substrates;
- Dr. Luisa Fiocca, ENI-Polimeri Europa, Novara, for performing the synthesis of the oxazolines, and for her precision and helpfulness;
- Prof. L. Fambri, University of Trento, for performing the thermal analyses of the sol-gel hybrid materials;
- Prof. Giuseppe Resnati, Prof. Pierangelo Metrangolo, Dr. Fanny Chaux and Dr. Maurizio Sansotera, NFM Lab, Politecnico of Milano, and Dr. Tullio Pilati, ISTM-CNR in Milano, for the preparation and characterization of the supramolecular self-assemblies.

Now, I want to thank all those people who did not contribute directly to this thesis, but whose presence still permeates every line of it, because they *were there* during these three years. Being this part way more personal, I will here use the language of the persons for which the thanks are intended.

Voglio quindi ringraziare tutte queste persone:

- I miei genitori, Marilena e Paolo. A tre anni di distanza, il motivo è ancora lo stesso: se sono arrivato qui, e ovunque io arrivi da qui in avanti, lo devo innanzitutto a loro;
- mio fratello Mauro, perché so di poter contare su di lui;
- le mie due nonne, Stella e Maria, perché continuano a essere delle *fan* infaticabili;
- Luce, perché per quanto ci si veda poco, è sempre una delle persone migliori con cui chiacchierare;
- la grande schiera degli amici di Piove e dintorni, e che non nominerò uno a uno solo per questioni di spazio: quelli vecchi e quelli nuovi, quelli che ci si vede sempre e quelli che non ci si vede quasi più... ma che ci sono; dato che, dopo essersi illuso che stavolta l'avrebbe scampata, ha finito suo malgrado per essere tirato dentro ai miei lavori *in extremis*, ringrazio in particolare il solito Emilio;
- tutti coloro che, nelle forme più varie, si sono succeduti in questi tre anni nella stanza studenti del DPCI (Paolo, Er...ika, Silvia, Gil, Diego, BenBen, Betta, Cinzia e perfino lo Smemerone). Potrei parlare di passaggi saltati, chicche da antologia, cicche in compagnia, cose di cui non sospettavo neanche l'esistenza, mattanze di alci, assurdità varie, assurdità ancora più varie, Cucciolini, palloni kamikaze a due colli e saune, ma mi limiterò a definirvi così: degli amici, più che dei compagni di laboratorio;
- Ida, per tutti i motivi che lei sa;
- quelli del Branco (el Terso, Cioncy, Roberto, Linda, Ale e Serena), perché è magnifico poterli ringraziare ancora tre anni dopo: l'università può finire, ma il Branco perdura;
- il Tuttotranneuno, passato, presente e (si spera ancora a lungo) futuro (Daniel, Paolo, Alessio, Claudio e Stefano), perché restare *binbi* fa un mondo di bene, soprattutto a quelli che non ci credono;
- I Question Mark, ahimé ormai sciolti per la disperazione dei *fans*, in tutte le loro formazioni (Bea, Lara, Francesco, Edo, Rossi, Emilio, Ale, Alice): per tutto ciò che di buono abbiamo passato insieme, prima e durante questi tre anni.

Et enfin, des remerciements sont dus – et très volontiers donnés – à tous ceux que j’ai connu pendant mon séjour en France. J’avais pas mal de doutes avant mon départ, mais à la fin ça s’est avéré être une expérience qui a fait de moi quelqu’un de meilleur. Encore une fois, j’aimerais bien tous nommer, mais lorsque j’ai essayé de faire une liste, j’ai été étonné de la quantité de noms qu’il y avait dedans. Ne m’en voulez pas donc si votre nom n’est pas ci-dessous, sachez que je ne vous ai pas oublié !

- Adriana, Ulises, Johnny, Enrico & Enrico, Tarik, Pedro et sa famille : vous avez été parmi mes premiers amis là bas, merci pour toutes les fois qu’on s’est amusés ensemble ;
- Alberto, perché neanche due giorni dopo il mio arrivo, mi trovavo a parlare di rock anni '70 sulla strada per Liegi;
- e con lui tutti gli *Italians*, in particolare Enrico (un altro ancora!), Fabrizio, Sara e Oliver, e *dulcis in fundo* Serafina, Silvia e Ada (quest’ultima perché se non la conosci non ci credi, e per la grande disponibilità dimostrata nell’*affaire* dello zaino smarrito);
- Sofie, because it was fun to work by her side. Ok, I should probably have put you in the first list, but somehow I think you’ll feel more at ease down here ;
- Erwan, parce que pouvoir te compter parmi ses propres potes, c’est ce qu’on appelle de la chance;
- Nico et Fanny, parce qu’ils sont géniaux : chez eux, même les toilettes sont de l’art;
- Laetitia et Bertrand pour m’avoir si souvent accueilli dans leur maison, et m’avoir initié aux gourmandises de la cuisine du Nord ;
- et enfin bon, pour toutes les autres filles et tous les autres mecs du labo et de ses alentours (Thao, Emilie, Alexandra, Sara, Séverine, Emmanuelle, Guillaume, Julien, Baptiste, Matthieu, Gilles, Vinh, Christophe, Nacer, Li, ...) y a quelque chose pour laquelle je dois les remercier : matchs de foot (joués, regardés ou pariés), barbecues et diners, musique, causettes, clopes en compagnie et rigolades... vous savez, quoi !
- Et un remerciement à tous ceux de l’Amaryllis, bien sûr !

Last but not least, and deserving three languages at once for his undeniable importance:

The Backpack, whose spiritual presence has never, *ever* abandoned me.

Le Sac à dos, dont la présence spirituelle ne semble toujours pas vouloir m’abandonner.

Lo Zaino, la cui presenza spirituale non accenna per niente ad abbandonarmi.